Université de Montréal

Towards Understanding the Functionality of Foot Orthosis Based on Foot Structure and Function

Par

Maryam Hajizadeh

Institut de Génie Biomédical, Département de Pharmacologie et Physiologie,

Faculté de Médecine

Thèse présentée en vue de l'obtention du grade de Philosophiæ Doctor (Ph.D.)

en Génie Biomédical

Août 2020

Institut de Génie Biomédical, Département de Pharmacologie et Physiologie, Faculté de Médecine

Towards Understanding the Functionality of Foot Orthosis Based on Foot structure and Function

Présenté par

Maryam Hajizadeh

A été évalué(e) par un jury composé des personnes suivantes

Dr. Jason Neva
Président-rapporteur

Dr. Mickael Begon
Directeur de recherche

Dr. Rachid Aissaoui
Membre du jury

Dr. Renate List
Examinateur externe

Dr. Pascal-André Vendittoli
Représentant de la doyenne

Résumé

Les orthèses plantaires (OP) sont des dispositifs médicaux fréquemment utilisés pour réduire les douleurs et blessures de surutilisation, notamment chez les personnes ayant les pieds plats. Le port d'OP permettrait de corriger les altérations biomécaniques attribuées à la déformation du pied plat, que sont la perte de l'arche longitudinale médiale et la pronation excessive du pied. Cependant, le manque de compréhension de la fonction des OP entraine une grande variabilité des OP prescrites en milieu clinique. L'objectif de cette thèse est d'approfondir les connaissances sur l'effet des OP sur la biomécanique, de quantifier les déformations des OP à la marche et de mettre en relation ces déformations avec la biomécanique du pied.

La première étude a évalué la manière dont les différentes conceptions d'OP imposent des modifications dans le mouvement et le chargement appliqué sur le pied. Cet objectif a été atteint grâce à une revue systématique traitant des effets des OP sur la cinématique et la cinétique du membre inférieur pendant la marche chez des personnes ayant des pieds normaux. Les critères d'inclusion ont réduit les études à celles qui ont fait état des résultats pour les géométries les plus fréquentes des OP, à savoir les biseaux, les supports d'arche et les stabilisateurs de talon. La revue a mis en évidence que les orthèses avec un biseau médial peuvent réduire le moment d'éversion de la cheville. Aucune évidence significative n'a été trouvée dans notre méta-analyse sur l'efficacité des orthèses incluant des supports d'arche ou des stabilisateurs de talon. Les différents procédés et matériaux utilisés dans la conception des OP ainsi que les caractéristiques des pieds des participants pourraient expliquer la variabilité retrouvée au regard des effets des OP sur la biomécanique.

La deuxième étude a apporté des informations précieuses et inédites sur le comportement dynamique des OP à la marche. La cinématique du contour des OP a été utilisée pour prédire la déformation de leur surface plantaire pendant la marche chez 13 individus ayant des pieds normaux en utilisant un réseau de neurones artificiels. Une erreur moyenne inférieure à 0,6 mm a été obtenue pour nos prédictions. En plus de la précision des prédictions, le modèle a été capable de différencier le patron de déformations pour deux OP de rigidités différentes et entre les participants inclus dans l'étude.

Enfin, dans une troisième étude, nous avons identifié la relation entre la déformation des OP personnalisées et la biomécanique du pied à la marche chez 17 personnes avec des pieds plats.

L'utilisation de modèles linéaires mixtes a permis d’exprimer les variations de la déformation des OP dans différentes régions en fonction des variables cinématiques du pied et de pressions plantaires. Cette étude a montré que l'interaction pied-OP varie selon les différentes régions de l’OP et les différentes phases du cycle de marche. Ainsi, des lignes directrices préliminaires ont été fournies afin de standardiser et optimiser la conception des OP.

Dans l'ensemble, les résultats de cette thèse justifient l'importance d’'intégrer des caractéristiques dynamiques du pied de chaque individu dans la conception d'OP personnalisées. Des études futures pourraient étendre les modèles de prédiction de l'interaction pied-OP en incluant d'autres paramètres biomécaniques tels que les moments articulaires, les activations musculaires et la morphologie du pied. De tels modèles pourraient être utilisés pour développer des fonctions coût pour l'optimisation de la conception des OP par une approche itérative utilisant la simulation par les éléments finis.

Mots-clés: orthèse plantaire, pied plat, déformation, cinématique du pied, pression plantaire, interaction pied-orthèse plantaire, revue systématique, intelligence artificielle, modèle linéaire mixte

Abstract

Foot orthoses (FOs) are frequently used medical devices to manage overuse injuries and pain in flatfoot individuals. Wearing FOs can result in improving the biomechanical alterations attributed to flatfoot deformity such as the loss of medial longitudinal arch and excessive foot pronation. However, a lack of a clear understanding of the function of FOs contributes to the highly variable FOs prescribed in clinical practice. The objective of this thesis was to deepen the knowledge about the biomechanical outcomes of FOs and to formulate the dynamic behaviour of FOs as a function of foot biomechanics during gait.

The primary study investigated how different designs of FOs impose alterations in foot motion and loading. This objective was achieved through a systematic review of all literature reporting the kinematics and kinetics of the lower body during walking with FOs in healthy individuals. The inclusion criteria narrowed the studies to the ones which reported the outcomes for common designs of FOs, namely posting, arch support, and heel support. The review identified some evidence that FOs with medial posting can decrease ankle eversion moment. No significant evidence was found in our meta-analysis for the efficiency of arch supported and heel supported FOs. The findings of this study revealed that differences in FO design and material as well as foot characteristics of participants could explain the variations in biomechanical outcomes of FOs.

The second study provided valuable information on the dynamic behaviour of customized FOs. The kinematics of FO contour was used to predict the deformation of FO plantar surface in 13 healthy individuals during walking using an artificial intelligence approach. An average error below 0.6 mm was achieved for our predictions. In addition to the prediction accuracy, the model was capable to differentiate between different rigidities of FOs and between included participants in terms of range and pattern of deformation.

Finally, the third study identified the relationship between the deformation of customized FOs and foot biomechanics in 17 flatfoot individuals during walking. The use of linear mixed models made it possible to identify the variables of foot kinematics and region-dependent plantar pressure that could explain the variations in FO deformation. This study showed that the foot-FO interaction changes over different regions of FO and different phases of gait cycle. In addition, some preliminary guidelines were provided to standardize and optimize the design of FOs.

Overall, the results of this thesis justify the importance of incorporating the dynamic characteristics of each individual's foot into the design of customized FOs. Future studies can extend the predictive models for foot-FO interactions by including other determinants of foot biomechanics such as joint moments, muscle activation, and foot morphology. Based on such extended models, the cost functions could be devised for optimizing the designs of customized 3D printed FOs through an iterative approach using finite element modeling.

Keywords: foot orthosis, flatfoot, deformation, kinematics, foot plantar pressure, foot-foot orthosis interaction, systematic review, artificial intelligence, linear mixed model

Table of Contents

List of Tables

Supplementary Tables

List of Figures

Supplementary Figures

Abbreviations

FO: Foot Orthosis

FE: Finite Element

AI: Artificial Intelligence

ROI: Region of Interest

EVA: Ethylene-Vinyl Acetate

MRI: Magnetic Resonance Imaging

CT: Computed Tomography

GRF: Ground Reaction Force

ES: Effect Size

CI: Confidence Interval

CoP: Center of Pressure

SPM: Statistical Parametric Mapping

RMSE: Root Mean Square Error

NRMSE: Normalized Root Mean Square Error

1D: One-Dimensional

2D: Two-Dimensional

3D: Three-Dimensional

GP: Gait Phase

RoM: Range of Motion

LAA: Longitudinal Arch Angle

VIF: Variance Inflation Factor

rmcorr: Repeated Measures Correlation

FEM: Finite Element Method

List of publications

Journal publications

Hajizadeh M, Desmyttere G, Ménard AL, Bleau J, Begon M (2020) Understanding the role of foot biomechanics on regional foot orthosis deformation during walking in flatfoot individuals. Submitted to *Journal of Biomechanics*

Desmyttere G, Leteneur, S, **Hajizadeh M**, Bleau J, Begon, M (2020) Effect of 3D printed foot orthoses stiffness and design on foot kinematics and plantar pressures in healthy people. *Gait & Posture*, 81:247:253.

Hajizadeh M, Michaud B, Desmyttere G, Carmona JP, Begon M (2020) Predicting foot orthosis deformation based on its contour kinematics during walking. *PLoS ONE*, 15 (5): e0232677.

Hajizadeh M, Desmyttere G, Carmona JP, Bleau J, Begon M (2020) Can foot orthoses impose different gait features based on geometrical design in healthy subjects? A systematic review and meta-analysis. *The Foot*, 42: 101646.

Hajizadeh M, Michaud B, Begon M (2019) The effect of intracortical bone pin on shoulder kinematics during dynamic activities." *International Biomechanics*, 6(1): 47-53.

Cherni Y, **Hajizadeh M**, Begon M, Turpin NA (2019) Muscle coordination during robotic assisted walking using Lokomat. *Computer Methods in Biomechanics and Biomedical Engineering*. 22(sup1): S216-8.

Desmyttere G., **Hajizadeh M**, Bleau J, Begon M (2018) Effect of foot orthosis design on lower limb joint kinematics and kinetics during walking in flexible pes planovalgus: A systematic review and meta-analysis. *Clinical Biomechanics*, 59:117-129.

Conferences

Cherni Y, **Hajizadeh M**, Begon M, Turpin NA (2019) Muscle coordination during robotic assisted walking using Lokomat", *SB conference- Poitiers*, France.

Hajizadeh M, Michaud B, Desmyttere G, Carmona JP, Begon M (2019) The rigidity of foot orthosis will alter its predicted deformation during walking*, ISB Conference- Calgary*, Canada.

Hajizadeh M, Ménard AL, Desmyttere G, Lagarenne L, Carmona JP, Begon M (2019) Foot orthosis deformations following dynamic loading: a 3D finite element study*, ISB Conference- Calgary*, Canada.

Desmyttere G, **Hajizadeh M,** Bleau J, Begon M (2019) Foot orthosis with add-on rearfoot postings can alter foot kinematics*, ISB Conference- Calgary*, Canada.

Hajizadeh M, Desmyttere G, Michaud B, Carmona JP, Begon M (2018) A novel approach to predict foot orthosis deformation during dynamic loading, *CSB conference- Halifax*, Canada.

Dedication

To my mom and dad

"Living Life Tomorrow's fate,
though thou be wise,
Thou canst not tell nor yet surmise;
Pass, therefore, not today in vain,
For it will never come again."

- Omar Khayyam

Acknowledgement

This long journey of my life was not feasible without the enormous support and assistance from my supervisor, colleagues, and family members.

Foremost, I would like to express my sincere gratitude to my supervisor, *Dr. Mickael Begon*, for his continuous and kind support during the course of my Ph.D. research and writing of this thesis. Thank you, *Mickael*, for your advices, motivation, patience, enthusiasm, and immense knowledge. Your daily follow-ups with "Quoi de neuf?" and your encouraging responses with "Good idea" and "Excellent" had a broad impact, from pressure to motivation, on the way to fulfill this Ph.D.!

My sincere gratitude goes to all my colleagues in *S2M team* who have created a friendly and warm atmosphere. I did not only pursued research in the lab, but also lived a joyful life there. Thank you all for the days we worked together and for all the fun we had during lunch time, Thursday pastries, coffee breaks, and insanity time!

All the members of *FOOT¡ Team* deserve very special thanks for all the support and encouragement they gave me. Without their guidance and feedback this Ph.D. would not have been achievable. Thanks to both of you, *Anne-Laure* and *Gauthier*, it was a real joy to do data collections, group meetings, and all other stages of this project in your accompaniment and assistance. I appreciate your valuable insights and comments on my thesis writings. I also acknowledge the valuable advices provided by the partners of this project, especially *Dr. Jacinte Bleau, Mr. Olivier Bisson,* and *Mr. Jean-Phillipe Carmona*.

I gratefully acknowledge the financial support of this project by Natural Sciences and Engineering Research Council (*NSERC*) R&D Coop with *Medicus, Caboma,* and *MedTech*. I am also thankful to the financial support I received from *FRQNT* in the form of doctoral research scholarship program.

Last but not the least, I would like to thank my family for all their love and inspiration. To my parents, *Nahid* and *Esmaeil*, thank you for being my champions and for your unrestricted support. You taught me that achieving my goals is the only thing that will bring me the real happiness. To reach my goals, you backed me up to step in the challenging route of loving each other remotely, from two different lands. To my lovely sister, *Marjan*, thank you for always motivating me, being here beside me, and cheering me up in tough situations. To my brothers, *Mehdi* and *Meraj*, thank

you for supporting me throughout all difficulties and challenges during my life. Finally, this thesis is also a fruit of love and unconditional support from my beloved husband *Bijan*. At the end of the day, he listened, or at least pretended to listen, to the challenges of my research life. He always ensured me that there is an end to a PhD when it was impossible for me to see it. I am there now, my love!!

Introduction

Context and general objective

Flatfoot deformity is a frequent pathology with a prevalence of 20-25% in the general population, characterized by a partial or complete collapse of the medial longitudinal arch [1]. This deformity can impose various alterations in the motion of foot joints and the operation of functional mechanisms [2]. Excessive pronation is usually observed during the early stance phase in flatfoot individuals due to the orientation of the subtalar joint [3-5]. In addition, the medial longitudinal arch cannot shift from a mobile adaptor in weight-bearing phase to a rigid lever in the propulsion phase, resulting in excessive stress on the midfoot and inefficient propulsion [6-8]. A further common alteration is forefoot abduction, which deteriorates the biomechanical function during propulsion. These alterations in foot motion and function make the foot susceptible to a diversity of symptoms such as increased lower limb fatigue and overuse injuries, Achilles tendinopathy, stress fractures, osteoarthritis, and patellofemoral pain [2, 9, 10]. In order to avoid or ameliorate these consequences, clinical interventions are required to control the recognized alterations in foot biomechanics [11-13].

Foot orthoses (FOs) are one of the most common interventions to restore normal foot mechanics and release additional stress in flatfoot individuals [10]. FOs can be either prefabricated or customized. While prefabricated FOs are general medical devices and accessible to people with different foot types, customized FOs are administered to each individual foot based on their biomechanical demands and symptoms [12, 14]. Therefore, customized FOs are more likely to direct the treatment plans and attain higher levels of quality and satisfaction [6, 10]. The introduction of computer aided technologies such as 3D scanning, computer aided design, and 3D printing to the fabrication process of FOs have facilitated the integration of more details within the FO design and subsequently the region-dependent control of foot motion [15]. The process of delivering customized FOs starts with foot assessment by a clinical practitioner and obtaining the shape of its plantar surface. Then, the geometry of the foot is modified by identifying the potential structural and functional deficits contributing to the outbreak of symptoms. Finally, the FOs are developed and fabricated by implementing the design features that are thought to selectively modify the identified deficits [13, 16]. Certain levels of variation exist in each of these steps due

to the foot complexity as well as the different training and experience of clinical practitioners. For example, there are different tools to assess the foot and different approaches to identify foot type [17-19]. Defining the foot type can be in a static or a dynamic posture and be based on foot motion or plantar loading. Furthermore, the foot shape can be obtained using different techniques such as casts, foam boxes or 3D scanners, in non-weight bearing or semi-weight bearing positions [20]. Finally, considerable variation exists on the approach that foot motion and function are modified between clinicians leading to the large variation in FO design and material [12, 21]. The most reported differences in the designs of FOs for flatfoot individuals are the placement and the level of posting and supports as well as the rigidity of FOs [22]. This high variation in the FO design shows that no consensus still exists between clinicians, which is a consequence of uncertainty and controversy in the available knowledge [13, 22, 23]. In order to overcome this uncertainty and enhance our knowledge in this field, it is primarily required to measure the biomechanical outcomes from these orthoses.

Depending on the design and rigidity of FOs, the response of flatfoot individuals to this intervention tool might vary. When it comes to similar designs of FOs, it is expected to see consistent outcome measures between included participants and between studies. However, this prospect has not been met in the available literature. For example, the efficiency of medial rearfoot posting to decrease the excessive rearfoot eversion in flatfoot individuals has been either confirmed [24-26] or rejected [27, 28] in previous studies. The same controversy exists for the applicability of neutral rearfoot posting to control foot pronation [26, 29]. Regarding the arch-supported FOs, even single studies could not find any evidence of efficiency to modify the subtalar joint orientation and support the medial longitudinal arch [30, 31]. Different rigidities of FOs were found to have similar impacts on supporting the medial longitudinal arch by Balsdon, et al. [32], while higher efficiency of hard insoles to support the medial longitudinal arch compared to soft insoles accompanied by higher plantar pressure was indicated by Su, et al. [33]. The source of these inconsistencies should be differences in the structural and functional characteristics of the foot between individuals. As the foot and FO are in direct contact during dynamic activities, any changes in the characteristics of one component might emerge as a different response from the other component. Limited evidence exists on the dependency between the characteristics of feet and FOs in a predictable manner. An assessment of the dose-response effect of customized contoured FOs with different levels of postings in flatfoot individuals showed a linear relationship between the levels of posting and

changes in rearfoot eversion [26]. In fact, each 2° of increase in the level of medial posting was associated with a mean reduction of 0.28° in rearfoot eversion [26]. In addition, a dose-response effect of customized FOs with different levels of heel support, ranging from 0 mm to 6 mm, on plantar pressure distribution was investigated in flatfoot individuals, but no systematic relationship between plantar pressure and the level of heel support was achieved [34]. Although these studies provide useful insights on the association between FO design in overall and foot characteristics, the interaction between regional behaviour of FO and foot motion might vary depending on the contour and rigidity of the region. This unknown aspect is important to be evaluated since customized FOs can entail different design features over their plantar surface.

Based on these issues, **the general objective of this thesis was to estimate the relationship between region-dependent behaviour of FOs and the biomechanical characteristics of flatfoot individuals during walking.** This objective was designated to respond to some of the ambiguous points in the process of treating flatfoot individuals as illustrated in Figure 1. Although this treatment process looks straightforward at first glance, it contains considerable uncertainties for clinicians due to a lack of a single algorithm for FO prescription. Following the assessment of flatfoot individuals, the primary option coming to the mind of the clinical practitioner is prescribing FOs. Based on their training and experience, all clinicians could fulfil the goal of delivering FOs to the patients. However, they still hold the questions of whether they have chosen the best material and design of FO, and whether their prescription could enhance the foot motion and function of patients to relieve their symptoms [21]. They are not sure "what is the best orthotic practice" to treat each patient due to the complexity and variations in the individuals' feet. To help clinicians to standardize the execution of their training into actual practice and introduce guidelines to the adoption of technology within FO designs, three steps were pursued in this thesis. We primarily sought to gain insights on the effect of different designs of FOs on foot function. Then, we focused on quantifying the deformation of customized FOs during dynamic activities. The predicted deformation was a continuous variable over time and the plantar surface of FO which could identify the region-dependent mechanical behaviour of FOs. Quantification of FO deformation enabled us to find the linkage between foot biomechanics and regional behaviour of FO over different phases of the gait cycle.

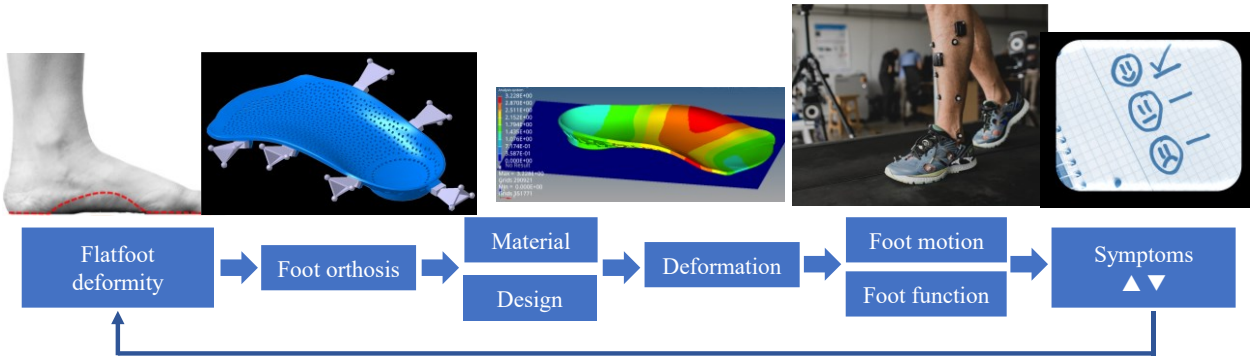

Figure 1: Schematic illustration of general problem and objective of this thesis.

Detailed structure of the thesis

In order to address the thesis objective, this report is structured as follows:

Chapter 1 is dedicated to the review of relevant scientific literature. In this chapter, the general concepts of foot anatomy and physiology, different techniques for assessing and quantifying flatfoot deformity, as well as the fabrication process of FOs were shortly reviewed. Then, the techniques to quantify FOs and foot biomechanics in accompany with their application in flatfoot individuals were summarized. Finally, the available knowledge on the interaction between foot and FOs were overviewed, and the specific objectives of this work were identified.

The heart of this thesis lies in three studies which constitute the three subsequent chapters. In the first study (**Chapter 2**), a systematic review was conducted to comprehensively compare the effect of different designs of FOs on the kinematics and kinetics of the lower body. In addition, the level of evidence in the available literature and guidelines for standardizing the methodological approaches was extracted. In the second study (**Chapter 3**), we sought to predict foot orthosis deformation during walking using an artificial neural network. This variable was relevant to deepen our knowledge on time-dependent and region-dependent behaviour of customized FOs. In the third study (**Chapter 4**), we investigated the relationship between foot biomechanics and FO behaviour during walking. We were interested to formulate the region-dependent FO deformation as a function of the most correlated variables of foot biomechanics. These relationships could establish preliminary guidelines to be practiced in clinics and industry with the purpose of standardizing and optimizing FO designs.

Finally, **Chapter 5** discusses the key findings of all three studies in addition to highlighting their limitations and directions for future research and practice. To close this thesis, a general conclusion was added to summarize the main points addressed in this thesis.

Chapter 1 - Literature Review

1.1. Anatomy and physiology of the foot

The foot is a complex structure consisting of 26 bones, 33 joints, muscles, tendons, ligaments, and a network of blood vessels and nerves, surrounded by other soft tissues and skin [35]. These components work together to provide stability, body weight support, and mobility. Understanding foot anatomy and physiology will help to reach a better understanding of the mechanisms underlying foot motion and loading. In this section, common terms for addressing relative positions and orientations will be primarily introduced. Then, the anatomy of the foot as well as the mechanisms of foot function will be shortly overviewed.

1.1.1. Common terms to address the position and motion of the foot

In order to address the anatomical and biomechanical features of the foot, it is important to refer to standard agreements on the directions and planes of movement. The *medial* side is referred to the inner side or bigger toe, while the outer side or the side of the fifth toe is called *lateral*. Furthermore, the front side is named as *anterior*, where the rear side as *posterior*. To describe the foot function, three cardinal planes are additionally defined as sagittal, frontal, and transverse (Figure 1.1). Movement of the foot occurring in the sagittal plane is labeled as plantarflexion/dorsiflexion, in the frontal plane as eversion/inversion, and in the transverse plane as abduction/adduction [20].

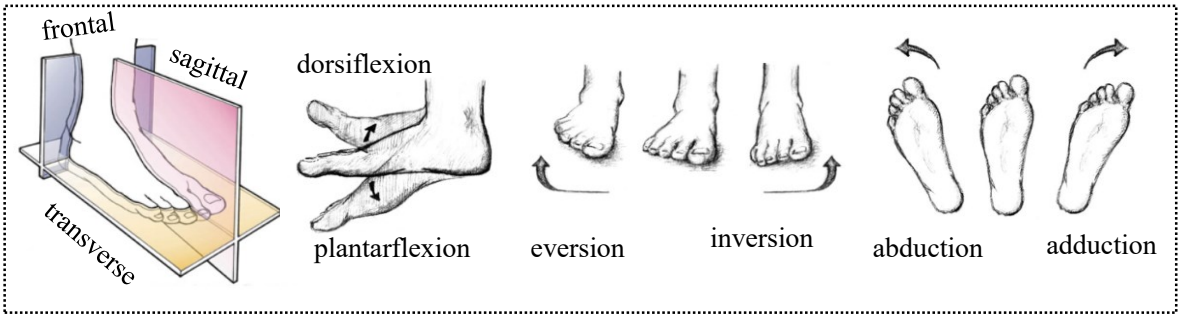

Figure 1.1: Foot anatomical planes and corresponding motions of foot. Image reprinted from https://www.footmaxx.com/component/content/article?id=98:basic-anatomical-concepts&catid=24&Itemid=1730.

1.1.2. Foot bones

In order to simplify the complex bony structure of the foot, especially for biomechanical studies, including this thesis, three main segments have been defined for foot bones based on their location and function: rearfoot, midfoot, and forefoot (Figure 1.2).

The rearfoot is made up of the calcaneus which is the largest and most posterior bone in the foot and the talus which is anterior to the calcaneus. Calcaneus can bear high tensile, compressive and bending forces thanks to its structure. It also provides a lever arm for the insertion of the Achilles tendon, which contributes to plantarflexion. The structure of the talus enables it to transmit the reaction forces from foot to ankle and leg [35, 36].

The midfoot is anterior to the rearfoot and is composed of the navicular, cuboid and the three cuneiform bones [20]. Navicular is proximally articulated with the talus and distally with the three cuneiforms. Navicular is counted as a key component in the structure of the medial longitudinal arch. The cuboid articulates proximally with the calcaneus, distally with fourth and fifth metatarsals, and medially with the lateral cuneiform. The cuneiforms articulate with first to third metatarsals and form the structure of the transverse arch.

The forefoot is anterior to the midfoot and is composed of five metatarsals and fourteen phalanges [20]. The metatarsals articulate distally with phalanges. The first metatarsal articulates with two sesamoids. The second metatarsal is locked in place because it is surrounded by the apexes of the medial and lateral cuneiforms and articulated with the intermediate cuneiform. The peroneus brevis tendon and plantar fascia are attached to the proximal surface of the fifth metatarsal.

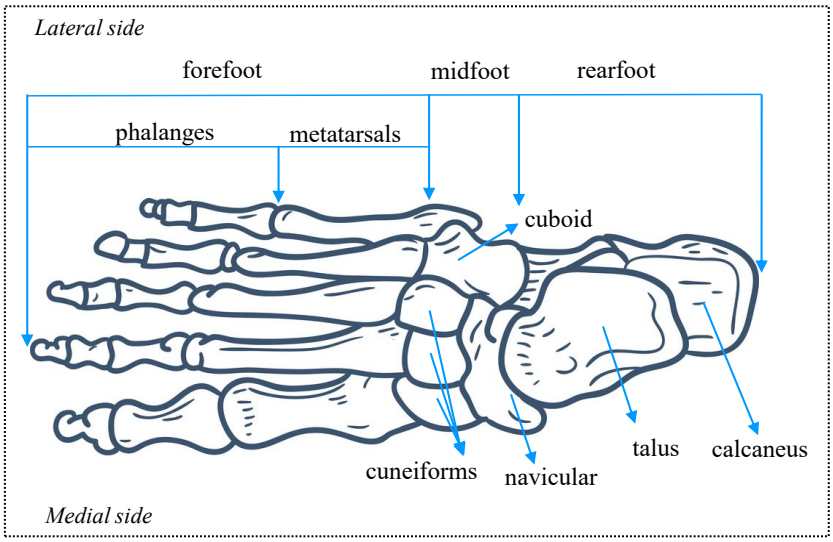

Figure 1.2: A transverse view of the 26 bones of the foot and their division into rearfoot, midfoot, and forefoot. Foot skeleton reprinted from VectorStock® (VectorStock.com/1851626).

1.1.3. Foot joints

A total of 33 joints exist in the foot, constructed by the connection of two or more bones, to provide mechanical support and facilitate foot dynamics [35]. The ankle joint is a synovial hinge joint, generated by talus, tibia, and fibula, and enables plantarflexion/dorsiflexion [35, 36]. The medial and lateral ligaments are responsible to provide medial and lateral joint stability during dynamic activities [35]. Intertarsal joints, including the subtalar (talocalcaneal) joint and transverse tarsal joint (talonavicular and calcaneocuboid joints), are constructed by tarsal bones. These joints are mainly responsible for eversion/inversion and pronation/supination. In fact, the oval shape of the articular surfaces and oblique orientation of the subtalar joint facilitates the coupled movement of pronation/supination (Figure 1.3). This feature also enables the joint to convert the rotation of the vertical axis to the rotation of the horizontal axis [36]. Ankle joint together with subtalar joint are responsible for the ankle dorsiflexion, tibia internal rotation, and calcaneus eversion at the early stance, while the movement shifts to ankle plantarflexion, external tibia rotation, and calcaneus inversion during late stance [36]. Transverse tarsal joints help the motion at the midfoot level and enable the transition from a flexible to a rigid structure during gait. In fact, talonavicular joint and calcaneocuboid joints are parallel during calcaneus eversion and non-parallel during inversion. When they are parallel, they provide flexibility and absorb shock. When the joints diverge and become non-parallel, it helps the foot to provide a rigid lever and the Achilles tendon can act to

push-off [37]. The naviculocuneiform, naviculocuboid, and intercuneiform joints construct the midfoot arch and are relatively rigid. Their cumulative motion, however, helps to flatten or elevate the transverse arch with rearfoot eversion/inversion. Tarsometatarsal joints have limited movements [36]. However, the metatarsophalangeal joint can facilitate gliding as well as eversion/inversion and pronation/supination rotations. Interphalangeal joint additionally articulate phalanges with each other and has flexion/extension motion [35].

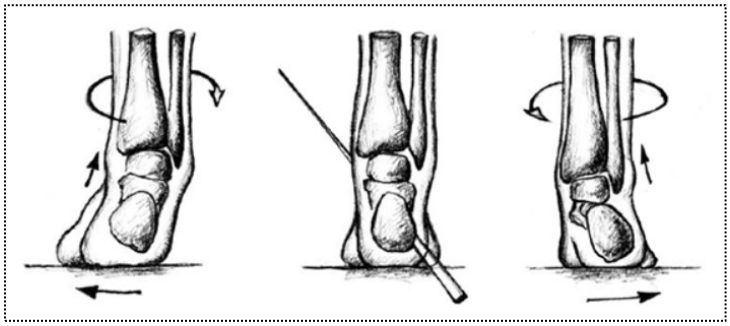

Figure 1.3: Subtalar joint axis in neutral (center), supination (left) and pronation (right) positions. Image Reprinted from https://www.footmaxx.com/invest/basic-biomechanics.

1.1.4. Foot arches

In addition to defining the foot regions based on the position of bones, the foot can also be divided based on its three linked arches: *medial* longitudinal arch, *lateral* longitudinal arch, and *transverse* arch (Figure 1.4). Any abnormal function of one of these arches would affect the function of the other two arches [38]. The medial longitudinal arch is made up of calcaneum, talus, navicular, cuneiform, and the first, second and third metatarsals. It is higher and more flexible compared to the lateral longitudinal arch. The structure of the medial arch enables it to vary in shape and configuration during dynamic activities [8, 38]. The lateral longitudinal arch, which is made up of the calcaneum, the cuboid bone and the fourth and fifth metatarsals, has a rigid structure and helps to support the body weight [38]. The transverse arch consists of metatarsal bases and the cuneiform and cuboid bones [8]. The arches of the foot are responsible for shock absorption and storing mechanical energy for more efficiency and less joint loads [39]. They also prevent the compression on plantar regions where muscles and nerves are located [20]. Individuals with flatfoot deformity, which are the target population of this thesis, exhibit a partial or complete collapse of the medial longitudinal arch during weight-bearing, which could lead to muscle fatigue, pain and further

injuries [1]. Foot orthoses are commonly suggested to this group of patients to support the medial longitudinal arch and improve the abnormal foot posture and loading [12, 13]. Therefore, reaching a good knowledge of the anatomy of the medial longitudinal arch and the underlying mechanisms of its function will be useful to assess the efficiency of customized foot orthoses or presenting guidelines to optimize their design.

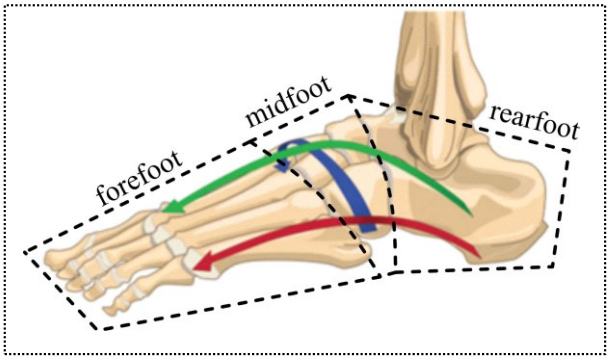

Figure 1.4: Illustration of the three foot segments (rearfoot, midfoot and forefoot), and three intersecting arches of the foot (the medial longitudinal arch in green, the lateral longitudinal arch in red, and the transverse arch in blue). Reprinted from Flores, et al. [8]; Copyright (2020), with permission from Radiographic Society of North America (RSNA®).

1.1.5. Foot muscles and ligaments

Foot muscles can be divided into extrinsic or intrinsic muscles. The origin of extrinsic muscles are the compartments of the leg, and they mainly contribute to foot rotations such as plantarflexion/dorsiflexion and eversion/inversion. On the other hand, the origin and insertion of intrinsic muscles are in the foot and can be found in two layers on the dorsal foot surface and in four layers on the plantar foot surface [40, 41]. The activation of plantar intrinsic muscles is usually simultaneous so that they are considered as a functional unit [41]. They might help extrinsic muscles in their actions. They also increase the foot capacity to adapt to the variation of external loading, so that an efficient transition of loading between foot and ground is reached during walking [40]. In addition, a total of 30 ligaments exist in the foot. Plantar ligaments are stronger than dorsal ligaments since they are under more functional demands, such as the tension to hold talonavicular joint and their contribution to lock the midfoot [36].

1.1.6. Mechanisms of foot function

The complexity of the musculoskeletal system of the foot is in accordance with the complexity of the underlying mechanisms that govern foot motion. The foot should be flexible during weight acceptance to adapt to the terrain, support body weight at midstance, then provide a rigid lever arm for propulsion [42]. The most popular mechanisms to explain the transition of the foot from flexible to the rigid structure during gait can be mentioned as the windlass mechanism [43] and midtarsal locking mechanism [37].

Windlass mechanism: This mechanism assumes that a triangular arch form can be arranged by the bones and ligaments of the foot. This triangle, in fact, consists of the midtarsal joint and metatarsophalangeal joint, and plantar fascia stretching from the calcaneus to proximal phalanges of toes as the triangle base [44, 45]. The dorsiflexion of hallux winds the plantar fascia around the metatarsal heads and makes it tight. This will consequently elevate the arch, which is ideal for absorbing the shock of body weight during early stance (Figure 1.5). From early stance to midstance, the plantar fascia stretches, and the arch flattens under body weight [44]. This will help the foot to organize and distribute the load on foot regions. After midstance, when the foot prepares to lift off the ground, the heel lift makes the toes dorsiflex. The plantar fascia will subsequently be tightened, and arrange the foot as a rigid lever to successfully provide the propulsion phase [45].

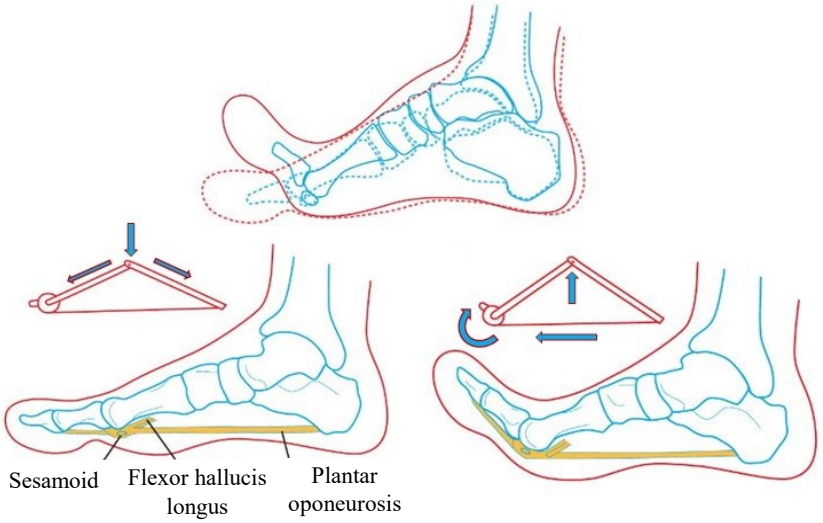

Figure 1.5: Windlass mechanism describing the functional behaviour of the arch through the rigidity of arch spanning tissues. The inactive windlass during lengthening of the arch at midstance is followed by metatarsophalangeal dorsiflexion and active windlass. ©Docpods.

Midtarsal joint locking mechanism: In this theory, the changes in foot shape from mobile structure to the rigid lever is referred to the shape of tarsal bones and changes in their axes [46]. As mentioned, the midtarsal joint reflects the movement between rearfoot and midfoot and is a combined articulation of talonavicular and calcaneocuboid joints. Tweed, et al. [47] reported that the convex curvature axes of these articulated joints changes by the inversion or eversion of the subtalar joint, leading to lock or unlock the midtarsal joint and subsequently resulting in rigid or flexible foot structure. In fact, the non-synchronous movement of talonavicular and calcaneocuboid joint axes might explain this changeover from flexible to rigid [48].

Summary: The complexity of foot structure enables it to satisfy the multiple biomechanical demands during dynamic activities such as walking. During the early stance, the parallel structure of midtarsal joints and the flexible arch enable the foot to act as a mobile adapter for weight-bearing and shock absorption. In midstance, the tension of plantar ligaments holds the talonavicular joint, and the foot reaches its minimum height relative to its interaction surface to distribute the pressure over the foot plantar surface. During push-off, the midtarsal joints become non-parallel, and the medial arch recoils, letting the foot act as a rigid lever for efficient propulsion. Malfunctioning or failure of any of these components can lead to foot injuries and pain or even affect the function of other body joints. Therefore, it is important to understand the foot anatomy and physiology in order to reach a deeper understanding of its biomechanical function and the requirements for designing customized foot orthoses.

1.2. Flatfoot deformity

Abnormal foot structure can make the foot prone to pain and injury during dynamic activities [49]. To simplify the anatomical complexities of the foot for clinical applications, the feet are categorized into three types based on their structure and the orientation of bones. The feet with low medial arch, everted rearfoot, and/or abducted forefoot are classified as planus, well aligned feet in rearfoot and forefoot as rectus, and high arched feet with inverted rearfoot and/or adducted forefoot are classified as cavus. The over-pronation in planus feet (flatfeet) results in the medial displacement of ground reaction force during the stance phase of the gait, while the over-supination in cavus leads to a lateral displacement of the ground reaction force [50].

According to previous studies, the prevalence of flatfeet is reported to be around 20-25% in the general population [51, 52]. Flatfeet are the leading cause of visits for pediatric foot problems [4]. The prevalence appears to be higher in females [51], individuals with high body mass index [53], and individuals with larger foot sizes [51]. Most children are born with flatfeet, and a normal foot arch develops spontaneously during the first 10 years of life. The flatfoot can be congenital or acquired [54, 55], rigid or flexible, adult or pediatric, idiopathic (*i.e.* of unknown cause), or neurological as in patients with cerebral palsy [56]. Developmental flatfoot normally occurs in toddlers and occasionally persists into adulthood without symptoms [8].

A variety of measures exist to quantify foot type based on foot morphology including visual inspection, anthropometric measures, footprint evaluations, radiographic techniques and dynamic laboratory analyses [57]. In clinical practice, some of these measures have gained more popularity due to their reliability and lower cost, namely foot posture index, arch height index, and arch height flexibility. These clinical measures classify the foot type based on foot function (over-pronation, normal, over-supination), foot structure (high arch, normal arch, low arch), and arch flexibility (reduced, normal, excessive), respectively [58]. In this section, different measures to classify foot types will be presented.

1.2.1. Visual inspection

Visual assessment is a simple method in clinical practice to examine the alignment of the foot and look for the presence of any problems, which can be the inspections from front, sides and back, during weight-bearing or non-weight bearing, or in static posture *versus* walking [49]. Dahle, et al. [59] investigated the inter-rater reliability of classifying foot types into three groups of pronated, supinated and neutral using visual inspection, and found a 73.3% agreement between the examiners. Foot posture index (FPI) is one of the popular measures in this category, which has been reported as an accurate and reliable method of classifying foot types [57].

Foot Posture Index: Redmond, et al. [57] designed the six-item Foot Posture Index (FPI-6) to overcome the cost and time issues. FPI-6 is a simple method giving an indication of the overall foot posture across the three planes of the foot (sagittal, frontal, transverse) and anatomical segments (rearfoot/midfoot/forefoot). A static bipedal position is used for this clinical test, where the participant is blinded to the measurement to avoid alterations in foot posture. Double limb

support position could reflect the foot function better than non-weight-bearing measures, and represents an approximation of foot function during the gait cycle [57].

The evaluation of FPI-6 includes a series of six observations achieved by a clinician, and each measurement is scored from -2 to 2. These items include [60] : (1) talar head palpation, (2) curves above and below the lateral malleolus, (3) inversion/eversion of the calcaneus, (4) prominence in the region of the talonavicular joint, (5) congruence of the medial longitudinal arch, and (6) adduction/abduction of the forefoot relative to the rearfoot (Figure 1.6). Characteristics corresponding to a neutral foot posture are scored as zero, while pronation postures deliver positive values and supination characteristics negative values. Foot type would then be specified based on the raw scores as strong supination [-5 to -12], supination [-4 to -1], normal position [0 to 5], pronation [6 to 9] and strong pronation [10 to 12] [57]. Being able to fit the individuals' feet into five categories would handle a reasonable compromise between sensitivity, reliability and ease of use [61]. FPI-6 was used in this thesis to differentiate between the recruited flatfoot individuals.

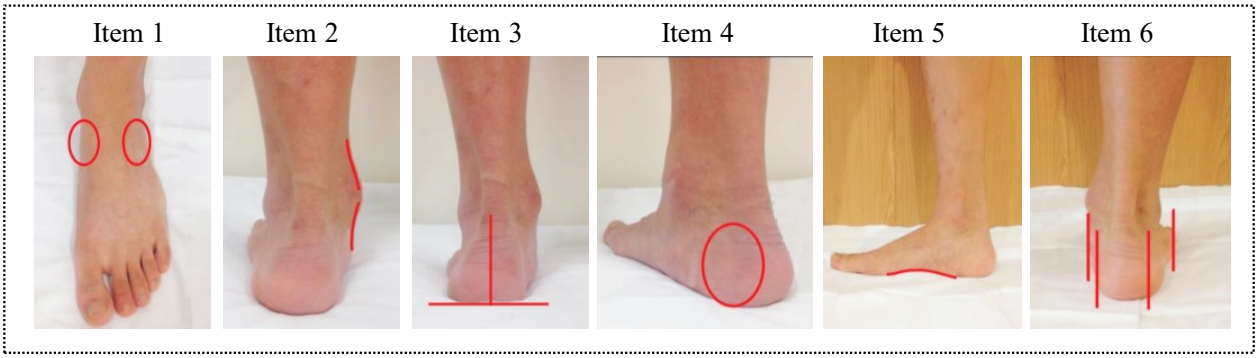

Figure 1.6: The six items of the foot posture index. Item 1: talar head palpation, Item 2: supra & infra lateral malleolar curve, Item 3: inversion/eversion of the calcaneus, Item 4: bulging in the talonavicular joint, Item 5: congruence of the medial longitudinal arch, Item 6: adduction/abduction of the forefoot. Published by Lee, et al. [62]; Copyright (2020) with permission from the Korean Academy of Rehabilitation Medicine.

1.2.2. Anthropometric measures

The characterization of foot type can be performed by anthropometric approaches, which are based on the direct measurements of bony landmarks that represent important foot structures such as the medial arch or rearfoot orientation. A summary of some popular anthropometrical measures is provided in this section.

Longitudinal arch angle: This angle is formed by two lines connecting the medial malleolus to the navicular tuberosity, and from there to the first metatarsal head [63]. This parameter has been measured in either static posture [64] or during walking [65] to classify the individuals into three groups of low, normal, and high arched feet. The intratester and inter-tester reliabilities were reported as 0.90 and 0.81 for measuring longitudinal arch angle in static posture [64].

Rearfoot angle: This angle is measured between a longitudinal line on the calcaneus and a line on the distal one-third of the lower leg. The rearfoot angle can be measured in static posture using goniometers, or by inserting four markers to represent these lines during dynamic activities. This measure has been suggested to provide information about subtalar joint motion [64]. However, rearfoot angle in static posture has been reported to be poorly correlated with the dynamic rearfoot orientation [66]. Therefore, the rearfoot angle in static posture was not used to assess the functionality of FOs in this study.

Navicular drop: This parameter is measured as the excursion of the navicular bone in the sagittal plane, by subtracting the height of navicular tuberosity in non-weight bearing position from 50% weight-bearing position [67]. The navicular drop could reflect the excessive pronation due to the insufficient support of the medial longitudinal arch. Moderate intertester and intratester reliability have been reported for this technique [68]. Arch height index, which represents a similar concept to navicular drop, and has been validated with radiographic images [19], was measured in this study during the assessment of feet by podiatrists.

Arch Height Index (AHI): The height of the medial arch is an important variable that can quantify foot structure [69]. Williams and McClay [19] introduced the arch height index (AHI) as the ratio of medial arch height of the foot normalized by the truncated foot length, in both sitting and standing positions (Figure 1.7). For this test, arch height (AH) is measured from the floor to the dorsal surface of the foot at half of the total foot length. In addition, truncated foot length is the distance from the posterior heel to the first metatarsal head, measured along the medial border of the foot. This tool is used to classify the feet as planus, rectus or cavus [70]. This index has been shown to be reliable and an accurate measure [19, 71] and was validated by equivalent radiographic measurements [19]. Arch height flexibility is a good complement for AHI to classify foot structure [69].

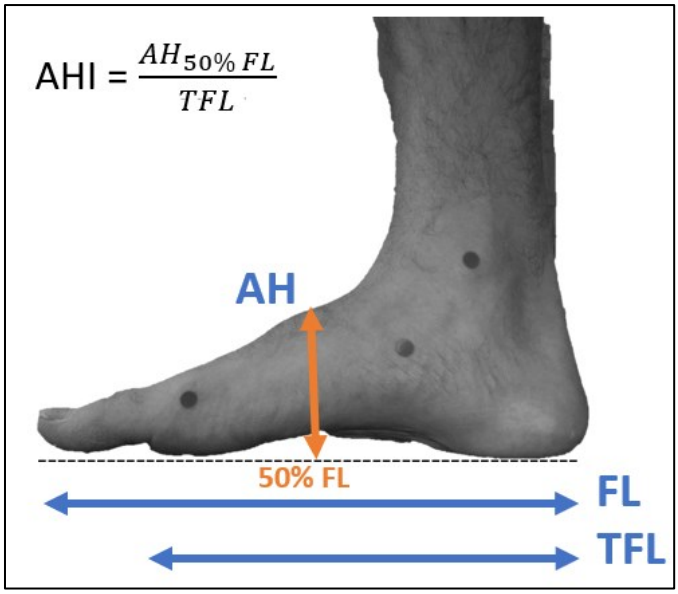

Figure 1.7: Depiction of measurements taken for arch height index (AHI) calculation. AH indicates arch height at half resting foot length; FL, foot length; and TFL, truncated foot length.

Arch Height Flexibility (AHF): In addition to foot structure and function, studies have suggested that foot flexibility plays an important role in foot biomechanics and allows for an adapted treatment [17, 58]. Arch height flexibility (AHF) is a measure for categorizing the foot type from very stiff to very flexible based on reduced, normal or excessive flexibility. AHF is calculated as the variation in arch height between sitting and standing positions, normalized to the variation in foot loading, *i.e.* AHF= $\frac{AH_{sitting} - AH_{standing}}{0.4 \times body\ weight} \times 100\ [mm/N]$. Arch height is measured in a similar way to arch height index. The change in load is based on an assumed change in body weight from sitting to standing, which is equal to 40% of body weight. In fact, the load on the foot is assumed to be equal to 50% of the body weight in standing position, and 10% of the body weight in sitting position [69]. Zifchock, et al. [69] used a large dataset including 1056 feet to classify them based on the arch height flexibility. Five categories were finally defined as very stiff [AHF<9.91], stiff [9.91≤AHF<13.54], neutral [13.54≤AHF<16.00], flexible [16.00≤AHF<20.54], and very flexible [AHF≥20.54] with values expressed in mm/N. Thanks to AHF, subjects with flatfoot deformity can be discriminated based on the medial arch function, and the designs of customized FOs were mainly adjusted based on AHF and body mass index in this project.

1.2.3. Footprint evaluations

Imprints of foot provided by ink pads or pressure transducers can also be used for foot classification. This technique is based on the fact that alteration in the structure and orientation of feet would be reflected in the footprints. In this section, three measures calculated from footprints will be presented.

Arch index: This index is calculated as the ratio between the areas of different regions of toeless footprint [72] defined in the following sentences. Four lines are used to create these regions: the first line connects the center of the heel to the tip of the second toe, another line is created at the most anterior point of footprint and perpendicular to the first line; then two other lines would be drawn parallel to the anterior line to divide the foot length to three equal parts. The arch index is then calculated as the ratio of the area in the middle one-third footprint region to the entire area (Figure 1.8-a). This method has been reported to be inefficient to explain the dynamic between-individual variations [73].

Arch angle: This measure is defined as the angle between a line that connects the most medial part of the heel to the most medial part of the metatarsal and a second line that connects the most medial part of the metatarsal to the point where the shape of medial arch segment firstly touches the metatarsal outline of the arch (Figure 1.8-b) [35].

Footprint index: It is defined as the ratio of the non-contact to the contact areas of the toeless footprint (Figure 1.8-c). The non-contact area is calculated from the region located between the medial border of footprint and medial footprint contour [74].

Although footprint evaluations could provide useful information about the arch structure, they were not used to differentiate between flatfoot individuals in this study. However, the foot plantar pressure was recorded during walking with customized FOs and was analyzed to represent the dynamic loading of the foot over the gait cycle.

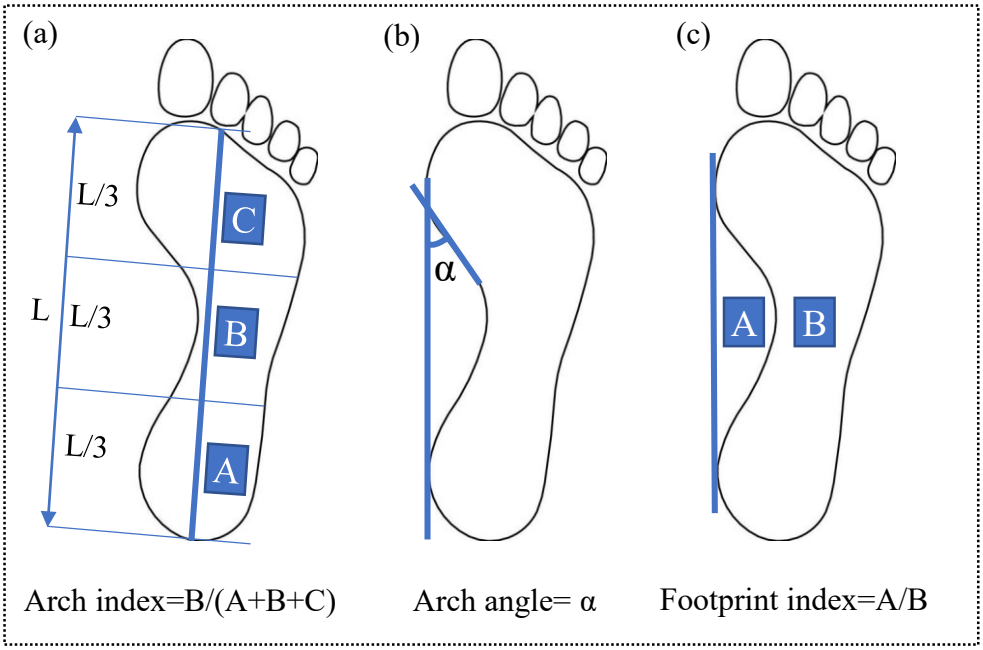

Figure 1.8: Graphical view of footprint parameters: (a) Arch index, (b) Arch angle, (c) Footprint index.

1.2.4. Radiographic techniques

Radiographs taken from the standing weight-bearing position of individuals can be used to extract different characteristics of the foot, such as the medial longitudinal arch. From a lateral radiograph, calcaneal inclination angle can be defined as the angle between a line tangent to the inferior surface of the calcaneus and a line tangent to the foot interaction surface (CAI in Figure 1.9). The ratio between height to length can also be calculated, where the height is the distance from the platform to the inferior surface of the talar head, and the length is the distance between the posterior surface of the calcaneus to the anterior surface of the first metatarsal head (H/L in Figure 1.9) [75]. In addition, the calcaneal- first metatarsal angle can be estimated by a line tangent to the inferior surface of the calcaneus and a line along the dorsal surface of the first metatarsal (CA-MT1 in Figure 1.9) [76]. Depending on the purpose of the study and the population that is targeted, several other measures can be calculated from radiograph images. Videofluoroscopy measurements have been also employed recently to determine the foot function during dynamic activities such as walking [77, 78]. Both radiographic and videofluoroscopy measurements have high reliability but are expensive and expose the patients to radiation [49]. They can be used as beneficial tools for

validating the clinical measurements [49]. Radiographic techniques were not used in this study due to their high cost and radiation exposure.

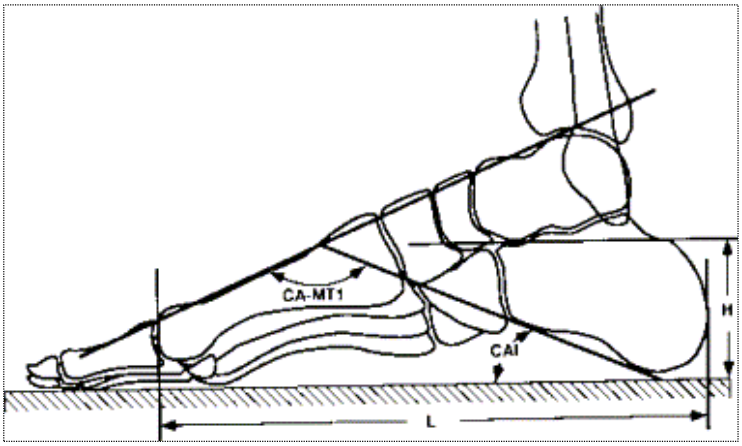

Figure 1.9: Radiographic parameters defining the medial longitudinal arch of the foot, measured on a standing lateral x-ray. Abbreviations: CA-MT1, Calcaneal-first metatarsal angle; CAI, calcaneal inclination; H, arch height; L, arch length. Reprinted from Saltzman, et al. [79]; Copyright (2020) with permission from Elsevier Inc.

1.2.5. Dynamic laboratory analyses

The dynamics of the foot can be recorded and processed in gait labs equipped with optoelectronic motion analysis systems, force plates, and plantar pressure systems. The optoelectronic cameras can provide accurate data on foot kinematics, the force plates reflect the ground reaction forces and center of pressure, and plantar pressure systems can estimate the distribution of plantar pressure at each moment of dynamic activities. In this study, multi-segment foot kinematics and plantar pressure distribution were used to characterize the foot biomechanics of individuals with flatfoot deformity during walking.

Summary: Several techniques exist to determine foot characteristics and classify the foot type. While the radiographic measures provide more accurate and reliable results which have a high correlation with injury, they are expensive and expose the patients to radiation. In addition, the dynamic laboratory analysis could reflect the dynamic foot characteristics, but they are time-consuming and expensive to be used during daily practice for clinicians. Visual techniques, anthropometric measures, and footprint indices can be used as alternative techniques with an acceptable level of reliability and repeatability to recognize and differentiate between foot types.

1.3. Foot orthosis

Foot orthoses (FOs) are used as functional devices to modify abnormal foot motion, help to redistribute plantar pressure, and prevent pain and further injuries [14, 16, 28]. FOs can fall into three categories: *prefabricated* FOs which have generic contours and are available over the counter in shoe stores and pharmacies, *semi-customized* FOs which are fabricated from a mold-of-best-fit chosen from a library of template orthotic shapes and can be later heated to modify their shapes based on individual needs, and the *customized* FOs which are specifically manually made (traditional methods) or CAD/CAM designed (modern methods) based on the cast or foot scan of each individual. Some negative points of *prefabricated* FOs can be listed as (1) low arch profile which cannot sufficiently control rearfoot motion and support medial longitudinal arch; (2) little or no heel cup which leads to a lack of control of heel motion; (3) soft materials on the medial arch which cannot resist against the downward motion of the arch; (4) the possibility of losing their shape over time, making them inefficient to control rearfoot motion; (5) the top cover of FO which might get loose or tear, and could be followed by skin irritation as well as reducing the level of comfort; (6) limited sizes ranges, which can be accompanied by poor fit inside the shoes. Semi-customized FOs are usually developed for the purpose of lower cost compared to customized FOs and mass production, and are, in fact, a compromise between cost, fit, and function [28, 80]. Semi-customized and customized FOs are capable to overcome the issues of prefabricated insoles, but no broad consensus exists on how these FOs should be prescribed and controversial arguments still remain on their functionality [12]. All these issues emphasize the necessity of conducting more research in this area. In this section, the clinical theories to explain the therapeutic effect of FOs will be firstly reviewed [81]. These theories could help us to realize and remove the obstacles that are present in current designs. Then, the existing approaches to fabricate FOs and available designs will be summarized, since the biomechanical effect of FOs is changed based on their fabrication technique, design, and material properties [82-84].

1.3.1. Foot orthosis theories

Different clinical and biomechanical theories exist to explain the therapeutic mechanism that FOs exert. All these theories have been established based on foot structure or foot function. However, no single theory has been yet introduced to explain the therapeutic mechanism, which might be due

to the variation that exists between the individuals' feet. Three main podiatric theories are summarized in this section.

Foot morphology theory: In this theory, known as the "Root model" [85-87], foot morphology is referred to as subtalar joint neutral position during non-weight bearing stance phase [88]. Through the prescription protocol, a cast of the foot is prepared in subtalar joint neutral position with correct rearfoot to forefoot alignment [88]. The neutral position of the subtalar joint has been regarded as an important parameter, since it is supposed to minimize stress on the surrounding joints and ligaments, provide an efficient position for muscle function and reduce the impact force at initial foot contact, and represent a point where the foot shifts from a mobile adaptor to rigid lever [89]. An intrinsically forefoot/rearfoot posting is added to the cast to place the heel bisection in the required position. The degree of posting is calculated based on the patient's neutral calcaneal stance position in order to have a normal amount of pronation. The amount of normal pronation is estimated based on the height of the subtalar joint axis [88, 90].

Sagittal plane facilitation theory: This theory, firstly developed by Dananberg [91], considers the foot as a pivot rocking forward from heel to toe. This movement enables the hip extension which then provides gait propulsion. Therefore, any kind of pathology which limits the foot range of motion in the sagittal plane would lead to an inadequate hip extension to provide normal propulsion and stride [92-94]. Any kind of posting or material modifications in FO would be based on trial and error observations using video gait analysis and in-shoe pressure systems [93, 95]. Although this theory is based on foot dynamics, the actual prescription methods are sparsely documented [88]. This makes it difficult for clinicians to find a link between deformities of the foot and sagittal plane theory prescription methodology.

Tissue stress theory: This theory, developed by Kirby [96], works based on the assessment and modification of the moments across the subtalar joint in order to reduce the stress on anatomical structures. A medial/lateral deviation on the center of pressure is modulated by a posting to generate opposing moments (pronation/supination) and provide rotational equilibrium for foot motion. The prescription of FO is based on symptom reduction by applying proper moments to the subtalar joint and decreasing the abnormal forces on injured structures [88, 96]. Similar to sagittal plane theory, no prescription protocol exist for producing FOs based on this theory [88].

Although the aforementioned theories seem diverse at first glance, they have shown some common outcomes for treatment [88]. These theories are then integrated within the fabricate process, detailed in the following section, for extracting the foot geometry and subsequently developing FO geometry. Foot morphology theory was followed in this thesis for extracting the geometry of customized FOs.

1.3.2. Towards design and fabrication of customized foot orthosis

Customized FOs can be developed by traditional *versus* modern methods. The traditional fabrication needs to be done by an expert prosthetist, while the quality, cost and time to design FO is negatively affected by this fabrication approach. On the other hand, access to technologies such as 3D scanners, CAD/CAM design, and 3D printers have facilitated the modern approach of fabricating FOs. This technique can be more efficient in terms of time and cost, more accurate, and contain more details for subject-specific designs [14]. Both methods follow some common steps for FO fabrication, namely (1) assessment of patients, (2) acquiring the geometry of foot, (3) developing the geometry of FO, (4) fabricating FO, and (5) fitting and adjustment of FO. These steps and the differences between traditional and modern models will be summarized in this section.

Assessment of patients: The patient can be assessed in both non weight-bearing and weight-bearing stance positions as well as walking. Visual assessments of foot and anthropometric measurements will be performed by the clinical practitioners to decide about the required forefoot and rearfoot modifications. In addition, the collapse of the medial arch and other foot deformities will be detected through this examination. In fact, decisions on several characteristics of FO such as design, material, and modifications in FO regions are made in this step [14, 16]. Integrating FO theories (refer to section 1.3.1) into the design of FO is common to control the foot posture or re-distribute plantar pressure [16]. Following the Root model, in which static foot assessment is used to infer foot dynamics, is one of the most popular theories implemented in the traditional approach [87]. On the other hand, advances in technology have made the modern approaches more robust in the reliability of anthropometric measurements, the possibility of capturing the foot motion and pressure during dynamic activities, and integrating the patients' needs into FO design [14]. As shown in research projects, modern approaches may also take advantage of finite element methods to optimize the postural corrections, which yield more repeatable designs and can prevent the

distortion of plantar soft tissues [20]. However, this optimization step will add time and cost to the fabrication process. In this thesis, podiatrists performed some static and dynamic evaluations of individuals with flatfoot deformity, including arch height index and arch height flexibility using arch height measurement system [69], plantar pressure distribution in standing posture and during walking, and visual assessment of walking to decide about the rigidity and design of customized ¾-length FOs in several regions.

Foot geometry extraction: In the traditional approach, the cast of the foot is made in the subtalar joint neutral position as well as neutral ankle position, *i.e.* no plantarflexion nor dorsiflexion (Figure 1.10-a). A positive cast is then constructed by pouring plaster into the negative cats [16]. The foot casts are sometimes replaced by using foam boxes for capturing the geometry. Foam boxes are easier and faster for further processing and were used in this thesis to capture the foot geometry (Figure 1.10-b). In modern approaches, scanners are used to generate the geometrically accurate shape of the foot surface (Figure 1.10-c) [16]. In addition to higher accuracy, the patients would experience more comfort during the prescription process [97].

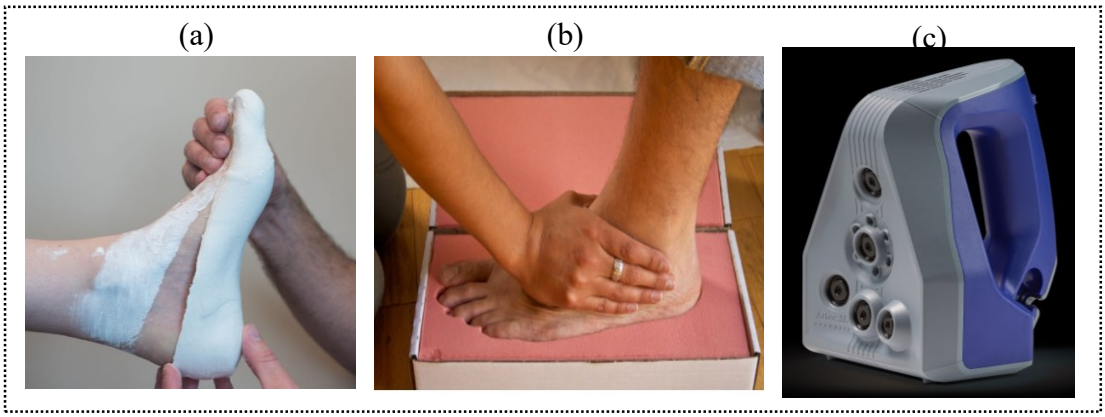

Figure 1.10: (a) Negative cast impression by the direct pressure technique; the foot is maintained in the subtalar neutral position while the plaster hardens, Image reprinted from http://www.fishmanfootcare.com/custom-molded-orthotics/ (b) Negative cast impression using the foam box technique, Image reprinted from http://www.levyandrappel.com/orthotic-products/levy-foam/ (c) Artec MH 3D-scanner (Courtesy of Artec3D Inc., Luxemburg, https://www.artec3d.com/).

Foot orthosis geometry: In the traditional approach, the positive cast of the foot is used to form a mold for developing the FO design. Then, the primary mold is modified by adding or subtracting

plaster to adjust for the modifications of foot posture and pressure which were suggested by the clinician [16, 89]. In the modern approach, the 3D scan of the foot or positive casts are imported into CAD/CAM software to design the customized FOs for each individual. The advantage of using CAD/CAM can be counted as saving time and labor work, adding more precision and accuracy, and the possibility of including the iterative optimization routines for FO design [16, 20]. Some studies exist which used optimization approaches to improve the function of FOs, such as the cushioning properties and pressure distribution in customized diabetic insoles [15, 98]. In addition, the orthosis designs can be archived and reproduced if needed [97]. For the purpose of this thesis, three-quarter length customized contoured FOs were designed based on 3D surface scans of each participant's foot in its neutral subtalar joint position using SpecifX (Shapeshift3D Inc., Montréal, Canada). The rigidity of different regions of FO was adjusted based on the arch height flexibility and body weight.

FOs for individuals with flatfoot deformity are mainly designed with the purpose of reducing excessive rearfoot eversion and forefoot abduction and supporting the medial longitudinal arch [26, 99]. Therefore, the design of customized FOs might not only follow the shape of the foot but also contain some additions on the medial arch, heel, or forefoot to impose motion correction during dynamic activities. The most common additions used for this population can be considered as FOs with medial rearfoot posting, medial forefoot posting, neutral rearfoot posting, and medial arch support (Figure 1.11) [22]. The biomechanical effects of these common designs have been evaluated in previous literature, which will be furtherly discussed in this chapter (section 1.5.4).

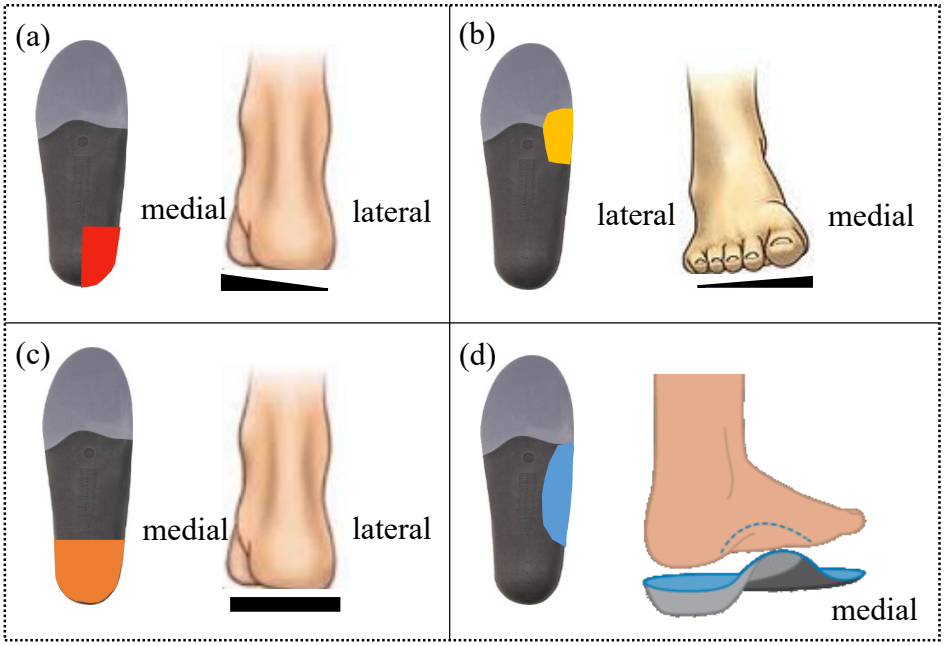

Figure 1.11: Common additions to the design of foot orthoses for individuals with flatfoot deformity, (a) Medial rearfoot posting, (b) Medial forefoot posting, (c) Neutral rearfoot posting, (d) Arch support.

Foot orthosis fabrication: The FO can be fabricated after finalizing the geometry of FO. The plantar surface of FO matches the altered shape of the positive cast. Then, support materials or posting would be added to the base surface to ensure the efficiency of FO on modifying foot posture. In the modern approach, 3D printers can be used to automatically fabricate FOs, which are more efficient in terms of production time and labor work. Less storage space and less equipment for production purposes are other advantages of modern fabrication techniques [97].

A wide variety of materials have been used to fabricate FOs [89, 100]. Primary FOs were originally fabricated using fabric, metal, and leather. However, technological advancement in developing strong and light materials for aerospace and marine industries have made these components available for orthoses manufacturing. The most commonly used materials for orthoses and prostheses can be regarded as leather, metal, wood, thermoplastic materials, foamed plastics, and viscoelastic polymers. These materials could be differentiated based on strength, stiffness, durability, density, and corrosion resistance [101]. The final selection of materials depends on the individuals' needs of each patient and the training and experience of orthotist and prosthetist. The customized FOs used in this study were 3D printed in Nylon12, which is distinguished for its

exceptional impact strength, stress cracking, and abrasion resistance, low coefficient of sliding friction, high fatigue resistant, and high processability.

Foot orthosis delivery: The podiatrist should finally deliver the FO to the patients and help them for fitting the FO inside the shoes.

1.4. Evaluation of foot orthosis function

FOs are prescribed through clinical examination and detecting the biomechanical needs of patients. In order to translate such biomechanical needs into FO design, it is important to characterize the dynamic behaviour of FO [102]. The dynamic function of FO cannot be captured with optoelectronic cameras, since the plantar surface of FO is hidden by the contact of the foot plantar surface. Therefore, alternative techniques are inquired in this area, which could be finite element analysis (section 1.4.1), mechanical testing (section 1.4.2), *in-vitro* measurement (section 1.4.3), or artificial intelligence method (section 1.4.4) for predicting the deformation and optimizing the structure and design of FO.

1.4.1. Finite element analysis

Finite element (FE) analysis has shown potentials in evaluating different structural and material configurations of footwear and FOs and their subsequent effects on foot biomechanics. A huge variety of materials and designs has been introduced to the market of insole manufacturing, while their mechanical compatibility with foot function remains unknown. Efficient insoles could be regarded as the ones that fulfill multiple requirements such as cushioning and stability, as well as responding to the subject-specific biomechanical demands such as anthropometric data, gait features, and foot type [98, 103]. Numerical analysis has been used to simulate and validate the interaction between foot and FO, especially for normal feet or diabetic feet [104, 105]. In addition, some research has gone a step forward and used FE to characterize [106] or optimize the properties [98, 107] or design [108] of FOs. While some studies used a detailed geometry of the entire foot obtained from MRI and CT scans to present accurate simulations for foot-insole interfaces [109], others have used geometry-based simplified models [110] or specific anatomical sites [98] to overcome the problems of time-consuming modeling and expensive computations. Furthermore, several FE studies about insole/footwear modeling used static loading conditions, while a few studies refined their FE analysis to consider impact dynamics [103]. The dynamic loading for FE

analysis can consider not only the time-dependent changes in foot loading during dynamic activities [103, 111] but also the shifting of load from one foot region to other regions [103, 112, 113]. Therefore, an important drawback of FE analysis is that a compromise should always be sought between the cost of modeling and the accuracy of the outcomes.

In this section, some studies using FE modeling with the objectives of (a) quantifying the deformation and flexibility of footwear or FO, (b) evaluating the insoles with different materials and optimizing their mechanical properties, and (c) evaluating the insoles with different designs are summarized.

a) **FO deformation and flexibility**: The deformation of footwear and insoles has been evaluated in some FE models to adjust the level of flexibility. Although the footwear should provide a certain level of flexibility and stability, high cushioning due to sole compressive deformation could result in significant loss of energy and smooth guidance during the contact phase [106]. Nishiwaki [106] used motion analysis to determine the relationship between propulsion impulse and shoe sole deformation during running. A reduction in propulsion impulse, calculated from the propulsive phase of anterior-posterior ground reaction force, can help to reduce the running fatigue with constant running speed. In addition, shoe sole bending deformation which is a function of sole stiffness has also been regarded as a determinant factor to control the magnitude of propulsion impulse [106, 114]. Motion analysis was used in this study rather than conventional mechanical tests to reproduce the sole bending and the torsional moduli that occur during gait. Nine retroreflective markers were attached to the shoe sole, where the sole was divided into front, middle, and back regions to determine the relative bending and torsional deformations (Figure 1.12). Then, they represented a numerical method that used the CAD model of shoe sole loaded by foot plantar pressure to predict sole stiffness and deformation during gait based on eigen-vibration analysis [106, 114]. They concluded that controlling shoe sole stiffness under the metatarsophalangeal joint is a key area to fabricate efficient walking and running soles. In addition, Rupérez, et al. [115] developed a FE model to simulate the deformation of the shoe upper for three different materials by using the contact interfaces that were estimated from the movements of a foot during walking, from midstance to push off. The pressure distribution on the foot contact surface was then estimated. The results of these studies show that the functionality of footwear or

FO can be assessed using FE analysis, without the need for manufacturing prototypes, which subsequently saves time and cost.

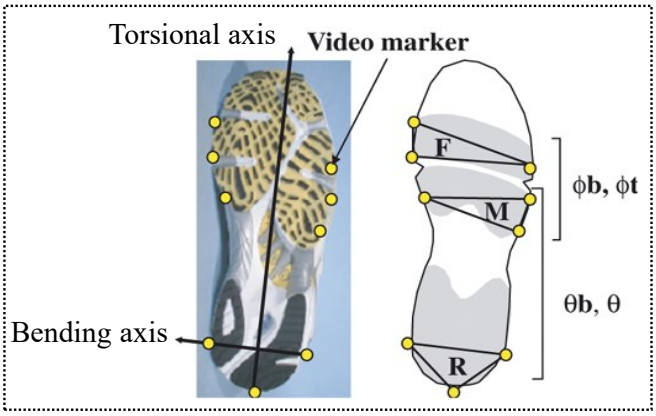

Figure 1.12: Arrangement of reflective markers. Long and short arrows denote longitudinal and width directions used in the calculation of bending (Θ_b, ϕ_b) and torsional (Θ, ϕ_t) angles. Reprinted from Nishiwaki [106]; Copyright (2020) with permission from Taylor & Francis.

b) **Quantification and optimization of materials**: In addition to characterizing FO, some FE models have been developed to optimize the mechanical properties of insole material. The insole material is believed to significantly influence the deformation [116], comfort [117], pressure-relieving behaviour of footwear [109, 118], and cushioning capacity [103]. Chatzistergos, et al. [98] targeted the individual demands of the diabetic foot and implemented parametric analysis on a simplified two-dimensional FE model to optimize the cushioning properties of the insole materials. The information for designing the model and reverse engineering of material properties of the heel pad was provided from the ultrasound indentation and plantar pressure measurements in this study (Figure 1.13). The assessment of different foam materials showed that the optimum mechanical property could be regarded as the one that maximizes the insole capacity to reduce pressure and absorb energy. The results of this study indicated that subject-specific foot properties such as tissue stiffness and thickness did not influence the optimum properties of insole material, while the subject-specific loading significantly altered the optimal properties. Not only the optimization of insoles has been performed for pathological feet, but also some studies have focused on the three-dimensional response of composite material and complex midsole designs with the final goal of preventing sports injuries [113, 119, 120]. Drougkas, et al. [103] used a geometrically accurate midsole model, reconstructed from micro CT scans, and implemented gait specific dynamic loading to optimize the shock-mitigating capacity of midsoles. Time-dependent

plantar pressure distribution during running was used for loading and time-dependent shoe-ground contact was obtained for applying boundary conditions. The optimization function was based on the effectiveness of different positions and shapes of gel pads in the midsole space. This effectiveness was defined as high-energy absorption and support. This study concluded that irrespective of the nonlinear relationship between midsole material allocation and optimization criteria, a significant effect on both cushioning and stability was reached. Unfortunately, there is no similar study available to investigate the optimization of insoles or FOs for flatfoot patients, the population of interest in the present thesis.

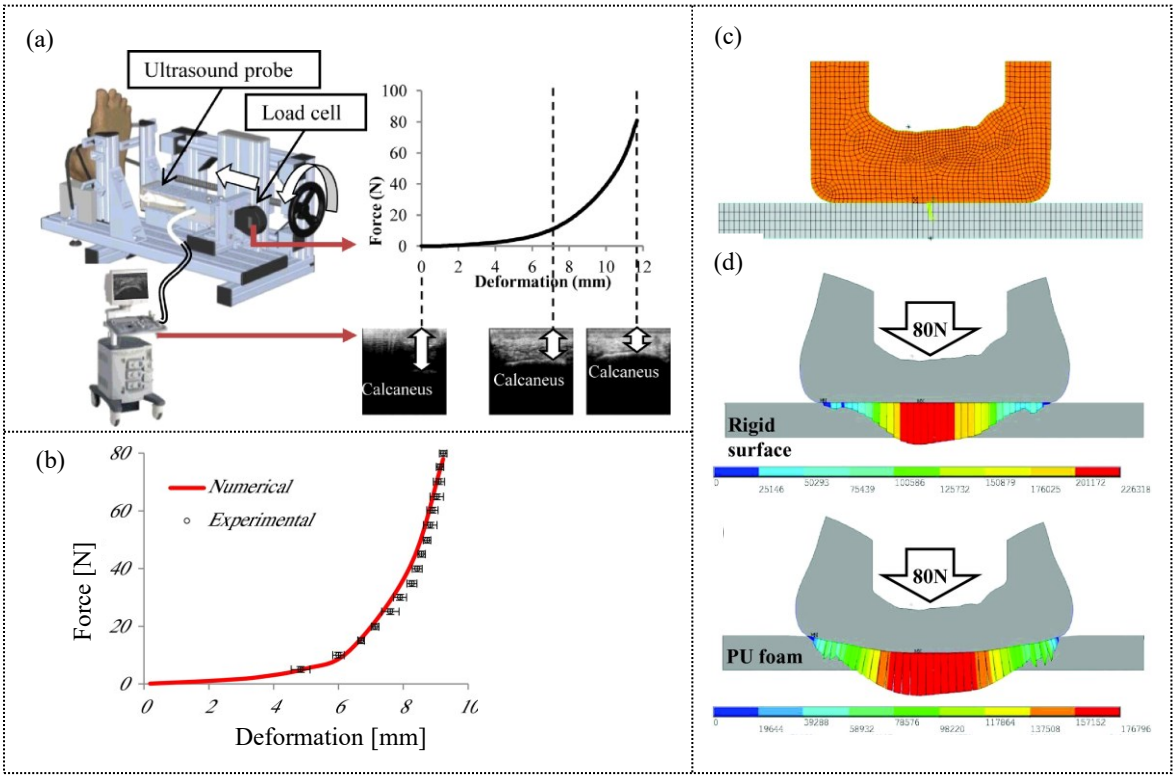

Figure 1.13: (a) Ultrasound indentation device and procedure to extract force/deformation curve, (b) Experimental *versus* best solution numerical curve for force-deformation, (c) The finite element model for estimating plantar pressure, (d) The plantar pressure estimation with a sheet of insole material and polyurethane foam. Reprinted from Chatzistergos, et al. [98]; Copyright (2020) with permission from Elsevier Inc.

c) **<u>Evaluation and optimization of FO design</u>**: On the other hand, some computational models evaluated the behaviour of FOs based on different design configurations. Although the main criteria for customizing the therapeutic insoles is to follow the patient foot shape, the human foot might exhibit different physiological behaviours in several regions [15]. It is possible to respond to such

region-dependent biomechanical demands of the foot by designing adds-on such as posting, arch support, heel height, etc., or by designing insoles with different mechanical properties over foot regions. Cheung, et al. [109] used a three-dimensional FE model, where foot bones were reconstructed from MR images and FO geometry followed the foot shape scan (Figure 1.14). In this study, the sensitivity of different designs of FO, namely arch shape, insole thickness, midsole thickness, midsole stiffness, and insole stiffness on peak plantar pressure were evaluated. They found out that arch-conforming FO and softer material are more effective in reducing plantar pressure, while the optimal configuration of the arch could vary depending on the arch flexibility or the target region of pressure relief for each individual [109]. In addition, Alemany, et al. [121] used the insole deformation and smoothing its gradient as the target parameters to optimize the shankpiece design for high heel shoes through a three-dimensional FE model. The optimization function had to minimize the maximum insole deformation by modifying three design parameters, namely the orientation angle between the shankpiece and the rear axis of the insole, the transverse position of shankpiece, and the longitudinal position of a joint dividing shankpiece in two parts.

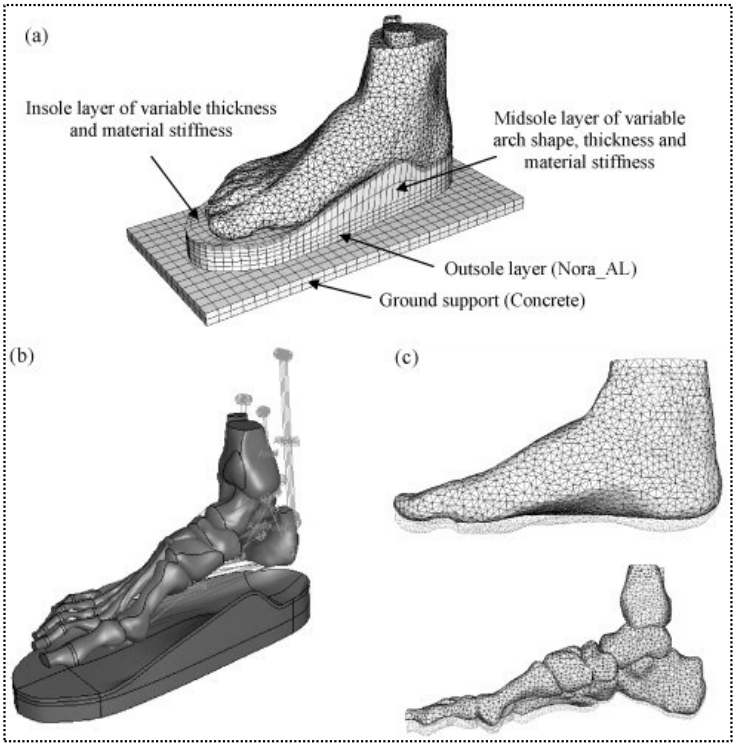

Figure 1.14: (a) The FE meshes of the ankle-foot structures, foot orthosis and ground support, (b) The connector elements for the applications of muscular forces during simulated midstance and (c) The deformed plot of the soft tissue and bony structures. Reprinted from Cheung, et al. [109]; Copyright (2020) with permission from Elsevier Inc.

Furthermore, a recent research [15] proposed a new technique of embedding different unit cells on the surface of FOs to generate heterogeneous mechanical properties. In this study three-dimensional FE modeling has been used for optimizing the stress distribution on the foot-insole contact surface in the diabetic foot by applying functional gradient properties to the customized insole. They used a variety of porous unit cells with different structures to represent different moduli of the materials. The optimized insole with heterogeneous mechanical properties was designed and 3D printed using thermoplastic polyurethane for the experimental test of plantar pressure distribution (Figure 1.15). The results of this study suggested that the optimized customized insole could homogenize the contact pressure in the forefoot and rearfoot as well as reduce the peak plantar pressure. The developed approach in their study makes it feasible to embed several mechanical properties on the insole plantar surface accompanied by a smooth transfer of properties between regions, which could be a good alternative for traditional multi-material insoles.

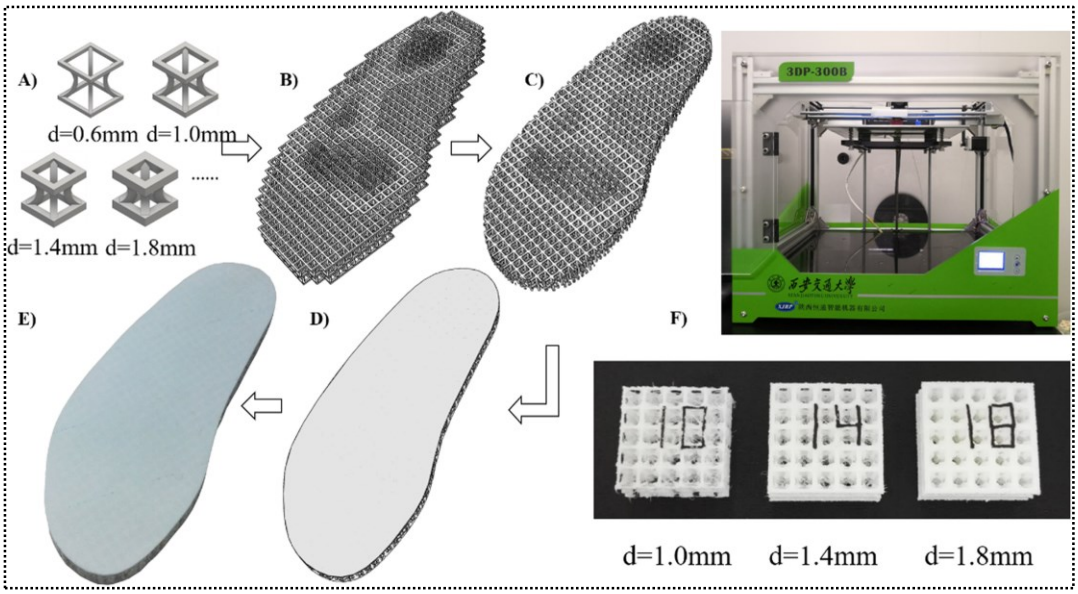

Figure 1.15: Assembly and manufacturing process of the customized porous insole A) Different porous units to be assembled B) Porous substrate C) Boolean intersection of the porous substrate and the original insole D) The complete customized porous insole model E) Manufactured porous customized flat insole and full contact insole F) The printing machine and the 3D-printed testing samples. Reprinted from Tang, et al. [15]; Copyright (2020) with permission from Elsevier Inc.

In order to quantify the displacement of FO under loading, a preliminary study was developed in our lab. In this study, the results of FE analysis were validated with experimental results. In fact, the VICON motion analysis system was used to capture the deformation of FO when manual loads

with known controlled magnitudes and application points were applied on FO plantar surface using a stick. A FE model was developed by simulating a similar matching model, loading, and boundary condition to the experimental conditions. The results showed that FEM could predict a similar range of displacement values as the experimental setup following different loading application points on both medial and lateral sides of the FO. Developing such FE models could be helpful in optimizing FO design following patient-specific variations. In addition, they can be replaced by time-consuming experimental tests to come up with a comprehensive dataset as input data for training the artificial neural network models. These preliminary results were presented as a poster at the ISB 2019 conference in Calgary (Appendices section- Appendix 1.). A common problem with FE modeling is analysis time. Our FE model was a very simple model that included the geometry of FO without any foot model, assigned linear elastic mechanical property to FO material, and applied static loading, but it took one hour for analysis on a computer with 18 GB of RAM, and processor of Intel® Xeon® CPU, W3670 @3.20GHz. Analyzing more complex models such as the foot complex, nonlinear mechanical properties, and dynamic loading might take several days depending on the model details. The limitation of FE models is not just restricted to their inefficiency in time and cost, but also to their ability to accurately simulate mechanical properties, loading, and boundary conditions based on the underlying modeling assumptions concerning interactions between structures (*e.g.* contact type). Using mechanical testing as well as in-vitro techniques make it easier to directly test the real foot structure and FO as well as to simulate closer to real conditions in terms of loading and constraints.

1.4.2. Mechanical testing

The quantification of FO parameters has also been investigated using mechanical testing. It is a rough simplification to use traditional mechanical tests which quantify FOs based on their material samples. The 3D printed FOs are fabricated based on different production techniques, specific-region material or multi-materials, and different designs such as the contour, wedges or postings, which require more robust techniques to quantify FOs rather than traditional mechanical tests. Cuppens, et al. [102] proposed an experimental set-up which was capable to measure FO properties as a function of material and design. A texture analyzer with a spherical probe of 0.5-inch diameter was used to measure force and displacement imposed on different locations of three FOs surfaces produced from different densities of ethylene-vinyl acetate (Figure 1.16). The sequential

compression forces with a certain maximum value were applied at different speeds to reach a certain maximum displacement at pre-defined points on four regions of medial arch, heel, metatarsal heads, and forefoot. FOs were finally characterized by determining stiffness (*via* displacement), compression set, and the shape (*via* height) at the four aforementioned foot regions. The suggested technique in this study was capable to differentiate between the material as well as the shape of FO in several regions.

A further study used a combination of the shoe sole model with the equations of whole-body motion to quantify the relationship between the compressive characteristic of the shoe sole and the body dynamic function [122]. To partition the regions with different structures, the sole was divided into four regions. Then, an impact test set-up made from an arm, accelerometer, and impactor lever with a spherical tip was used to estimate the force response information for each region. They observed that the ankle joint torque related to the elastic property of the frontal region of the shoe sole contributed to body propulsion and support, whereas the knee joint torque related to the viscous property of the shoe sole contributed to body propulsion [122].

Figure 1.16: Measurement set-up using a texture analyzer. Reprinted from Cuppens, et al. [102]; Copyright (2020) with permission from IEEE.

To our observation, some recent literature using mechanical testing is introducing a better reality of footwear and FOs characteristics by considering their contour and dynamic loading. However, some negative points still exist with this technique that can be counted as: (a) characteristics of customized FOs are unique depending on FO designs, and performing mechanical tests for each FO can be expensive in terms of time and labor cost. In addition, designing a repeatable set-up might be difficult to compare the characterization of different FOs; (b) mechanical tests could simulate the dynamic loading in discrete points rather than reflecting continuous loading.

1.4.3. *In-vitro* techniques

Some studies used experimental set-ups with cadaveric lower limbs to evaluate the efficiency of several types of FOs with arch support [123-126]. Kogler, et al. [125] used different designs of FOs consisting of prefabricated FO and four customized FOs of different levels of stiffness and arch heights to investigate their efficiency in supporting the medial longitudinal arch. The amount of strain experienced by the plantar aponeurosis was considered to quantify the efficiency of each FO. The compressive load was applied *via* a compression plate on the proximal portion of the tibia, where the amount of load was controlled by a load cell. To measure the strain, the plantar aponeurosis was exposed by blunt dissection, and a differential variable reluctance transducer was inserted parallel to the natural fiber orientation of plantar aponeurosis with a designed insertion tool (Figure 1.17). The results of this study showed that customized FOs made from viscoelastic and semi-rigid material as well as the ones with the higher arch support were more effective than other FOs in supporting the medial arch. The reason for more efficiency in supporting the medial arch was referred to as the capacity of transferring loads from plantar soft tissues to the apical bony structure of the arch. In a further study, cadaver specimens were used to evaluate the effectiveness of corrective FOs *versus* surgical reconstruction in acquired flatfoot deformity [24]. The loads which simulated the midstance phase of gait were applied on the lower limbs of cadavers. The effectiveness was evaluated based on modifying the contact area and plantar pressure distribution in weight-bearing conditions. This study proposed that both FO with arch support and calcaneal osteotomy surgery could decrease peak pressure, mean contact pressure, as well as the lateral shift of peak pressure spot. However, their arch-supported FO could correct ankle malalignment better than the calcaneal osteotomy surgery.

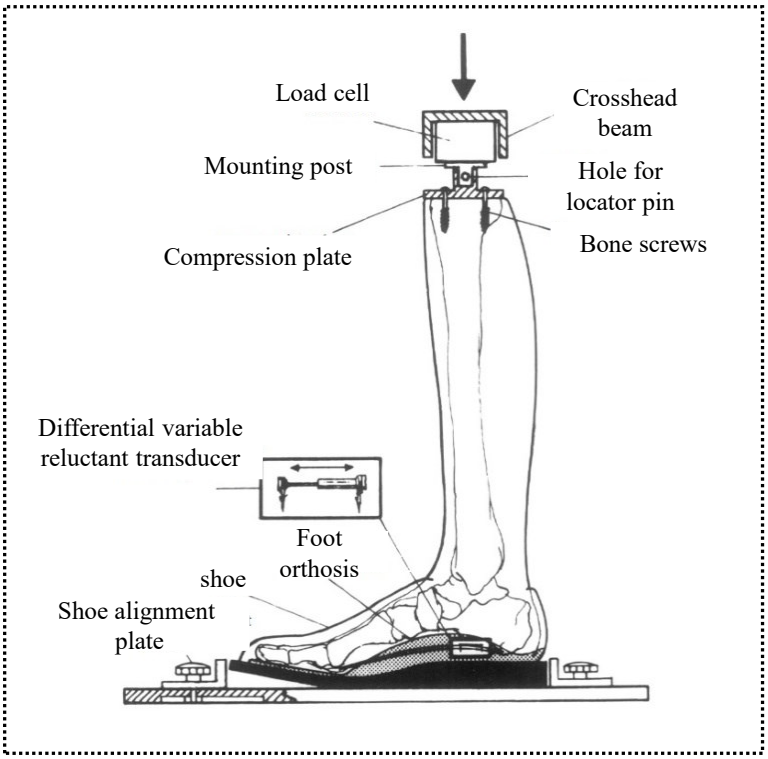

Figure 1.17: Diagrammatic representation of the experimental setup for testing the longitudinal arch support mechanism of foot orthoses. Reprinted from Kogler, et al. [125]; Copyright (2020) with permission from Elsevier Inc.

Quantifying the time-dependent changes in the behaviour of foot or FO is important for explaining their dynamic functionality. Saito, et al. [126] used a cadaver specimen to measure the time-dependent changes of foot arch height when applying repetitive loading of midstance in three groups of normal, obese individuals and obese individuals with the insoles. Time-dependent changes in the arch index, arch height flexibility, and energy absorption were then calculated for each group during 10,000 cyclic loadings. The results of this study showed that using insole for obese individuals could slow down the progression of flatfoot deformity. While using insole for the group with obesity could decrease the arch flexibility and energy absorption at the beginning of loading, these positive effects could not be preserved over the whole sequence of cyclic loading. Therefore, the positive effect of insoles for obese individuals might be limited to the number of steps [126].

Studies on cadaver specimens have provided useful information about the effect of insoles/ FOs on the deformation of soft tissues and bony structures. However, these studies are limited to simulating

the load of midstance rather than the whole stance phase. Due to the difficulty of simulating different phases of walking in cadaveric studies, alternative techniques might be used for quantification of foot or FO during walking. A further point is that while the changes of the foot have been characterized in previous studies, no information has yet been reported for the dynamic quantification of the FOs.

1.4.4. Artificial neural network

Artificial intelligence (AI) has achieved significant popularity in science, engineering, and medicine to support and guide decisions, provide recommendations, and predict features. For the application of AI in biomechanics, it is important to choose the input parameters (predictors) which could be clinically relevant to the output metrics and perform a proper standardization of data [127]. After preparing the data, the neural network model can be designed and tuned in order to find the dependency between input and output metrics [128]. Once the neural network is trained, it can accept a new set of input data, as unseen data, and predicts the output metrics [129]. In the following sections, the basic concepts for building deep learning models will be introduced, and the application of AI in foot biomechanics will be summarized. Since the application of AI in biomechanics is relatively new and limited, more details will be provided regarding the primary steps to build neural networks. It is also important to take advantage of this technique to cope with problems where the mechanical relationship between cause and effect is difficult or impossible to reach [130]. In this thesis, a deep learning model was built to predict the dynamic behaviour of FO. The main advantage of using AI over the previously mentioned techniques is that it can predict a continuous dynamic behaviour of FO rather than discrete points. In addition, the predictions can be done for different subjects with customized FOs with lower time and labor costs and more realistic loading and boundary conditions compared to FE analysis.

1.4.4.1. Building deep learning models

Neural networks are used to develop robust algorithms that can model difficult problems. The neural network takes the inputs and learns the dependency between inputs and outputs. In fact, the inputs go through the hidden layers, where their weights are adjusted to provide the best predictions. *Keras* can be used as an open-source user-friendly library in Python for building neural

networks. Some concepts are introduced here to better understand the structure and function of neural networks:

Neurons: These are building blocks of neural networks that take the weighted inputs and produce an output using an activation function [131].

Weight of neurons: They are in fact very similar to the coefficients that are used to define a regression equation [131].

Activation: The summation of weighted inputs would pass an activation function to yield the output of the neuron [131].

Networks of neurons: Neurons are arranged into networks, where a row of neurons is called layers. For dense layer type, all neurons in the previous layer would be connected to the neurons in the current layer. A network can have multiple layers including an input layer, hidden layers, and an output layer (Figure 1.18). The *input layer* takes the input from the dataset and usually assigns one neuron per input. In fact, the input neurons simply transmit the inputs to the next layer. *Hidden layers* are the ones located between the input and the output layer. Deep learning is referred to as having a large number of hidden layers in the network. The final hidden layer is called the *output layer*, and the requirement for this layer is to handle output in the format of the required problem [132].

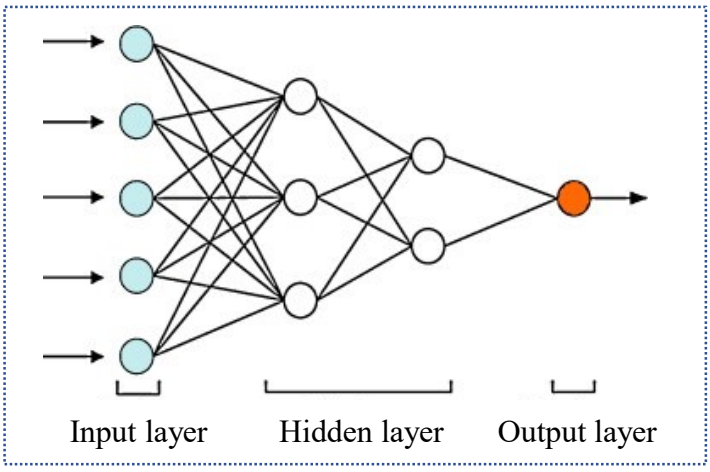

Figure 1.18: Artificial neural network structure. Reprinted from Sayadi, et al. [133]; Copyright (2020) with permission from IEEE

Learning process of the neural network: After building the network structure, training the neural network, *i.e.* learning the values of parameters including weights and biases, is a key step of deep learning. These parameters are optimized through an iterative process of forward and backward propagation. The first phase starts with forward propagation where the input data is fed into the network and all the neurons in a current layer apply their transformation to the information received from the neurons of the previous layer and pass them to the next layer. The loss function would then be used to compare the prediction data, which is the data of the final layer, to the real data, and measures how good the neural network has performed [132]. A popular loss function for regression problems is "mean-squared-error" which estimates the average squared difference between the predicted and actual values. The error can vary between 0 and 1, and the closer to 0 can be interpreted as the better performance of the model. The second phase is backpropagation through which the loss information is propagated backwards from the output layer to all hidden layers. In this process, the loss information distributes to all neurons depending on the relative contribution of each neuron to the total loss on the original output. The next phase would be to use gradient descent to change the weights in small increments by calculating the derivative of the loss function in order to adjust the weights for reaching a global minimum loss (Figure 1.19). In fact, the learning process might be seen as an optimization problem where the parameters (weights and biases) should be adjusted to minimize the loss function [131, 132, 134].

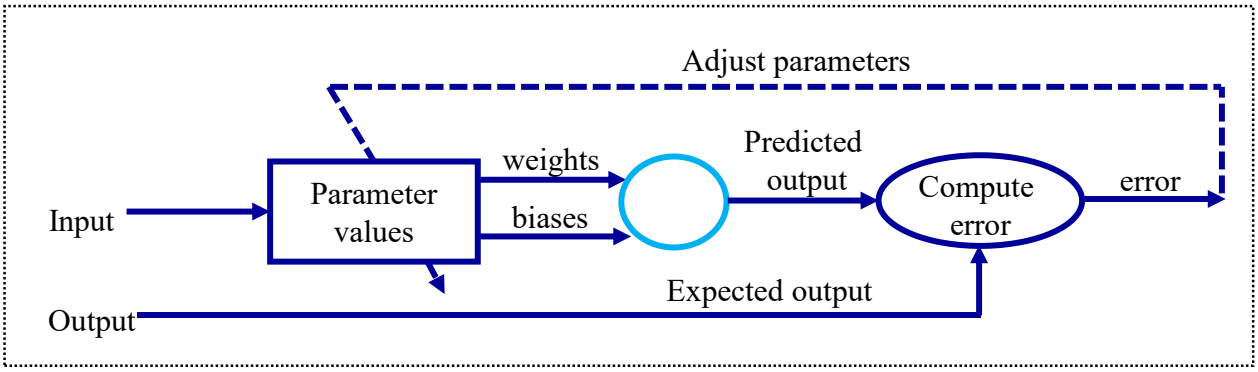

Figure 1.19: Flowchart for the process of learning, reproduced from https://towardsdatascience.com/how-do-artificial-neural-networks-learn-773e46399fc7.

In terms of input data, the neural network needs to be trained on a dataset that has been already well prepared. The primary requirement is to standardize or normalize both input and target variables. Unscaled input variables might lead to a slower or unstable learning process, and

unscaled target variables can lead to exploding gradients which could consequently cause a fail in learning process [134].

1.4.4.2. Applications of neural network in foot biomechanics

Due to the complexity of objectives in clinical biomechanics, a breakdown of the objects into subsystems is performed, which consequently increases the number of available variables. A common application of AI in clinical biomechanics is to deal with the multi-dimensional and multi-correlated nature of gait data [130]. AI can assist in such cases to either classify the group of patients or make decisions for their treatment and rehabilitation. A further application of AI in clinical biomechanics is to predict the metrics which cannot be directly measured [127, 130]. This could originate from either the difficulty for providing equipment such as exterior or far-distancing data collections or the impossibility of reaching the favorable metrics due to invasiveness or physical constraints [127]. The use of AI is still limited in the biomechanical fields related to footwear and FO. Some previous applications of neural networks in this area have been evaluating the functionality of footwear and selection of the material or design for footwear and insoles.

AI has been implemented to reach the principal aim of therapeutic footwear or insoles, which is reducing pain, improving comfort, and redistributing plantar pressure and loading based on the patients' needs. Wang, et al. [35] used an unsupervised learning system in AI to propose mass customization of shoe development for diabetic patients based on seven characteristics of foot girth. The shoe lasts for this group of patients were optimized such that they conform to the shape of the foot and satisfy some biomechanical needs such as reducing plantar and dorsal pressure of the foot. In this study, 60 shoe lasts were firstly categorized based on the girth characteristics using an artificial neural network, and then a relative fitness function between foot girths of patients and corresponding ranges of shoe last categories were calculated to achieve the optimal shoe last design (Figure 1.20). Kirk, et al. [135] used neural networks to predict the dependency between different parameters of studded footwear, such as cross-sectional area and shape coefficients, as input and dynamic traction as output. This study showed a rapid prediction of traction forces with a low prediction error of 10%.

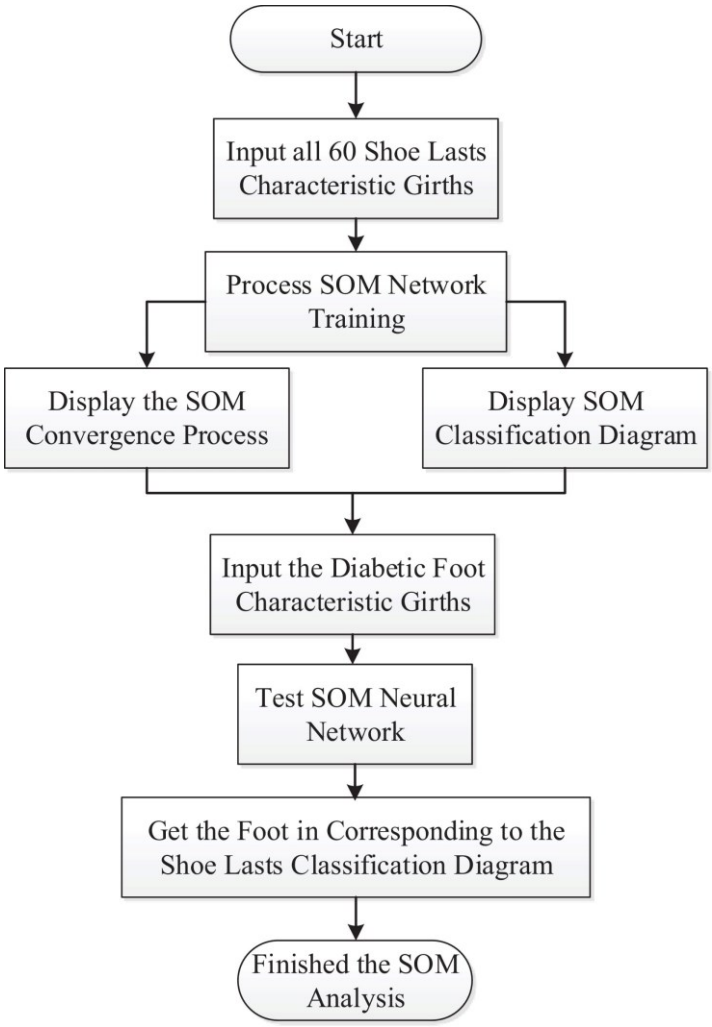

Figure 1.20: Systematic approach self-organizing map (SOM) to categorize shoe lasts and the corresponding diabetic foot, Reprinted from Wang, et al. [136]; Copyright (2020) with permission from Elsevier Inc.

Some literature exists that have utilized AI for predicting the characteristic and function of footwear materials to replace mechanical testing. José Rupérez, et al. [137] proposed an AI model to characterize the contact between shoe upper and foot surface. In this study, tests of flexibility were performed on three commonly used materials in footwear manufacturing to deform the materials. An artificial neural network was then trained to characterize the three materials with a unique equation. The results of this study could be used for characterizing the new materials based on their elastic parameters (Young modulus and Poisson ratio), and their thickness without the need to repeat the experiments. In addition, multilayer perceptron AI was used by Rupérez, et al. [138] to predict the dorsal pressure applied by shoe upper on the foot, which is known as a measure of

comfort and functionality in footwear. The data was collected on four healthy subjects during walking on a platform with five shoes from the same design but different upper shoe material. Pressure sensors were placed on 14 anatomical landmarks of the foot surface between the foot and shoe upper, where the positions of landmarks were previously recorded with respect to the global coordinate system. The inputs for training AI were Young's moduli and Poison's ratio of materials and the coordinates for the position of 14 pressure sensors during the whole step, and the output were the pressures recorded by sensors. The predictions showed high accuracy and reliability, and the correlations between actual pressure and predicted pressure was over 0.9. The results of their study offered that the single equation obtained from AI could estimate the pressure for several materials of upper shoes without the need for time-consuming and expensive experiments to test each individual material.

AI has also been used to see whether gait features can be differentiated between different footwear. Wang, et al. [139] investigated the relationship between muscle activations and footwear conditions including sneakers, high heel shoes *versus* barefoot. They observed that their neural network could properly classify different footwear conditions. Barton, et al. [140] examined whether their back-propagation neural network model could distinguish the differences in plantar pressure distribution between two insoles with different materials *versus* no insole condition. They used total contact area, total force, peak pressure, coordinate of peak pressure, and coordinate of the center of pressure of seven healthy subjects during walking on a treadmill as the input for classification. Their results showed that the neural network was capable to differentiate between insoles especially for maximum contact area and peak pressure, even though the statistical analysis, ANOVA, did not show significant differences between conditions.

The overview of the literature related to AI shows that it is possible to use AI as a powerful tool in the FO industry for a wide range of applications such as providing optimal models for mass production of customized FOs, predicting the functionality of FO during dynamic activities, and differentiating between FOs with different configurations of design or material.

Summary: Four approaches introduced in this section could be used to quantify the dynamic characteristic of footwear and FOs. Each technique is accompanied by some advantages and disadvantages. FE analysis is costly in terms of the time for generating the model and numerical analysis. It also requires a significant amount of information for either geometry or mechanical properties. Therefore, anatomically simplified models are usually replaced by the real existing model which will subsequently affect the accuracy of results. Regarding mechanical testing and *in-vitro* measurements, physiological loading conditions cannot be accurately simulated, and the applied loads introduce a limited number of discrete points rather than providing the whole cycle of dynamic activity such as walking. AI is a further promising approach to predict the biomechanical parameters which cannot be directly measured. A robust and comprehensive training data is a primary requirement of minimal prediction error. This technique might be costly in terms of data collection and preparation for training the neural network model. However, it is easier to be applied for larger sample size, and the predictions can be performed for the whole phase of dynamic activity.

1.5. Foot kinematics

The kinematics represents the joints' motion and the orientation of body segments relative to each other during dynamic activities, without considering the underlying forces that generate the motion [35]. Since the foot is composed of several bones, joints, ligaments and tendons, interpreting the motion of the foot complex by analyzing the foot kinematics as one rigid segment is an oversimplification. Some invasive *in-vivo* measures of foot kinematics have confirmed the importance of the motion generated by the joints distal to the rearfoot, i.e. talonavicular, navicular-cuneiform, metatarsal cuneiform, and metatarsal-cuboid joints [141, 142]. The expansion of multi-segment foot models during recent years have enhanced our understanding of the motion of foot and ankle [143]. The clinical application of these models to better characterize the pathological gait has been also verified [144]. However, the application of these models in FO studies has been limited, which might be due to the difficulty of attaching more markers directly on the skin in the presence of shoes. In this section, some popular multi-segment foot models will be introduced. Then, the kinematics of normal foot during walking and the abnormalities that happen due to flatfoot deformity will be briefly reviewed. Finally, the available knowledge on the effect of FOs on modifying the abnormal foot motion of flatfoot individuals will be discussed.

1.5.1. The foot kinematics models

Technological advancements in motion analysis systems have made it possible to capture the position of smaller markers placed closer to each other, on the smaller segments of the foot. To date, several multi-segment foot models have been used for analyzing the kinematics of both healthy individuals and the ones with biomechanical dysfunction, from which the most popular ones are Milwaukee foot model [145], Oxford foot model [146], Heidelberg foot measurement method [147], Rao model [148], and Rizzoli foot model [149]. The major differences between these models can be stated as: (a) the number of segments (Figure 1.21), (b) the location of markers, the involved anatomical landmarks, and the accuracy and reliability of marker placement, (c) the definition of segments and the underlying anatomical structure of each segment, (d) the definition of local coordinate system for each segment, (e) the method to estimate joint center (functional *versus* anatomical), the method to define the axes and order of rotations of segments around their corresponding joints (Euler, Joint Coordinate System [150], projection angles), and the degrees of freedom for each joint, and (f) the reliability of joint kinematics [143]. These differences between the aforementioned models are summarized in Table 1.1.

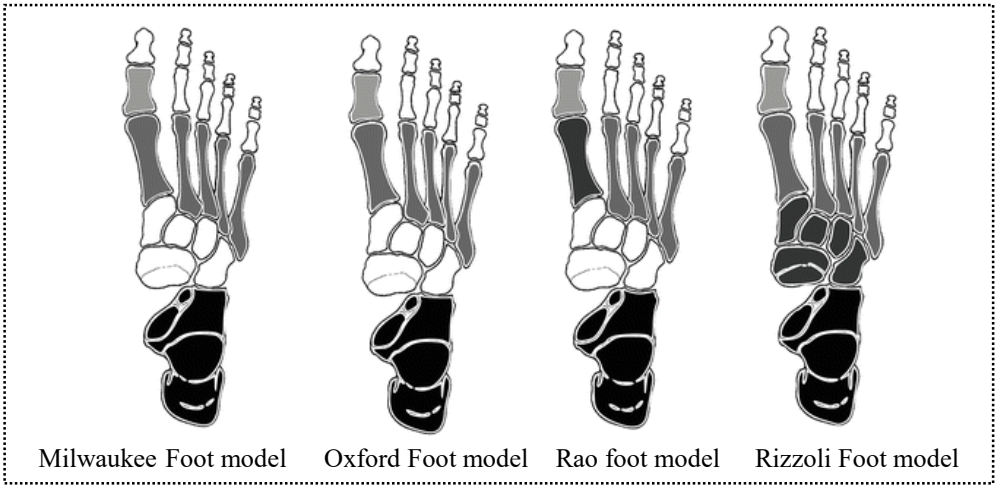

Figure 1.21: Diagrammatic representation of the foot segment subdivisions (different gray tones) for the main multi-segment foot models. Reprinted from Leardini and Caravaggi [151]; Copyright (2020) with permission from Springer Nature.

Table 1.1: Summary of determinant components of different multi-segment foot models

Foot model	# segments	# markers	Precision on location and orientation of reference frames	Method to calculate 3D orientation	Reliability of joint kinematics
Milwaukee **[145]**	4	9+1 triad	limited	Euler	Not reported
Oxford **[146]**	4	15+2 stick markers	adequate	Joint coordinate system	Systematic/Between-trial/between-day/between-tester variability/2 testers, 2 healthy subjects, 4 days
Heidelberg **[147]**	7	17	adequate	Projection angles	Inter-tester/inter-day/inter-trial repeatability/ 1 subject, 5 testers (SD, CMC)
Rao **[148]**	4	9+1 rigid plate	adequate	Euler	Inter-subject variability of waveforms (mean± SD)
Rizzoli **[149]**	5	14	adequate	Joint coordinate system	Inter-subject variability of waveforms (mean± SD); inter-trial/inter-tester/inter-session variability [152]

The segments for Milwaukee **[145]** and Oxford **[146]** foot models are Tibia/rearfoot/forefoot/hallux, for Heidelberg model are Tibia/rearfoot/midfoot/forefoot/hallux/first ray/fifth ray (+functional angles), for Rao model are Tibia/calcaneus/lateral forefoot/first metatarsal, and for Rizzoli model are Tibia/calcaneus/midfoot/metatarsus/hallux (+functional angles).
Abbreviations: SD: standard deviation, CMC: coefficient of multiple correlation

Some review papers provide valuable sources of an overview of multi-segment foot models [143, 144, 151, 153]. Deschamps, et al. [153] performed a systematic review study to assess different multi-segment foot models with regards to their applications in the clinical context. In addition, van Hoeve, et al. [154] reviewed the available literature using multi-segment foot models in patients suffering from foot and ankle trauma to determine the diagnostic values of these models. The consistent findings of both studies indicated that in the presence of skin motion artifacts and the difficulty of capturing some foot bones, these models still provide valuable biomechanical insights and can be used as promising diagnostic tools for evaluating foot and ankle kinematics in the presence of injuries [153, 154]. Deschamps, et al. [153] added that a certain number of the calculated joint rotations was consistent and repeatable, but some of these measures were critical to be used for clinical purposes. A further review study was done by Bishop, et al. [143], where they stated that the source of inconsistent results in multi-segment foot kinematics refers to a lack of transparent explanation of the methodological and technical details, especially in defining the

segments and reliability analysis. The existing ambiguity in these aspects makes it difficult for further studies to reproduce the same model and algorithm. Rizzoli foot model [149], chosen for our thesis data collections, provided enough details on the placement of markers based on the position of bony landmarks as well as defining the joint centers, local coordinate system, and calculating 3D joint orientations. The position of anatomical landmarks could be easily identified under the skin by manual palpation, and the markerset was fully visible for normal feet as well as deformed feet. Using this model, it is also feasible to calculate functional angles such as the longitudinal arch angle, which is crucial in the presence of flatfoot deformity. In addition, the repeatability of this foot model was examined by measuring inter-tester (four examiners), inter-trial (five trials of level walking), and inter-session (three sessions, two to four weeks apart) variabilities on two healthy individuals [152]. The inter-trial variabilities were small across all kinematic variables, while the inter-session variability was low just for two experienced testers. Since the position of markers significantly affects the variability of foot kinematics, it is important to use the data collected by experienced examiners who have sufficient knowledge of foot biomechanics [152]. This aspect was considered in our study, and the marker placements were performed by two Ph.D. students (MH and GD) who were well trained and experienced. The repeatability of this foot model was additionally compared to the Oxford foot model, one of the most commonly used techniques, using intra-class correlation coefficient and standard error of measurement in 17 children between two testing sessions [155]. Both models showed moderate repeatability and reasonable test-retest error, while the Rizzoli foot model [149] provided additional data on midfoot kinematics and functional angles compared to the Oxford foot model.

1.5.2. The normal foot motion during walking

Walking, unlike other forms of bipedal movement such as running, does not involve a phase where there is no foot contact with the ground. Thus, walking is composed of alternating stance phases of the left and right foot. The gait cycle consists of five key points as shown in Figure 1.22: heel strike (0% of stance phase), foot flat (about 17% of stance phase), midstance (50% of stance phase), heel off (83% of stance phase), and toe-off (100% of stance phase). A gait cycle starts with a heel strike, and the entire plantar surface of the foot comes into contact with the ground in foot flat. Heel strike to foot flat is accompanied with pronation, and the corresponding rearfoot eversion when the impact force of the ground is absorbed. At midstance, the rearfoot eversion, and subsequently foot

pronation reaches its maximum range (Dugan and Bhat, 2005), and the foot should survive downward forces. The propulsion occurs from midstance to toe off when the foot supinates and the medial longitudinal arch recoils to provide a rigid lever for efficient propulsion. Individuals with foot deformities might alter their foot motion so that they cannot respond to the requirements of different phases of the gait cycle and consequently cannot regenerate an efficient gait. In order to give clinical suggestions to these individuals, it is primarily necessary to understand what happens during normal gait.

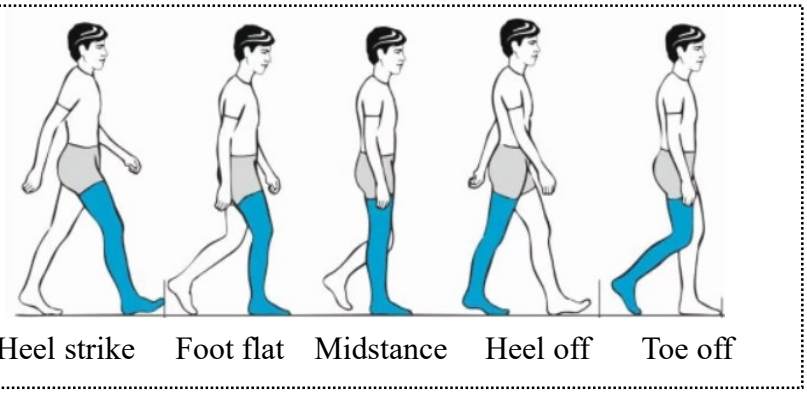

Figure 1.22: The five key points of gait cycle. Reprinted from Pirker and Katzenschlager [156]; Copyright (2020) with permission from Springer Nature.

The kinematics of normal foot during walking was reviewed by Rankine, et al. [144] using 23 studies considering multi-segment foot models. They reported the pattern and range of motion for three segments of rearfoot, midfoot, and forefoot in sagittal, frontal, and transverse planes, which is summarized as follows:

Rearfoot: In the *sagittal plane,* a similar pattern was reported between studies. Generally, dorsiflexion at heel strike was followed by a rapid plantarflexion motion, then gradual dorsiflexion until heel off. From heel off to toe off, a rapid shift to plantarflexion occurred. The average reported range of motion was 18.5° in the sagittal plane. In the *coronal plane*, most models confirmed an inversion position at heel strike, and eversion position at midstance, followed by a shift to inversion at toe off. The consensus pattern of motion in the coronal plane included an inversion position at heel strike moving toward eversion and continued into midstance. Then, the rearfoot inverts during pre-swing phase (heel off to toe off), having an inverted position at toe off. The average range of motion among 21 studies was 10.5° in the coronal plane. In the *transverse plane*, a limited

consensus was found between different models. Regarding the pattern of motion, most studies reported abduction at heel strike which decreases at midstance and converts to adduction at toe off. Gradual adduction throughout the stance phase of gait with an average range of 7.4° was reported among 18 studies [144].

Midfoot: Four models were found to report the midfoot kinematics in the sagittal plane and five models in coronal and transverse planes. In the *sagittal plane*, the consensus pattern of motion included plantarflexion at heel strike, which would be followed by dorsiflexion in midstance, where it starts to dorsiflex during pre-swing phase. The average range of motion in this plane was 8.7°. In the *coronal plane*, the eversion at heel strike continued into midstance and converted to inversion at toe off with an average of 6.3° for the range of motion. In the *transverse plane*, a very little consensus was reported between available studies, where the average range of motion was 3.8° [144].

Forefoot: In the *sagittal plane*, a majority of models indicated plantarflexion at heel strike, converting to dorsiflexion at midstance, followed by plantarflexion at toe off. The average range of motion in this plane was 13.7° among 17 studies. In the *coronal plane*, the midfoot exhibited eversion at heel strike, continuing into the midstance point, whereas it was followed by inversion at toe off. An average of 8.8° was achieved for the range of motion. In the *transverse plane*, the consensus motion showed abduction at heel strike, neutral motion at midstance, and adduction at toe off, while the consensus was weak. The forefoot transverse plane range of motion was 8.8° among studies [144].

To date, several studies on multi-segment foot models have provided useful information regarding the motion of the foot. These models could present the complexity of foot structure better than single segment models. The results of these studies would be valuable for the context of this thesis, in which multi-segment foot models were used for analyzing foot kinematics. Reviewing the pattern and range of motion of different segments during walking provided a baseline to compare and validate our kinematic results. In addition, they could be useful in realizing the abnormalities that might occur due to flatfoot deformity.

1.5.3. The effect of flatfoot deformity on foot motion

Excessive foot pronation during early stance is usually observed in flatfoot individuals, which is accompanied by the collapse of the medial longitudinal arch [4, 157]. Due to the difficulty of measuring foot pronation directly, it is commonly considered as a combination of rearfoot eversion, forefoot abduction, and ankle dorsiflexion.

Rearfoot motion is an important element of gait mechanics because it is the first body part that comes into contact with the ground during normal g, in addition to transferring the external forces from the ground to the lower limb [158]. Excessive eversion of the rearfoot can be considered as a common component of flatfoot deformity, which happens during weight-bearing at the early stance phase (Figure 1.23) [159]. It results in the excessive use of muscles and tendons to control the abnormal movement of the lower limbs [160]. Excessive eversion during early stance also imposes a late inversion during the propulsion phase, which inhibits proper propulsion [159].

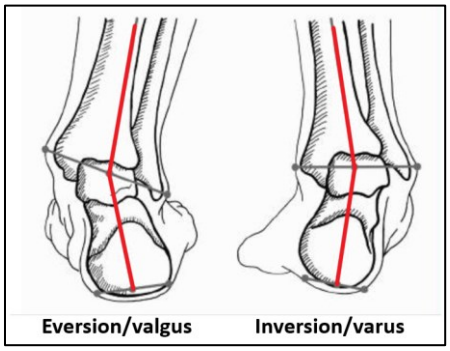

Figure 1.23: Position of right rearfoot in the frontal plane.

The most dominant alteration in the kinematics of the midfoot region in flatfoot individuals is the collapse of the medial longitudinal arch (Figure 1.24). In weight bearing, the collapse of the medial arch results in a significantly higher contact area in the medial region of the foot [55, 161]. The medial longitudinal arch cannot form a rigid lever arm for efficient propulsion during gait, and the forward propulsion is imposed on the midfoot instead of the metatarsal heads [162]. This increases the stress on the midfoot and results in more arch collapse and midfoot abduction [163]. Due to excessive arch collapse, the foot rolls forward like a rocker bottom and loses the force that is needed for efficient gait. Poor propulsion in flatfoot individuals could also result in a decrease in stride length [5].

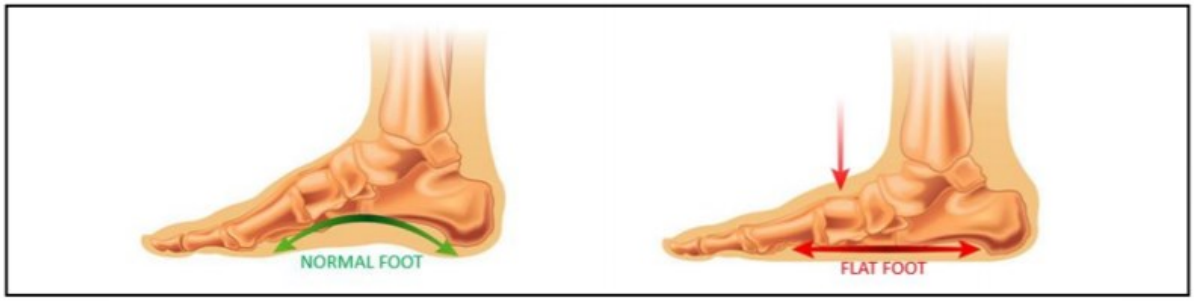

Figure 1.24: Comparison of the medial longitudinal arch of normal arched foot and flatfoot. Image reprinted from http://footmindbody.blogspot.com/2014/07/insoles-for-flat-feet.html.

Regarding the alterations in forefoot kinematics, reduced peak adduction during late stance [159, 164] and higher plantarflexion during the propulsion/push-off phase [159, 165] have been reported in people with flatfeet compared to normal feet. As adduction of the forefoot is part of foot supination during push off, this reduction might impact the foot's biomechanical function during the propulsion phase of the gait cycle [159]. In addition, various degrees of forefoot inversion have been observed in people with flatfeet [166]. Forefoot inversion is a malalignment of the foot in which the forefoot is in supination relative to the rearfoot when the subtalar joint is in its neutral unloaded position [167]. In weight bearing, the forefoot shifts to an eversion orientation to allow the medial border of the foot to reach the ground [31]. In fact, when the body weight transfers to the forefoot region, the first metatarsal is forced to lower from its elevated position. This is accomplished by midfoot and/or rearfoot compensatory pronation, which is accompanied by the collapse of the medial longitudinal arch and an increase in rearfoot eversion [31].

Therefore, the main biomechanical changes of flatfeet relative to neutral feet can be mentioned as eversion-inversion of the rearfoot, abduction-adduction of the forefoot, and collapse-recoil of the medial longitudinal arch, which are summarized in Figure 1.25.

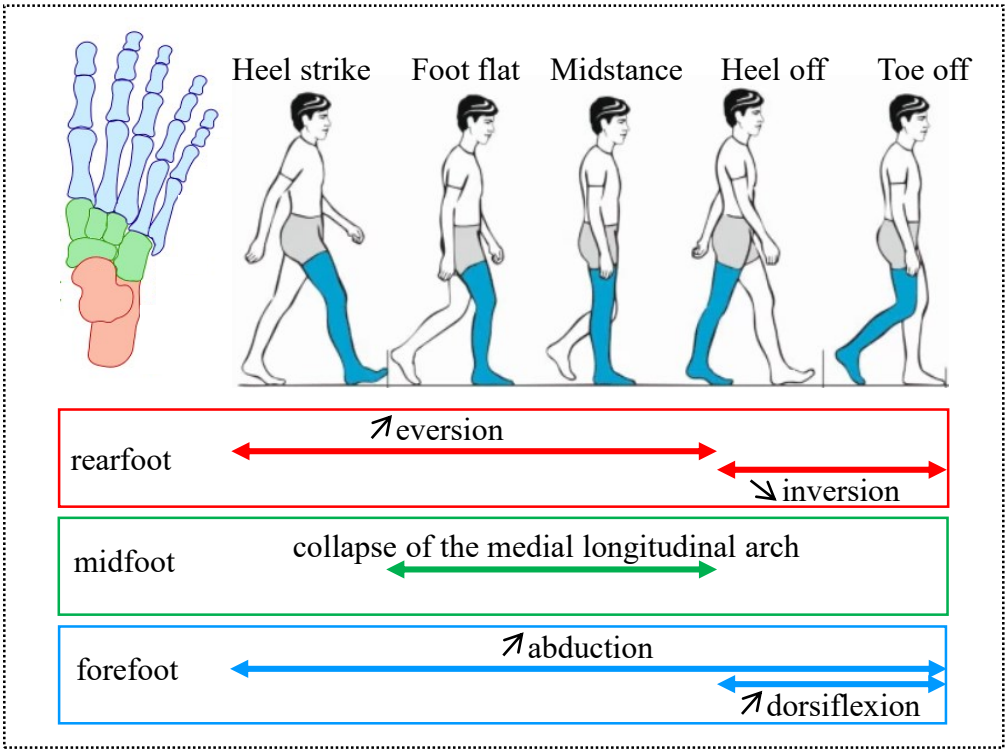

Figure 1.25: Main biomechanical changes of flatfeet individuals during the stance phase.

1.5.4. The effect of foot orthosis on the kinematics of flatfoot

The function of FOs was assessed by comparing the kinematics of flatfoot individuals during walking with- and without- FOs in a few studies. As mentioned in section 1.3.2, the design of FOs might be different depending on the experience and training of health practitioners. The most common geometrical modifications applied to the FO design for individuals with flatfoot deformity could be regarded as medial rearfoot posting, medial forefoot posting, neutral rearfoot posting, and medial arch support [22]. These modifications are in fact added with the purpose of preventing excessive rearfoot eversion and forefoot abduction as well as supporting the medial longitudinal arch during propulsion [26]. However, limited consensus exists among available studies about the efficiency of these FOs. While some studies found them efficient for assisting individuals with flatfoot deformity to overcome their abnormal gait [25, 26], others did not find any evidence of alterations compared to flat insoles or shoe-only condition [28, 31]. These controversial results might be due to different reasons such as differences in the design and material of FOs and their levels of customization [22, 26, 168], differences in foot kinematic models and analysis approach

[143], and the variations in the foot structures between individuals [169]. In this section, the available knowledge on the relationship between FO design and foot kinematics will be summarized.

Desmyttere, et al. [22] did a meta-analysis study to gather and analyze the available knowledge on FO design and foot motion of individuals with flatfoot deformity. Five subgroups of included studies were formed based on the adds-on of FOs, namely as medial rearfoot posting (five studies), medial forefoot posting (two studies), a combination of medial rearfoot and forefoot posting (four studies), neutral rearfoot posting (two studies), and arch support (three studies). The main findings of this review can be summarized as follows:

Medial rearfoot posting was originally added to FOs with the purpose of imposing a neutral subtalar joint position at heel strike based on Root theory for controlling the excessive eversion occurring during the early stance phase [170, 171]. However, the application of these FOs did not yield consistent results between studies. While three studies reported lower rearfoot eversion during walking [24-26], two other studies addressed an increase in rearfoot eversion [27, 28] (Figure 1.26). In addition, a decrease in forefoot abduction was reported by Telfer, et al. [26] during walking with this FO design.

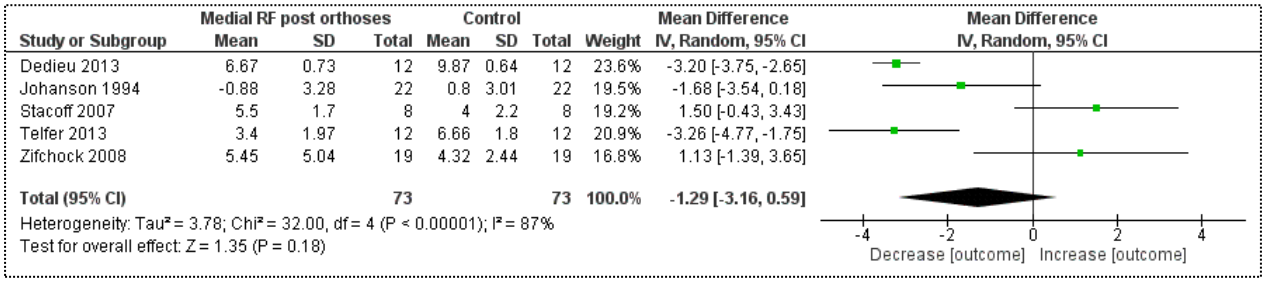

Figure 1.26: Forest plot of the effect of foot orthoses with medial rearfoot posting on rearfoot eversion during walking in people with flexible flatfoot. The total effect was calculated as the mean difference (95% CI). SD: Standard Deviation, CI: Confidence Interval. Reproduced from Desmyttere, et al. [22]; Copyright (2020) with permission from Elsevier Inc.

FOs with medial forefoot posting is usually prescribed for individuals with excessive forefoot abduction. The rearfoot posting is added to the forefoot posting when this excessive abduction leads to excessive eversion [25]. Walking with medially forefoot posting as well as medially forefoot plus rearfoot posting resulted in a significant decrease of 2.2° (Figure 1.27) and 2° (Figure 1.28) in rearfoot eversion, respectively. The effect of forefoot posting on the level of rearfoot

eversion might be addressed to the presence of coupling in the motion of the three foot segments [172].

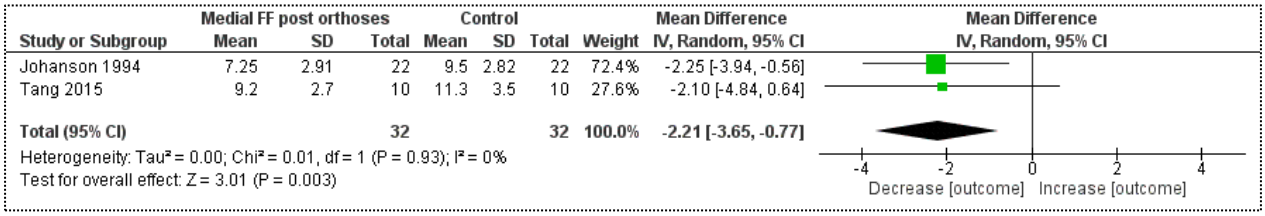

Figure 1.27: Forest plot of the effect of foot orthoses with medial forefoot posting on rearfoot eversion during walking in people with flexible flatfoot. The total effect was calculated as the mean difference (95% CI). SD: Standard Deviation, CI: Confidence Interval. Reproduced from Desmyttere, et al. [22]; Copyright (2020) with permission from Elsevier Inc.

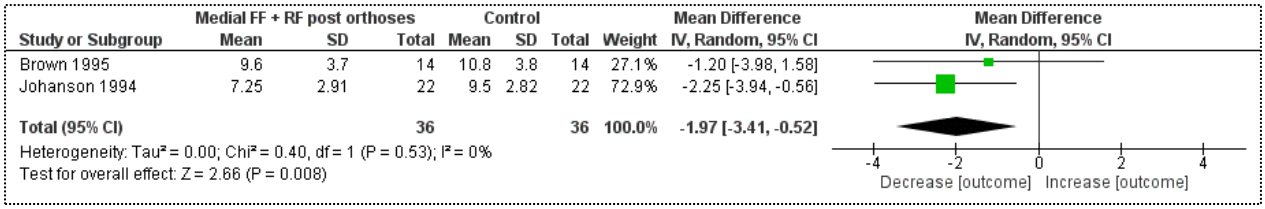

Figure 1.28: Forest plot of the effect of foot orthoses with medial forefoot & rearfoot posting on rearfoot eversion during walking in people with flexible flatfoot. The total effect was calculated as the mean difference (95% CI). SD: Standard Deviation, CI: Confidence Interval. Reproduced from Desmyttere, et al. [22]; Copyright (2020) with permission from Elsevier Inc.

Neutral posting is added to the design of FO to fulfill the purposes of stabilization and preventing the subtalar joint to rock to excessive pronation [173]. However, the two available studies reported controversial results in rearfoot eversion during walking with these FOs. While Telfer, et al. [26] indicated lower rearfoot eversion, Bishop, et al. [29] showed a small but significant increase in this variable (Figure 1.29). Neutral rearfoot posting was also reported to decrease peak forefoot adduction during walking [173].

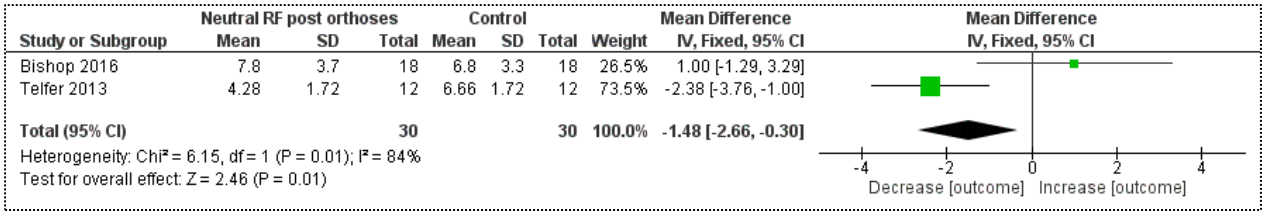

Figure 1.29: Forest plot of the effect of foot orthoses with neutral rearfoot posting on rearfoot eversion during walking in people with flexible flatfoot. The total effect was calculated as the mean difference (95% CI). SD: Standard Deviation, CI: Confidence Interval. Reproduced from Desmyttere, et al. [22]; Copyright (2020) with permission from Elsevier Inc.

Finally, FOs with medial arch support are designed to assist the medial longitudinal arch in retrieving its form after midstance and providing a rigid lever for efficient propulsion. The efficiency of these FOs in reducing rearfoot eversion was examined by two studies, but no significant effect was observed (Figure 1.30) [30, 31]. However, a recent study [158] showed that insoles with arch support could significantly reduce the peak rearfoot eversion in flexible flatfoot individuals. Based on the findings of these studies, it is possible that the efficiency of the arch supported FOs depends on the level of flexibility and the weakness of muscles, tendons, and ligaments that support the medial longitudinal arch. This review paper gathered extensive data on the impact of different designs of FO. These results provided useful biomechanical insights for this thesis, especially for analyzing and interpreting the relationship between the deformation of FO and foot biomechanics (Chapter 4).

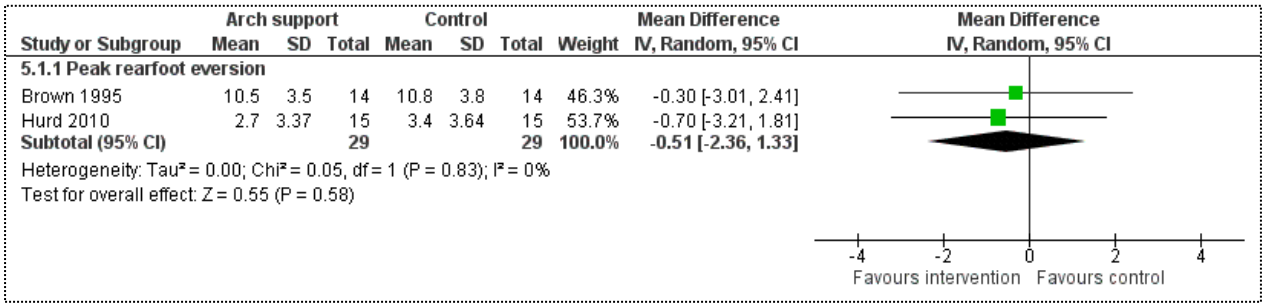

Figure 1.30: Forest plot of the effect of foot orthoses with arch support on rearfoot eversion during walking in people with flexible flatfoot. The total effect was calculated as the mean difference (95% CI). SD: Standard Deviation, CI: Confidence Interval. Reproduced from Desmyttere, et al. [22]; Copyright (2020) with permission from Elsevier Inc.

In addition to different designs of FOs, the rigidity of FOs as well as the customization might be regarded as other important factors to alter the foot kinematics in flatfoot individuals. Cheung, et al. [10] performed a meta-analysis study, where they found out that customized FOs could control the rearfoot eversion and subsequently excessive foot pronation more efficiently than prefabricated FOs. In addition, Prachgosin, et al. [6] compared the total-contact customized FOs to the shoe-only condition in flexible flatfoot individuals. They observed that customized FOs were more efficient to support the medial longitudinal arch and correct the biomechanical alteration in flexible flatfoot. This higher efficiency might be referred to as the design of customized FOs which can be adjusted for each individual foot structure to better manage the alterations in foot motion. Regarding the rigidity, Balsdon, et al. [32] compared the biomechanical effect of hard (Suborthlen) and soft (Plastazote) customized orthoses *versus* shoe only condition during walking using videofluoroscopy. They found out that both hard and soft customized FOs could similarly support the medial longitudinal arch of flatfoot individuals better than shoe only condition. However, no significant difference in medial arch angle was achieved between hard and soft customized FOs in this study.

Summary: Foot kinematics provide useful insights into the dynamic alterations related to the flatfoot deformity. Such information can be implemented in evaluating the function of foot orthoses or optimizing their design. The reliability and accuracy of foot kinematics data, therefore, play an important role in clinical practice in recognizing the abnormalities and prescribing orthoses. The development of multi-segment foot models has made it feasible to quantify the three-dimensional rotations of different foot joints, which provide additional useful information for clinical use. The major alterations in the kinematics of flexible flatfoot individuals can be mentioned as early and excessive rearfoot eversion which might eventually be accompanied by forefoot abduction. In addition, at the midfoot level, the medial longitudinal arch collapses under body weight, and cannot recoil properly to provide a rigid lever during the propulsion phase. Foot orthoses, as common treatment tools for flatfoot deformity, could ameliorate these alterations to some extent. However, depending on the design, rigidity, and level of customization, these corrective effects change. Variation in FO designs has led to inconsistencies in the findings of available literature. In order to clarify this issue, it is important to find a direct association between foot kinematics and foot orthosis dynamic behaviour.

1.6. Foot plantar pressure

Plantar pressure analysis is a widely used tool in research and clinics to represent the foot function. Plantar pressure data can be used for the assessment of abnormal foot loading, the treatment of patients with a variety of pathological symptoms and improving the design and functionality of treatment tools such as foot orthosis and footwear. Choosing an appropriate technique for processing pressure data is important for further clinical interpretation, transfer, and relevance. In this section, different available systems for measuring plantar pressure will be shortly introduced (section 1.6.1), and the techniques for analyzing plantar pressure data will be summarized (section 1.6.2). Finally, the effect of FOs in improving the plantar pressure distribution in flatfoot subjects will be presented (section 1.6.3).

1.6.1. Plantar pressure measurement system

Plantar pressure measurements could provide information about the magnitude and distribution of force that is applied to the plantar surface of each individual foot with respect to the supporting surface during dynamic loading [35, 99]. Although the force plates provide the vertical and shear components of ground reaction force, they have limited value in providing the distribution of load [174]). Any abnormal foot posture might alter the normal plantar pressure distribution or impose excessive pressure under some foot regions which leads to pain and further injuries [35, 99, 175]. In athletes, the foot pressure distribution and the region of peak pressure vary by sport type [175], depending on shoe type and comfort which was found to be related to plantar pressure distribution. Therefore, commercial plantar pressure measuring devices are gaining more popularity as standard evaluation tools for clinical application, prescription of orthosis and athletic footwear design [35]. Foot plantar pressure analysis could additionally be used for statistical and modelling analyses to understand the relationship between footwear, gait features and plantar pressure for decision-making process [176-181].

The key requirements in the design of plantar pressure measurement systems are spatial resolution, sampling frequency, accuracy, sensitivity, and calibration [182]. Foot plantar pressure could be recorded using either platform systems (Figure 1.31-a) or in-shoe systems (Figure 1.31-b). Each system has unique functions and features for data collection and analysis and can be selected based on the study aim and costs [175]. The platform systems are easy to use since they are stationary

and flat. However, they inquire a familiarization time for the participant to ensure natural gait and contact with the platform. On the other hand, in-shoe plantar pressure devices, which are used in this thesis, are known for their higher efficiency, mobility, applicability, and reduced cost compared to platform systems [175, 182, 183]. In addition, the participant would not have to alter gait features to target the platform during walking [183]. The system is flexible and portable which makes it suitable for several gait tasks, footwear designs, and terrains, and they have been highly recommended for studying orthotics designs [182]. In-shoe systems contain much separate force measuring sensors that are distributed within the region of foot and ground/shoe contact. However, their spatial resolution is usually lower than platform systems due to fewer sensors [182].

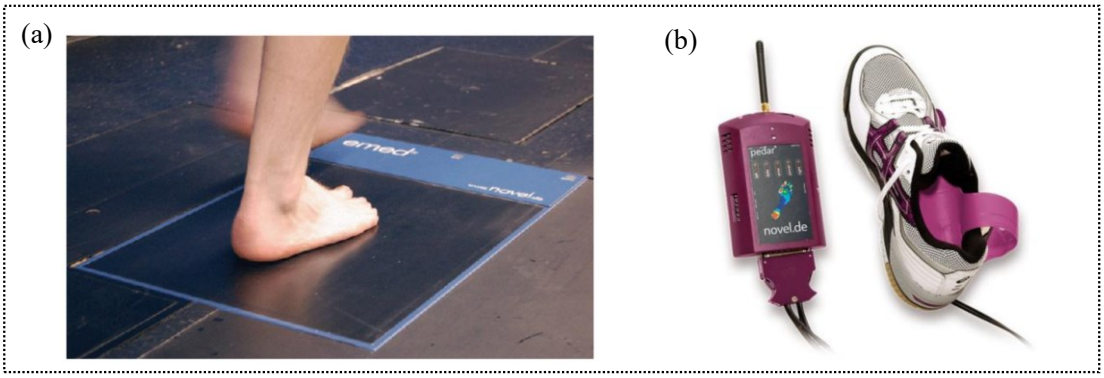

Figure 1.31: (a) Platform plantar pressure system, (b) In-shoe plantar pressure system. Reprinted from Abdul Razak, et al. [182]; Copyright (2020) with permission from MDPI (http://www.mdpi.org).

Price, et al. [184] compared the accuracy and repeatability of three in-shoe pressure measurement systems, namely *Medilogic, Pedar,* and *Tekscan*, for which the differences in size, sensor number, and type are detailed in Table 1.2. *Medilogic* insoles had a lower cost, a higher number of sensors, lower sensor thickness, higher sampling rate, and higher measurement range compared to *Pedar* insoles. *Medilogic* insoles were more proper to be used inside shoes compared to *Tekscan* insoles since *Tekscan* insoles slip easily inside the shoes during dynamic activities, which impose error in the pressure results. Price, et al. [184] indicated that all three insoles exhibited high between-day repeatability. Regarding the validity for pressure data, *Pedar* got the first rank followed by *Medilogic* in the second rank. Regarding the validity of the contact area, *Medilogic* performance was the best [184]. Furthermore, Koch, et al. [185] evaluated the validity and reliability of *Medilogic* pressure insoles for measuring the vertical ground reaction forces. Their tests included

static mechanical tests during loading and unloading the pressure insoles and the tests of participants with insoles inside their shoes, where the forces were recorded by both insoles and force plates. The reliability testing during such mechanical tests yielded an average intraclass correlation coefficient of 0.998. In addition, the average root mean square error was 6.6% and 17.7% between the insoles and force plates during standing and walking respectively [185]. Using pressure insoles is also accompanied by some limitations. A common problem of using all pressure insoles is the shear effect because the sensors measure the forces normal to the sensor surface. When the pressure insoles are put on shoes or contoured orthosis, the angle of the sensor surface would not be parallel to the ground surface. As a result, the pressure measurements might not represent the vertical ground reaction force [185]. Other limitations of in-shoe plantar pressure systems might be counted as the limited number of sensors, the effect of trapped heat and sweat of the foot on the results, and sensor slipping inside shoes [175].

Table 1.2: Definition of variables quantified for in-shoe pressure measurement comparison. Reprinted from Price, et al. [184]; Copyright (2020) with permission from Elsevier Inc.

Feature	***Medilogic***	***Pedar***	***Tekscan***
Sensor model	SohleFlex Sport	Pedar-X	F Scan 3000E Sport
System cost (quote 2016)	£10500 (including insoles)	£12600 (not including software+ insoles)	£14000 (including insoles)
Sensor technology	Resistive	Capacitive	Resistive
Number of sensors	Variable based on insole size (≤240)	99	Variable based on insole size (≤960)
Sensor density	0.79 per cm^2	0.57-0.78 per cm^2	3.9 per cm^2
Insole thickness	1.6 mm	2.2 mm	0.2 mm
Maximum sampling rate	300 Hz	100 Hz	169 Hz
Measurement range	6- 640 KPa	20-600 KPa	345-862 KPa
The recommended time between calibrations	1 year or 5000 steps	Variable	Disposable insoles-calibrate at each use

Plantar pressure data used in this thesis were recorded by *Medilogic® WLAN insoles* after considering several parameters of accuracy, repeatability, spatial resolution, frequency rate, the purpose of study, and costs. The plantar pressure system had a maximum of 240 sensors per insole, depending on the insole size, and was capable to collect 8-hour raw data for each sensor [185, 186]. The sensors are 0.75 cm× 1.5 cm rectangles, with a corresponding area of 1.125 cm^2. They measure the changes in electrical resistance which is proportional to the applied pressure. Each sensor can measure a range of 0.6 to 64 N/cm^2, and the sampling rate could vary between 100 Hz and 400 Hz (Figure 1.32).

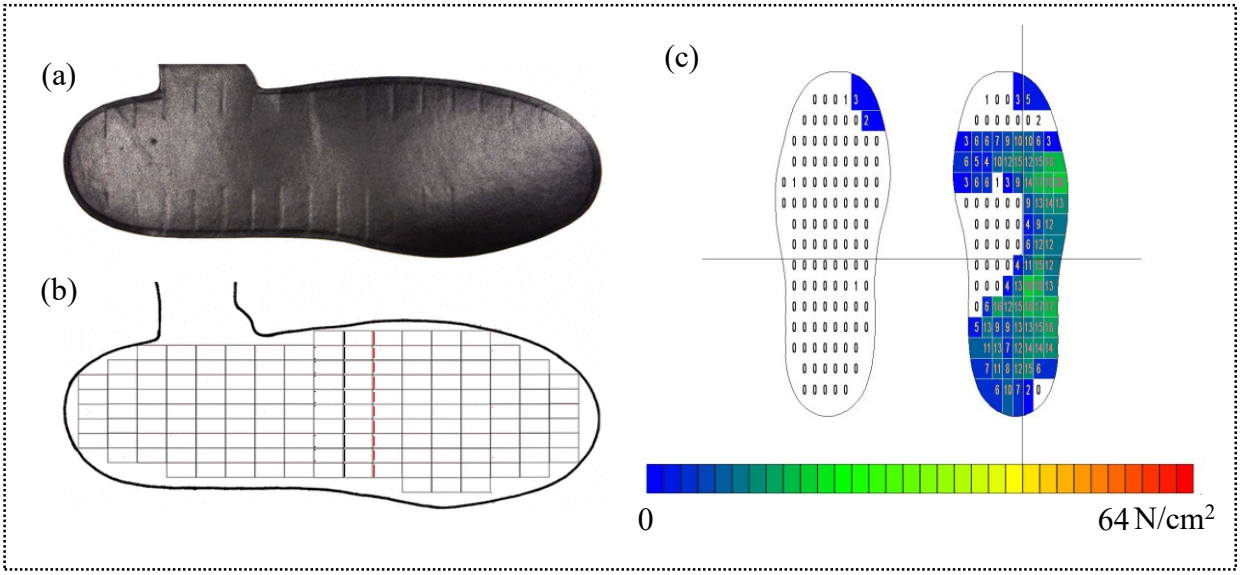

Figure 1.32: (a) Medilogic® left insole of in-shoe pressure system, (b) Its corresponding sensor map where each rectangle represents a sensor, (c) Pressure map of a subject with Medilogic software. Reprinted from DeBerardinis, et al. [187]; Copyright (2020) with permission from SAGE (https://us.sagepub.com/en-us/nam/open-access-at-sage).

1.6.2. Analysis and interpretation of plantar pressure data

Numerical and statistical analysis of pressure data can be performed in either one dimension as temporal mean and peak pressure or two dimensions as pressure maps for pixel-level analysis. For one-dimensional analysis, the plantar pressure data are divided into different meaningful regions of interest (ROIs), which is called masking [35]. The masking algorithms might be grouped as *i)* manual masking, *ii)* automatic anatomical making, and *iii)* integrated anatomical masking.

i) The accuracy of manual masking depends on the quality of pressure images, which is a function of the number of sensors and sensor density, as well as the anatomical knowledge of clinicians. This method has a low level of repeatability and is rarely used nowadays.

ii) Several reliable and automatic algorithms to date have been introduced for automatic masking, which do not hold the inaccuracies of manual masking. These techniques provide more information compared to analyzing the whole plantar surface of the foot [188, 189]. After an appropriate masking, different pressure variables such as peak pressure, mean pressure, contact area, and other relevant variables can be calculated for each region [35]. These results provide information on the foot function of the abnormal foot or the effect of rehabilitation tools such as FOs. They also provide valuable results for researchers and footwear industries to find out the correlations between foot posture, foot motion, and foot function.

Most studies have used automatic masking for reporting and interpreting the results of plantar pressure. Through this technique, the ROIs are generated based on anatomical features of the foot by using longitudinal lines for dividing the foot mediolaterally and horizontal lines for dividing the foot to rearfoot, midfoot, and forefoot [188]. Different approaches have been suggested for automated masking. One common algorithm was suggested by *Novel*® which generates 10 regions of interest. These regions included first toe, second toe, third to fifth toes, five regions for each metatarsal, midfoot, and rearfoot. The geometrical features to divide the regions were medial and lateral border lines, as well as horizontal lines at 45% and 73% of foot length. The intersection of medial and lateral border lines defined the long plantar angle, which was used to generate the metatarsal regions. The horizontal lines divided the foot to rearfoot, midfoot, metatarsals, and toes (Figure 1.33-a). Ellis, et al. [188] assessed the accuracy of this algorithm during static and dynamic activities in normal feet and found out that most foot regions were identified accurately. Other studies exist which used *Novel*® auto-masking technique, but for the purpose of simplification or clinical goal generated different masking regions, such as eight ROIs including medial and lateral regions for rearfoot, midfoot, and forefoot, hallux, and lesser toes [190]. Furthermore, other manufacturers of in-shoe pressure insoles have suggested different masking regions. *Footscan*® software (*RSscan International*) suggests a 10-region automatic masking, which divides the foot into hallux, toes 2-5, five metatarsal regions, midfoot, medial heel, and lateral heel (Figure 1.33-b) [191]. Using *Medilogic* pressure insoles, Pauk, et al. [192] performed 5-region anatomical masking

including the toes, metatarsal heads, navicular bone, cuboid bone, and heel to compare the foot loading in pathological feet (Figure 1.33-c). This overview shows that substantial variation exists in masking techniques between studies that make the comparisons of results very difficult [99]. No agreed and standard method has yet been proposed to be used by all studies. A further important problem is that most masking techniques identify the regions based on geometrical features of pressure maps and ignore the association of these regions with foot anatomy. If the regions are established based on foot anatomy, the interpretations will be more reliable. The integrated anatomical masking has been developed recently to reach this goal.

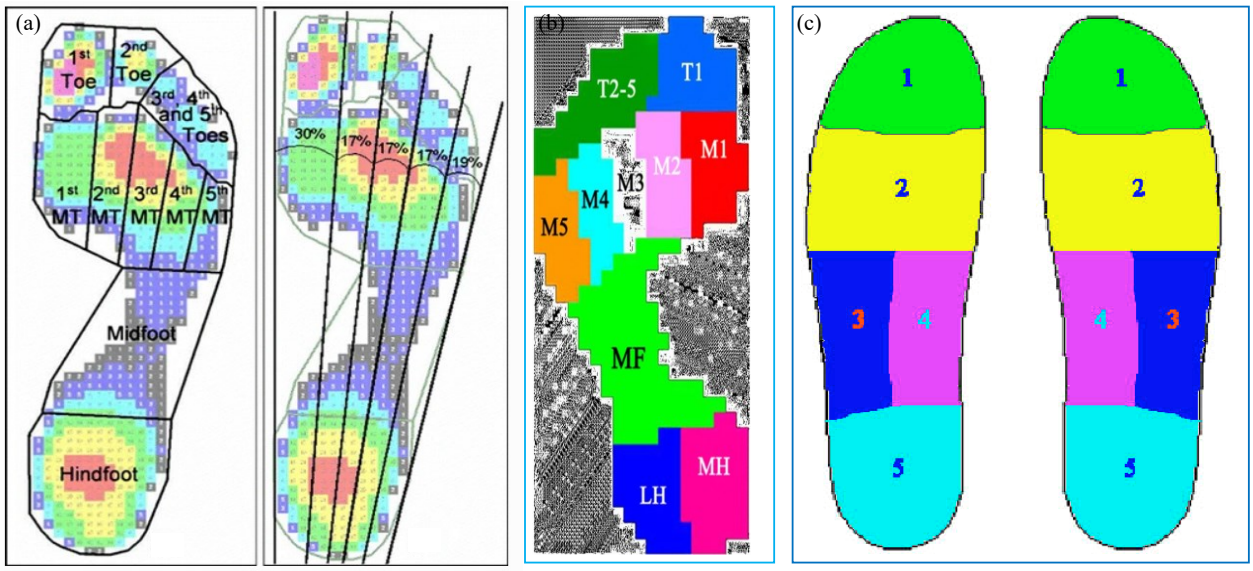

Figure 1.33: (a) The Novel® standard for 10-region anatomical masking; mask regions; medial and lateral border lines and the midlines for generating metatarsal regions, Reprinted from Ellis, et al. [188]. Copyright (2020) with permission from Springer Nature; (b) *Footscan*® standard for automatic masking, Reprinted from Xu, et al. [191]; Copyright (2020) with permission from International Scientific Information; (c) Anatomical masking for *Medilogic* pressure insoles, Reprinted from Pauk, et al. [192]; Copyright (2020) with permission from Oficyna Wydawnicza Politechniki Wrocławskiej

iii) In order to overcome some limitations of the manual and automatic masking techniques, some studies have suggested the integrated anatomical masking approach based on objective anatomical landmarks to divide the plantar foot surface. In addition to their repeatability, these techniques provide the capability to integrate foot joint kinematics and foot pressure in the corresponding anatomical regions to help clinicians for more suitable treatment plans [189, 193]. To implement the methodology of an integrated approach, it is not necessary to use a specific foot model.

However, it is important to primarily synchronize and align the kinematics and pressure data, and then identify the clinically relevant foot segments and plantar regions. This technique has been developed and implemented for some commonly used foot kinematic models, including the Rizzoli foot model [149], the Oxford foot model [193, 194], and the Padua foot model [195].

The anatomical masking which leads to integrated pressure-kinematics has been used in some studies investigating pathological cases. Giacomozzi, et al. [196] used this approach to assess the functional performance of patients with the talocalcaneal condition in surgical and non-surgical conditions. In this study, the bony segment position using the Rizzoli foot model, ground reaction force, and plantar pressure were synchronized and measured. Anatomical masking was used to define three ROIs of rearfoot, midfoot, and forefoot. For each ROI, kinematics as well as the shear and vertical components of ground reaction force, were estimated. Surgical patients were found to restore the subtalar and forefoot motion as well as shear ground reaction forces. The finding of this study showed the efficiency of such anatomical masking techniques in an accurate inspection of this surgical treatment for either follow-up or decision-making purposes. Furthermore, Oxford Gait Laboratory implemented this integrated approach in several published studies of children, patients with cerebral palsy, or other foot deformities [193, 194, 197]. The integration was performed by projecting the foot anatomical landmarks of the Oxford foot model onto the foot plantar pressure map to identify five anatomical ROIs, namely medial and lateral rearfoot, midfoot, medial, and forefoot (Figure 1.34). The beneficial aspects of such anatomical masking were reported in these studies for clinicians to prescribe orthotics and making further treatment plans.

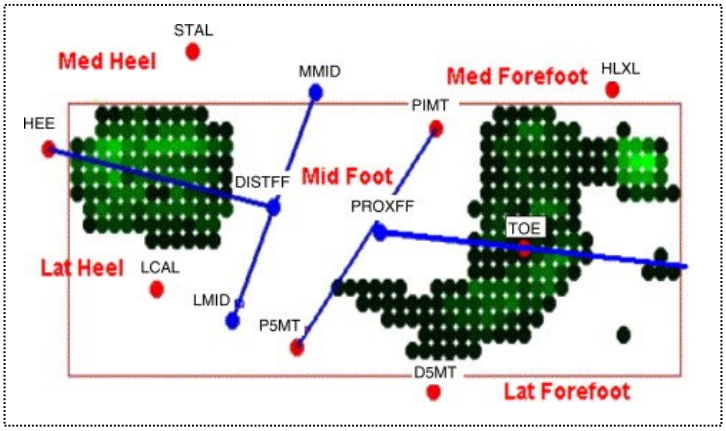

Figure 1.34: Pressure footprint showing five sub-areas: medial heel, lateral heel, midfoot, medial forefoot, and lateral forefoot. The labelled circles represent the projected positions of markers on the foot. Reprinted from [193]; Copyright (2020) with permission from Elsevier Inc.

In addition to helping in clinical decision making, anatomical masking techniques have shown their potential to be used for identifying the correlation between the kinematics of foot segments and regional loading, with more accurate identification of ROIs. Giacomozzi, et al. [178] used an integrated kinematics-force-pressure system to measure Rizzoli multi-segment foot kinematics and plantar pressure in healthy individuals during walking. Anatomical masking was implemented to pair the kinematic segments with the corresponding regions in the plantar pressure map (Figure 1.35), and through correlation analyses, the regional kinematics-pressure associations were sought. Weak to moderate correlations were observed in all regions especially between sagittal-plane foot segment kinematics and plantar pressure. The findings of this study indicated that foot joint mobility was inversely correlated to plantar pressure, meaning that the higher joint mobility would be accompanied by the lower plantar pressure. A further step was taken by Caravaggi, et al. [176] who used stepwise multiple regression analysis to find the relationship between walking speed, segmental foot kinematics, and corresponding plantar pressure regions in healthy normal-arched individuals. The anatomical masking was done similarly to Giacomozzi, et al. [178]. Six corresponding ROIs were obtained, where the joint ranges of motion and mean/peak regional plantar pressure were extracted. The results of this study indicated that joint rotations, especially in the sagittal and the frontal planes, as well as walking speed could account for between 6% and 43% of the variation in plantar pressure depending on ROI. In addition, the lower joint mobility was associated with higher plantar pressure in the rearfoot and forefoot which was consistent with the previous studies. The findings of available literature, therefore, suggest the capability of anatomical masking in detecting a close relationship between joint motion and plantar loading.

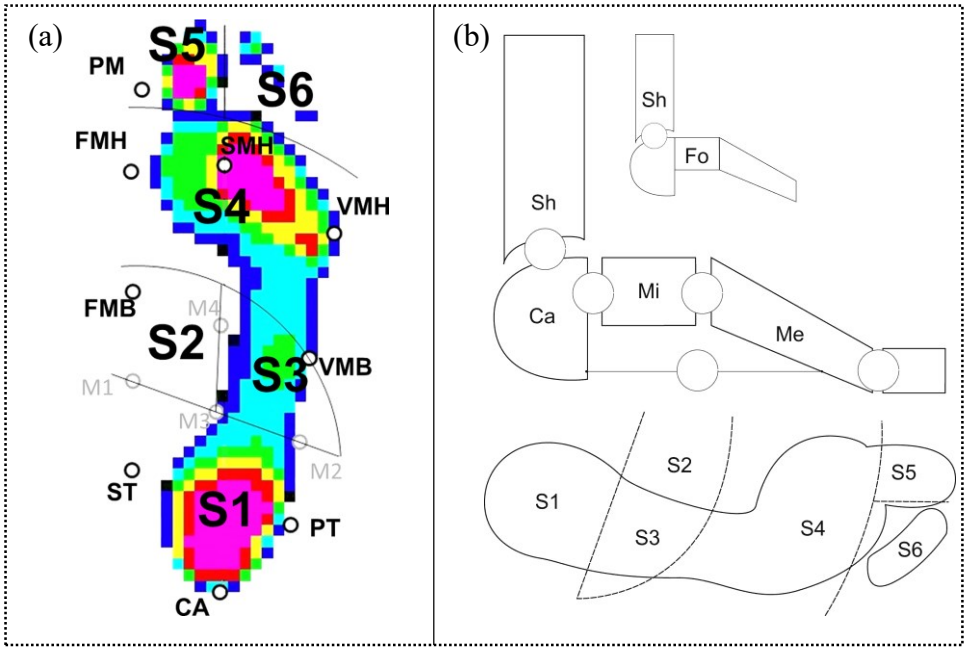

Figure 1.35: (a) Anatomical identification of regions for Rizzoli foot model, (b) Diagram of foot segments and corresponding plantar pressure regions. Reprinted from Giacomozzi, et al. [178]; Copyright (2020) with permission from Elsevier Inc.

This integrated approach suggests an inevitable improvement in reporting regional foot function because it defines meaningful regions adapted to the foot anatomical structure of the target population rather than the plantar surface geometry. Furthermore, the correlation and regression models of the aligned segmental foot motion and regional pressure obtained from this technique will be more reliable for clinical use [178, 189]. Another benefit of this technique is to facilitate the path to standardize the definition for ROIs, and to overcome the heterogeneity that exists in common masking techniques. Following a standard approach would enable clinicians and researchers to compare pressure-related regional datasets and facilitate making decisions for treatment and rehabilitation [178, 189]. On the other hand, developing such integrated anatomical masking algorithms is accompanied with some challenges. Since the location of foot markers plays an important role in this approach, the marker placement should be done by an expert practitioner. In addition, it is suggested to use the acquisition of at least five trials rather than a single trial [198]. Another challenge is using reliable and accurate hardware and software tools for temporal synchronization as well as the alignment of kinematics and pressure data [189]. Since anatomical masking proposes several clinical and biomechanical benefits compared to other masking

techniques, and it has been validated before, this approach will be used in this thesis to create corresponding regions for foot kinematics, foot plantar pressure, and FO deformation. The relationship between integrated segmental kinematics- plantar pressure- FO deformation will then be determined using linear mixed models.

1.6.3. Application of plantar pressure for flatfoot subjects

Plantar pressure analysis is a good technique to assess the relationship between the abnormal foot posture in flatfoot subjects and foot function. A recent systematic review study [99] summarized the results of available literature on the alteration of plantar pressure in flatfeet compared to normal feet subjects. Flatfoot subjects showed the most substantial difference in forefoot and hallux regions compared to normal feet. In general, flatfoot subjects exhibited higher peak pressure, maximum force, and contact area under the regions of medial arch, central forefoot, and hallux, whereas they exhibited lower peak pressure and maximum force in the lateral forefoot compared to normal foot [50, 199]. Based on these observations, it is expected that FOs could alter such an imbalance of pressure and ameliorate the loading distribution in flatfoot subjects.

There are just a few studies that reported the effect of FO on plantar pressure distribution in adult flatfoot subjects. The FOs for flatfeet subjects have been mostly designed with the goal of increasing the support and contact area in the medial arch [84, 200]. They are also favored to attenuate the force at heel strike and distribute pressure at midstance to facilitate a proper push off [84]. Some studies reported similar efficiency for customized *versus* prefabricated FOs for flatfoot subjects [84, 201]. Khodaei, et al. [84] asked 19 flatfoot subjects to walk on a walkway equipped with *Pedar®-x platform* system for three different conditions, namely shoe-only, prefabricated FO, and customized FO. Ethylene vinyl acetate foam (EVA with shore 40) was used to fabricate both FOs with an average thickness of 3 mm in heel and forefoot regions. For data analysis, the plantar foot surface was divided into eight anatomical regions, namely heel, medial midfoot, lateral midfoot, first metatarsal, second metatarsal, third-fifth metatarsal, hallux, and lateral toes (Figure 1.36-a). In addition, Redmond, et al. [201] asked 15 flatfoot subjects to walk on a walkway at their comfortable speed, where the *Pedar* in-shoe pressure system was inserted inside the shoes. The customized FO was fabricated from the casts of each participant posted to their neutral calcaneus stance position. The prefabricated contoured FO had a 4° varus rearfoot post. Both FOs were made from EVA. Five masking regions were selected for comparing the pressure data which were

corresponding to foot anatomical areas, namely as the heel, midfoot, medial forefoot, lateral forefoot, and hallux (Figure 1.36-b). The results of both studies showed that both customized and contoured prefabricated FOs could decrease the peak pressure and force under metatarsal and heel regions and increase pressure and contact area under the midfoot region (medial midfoot region) compared to shoe-only condition [84, 201]. However, significant differences were not found between prefabricated and customized FOs in any of these anatomical regions. Therefore, it was concluded that the customized FO exhibited a similar level of efficiency to prefabricated contoured FO for flexible flatfoot subjects in terms of foot pressure distribution. In contrast to these observations, Xu, et al. [200] reported that customized FOs were more efficient than prefabricated FO for symptomatic flatfoot subjects. In this study, 80 subjects with bilateral flatfoot were divided into the control group and the experimental groups. The control group subjects were asked to wear the prefabricated FOs and the experimental group to wear customized FOs (made from EVA) for eight weeks, where the plantar pressure and comfort level were compared between groups. The *Footscan* platform system (*RSscan International*) was used to record the plantar pressure during walking, and 10 masking regions were applied to analyze the pressure data (refer to section 1.6.2). The results showed higher peak pressure in the midfoot and lower peak pressure at 3rd metatarsal for customized FO compared to prefabricated FO. The findings of this study suggested that customized FO performs better than prefabricated FO for distributing the load from forefoot to midfoot as well as comfort level. Due to the few number of available research as well as the controversy that exists between studies, further research is necessary for evaluating the pressure distribution in larger sample sizes, and standardizing the masking areas for plantar pressure analysis [84, 200, 201].

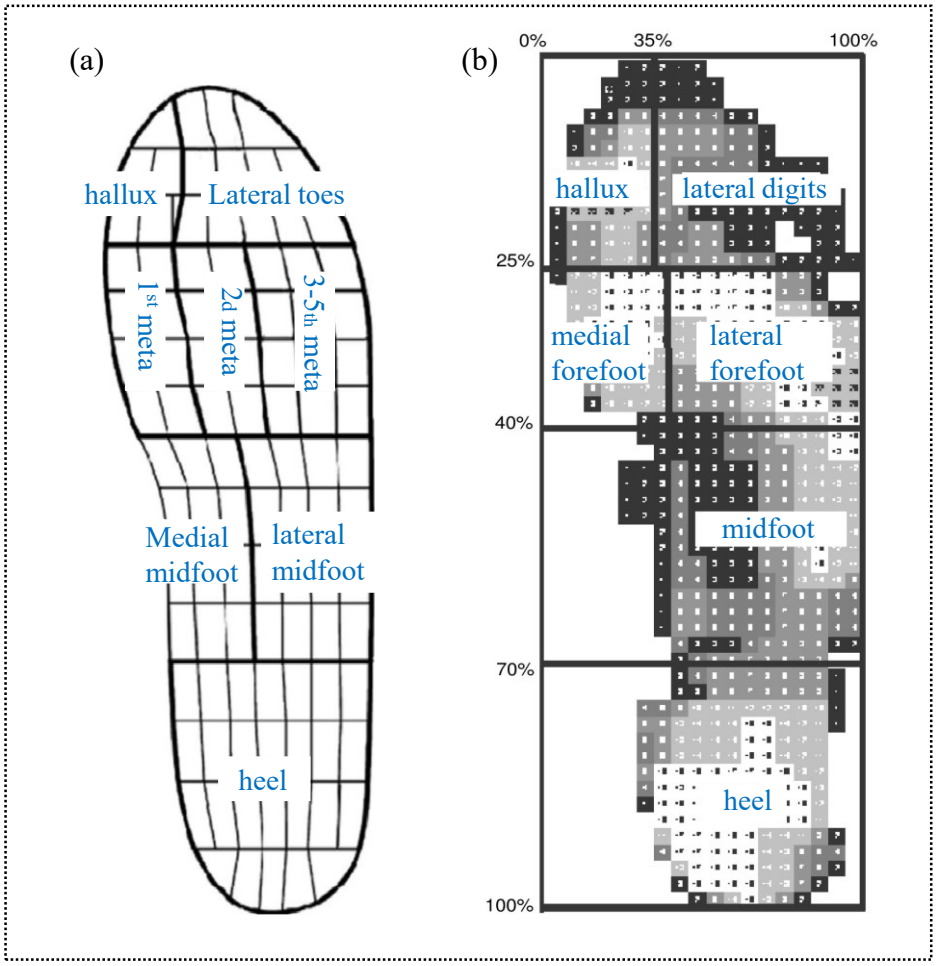

Figure 1.36: Masking areas, published by (a) Reprinted from Khodaei, et al. [84]. Copyright (2020) with permission from Elsevier Inc. (b) Reprinted from Redmond, et al. [201]; Copyright (2020) with permission from Elsevier Inc.

Summary: Plantar pressure measures can be used as a valuable dataset to realize the dynamic behaviour of the foot in the presence of abnormal foot postures such as flatfoot. Plantar pressure systems yield the distribution of the force in the whole contact area, in contrast to force platforms which provide a single resultant force. Anatomical masking of plantar pressure provides information about region-dependent foot loading, which enables researchers and clinicians to more accurately make decisions about treatment and rehabilitation plans, as well as orthosis design. Recent research showed the benefits of FOs in flatfoot subjects by transferring the pressure from the rearfoot and forefoot to the midfoot region. However, the advantage of customized design over prefabricated design is still unknown due to the heterogeneity between studies. One principal source of heterogeneity might originate from using different masking techniques. The new techniques of anatomical masking that are based on foot anatomical landmarks can be replaced by the common masking techniques that are based on the geometrical features of the plantar surface. These techniques have been confirmed to be repeatable and reliable and can be recommended as standard approach. Additionally, they integrate the regional pressure with foot multi-segment kinematics, which provide more robust variables for building correlation and regression models to extract the relationship between foot motion and foot loading.

1.7. The interaction between foot orthosis and foot biomechanics

Customized FOs are commonly prescribed with the purpose of neutralizing the static foot posture for flatfoot individuals following the Root model in clinical practice [171, 202, 203], and not the foot motion during dynamic activities. However, recent literature pointed out that static variables of foot posture are not good predictors of the response of patients to FOs [179, 202]. Foot motion and loading during dynamic activities might be among the variables that provide evidence of the patients' response to FOs. In previous sections, the approaches of dynamic characterization of FOs (section 1.4) and the determinants of foot biomechanics including kinematics (section 1.5) and foot plantar pressure (section 1.6) were reviewed. Referring to these sections, controversial results have led to limited evidence regarding the relationship between FO design and foot motion for individuals with flatfoot deformity. These controversies could originate from either inter-subject variability in foot characteristics or differences in the designs of FOs. Reaching a better understanding of this relationship could clarify the biomechanical needs of flatfoot individuals for designing customized FOs. In addition, the comparisons of the performance of FO designs have

been performed at a very general level such as the level of posting, arch height, or rigidity, while the response of individuals with flatfoot deformity to region-dependent behaviour of FO remains unknown. Multiple regression analysis and linear mixed models have the potential to assess the interaction between different variables, as shown in section 1.6.2 for the relationship between foot mobility and loading. In this section, the available knowledge on the relationship between FO design, foot motion and function, and comfort level will be overviewed.

Although foot posture has been reported to be associated with foot kinematics and plantar pressure during walking [9, 204], its contribution to account for the variations in FO characteristics has been questioned [179]. Lewinson, et al. [179] assessed whether there is any relationship between foot structure and knee joint kinetics during walking or the biomechanical response to medially and laterally wedged insoles in patients with knee osteoarthritis. The foot structure including foot mass, foot fat, foot length, foot width, arch height, and the rearfoot angle was obtained *via.* 3D foot scanning (Figure 1.37), and knee joint moment using gait analysis. Multiple regression analysis was used to assess the probable relationships. This study concluded that any parameters of foot structure did not play a significant role in predicting the individual knee joint loading during walking, and neither did it in predicting their response to wedged insoles. A further study was additionally developed by Jarvis, et al. [202] to investigate whether any correlation exists between the static foot structural deformities, which are dominantly used as determinant factors to design FOs in clinics (Root theory), and foot kinematic during gait. To reach this goal, a set of parameters in static foot posture and their corresponding foot kinematic parameters were measured and compared. The static assessment consisted of neutral and relaxed calcaneal stance positions, range of ankle dorsiflexion, range of motion for 1st ray, and frontal position of the forefoot relative to rearfoot. Foot kinematics during gait was additionally calculated using the six-segment model, consisting of leg, calcaneus, midfoot, lateral forefoot, medial forefoot, and hallux [205]. The results of this study indicated that no relationship existed between static foot assessments in the Root *et al*. protocol [171, 203] and foot kinematics during gait. The findings of these studies therefore raised the concern of using the factor of static foot structure for clinical evaluation of the foot and to prescribe FOs.

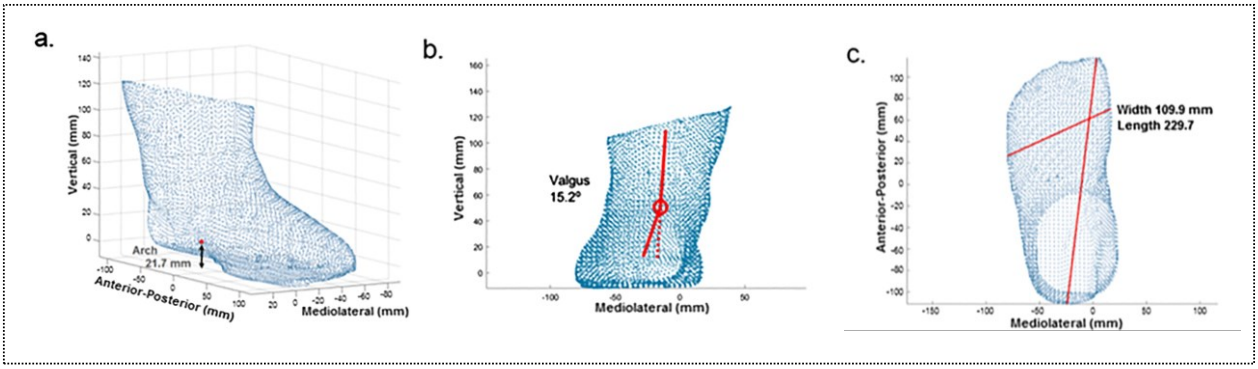

Figure 1.37: foot structure measurement example for one subject, (a) arch height, (b) rearfoot angle, (c) width and length of the foot. Reprinted from Lewinson, et al. [179]; Copyright (2020) with permission from Elsevier Inc.

Differences that exist in the responses of flatfoot subjects to customized FOs might originate from the variations in foot characteristics. In order to inspect this issue, Arnold, et al. [169] classified the individuals with flatfoot deformity into two groups of biomechanical "responders" who showed a reduction in peak calcaneal eversion during walking with customized FOs *versus* biomechanical "non-responders" who neither changed nor increased the peak calcaneal eversion. A set of outcome variables, namely peak and range of motion for calcaneal eversion, time to peak calcaneal eversion, peak rearfoot eversion moment, mediolateral excursion of the center of pressure, and peak dorsiflexion of 1st metatarsophalangeal joints, were specified for both groups during walking with footwear (baseline condition). Discriminant function analysis was performed for the variables that showed a significance level of $p < 0.1$ between the two groups, as potential variables, to determine which of them were significant predictors of the biomechanical response to FO condition. The results of this study showed that flatfoot individuals with higher rearfoot eversion at baseline condition (i.e. walking with footwear) were the ones who responded to FOs. Therefore, it was suggested that the response to FO is associated with foot motion during dynamic activity rather than its neutral static posture.

Another important factor in the design of FOs is their comfort besides their role to align skeleton and prevent pain or further injuries. In fact, comfort is the primary factor through which the individuals decide to continue or stop using their FOs [206]. The design and rigidity of FOs would impact foot kinematics and loading as well as the perceived comfort during dynamic activities [206]. Therefore, a study was designed with the purpose of assessing the interaction between the

changes in comfort and alteration in foot kinematics, kinetics, and muscles' activations [206]. To reach this goal, three orthosis conditions, namely posting, custom molding, and posting added to custom molding, as well as control condition were recorded during running. Multiple linear regression was then used to evaluate how much variation in the comfort level could be accounted by the changes in the foot motion variables. In addition, discriminant analysis was performed to determine whether the predictors from the regression analysis could discriminate between different FO conditions. The results of this study showed that foot kinematics, kinetics and muscle activation could partially predict (R^2 =34.9%) the comfort level during running. In addition, the variables of foot biomechanics could classify 75% of cases correctly to their corresponding FO conditions. This finding proposed that multiple regression analysis was able to establish the relationship between FO behaviour, *i.e.* comfort level, and foot biomechanics, *i.e.* kinematics, kinetics, and muscle activations.

Some other studies exist assessing the relationship between FO and foot biomechanics by testing and comparing the effects of different designs. Telfer, et al. [207] compared the effect of ¾ length semi-rigid customized FOs with different levels of postings, changing from 6° of lateral posting with 2° increments to 10° of medial posting, on rearfoot kinematics (Figure 1.38), ankle joint kinetics, and plantar pressure of flatfoot individuals. A linear significant relationship was observed between the level of posting and rearfoot eversion, ankle eversion moment, and plantar pressure at the lateral rearfoot, midfoot, and lateral forefoot regions. Each 2° increase in the level of medial posting was accompanied by a mean of 0.15° decrease in rearfoot eversion. Based on these results, a dose-response effect of customized FOs with posting on rearfoot kinematics, kinetics, and plantar pressure could be concluded. A further study compared the effects of three types of insoles, namely flat insole, insole with arch support, and insole with arch support plus cushion pads, on rearfoot kinematics and kinetics of flexible flatfoot participants during walking [158]. The results showed a higher efficiency of insoles with arch support compared to flat insole in terms of reducing rearfoot eversion, which might be associated with their potential to decrease the risk of further injuries.

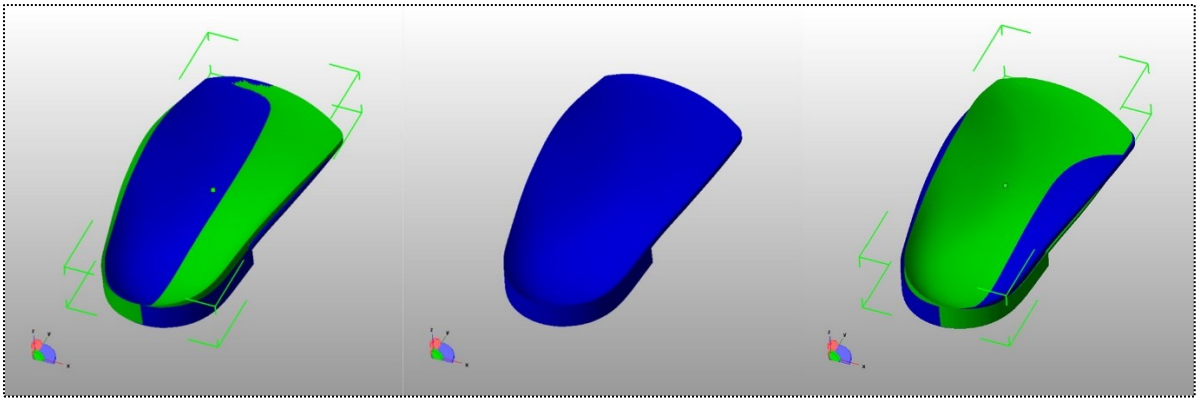

Figure 1.38: Extrinsic posting in customized foot orthosis design changing from lateral posting (left) to neutral posting (center) to medial posting (right). Reprinted from Telfer, et al. [26]; Copyright (2020) with permission from Elsevier Inc.

Furthermore, some studies have evaluated the effects of FO rigidity on foot motion and comfort level. Balsdon, et al. [32] assessed the efficiency of hard *versus* soft customized FOs for supporting the medial longitudinal arch compared to prefabricated FO and barefoot using fluoroscopic images during walking. The results on flatfoot participants suggested that both hard and soft customized FOs supported the medial longitudinal arch against collapsing more than prefabricated FO and barefoot. However, the hard and soft customized FOs showed similar levels of efficiency. In addition, Su, et al. [208] looked at the effects of the material hardness and the arch height support of customized FOs on foot motion, plantar pressure, and stress distribution of foot tissues of flatfoot individuals. FOs with three different arch heights (type I: 27 mm, type II: 30 mm, type III: 33 mm) and three levels of hardness (Shore A 30, Shore A 35, Shore A 40) were manufactured for experiments on one flatfoot participant, and stress in tissues was calculated using finite element analysis. The results of this study showed that the higher height of arch support and higher material hardness positively affected the support of the medial arch. However, higher rigidity was accompanied by higher plantar pressure regardless of the height of the medial arch, which was subsequently leading to greater foot ligaments and joint cartilage stress (Figure 1.39). Therefore, the design of customized FO should be based on a modulation between the level of correction in foot motion and the level of pressure and stress imposed on joints and ligaments. This study investigated just one subject with flatfoot, which cannot be representative of the whole population. To our knowledge, there is no exhaustive study that evaluates the interaction between FO dynamic behaviour and foot kinematics and plantar pressure in individuals with flatfoot deformity. In this

thesis, this interaction will be developed using anatomical masking techniques and linear mixed models. Using these techniques could enable us to extract the region-dependent relationships rather than the whole plantar surface.

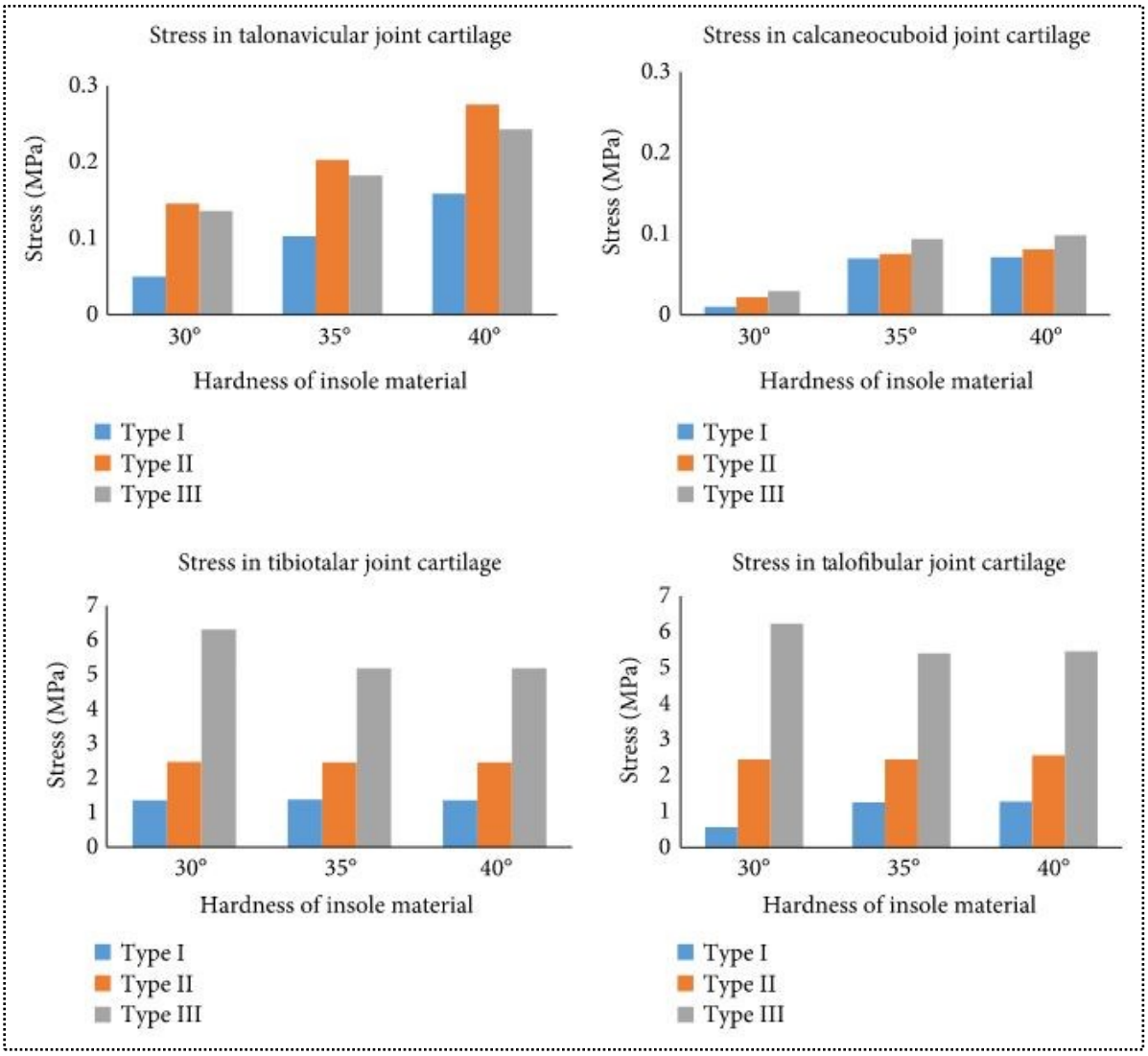

Figure 1.39: The maximum stress in joint cartilage for different arch heights and hardness of foot orthosis calculated from finite element analysis. The x-axis of each subplot represents three insoles with different levels of hardness. The type I, II, III in the plots show the insoles with different heights of the medial arch. Reprinted from Su, et al. [208]; Copyright (2020) with permission from Hindawi Publishing.

Summary: The design of customized FOs should be based on the demands of individuals with flatfoot deformity. Previous literature doubted whether static foot posture could provide useful information for prescribing FOs. The strategies to design FOs, therefore, should be guided towards the dynamic motion and loading of the foot. To date, some suggestions and guidelines have been provided for designing FOs. However, limited evidence exists on the efficiency of available FOs, which might be due to the variations between subjects or variations in the approaches for designing FOs. A necessary step to reach this goal is to find the relationship between the dynamic characterization of FO and the parameters of foot dynamics. Multiple regression analysis and linear mixed models are robust statistical approaches to find the interaction between multiple parameters, which have the potential to be used for this purpose.

1.8. Problem and specific objectives

The ultimate goal of this thesis is to realize the response of FOs to dynamic loading and its dependency on foot motion and function. Although FOs are commonly used to deal with foot deformities, there are still several uncertainties, controversies, and gaps in this field. The clinical practitioners have access to known FO theories such as the Root model to prescribe customized orthosis following visual and anthropometrical assessments. However, a limited consensus has yet been reached on the prescription criteria. In addition, industries that design and fabricate these medical devices have taken advantage of CAD/CAM to integrate more details and accuracy in the design of FOs. However, such designs have been established based on basic characteristics of the foot and through trial and error iterations. As a result, the target population of FOs will finally receive a product which holds uncertainties to optimally respond to the individuals' demands. To our view, the primary points that should be addressed before overcoming this issue are as follows. The first point is that there is no database or comprehensive research to gather all the available knowledge on different designs of FO and quantitatively ensemble their impact on lower body kinematics. While a systematic review and meta-analysis could reveal the alteration in foot biomechanics related to FO design, the mechanism underlying such relationship still remains unknown. In order to resolve this ambiguity, we primarily need some metrics which represent the time-dependent characterization of FO regions. Finally, the mentioned underlying mechanism can

be realized *via* the relationship between the determinants of foot biomechanics, *i.e.* foot kinematic and plantar pressure distribution, and FO behaviour. Regarding the mentioned gaps, the specific objectives of this thesis could fall into the following three categories:

Specific objective 1: Investigating the effects of common designs of foot orthosis on the motion of the lower body

The designs of foot orthosis might exert significant alterations on the motion of the foot, knee, and hip. A clear understanding of these alterations is important for informing the clinical practitioners that aim to restore or enhance the lower body function. Several independent studies have reported the interaction between FO design and body dynamics. However, no comprehensive assessment of the available literature on foot orthosis function has yet been performed.

Therefore, this thesis aimed to conduct a systematic review and meta-analysis on the reported quantitative data on lower body function as an effect of walking with foot orthosis. It was hypothesized that different additions to FO designs such as postings, heel supports, and arch supports would alter the kinematics and kinetics of the lower extremity differently. It was additionally assumed that this systematic review will enable us to report the methodological weaknesses of the included studies.

Specific objective 2: Representing the dynamic behaviour of foot orthosis

The deformation of FO is a potential variable to represent its response to different loading conditions. Using mechanical testing or cadaveric experiments, it is possible to simulate certain phases of walking to estimate the orthosis deformation. However, the responses would be limited to some discrete points in gait. Finite element analysis is an alternative approach, while it inquires some simplifications in modeling the geometry and boundary conditions. Artificial intelligence is a further approach which can yield the continuous dynamic behaviour of orthosis without any need for simplification, while it has not been previously implemented for this purpose.

Therefore, the second objective of this thesis was to predict the deformation of the plantar surface of FOs using an AI approach. It was hypothesized that the AI approach could differentiate between different regions and rigidities of FOs as well as different phases of the gait cycle.

Specific objective 3: Understanding the interaction between foot orthosis and foot biomechanics

The third objective of this thesis was to examine the presence of any dependency between FO deformation and foot motion and loading during gait. More specifically, we were interested to understand whether multi-segment foot kinematics and regional foot plantar pressure could predict the variations in the regional deformations of foot orthosis in individuals with flatfoot deformity. Linear mixed models were built for five regions of foot orthosis and over four phases of the gait cycle to examine this dependency. It was hypothesized that the alterations in the kinematics and plantar pressure of flatfoot individuals play an important role in deforming different regions of foot orthosis during the gait cycle.

Chapter 2 - Can Foot Orthoses Impose Different Gait Features Based on Geometrical Design in Healthy Subjects? A Systematic Review and Meta-analysis

This chapter is presented as an article, published in *The Foot* journal. This article was co-authored by Maryam Hajizadeh, Gauthier Desmyttere, Jean-Philippe Carmona, Jacinte Bleau, and Mickael Begon. Maryam hajizadeh had a major contribution and was the corresponding author for this article. Defining the question of this study and the inclusion criteria for articles, as well as comprehensive search in databases were performed by Maryam Hajizadeh. The review of papers for including/excluding them, the quality check of included articles, and extracting the results were performed by Maryam Hajizadeh and Gauthier Desmyttere. Data synthesis and analysis was performed by Maryam Hajizadeh in collaboration with all coauthors. This article was written by Maryam Hajizadeh and supervised by Mickael Begon. All co-authors contributed in reviewing the article and shared their comments and suggestions to improve its context.

Published as: Hajizadeh M, Desmyttere G, Carmona JP, Bleau J, Begon M (2020) Can foot orthoses impose different gait features based on geometrical design in healthy subjects? A systematic review and meta-analysis. *The Foot*; 42:101646. https://doi.org/10.1016/j.foot.2019.10.001

Abstract

Objective: Foot orthoses (FOs) are popular treatment to alleviate several abnormalities of lower extremity. FO designs might alter lower extremity biomechanics differently, but the association is not yet known. This review aimed to evaluate how different FO designs, namely FO with medial posting, lateral posting, arch support, or arch & heel support, change lower limb kinematics and kinetics during walking.

Literature Survey: Electronic database search were conducted from inception to March 2019, and 25 papers passed the inclusion criteria. Two independent reviewers checked the quality using a modified Downs and Black checklist (73.7±5.5%) and a biomechanical quality checklist (71.4±17.1%). Effect sizes for differences between with- and without- FO walking were calculated, and meta-analysis was performed whenever at least two studies reported the same variable.

Results: Medial posting reduced peak ankle eversion moment. Lateral posting brought about higher peak ankle dorsiflexion and peak ankle eversion for kinematics, as well as higher peak ankle abduction moment, lower peak knee adduction moment, and higher peak mediolateral ground reaction force (GRF) for kinetics. FOs with either arch support or arch & heel support tended to decrease vertical ground reaction force, but it was not significant.

Conclusion: The findings of this review reveal that medial or lateral posting work efficiently to change foot and knee kinematics and kinetics. However, the impact force is just slightly decreased by arch-supported and heel supported FOs. Due to the small number of available studies, and heterogeneity in meta-analysis findings, further research with more standardized biomechanical approach are required.

Keywords: foot orthosis, posting, arch support, arch & heel support, meta-analysis, gait analysis

2.1. Introduction

Foot orthosis (FO) has been suggested as an intervening tool to control the transmission of ground reaction force (GRF) to bony structures and soft tissues [209, 210]. The foot, as the in-contact segment, adapts primarily to FO effect by producing, attenuating or re-orienting motion [209]. The compensatory mechanisms are then generated by knee and hip, as non-contact segments, to response for inter-joint coordination and support movement propulsion [211]. Therefore, FO can be used to prevent and relieve not only foot injuries, but also knee and hip musculoskeletal disorders [212]. FOs might behave differently in terms of their contribution to control three-dimensional joint kinematics and kinetics based on their specific designs. Various designs of FO are available in the market, whereas a few studies evaluated their design impact on biomechanical outputs. Furthermore, there is no database to introduce classification of designs for common FOs based on their biomechanical effects.

Several studies have confirmed the synergic effect between musculoskeletal disorders and abnormal foot motion during walking [211, 213-215]. For example, in individuals with lateral ankle sprain, greater range of motion for subtalar joint has been observed, predisposing them to ankle osteoarthritis [216]. Generally, excessive foot motion due to flatfoot or pronated foot might lead to foot, knee and hip problems including joint and tendon damage in inflammatory conditions such as rheumatoid arthritis [173], anterior knee pain, tendinopathy and knee arthritis symptoms [217], and higher vulnerability of elderly individuals to hip osteoarthritis due to intersegmental coupling [218, 219]. In addition, plantar fasciitis can be prolonged due to higher first metatarsophalangeal joint dorsiflexion [220]. On the other hand, patients with medial knee osteoarthritis suffer from higher knee adduction moment and more medial knee contact force. To compensate, they might alter foot progression angle, by more lateral foot contacts, to reduce the lever arm between GRF and knee joint center in frontal plane. Such strategy could help them to reduce knee adduction moment as well as medial contact force [221, 222], and avoid pain [213]. Based on these evidences, a proper FO design can be an efficient candidate to deal with different musculoskeletal problems by controlling the foot posture.

Various modifications have been implemented in the design of FO to deal with several pathologies. When there is a need to incline the foot medially, a medial posting would be added to FO design. The medial posting might incline the rearfoot, forefoot, or full-length of the foot [173, 221]. On

the other hand, lateral postings are designed to incline the foot laterally either on rearfoot, forefoot, or all foot length [173, 223]. Adding arch support pads or designing a contoured FO that follows the arch shape can prevent the collapse of medial arch and provide stability and balance [222, 224]. FOs with heel cup have a concave shape at the heel region in order to absorb the shock of ground reaction force, maintain the foot alignment [225, 226]. Therefore, it is important to understand the biomechanical effect of each FO design in order to suggest proper FO to patients.

While some studies have suggested specific designs of FO to prevent or improve lower extremity injuries, controversies and variabilities exist between studies regarding their biomechanical performance. As the effect of walking with medial posting, studies found it both efficient [173, 210] and without significant effect [227, 228] to reduce rearfoot eversion and foot pronation. Increase in knee adduction moment with this orthosis has then been confirmed [210] or questioned [221]. Although lateral posting was shown to response for reduction in knee adduction moment [213, 222, 229-231], some contrary results were reported as well [173, 210, 232]. Inconsistencies also exists in higher [211, 228, 229] or lower [173, 221, 233] ankle eversion and ankle eversion moment with this posting. No evidence has yet been found as the effect of FO with medial arch support on either foot kinematics or GRF [217, 222, 226]. Similarly, there still remains ambiguity as to whether heel cup insoles are efficient to absorb the shock of impact force during walking [225, 226].

To our view, the necessity and benefit of a meta-analysis in this area fall into two main aspects. *(i)* As long as any individual study verifies a significant effect of a specific FO design, and this effect remains consistent between studies with similar FO, the applicability of that design could offer a guide reference for podiatrists and clinicians. The importance of providing such reference is highlighted when the clinicians do not have any database to detect which FO design could modify joint loading in order to help individuals walking more efficient and less painful. *(ii)* On the other hand, inconsistent findings between studies or lack of evidence in individual studies could be inferred to methodological weaknesses. Detecting and introducing such weaknesses could provide hints for further studies to pursue higher methodological and biomechanical standards and reduce the sources of error.

Although computer aided design and manufacturing technology have facilitated the production of customized FOs [173], the biomechanical effect of different designs of FO is still unknown. Some

previous reviews have assessed the effect of FO on kinematics, kinetics and impact forces [234, 235], but none of them evaluated how these effects change depending on FO geometrical design. The aim of this study was primarily to find previous literature for different designs of FO and categorize them based on FO design. Then a meta-analysis was performed to find any changes in kinematics and kinetics of lower extremity during walking with each design of FO compared to walking either with shoes or barefoot. We focused deliberately on healthy subjects to avoid the ambiguity on whether changes were due to the effect of FO design or a compensation for pathology.

2.2. Methods

2.2.1. Search strategy

Three main groups of keywords describing "foot orthosis", "design and geometrical modifications" and "biomechanical and locomotion metrics" were devised. Each group was a combination of several related MeSH terms and keywords. An electronic search was then performed in five databases namely Scopus, EMBASE, Medline, PubMed, and Cochrane library from their oldest available date to March 2019. The search string took advantage of the Boolean Operator "AND" to combine the three main groups, and "OR" to provide a comprehensive set of terms for each group (Supplementary materials: Groups of keywords). A double-screening method was used to detect the eligibility of studies by "MH" and "GD". The full text was reviewed for papers with lack of sufficient information in their title and abstract. Any disagreement between assessors was solved by argument and consensus.

2.2.2. Selection criteria

Eligible articles had to be peer-reviewed *in-vivo* studies (except pilot studies), written in English, based on gait analysis approach during walking either on treadmill or along walkway, and focusing on healthy adults with no history of lower extremity injury. Then, the publications evaluating the effect of FO material or production approach (casting, molding, etc.), or evaluation with high-heel shoes were excluded. The eligible articles were additionally narrowed to ones that considered the four most-common FO designs. These groups were medial posting, lateral posting, arch support, and arch & heel support. FO with medial posting was considered as FO inclining the foot medially with either rearfoot posting or a full-length wedge. Lateral posting was composed of the FO design

that inclined the lateral foot region with either rearfoot posting or full-length wedge. FOs with arch support used contour shape or pad in order to maintain the medial longitudinal arch. FOs with arch & heel support added a heel cup to arch-supported FO. FOs with total contact insert were included in the arch & heel support group. The articles with other types of FO or a combination of mentioned groups were excluded. Finally, eligible papers were limited to ones addressing kinematics and kinetics of lower extremity as well as GRF.

2.2.3. Methodological quality

The quality of included studies was assessed by two independent reviewers, MH and GD, using modified Downs & Black checklist for non-randomized trials [236]. This checklist included eight items for reporting, two for external validity, four for internal validity (bias), three for internal validity (confounding), and one for power, as used in previous reviews (Supplementary materials: Table S 2.I) [237, 238]. Each item was answered as 0 ("no"), 1 ("yes") or UD ("unable to determine"). Item 5 asking about principal confounders was the only item answered 0 ("no"), 1 ("partially"), 2 ("yes"), and UD ("unable to determine"). The confounders were regarded as walking speed, foot orthosis material, proof of healthy foot, and shoe model to answer this item. Here, the quality of each study was reported as a percentage of maximum possible score. A paper was classified as high quality for score $\geq 75\%$, moderate quality for $60\% \leq$ score $< 75\%$, and low quality for score $< 60\%$ [238]. Inter-rated agreement for quality assessment was estimated by κ level of agreement [239] for each question ranging from 0 to 1. The agreement was reported as slight $0.00 < \kappa \leq 0.20$, fair $0.21 < \kappa \leq 0.40$, moderate $0.41 < \kappa \leq 0.60$, substantial $0.61 < \kappa \leq 0.80$, and almost perfect $0.81 < \kappa \leq 1.00$ [240].

In addition, the quality of biomechanical measurement was estimated based on markerset and walking condition. The questions of this section were also answered as 1, 0, unable to determine (UD), and not applicable (NA). Placing markers on skin (1) or shoes (0), considering foot as multi-segment (1) or single segment (0), and using more than (1) or equal to (0) three markers on each segment were scored in markerset section. Studies which did not evaluate foot kinematics/kinetics got NA in the first two questions of this section. In addition, this section was not relevant for studies evaluating only GRF. The quality of walking condition was determined based on four parameters: walking with shoes (1) or barefoot (0); walking along walkway (1) or on treadmill (0); the number of cycles with more than or equal to 5 cycles (1), otherwise (0); monitoring and controlling the

speed of walking (1), otherwise (0). Those experimental aspects are known to affect the quality of outcome measures [241-246] and also the gait pattern [247-250]. The score was expressed in percentage and the biomechanical quality was classified similar to the methodological quality.

2.2.4. Data extraction and reporting

Several methodological details of studies including population (sample size, sex, and age), experimental protocol, foot model, foot orthosis (design and material), shoe model, and outcome measures were extracted. In addition, peak values [mean ± SD] of kinematics and kinetics in sagittal, frontal, and transverse planes for foot, knee and hip as well as vertical and mediolateral GRF were extracted as dependent variables. The authors who did not report the numerical values of mentioned outcomes were contacted [173, 230, 251-253]. We reported foot results as one segment, since only six studies used multi-segment foot models [173, 211, 217, 222, 223, 253, 254]. The extracted data were reported in any corresponding four groups of foot orthosis.

To extract and report data the following aspects were considered: the nearest value to normal walking speed [255] was selected for studies with different speeds [211, 252]; the more commonly-used wedging inclination was selected for studies with multiple wedging inclinations [173, 221, 223, 231, 251, 256, 257]; for peak knee flexion moment and peak knee adduction moment the higher peak value was selected [173, 213, 223, 230, 254]; one reference frame was selected in studies which reported kinematics in different frames [217, 254]; when the data were collected in different sessions, the results of first session were extracted [232]. The synthesis of this review followed the PRISMA guideline for reporting systematic reviews and meta-analysis.

2.2.5. Statistical analysis

RevMan (version 5.3, Copenhagen: The Nordic Cochrane Centre, The Cochrane Collaboration, 2014) was used to perform meta-analysis for variables reported by at least two studies in each group of foot orthosis. Forest plots enabled us to inspect the effect of foot orthosis on dependent variables by calculating effect size (ES) using standardized mean difference in a randomized effect model. In addition, they could reflect 95% confidence interval (95% CI), overall effect (p value), and heterogeneity index (I^2). Pooled ES were regarded as trivial ($ES \leq 0.2$), small ($0.2 < ES \leq 0.5$), moderate ($0.5 < ES \leq 0.8$), and large ($ES > 0.8$) [258]. When 95% CI crossed zero ($p > 0.05$), no significant differences could be inferred from meta-analysis. The level of inconsistency between

included studies was estimated as low, moderate, and high with thresholds of 25%, 50%, and 75% for I^2 [259]. Wherever a significant difference was observed for peak joint rotations, the mean difference (net difference in degree between with- and without- orthosis) was also calculated. Mean differences were easier than ESs to be interpreted clinically.

2.3. Results

2.3.1. Search results

Our literature search yielded 4756 articles, from which 1628 were removed as duplicates (*i.e.* 3128 articles). Initial screening based on title and abstract retrieved 386 relevant articles. There, the full texts of articles were reviewed to further check the inclusion criteria and details of orthosis design, where 361 papers were excluded. A final screening was performed with focus on reported outcome measures, which handled 25 papers for further processing (Figure 2.1).

As this review looked for the effect of each orthosis design, classification of included studies was done based on the design. Through this classification one study with medial posting [257], sixteen studies with lateral posting [210, 211, 213, 216, 223, 229-233, 251-254, 256, 260], four studies with both medial and lateral posting [173, 210, 221, 228], one study with lateral posting and arch support [222], and one study with arch support and arch & heel support [226], and three studies with arch & heel support [217, 224, 225] were detected. Details of studies are available in Table 2.1.

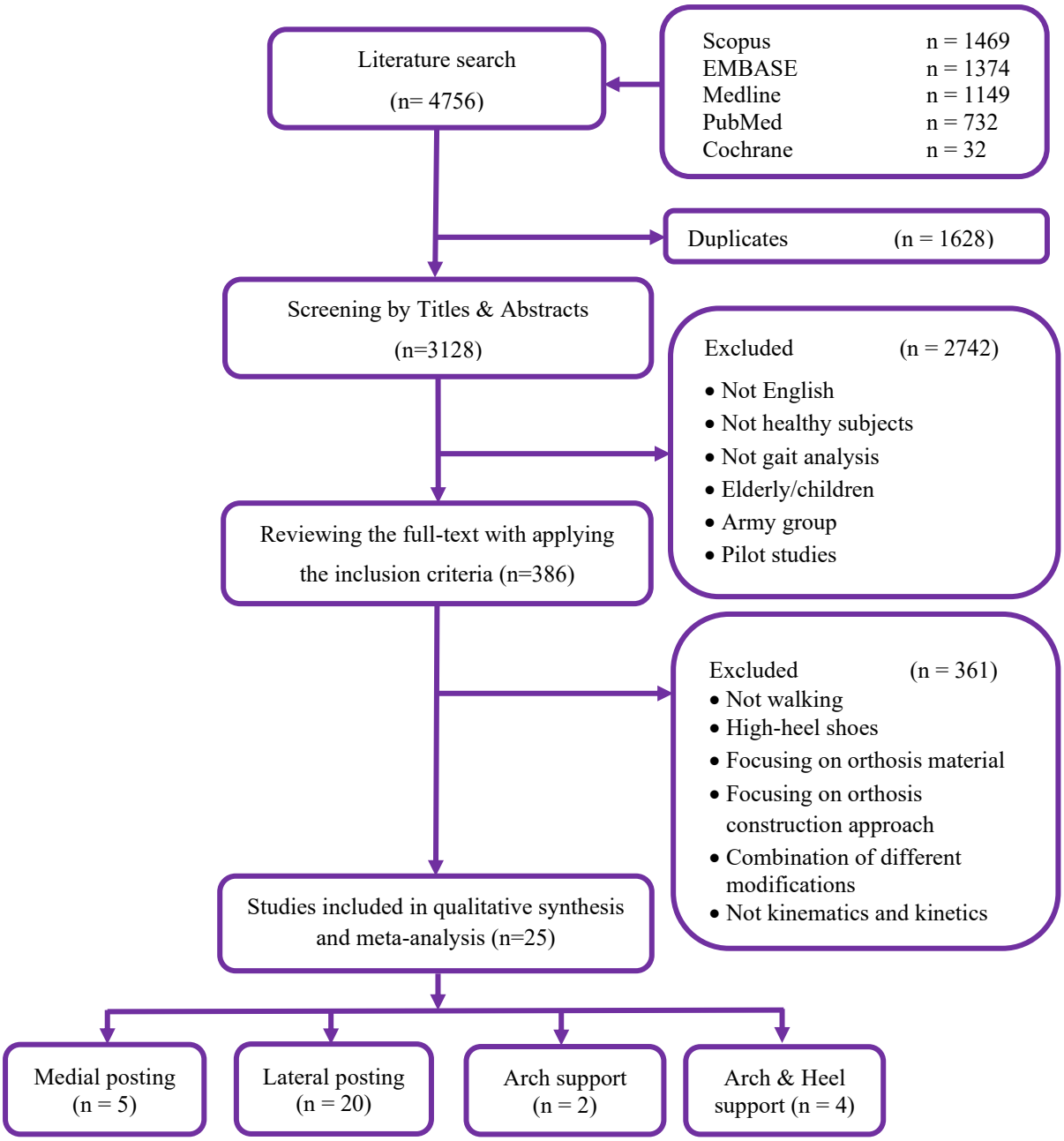

Figure 2.1 : Flow diagram of search strategy and study selection

2.3.2. Subject characteristics

The total number of participants for all included studies in the group of medial posting was 75 subjects (27 female and 48 male), with an average age of 28 ± 7 years old, height 176 ± 7 cm, and weight 70 ± 12 kg. In lateral posting group, a total number of 376 subjects (157 females, 184 males, 35 not mentioned), with age 27 ± 7 years old, height 170 ± 11 cm, and weight 66 ± 14 kg were

included. Studies with arch support included 30 subjects (19 females, 11 males), with averages of age 26 years old, height 164 cm, and weight 55 kg. Since one of two studies in this group did not report standard deviations, the subject characteristics are reported just by average value. The arch & heel support group included 71 subjects (41 females, 30 males), age of 28 ± 8 years old, height 167 ± 11 cm, and weight 61 ± 14 kg.

2.3.3. Study quality

The quality assessment showed a range from 68.4% to 84.2%. Moderate quality was achieved for 18 studies, while 7 other studies [173, 211, 222, 223, 231, 233, 260] were classified as high quality (Table 2.2). Overall, items about reporting got good scores by most of studies. The score for external validity items, however, were not met in most of studies. Only four studies [173, 211, 251, 260] reported the source of population and the criteria of selecting subjects. Out of the 25 papers, 2 studies [211, 260] stated the proportion of participants asked to attend and agreed. One paper [173] wrote about blinding for data processing in internal validity (bias). One paper [228] mentioned the time interval during which participants were recruited in internal validity (confounding) section. Finally, in power section five papers [222, 223, 231, 233, 260] declared the criteria for sample size. The κ level of agreement was substantial to almost perfect for scoring each individual item (Table 2.2). A complete agreement was achieved for all items except for item 5 about explaining the principal confounders ($\kappa = 0.74$), item 10 related to reporting actual probability values ($\kappa = 0.83$), item 11 ($\kappa = 0.96$) and item 22 ($\kappa = 0.96$) asking about the population selection.

In terms of biomechanical quality (Table 2.3) the scores ranged between 40% and 100% with nine high, eight moderate and eight low quality studies. Out of the 25 included papers, 6 studies placed the markers directly on skin [173, 211, 213, 217, 222, 228], 4 studies used multi-segment foot models for analysis [173, 211, 217, 222], 13 studies used marker redundancy (≥3 markers/segment) [173, 211, 213, 216, 217, 222, 229-233, 251-254], 19 studies asked the subjects to walk with shoes [173, 210, 211, 213, 221, 223-226, 229-233, 251, 252, 256, 257, 260], 22 on a walkway [173, 210, 213, 216, 221-226, 228-233, 251, 253, 254, 256, 257, 260], 20 collected more than or equal to 5 cycles [173, 210, 211, 213, 217, 221, 222, 225, 228-233, 251-254, 256, 257], and 18 studies monitored the walking speed [173, 210, 211, 216, 217, 221-226, 229-231, 233, 252, 253, 257].

Table 2.1. Summary of included studies

Study	Participants	Experimental protocol Task	 Foot model	Case condition: foot orthosis	Control condition: shod/bare	Outcome measures
Medial posting						
Burston, et al. [257]	n= 15 (8 F, 7M) age= 30.1 ± 10.0 y	Walking along walkway at self-selected speed 5 trials/ condition	>4 markers On shoes	5° medial wedge added to full-length Slimflex™ insoles Material: EVA	Individuals' training shoes	kinematics [°]: knee flexion kinetics [Nm]: knee flexion moment
Fukuchi, et al. [221]	n = 21 (21 M) age = 25 ± 3.4 y W=73.3 ± 9.1 kg H=178.1 ± 6.7 cm	walking along walkway at range of 1.4 m/s ≥5 trials/ condition	1 segment 3 markers on shoes	6° medial wedge added to insole, full-length material: EVA	standard neutral shoes (Aegis 2.0, Adidas international); with no extra insole	kinetics [Nm]: ankle inversion moment, knee abduction moment
Huerta, et al. [228]	n = 12 (6 F, 6 M) age = 24.6 ± 5.6 y W=62.8 ± 13.7 kg	walking along 20 m walkway at self-selected speed 10-12 trials/ condition	1 segment 3 markers on skin	7° medial wedge, rearfoot, 14 cm long and 4 cm width adhered to heel with double-sided tape material: high-density EVA	barefoot	kinematics [°]: ankle abduction, internal tibia rotation kinetics [Nm/kg]: ankle inversion moment
Nester, et al. [210]	n =15 (7 F, 8 M) age = [19-41] y	walking at a controlled cadence of 108 step/min 10 trials/ condition	1 segment 3 markers on shoes	10° medial wedge, extending from heel to 1st metatarsal placed under 3 mm orthosis material: high-density EVA	individual shoes	kinematics [°]: Internal tibia rotation relative to foot (pronation), External tibia rotation relative to foot (supination)
Telfer, et al. [173]	n = 12 (6 F, 6 M) age = 31.7 ± 10 y W=72.8 ± 12.3 kg H= 173 ± 7 cm	walking along walkway at controlled speed within 5% of individual pre-determined self-selected speed ≥7 strikes/ condition	2 segments 13 markers on skin	6° medial rearfoot posting, 3D foot surface scan and 3D printed, ¾ foot length material: semi-rigid, Polylactide	standard shoe, neutrally posted	kinematics [°]: rearfoot eversion, forefoot abduction, internal tibia rotation kinetics [%BW*height]: ankle eversion moment, knee adduction moment
Lateral posting						
Fischer, et al. [223]	N= 19 (7 F, 12 M) Age = 24 ± 3 y	Walking along 10 m walkway 3 trials/condition	3 segments Marker clusters On foot	5° lateral wedge attached under comfort insole material: High density EVA with durometer 60	Neutral frontal plane stability shoes (gel-beyond, Asics, JP)	kinetics [%BW*height]: knee adduction moment

Table 2.1 (continued)

Study	Participants	Experimental protocol		Case condition: foot orthosis	Control condition: shod/bare	Outcome measures
		Task	Foot model			
Forghany, et al. [251]	n = 8 (8 M) age = 33.5 ± 4.5 y W= 71.4 ± 10.6 kg H=170 ± 6 cm	walking along 10 m walkway at self-selected speed; 10 trials/ condition	1 segment 4 markers on shoes	5° lateral heel and sole wedge attached to flat insole material: high density vinyl acetate wedge, EVA flat insole	standard shoe	kinematics [°]: ankle eversion
Fukuchi, et al. [221]	n = 21 (21 M) age = 25 ± 3.4 y W= 73.0 ± 9.1 kg H= 178.1 ± 6.7 cm	walking along walkway at range of 1.4 m/s ≥5 trials/ condition	1 segment 3 markers on shoes	6° lateral wedge added to insole, full-length material: EVA	standard neutral shoes (Aegis 2.0, Adidas international); with no extra insole	kinetics [Nm]: ankle inversion moment, knee abduction moment
Hornestam, et al. [211]	n = 20 (14 F, 6 M) age = 23.7 ± 3.4 years W= 64.2 ± 12.1 kg H= 168 ± 6 cm	walking on treadmill (ProAction G635) at 5 km/h 30 trials/ condition	Rearfoot segment, 7 markers on skin	15° medially inclined insole, full-length material: high density EVA	standard neutral shoe (Crusader 4, Mizuno Inc); with flat insole made of high density EVA	kinematics [°]: rearfoot eversion
Huerta, et al. [228]	n = 12 (6 F, 6 M) age = 24.6 ± 5.6 y W= 62.8 ± 13.7 kg	walking along 20 m walkway at self-selected speed 10-12 trials/ condition	1 segment 3 markers on skin	7° lateral wedge, rearfoot, 14 cm long and 4 cm width adhered to heel with double-sided tape material: high-density EVA	barefoot	kinematics [°]: ankle abduction, internal tibia rotation kinetics [Nm/kg]: ankle inversion moment
Jones, et al. [229]	n = 15 (5 F, 10 M) age = 30.5 ± 8.6 y W= 66.9 ± 13.3 kg H= 169 ± 7 cm	walking along walkway at self-selected speed 10 trials/ condition	1 segment 6 markers on shoes	5° lateral wedge, full-length material: 70 shore A hardness	standard shoes (ECCO Zen)	kinematics [°]: subtalar joint eversion, knee flexion, knee varus kinetics [Nm/kg]: ankle/subtalar joint eversion moment, knee flexion moment, knee adduction moment

Table 2.1 (continued)

Study	Participants	Experimental protocol Task	 Foot model	Case condition: foot orthosis	Control condition: shod/bare	Outcome measures
Kakihana, et al. [216]	n = 25 (25 M) age = 20.7 ± 1.2 y W= 77.1 ± 13.1 kg H= 175.2 ± 4.8 cm	walking along 7 m walkway at self-selected cadence (95.8±4.0 step/min)	1 segment 7 markers on skin	6° lateral wedge insole, full-length material: EVA 8200	barefoot with 0° lateral wdge insole, flat insole, full-length, (material EVA 8200)	GRF [N/kg]: vertical GRF, mediolateral GRF
Kang, et al. [260]	n = 48 (24 F, 24 M) age = 23.5 ± 2.5 y W= 70.5 ± 21.5 kg H=170 ± 19 cm	walking along 6 m walkway at self-selected speed 3 trials/ condition	1 segment 3 markers on skin	5° lateral wedge insole, full-length	conventional shoes (flat, thin insoles)	kinetics [Nm/kg]: knee adduction moment
Kluge, et al. [252]	n = 22 (19 F, 3 M) age = 22.3 ± 2.2 y W= 62.1 ± 9.1 kg H= 166 + 8 cm	walking on instrumented treadmill at 1.3 m/s 1 minute/ condition	1 segment 6 markers on shoes	4-5° lateral wedge insole (placed under control condition insole), height of 4 mm, full-length material: cork	standard shoe model (Green Silence, Brooks) with unwedged insole and individualized arch support (igli insoles, medi)	kinematics [°]: ankle eversion kinetics [Nm/kg]: knee adduction moment GRF [N/BW]: vertical GRF, mediolateral GRF
Leitch, et al. [256]	n = 14 (10 F, 4 M) age = 44 ± 8 y W=70.4 ± 13.3 kg H= 168 ± 9 cm	walking along 8 m walkway at self-selected normal speed ≥5 trials/ condition	1 segment 3 markers	4° lateral wedge (placed under the control insole) material: EVA, 55 shore A durometer	standardized neutral shoe (New Balance 882) with no wedge insole	kinetics [%BW*height]: knee adduction moment
Molgaard, et al. [230]	n = 12 (4 F, 8 M) age = 31.9 y, range [22-50] y W= 73.5 kg H=175 cm, range [157-196] cm	walking along 10 m walkway at self-selected comfortable speed within ±5% 6 trials/ condition	1 segment 6 markers on shoes	10° lateral wedge insole, full-length model: Rehband, Technogel-Pes Velour	neutral running shoes (Nike Air Pegasus)	kinetics [%BW*height]: ankle abduction moment, knee flexion moment, knee adduction moment

Table 2.1 (continued)

Study	Participants	Experimental protocol Task	 Foot model	Case condition: foot orthosis	Control condition: shod/bare	Outcome measures
Nakajima, et al. [222]	n = 20 (9 F, 11 M) age = 28.4 ± 6.1 y W=59.8 ± 10.9 kg H=167.2 ± 9.4 cm	walking along 7 m walkway at self-selected speed with controlling cadence 5 trials/ condition	rearfoot segment on skin	6° lateral wedge insole, full-length material: EVA 8200	barefoot with 5-mm thick flat insole	kinematics [°]: knee valgus kinetics [%BW*height]: subtalar abduction moment, knee adduction moment
Nester, et al. [210]	n =15 (7 F, 8 M) age = [19-41] y	walking at a controlled cadence of 108 step/min 10 trials/ condition	1 segment 3 markers on shoes	10° lateral wedge (placed under 3mm base with cushioning material), full-length material: high-density EVA	individual shoes	kinematics [°]: ankle plantarflexion, ankle dorsiflexion, rearfoot abduction, Internal tibia rotation relative to foot (pronation), External tibia rotation relative to foot (supination) kinetics [Nm/kg]: ankle abduction moment
Russell and Hamill [233]	n = 14 (14 F) age = 26.1 ± 6.9 y W=60.1 ± 6.5 kg H= 164 ± 7 cm	walking along walkway at 1.24 m/s 10 trials/ condition	1 segment 8 markers, on shoes	8° lateral wedge insole, full-length material: EVA	same standard shoe model (New Balance RC 550)	kinematics [°]: ankle plantarflexion, ankle dorsiflexion, ankle eversion, knee flexion, knee adduction
Sawada, et al. [253]	n = 15 age = 22.5 ± 1.5 y W= 58.5 ± 10.1 kg H= 165 ± 10 cm	walking along 10 m walkway at self-selected speed 5 trials/ condition	3 segments Oxford foot model [261] on skin	5.3° lateral wedge insole (approximately) with base height equal to 5th metatarsal, ¾ foot length material: high-intensity silicon rubber	barefoot	kinetics [Nm/kg]: knee adduction moment
Telfer, et al. [173]	n = 12 (6 F, 6 M) age = 31.7 ± 10 y W=72.8 ± 12.3 kg H= 173 ± 7 cm	walking along walkway at controlled speed ≥7 trials/ condition	2 segments 13 markers on skin	6° lateral rearfoot posting, 3D foot surface scan and 3D printed, ¾ foot length material: semi-rigid, Polylactide	standard shoe, neutrally posted	kinematics [°]: rearfoot eversion, forefoot abduction, internal tibia rotation kinetics [%BW*height]: ankle eversion moment, knee adduction moment

Table 2.1 (continued)

Study	Participants	Experimental protocol Task	 Foot model	Case condition: foot orthosis	Control condition: shod/bare	Outcome measures
Tipnis, et al. [231]	n = 25 (13 F, 12 M) Age = 23.1 ± 2.3 y W= 60.9 ± 9.4 kg H= 166 ± 6 cm	walking along 23 m walkway at 1.46 m/s 5 trials/ condition	1 segment 5 markers on shoes	6° lateral wedge (Der-Tex Corp, Saco) adhered to full length orthosis (KLM lab Inc) material: crepe (70) and covered with micro-puff	standard shoe (Nike Air Pegasus) with 0° lateral wedge	kinematics [°]: knee flexion kinetics [Nm/BW*height]: knee adduction moment
Tokunaga, et al. [213]	n = 20 age = 23.1 ± 3.5 y W= 64.9 ± 12.6 kg H= 172 ± 7 cm	walking along 10 m walkway at comfortable speed 5 trials/ condition	1 segment 5 markers on skin	7° lateral wedge insole fixed to the sole, full-length material: EVA	flat insole, thickness 5mm, from EVA	kinetics [Nm/kg]: ankle abduction moment, knee adduction moment GRF [N/kg]: vertical GRF, mediolateral GRF
Weinhandl, et al. [232]	n = 10 (10 F) age = 21.8 ± 0.6 y W= 60.1 ± 4.63 kg H= 165 ± 5 cm	walking along 15 m walkway at self-selected speed 5 trials/ condition	1 segment 4-marker cluster on shoes	9° lateral wedge insole, along the rear lateral aspect of the insole material: EVA, 55 shore A durometer	individual athletic shoe with the shoe insole	kinetics [Nm/kg]: knee abduction moment GRF [N/kg]: vertical GRF, mediolateral GRF
Yamaguchi, et al. [254]	n = 29 (9 F, 20 M) age = 28 ± 4 y W= 59 ± 10 kg H= 166 ± 9 cm	walking along 8 m walkway at self-selected speed 5 trials/ condition	rearfoot segment 5 markers on skin	6° lateral wedge, full length	barefoot with flat insole, 5 mm thickness	kinetics [Nm/BW*height]: knee adduction moment
Arch support						
Nakajima, et al. [222]	n = 20 (9 F, 11 M) age = 28.4 ± 6.1 y W=59.8 ± 10.9 kg H=167.2 ± 9.4 cm	walking along 7 m walkway at self-selected speed with controlling cadence 5 trials/ condition	rearfoot segment on skin	flat insole with customized arch support, full-length material: EVA 8200	barefoot with 5 mm thickness flat insole	kinematics [°]: knee valgus kinetics [%BW*height]: subtalar abduction moment, knee adduction moment
Yung-Hui and Wei-Hsien [226]	n = 10 (10 F) age = 23 y, range [20-28] y W= 50 kg, range [47-53] kg H= 160 cm, range [156- 162] cm	walking on treadmill at 1.3 m/s 3 trials/ condition	NA	custom-made total contact insole with arch-support material: semi-rigid multi-form molded (AliMed Inc)	commercially available flat shoes, 1 cm thickness	GRF [%BW]: vertical GRF

Table 2.1 (continued)

Study	Participants	Experimental protocol Task	Foot model	Case condition: foot orthosis	Control condition: shod/bare	Outcome measures
Arch &heel support						
Creaby, et al. [225]	n = 22 (11 F, 11 M) age = 27 ± 5.6 y W= 66.2 ± 10.2 kg H= 170 ± 7 cm	walking along 10 m walkway at 1.20 m/s 5 trials/ condition	1 segment Plug-in-Gait markerset [262]	full-length insole with heel cup (Superfeet Blue, Superfeet Worldwide Inc) material: medium density foam footbed (A 45) with polypropylene shell	standard shoes (Nike Pegasus)	GRF [%BW]: vertical GRF
Hong, et al. [224]	N=20 (20 F) Age= 25.4 ± 3.8 y W= 50.5 ± 4.2 kg H= 157.8 ± 5.0 cm	Walking along a walkway at 1.3 m/s 3 cycles/condition	No markerset	Customized total contact insert orthosis Material: semi-rigid, multiform molded material, hardness 35 shore A, density 0.17 g/cm^3	Standard shoes with flat sole (1.0 cm)	GRF [%BW]: vertical GRF, anteroposterior force, mediolateral force
Wahmkow, et al. [217]	n =19 (19 M) age = 36 ± 11 y W= 79 ± 10 kg H= 180 ± 5 cm	walking on treadmill at 5 km/h 1 minute/ condition	3 segments Oxford foot model [261] on skin	medial arch support (height 30 mm) with a concave-shaped heel wearing with standardized silicon slippers, full-length material: polyurethane foam (shore 25; with an EVA core, shore 55)	barefoot	kinematics [°]: rearfoot eversion, internal tibia rotation
Yung-Hui and Wei-Hsien [226]	n = 10 (10 F) age = 23 y, range [20-28] W= 50 kg, range [47-53] kg H= 160 cm, range [156- 162] cm	walking on treadmill at 1.3 m/s 3 trials/ condition	NA	custom-made total contact insole with heel cup	commercially available flat shoes, 1 cm thickness	GRF [%BW]: vertical GRF

This table is arrayed based on the orthosis design. The papers which have more than one orthosis design are listed as duplicates with an update in the details of orthosis [173, 221, 222, 226, 228]; Some articles have more than one orthosis within the same group, but with different inclinations or heights. In such cases, the table just mentions the included design in our meta-analysis [173, 217, 221, 231, 251, 256]. The peak values of all outcome measures have been extracted for this systematic review and meta-analysis. Gray color shows the studies repeated in different categories.
F: female, M: male, y: years old, SD: standard deviation, EVA: ethylene vinyl acetate, GRF: ground reaction force, BW: body weight.

Table 2.2. Methodological quality assessment

Study	Reporting								External validity		Internal validity (bias)				Internal validity (confounding)			Power	Score	
	Q1	Q2	Q3	Q4	Q5[a]	Q6	Q7	Q10	Q11	Q12	Q15	Q16	Q18	Q20	Q21	Q22	Q25	Q27[b]	QS (%)	QC
Burston, et al. [257]	1	1	1	1	2	1	1	1	UD	UD	UD	1	1	1	1	UD	1	UD	73.7	MQ
Creaby, et al. [225]	1	1	1	1	2	1	1	1	UD	UD	UD	1	1	1	1	UD	1	UD	73.7	MQ
Fischer, et al. [223]	1	1	1	1	2	1	1	1	UD	UD	UD	1	1	1	1	UD	1	1	78.9	HQ
Forghany, et al. [251]	1	1	1	1	1	1	1	0	1	UD	UD	1	1	1	1	UD	1	0	68.4	MQ
Fukuchi, et al. [221]	1	1	1	1	2	1	1	1	UD	UD	UD	1	1	1	1	UD	1	UD	73.7	MQ
Hong, et al. [224]	1	1	1	1	2	1	1	0	UD	UD	UD	1	1	1	1	UD	1	UD	68.4	MQ
Hornestam, et al. [211]	1	1	1	1	2	1	1	1	1	1	UD	1	1	1	1	UD	1	UD	84.2	HQ
Huerta, et al. [228]	1	1	1	1	1	1	0	1	UD	UD	UD	1	1	1	1	1	1	UD	68.4	MQ
Jones, et al. [229]	1	1	1	1	1	1	1	1	UD	UD	UD	1	1	1	1	UD	1	UD	73.7	MQ
Kakihana, et al. [216]	1	1	1	1	2	1	1	1	UD	UD	UD	1	1	1	1	UD	1	UD	73.7	MQ
Kang, et al. [260]	1	1	1	1	1	1	1	1	1	1	UD	1	1	1	1	UD	1	1	84.2	HQ
Kluge, et al. [252]	1	1	1	1	2	1	1	1	UD	UD	UD	1	1	1	1	UD	1	UD	73.7	MQ
Leitch, et al. [256]	1	1	1	1	1	1	1	1	UD	UD	UD	1	1	1	1	UD	1	UD	68.4	MQ
Molgaard, et al. [230]	1	1	1	1	2	1	1	1	UD	UD	UD	1	1	1	1	UD	1	UD	73.7	MQ
Nakajima, et al. [222]	1	1	1	1	2	1	1	1	UD	UD	UD	1	1	1	1	UD	1	1	78.9	HQ

Table 2.2 (continued)

Study	Reporting								External validity		Internal validity (bias)				Internal validity (confounding)			Power	Score	
	Q1	Q2	Q3	Q4	Q5[a]	Q6	Q7	Q10	Q11	Q12	Q15	Q16	Q18	Q20	Q21	Q22	Q25	Q27[b]	QS (%)	QC
Nakajima, et al. [222]	1	1	1	1	2	1	1	1	UD	UD	UD	1	1	1	1	UD	1	1	78.9	HQ
Nester, et al. [210]	1	1	1	1	1	1	1	1	UD	UD	UD	1	1	1	1	UD	1	UD	68.4	MQ
Russell and Hamill [233]	1	1	1	1	2	1	1	1	UD	UD	UD	1	1	1	1	UD	1	1	78.9	HQ
Sawada, et al. [253]	1	1	1	1	2	1	1	1	UD	UD	UD	1	1	1	1	UD	1	UD	73.7	MQ
Telfer, et al. [173]	1	1	1	1	2	1	1	1	1	UD	1	1	1	1	1	UD	1	UD	84.2	HQ
Tipnis, et al. [231]	1	1	1	1	2	1	1	1	UD	UD	UD	1	1	1	1	UD	1	1	78.9	HQ
Tokunaga, et al. [213]	1	1	1	1	1	1	1	1	UD	UD	UD	1	1	1	1	UD	1	UD	68.4	MQ
Wahmkow, et al. [217]	1	1	1	1	2	1	1	0	UD	UD	UD	1	1	1	1	UD	1	UD	68.4	MQ
Weinhandl, et al. [232]	1	1	1	1	1	1	1	1	UD	UD	UD	1	1	1	1	UD	1	UD	68.4	MQ
Yamaguchi, et al. [254]	1	1	1	1	1	1	1	1	UD	UD	UD	1	1	1	1	UD	1	UD	68.4	MQ
Yung-Hui and Wei-Hsien [226]	1	1	1	1	2	1	1	0	UD	UD	UD	1	1	1	1	UD	1	UD	68.4	MQ
																			73.7 (5.5)	MQ
κ level of agreement	1	1	1	1	0.74	1	1	0.83	0.96	1	1	1	1	1	1	0.96	1	1	0.97	

Quality assessment of included studies using modified Downs & Black checklist; Q1: clear aim, Q2: clarity of reporting outcomes, Q3: clarity of patients' characteristics, Q4: describing interventions, Q5: explaining principal confounders, Q6: description of main findings, Q7: estimation and report of random variability, Q10: reporting actual probability values, Q11: asked participants well represent the whole population, Q12: the prepared participants well represent the whole recruited participants, Q15: blinding of who measure outcomes, Q16: clarity of probable data dredging, Q18: appropriate statistical tests, Q20: accuracy of outcome measures, Q21: recruiting cases and controls from same population, Q22: recruiting cases and controls over the same time interval, Q25: adequate adjustments for confounding in the analysis, Q27: sufficient statistical power. QS: quality score [0%-100%], 1: yes, 2: no, UD: unable to determine, QC: quality classification categorized as HQ: high quality (QS≥75%), MQ: moderate quality (60% ≤ QS< 75%), LQ: low quality (QS< 60%). [a] The score for this question is 0: no, 1: partially, and 2: yes similar Downs & Black checklist; [b] The score for this question was modified as 0,1, UD to facilitate comparison.

Table 2.3 : Biomechanical quality assessment

Study	Markerset			Walking condition				Score	
	Placement	Segment	Redundancy	Barefoot/ Shoes	Treadmill/ Walkway	Cycles	Speed	QS (%)	Quality classification
Burston, et al. [257]	NA	NA	1	1	1	1	1	100	HQ
Creaby, et al. [225]	NA	NA	NA	1	1	1	1	100	HQ
Fischer, et al. [223]	NA	NA	1	1	1	0	1	80	HQ
Forghany, et al. [251]	0	0	1	1	1	1	0	57.1	LQ
Fukuchi, et al. [221]	0	0	0	1	1	1	1	57.1	LQ
Hong, et al. [224]	NA	NA	NA	1	1	0	1	75	HQ
Hornestam, et al. [211]	1	1	1	1	0	1	1	85.7	HQ
Huerta, et al. [228]	1	0	0	0	1	1	0	42.9	LQ
Jones, et al. [229]	0	0	1	1	1	1	1	71.4	MQ
Kakihana, et al. [216]	NA	NA	NA	0	1	UD	1	50.0	LQ
Kang, et al. [260]	NA	NA	0	1	1	0	0	40.0	LQ
Kluge, et al. [252]	0	0	1	1	0	1	1	57.1	LQ
Leitch, et al. [256]	NA	NA	0	1	1	1	0	60.0	MQ
Molgaard, et al. [230]	0	0	1	1	1	1	1	71.4	MQ
Nakajima, et al. [222]	1	1	UD	0	1	1	1	71.4	MQ
Nakajima, et al. [222]	1	1	UD	0	1	1	1	71.4	MQ
Nester, et al. [210]	0	0	0	1	1	1	1	57.1	LQ
Russell and Hamill [233]	0	0	1	1	1	1	1	71.4	MQ
Sawada, et al. [253]	NA	NA	1	0	1	1	1	80.0	HQ
Telfer, et al. [173]	1	1	1	1	1	1	1	100	HQ
Tipnis, et al. [231]	NA	NA	1	1	1	1	1	100	HQ
Tokunaga, et al. [213]	1	0	1	1	1	1	0	71.4	MQ
Wahmkow, et al. [217]	1	1	1	0	0	1	1	71.4	MQ
Weinhandl, et al. [232]	NA	NA	1	1	1	1	0	80	HQ
Yamaguchi, et al. [254]	NA	NA	1	0	1	1	0	60.0	MQ
Yung-Hui and Wei-Hsien [226]	NA	NA	NA	1	1	0	1	75	HQ
								71.4 ± 17.1	MQ

Biomechanical quality assessment of studies: Foot markerset: placement: on skin (1) or on shoes (0); segment: multi-segment/ rearfoot segment (1) or one segment (0); redundancy: >3 markers (1) or 3 markers (0); Walking quality: shoes (1) or barefoot (0); walkway (1) or treadmill (0); ≥ 5 cycles (1) or < 5 cycles (0); speed monitored (1) or not monitored (0). T: treadmill, W: walkway, UD: unable to determine, NA: not applicable. For studies which did not calculate the foot kinematics or kinetics, the first two questions were not relevant. The placement of marker of foot does not affect the knee kinematics/kinetics or ground reaction force. For studies which report the ground reaction force, the first three questions were not relevant. The quality of studies was calculated by excluding the NAs from the scoring.

2.3.4. Medial posting

Regarding kinematics, one single study showed a decrease in peak ankle eversion with a mean difference -2.2°, (large ES -1.58; 95% CI -2.51 to - 0.64, $p = 0.001$) when wearing FO with medial posting [173] (Table 2.4 and Table 2.5). Single studies looked at peak ankle abduction [228], forefoot adduction [173], external shank rotation relative to rearfoot (inversion) [210], as well as peak knee flexion and knee flexion moment [257] without finding any significant differences between control and orthosis conditions. Similarly, our meta-analysis exhibited no significant difference for peak foot rotation angle (internal tibia rotation relative to rearfoot, or rearfoot eversion) reported by three studies [173, 210, 228] (Figure 2.2).

Table 2.4: Summary of statistical analysis for parameters explored in a single study

Outcome measure	Included study, quality [methodological, biomechanical], sample size (n)	*p* value	Effect size (95% CI)
Medial posting			
Peak ankle eversion	Telfer, et al. [173], [HQ, HQ], n = 12	0.001*	-1.58 [-2.51 to -0.64]
Peak ankle abduction	Huerta, et al. [228], [MQ, LQ], n = 12	0.39	-0.35 [-1.16 to 0.46]
Peak forefoot adduction	Telfer, et al. [173], [HQ, HQ], n = 12	0.14	-0.62 [-1.44 to 0.21]
Peak external shank rotation relative to foot	Nester, et al. [210], [MQ, LQ], n=15	0.54	0.22 [-0.49 to 0.94]
Peak knee flexion	Burston, et al. [257], [MQ, HQ], n=15	0.69	-0.15 [-0.86 to 0.57]
Peak knee flexion moment	Burston, et al. [257], [MQ, HQ], n=15	0.74	-0.12 [-0.84 to 0.59]
Lateral posting			
Peak forefoot adduction	Telfer, et al. [173], [HQ, HQ], n = 12	0.83	-0.09 [-0.89 to 0.71]
Peak external shank rotation relative to foot	Nester, et al. [210], [MQ, LQ], n=15	0.10	-0.61 [-1.34, 0.13]
Peak hip flexion	Russell and Hamill [233], [MQ, MQ], n = 14	0.85	-0.07 [-0.81 to 0.67]
Peak hip extension	Russell and Hamill [233], [MQ, MQ], n = 14	1.00	0.00 [-0.74 to 0.74]
Peak hip adduction	Russell and Hamill [233], [MQ, MQ], n = 14	0.66	0.17 [-0.58 to 0.91]
Peak knee extension moment	Molgaard, et al. [230], [MQ, LQ], n = 13	0.09	0.70 [-0.10 to 1.49]

Table 2.4 (continued)

Outcome measure	Included study, quality [methodological, biomechanical], sample size (n)	*p* value	Effect size (95% CI)
Arch support			
Peak knee adduction	Nakajima, et al. [222], [HQ, MQ], n=20	0.008*	-0.88 [-1.53 to -0.23]
Peak ankle abduction moment	Nakajima, et al. [222], [HQ, MQ], n = 20	0.72	0.11 [-0.51 to 0.74]
Peak knee adduction moment	Nakajima, et al. [222], [HQ, MQ], n = 20	0.26	-0.36 [-0.99 to 0.27]
Arch & heel support			
Peak ankle eversion	Wahmkow, et al. [217], [MQ, MQ], n = 19	0.14	-0.49 [-1.13 to 0.16]
Peak internal tibia rotation	Wahmkow, et al. [217], [MQ, MQ], n = 19	0.61	0.17 [-0.47 to 0.80]
Anteroposterior ground reaction force	Hong, et al. [224], [MQ, HQ], n = 20	0.56	-0.18 [-0.80 to 0.44]
Mediolateral ground reaction force	Hong, et al. [224], [MQ, HQ], n = 20	0.58	0.17 [-0.45 to 0.80]

Effect size is standardized mean difference. A positive value shows "increase", and negative value shows "decrease" for that parameter during wearing orthosis compared to no orthosis. HQ: high quality; MQ: moderate quality; LQ: low quality; GRF: ground reaction force. Where significant effect of wearing foot orthosis was found for single studies, it is shown with (*).

Table 2.5: Mean effect of walking with foot orthosis on joint rotations

Outcome measure	Included studies, quality [methodological, biomechanical], and sample size (n)	*p* value	Mean difference (95% CI) [°]
Medial posting			
Peak ankle eversion	Telfer, et al. [173], [HQ, HQ], n = 12	<0.0001	-2.15° [-3.20, -1.1]
Lateral posting			
Peak ankle dorsiflexion	Nester, et al. [263], [MQ, LQ], n = 15; Russell and Hamill [233], [MQ, MQ], n = 14	0.005	2.04° [0.60, 3.47]
Arch support			
Peak knee adduction	Nakajima, et al. [222], [HQ, MQ], n = 20	0.005	-1.36° [-2.30 to -0.42]

The mean differences are only reported for significant effect of foot orthosis on kinematics.
A positive value for mean difference shows "increase", and negative value shows "decrease" for that parameter during walking with orthosis compared to without orthosis.
HQ: high quality; MQ: moderate quality; LQ: low quality.

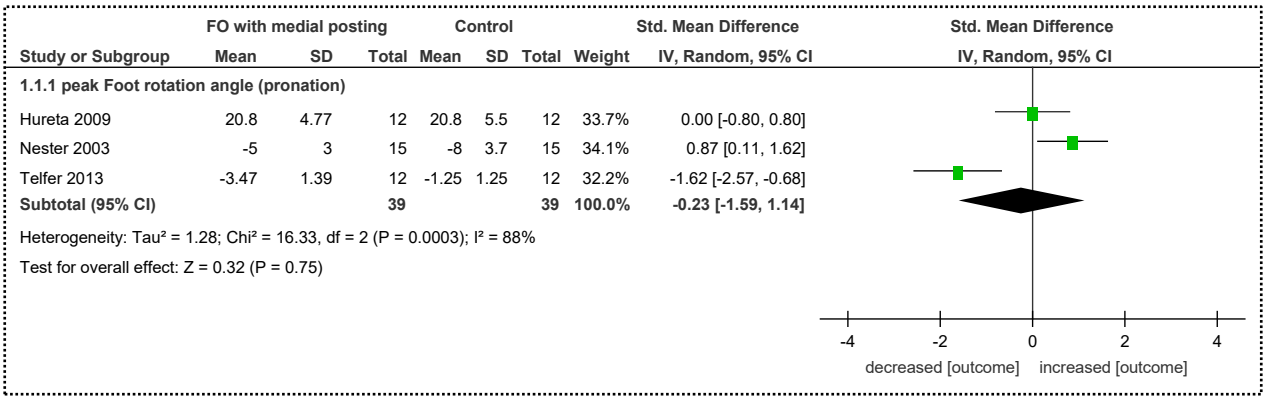

Figure 2.2 : Forest plot indicating the effect of foot orthosis with medial posting on lower extremity kinematics. The subtotal effect for each parameter and the total effect were calculated as standardized mean difference (95% CI). SD: standard deviation, std: standardized, CI: confidence interval, IV: inverse variance.

As for kinetics, three studies reported peak ankle eversion moment [173, 221, 228] and two compared peak knee adduction moment [173, 221]. Meta-analysis showed significant decrease in peak ankle eversion moment with medial posting (large ES -1.18; 95% CI -2.12 to -0.24, p=0.01, moderate heterogeneity I^2 = 75%). However, no significant effect for peak knee adduction moment was observed (95% CI cross zero, p> 0.05; Figure 2.3).

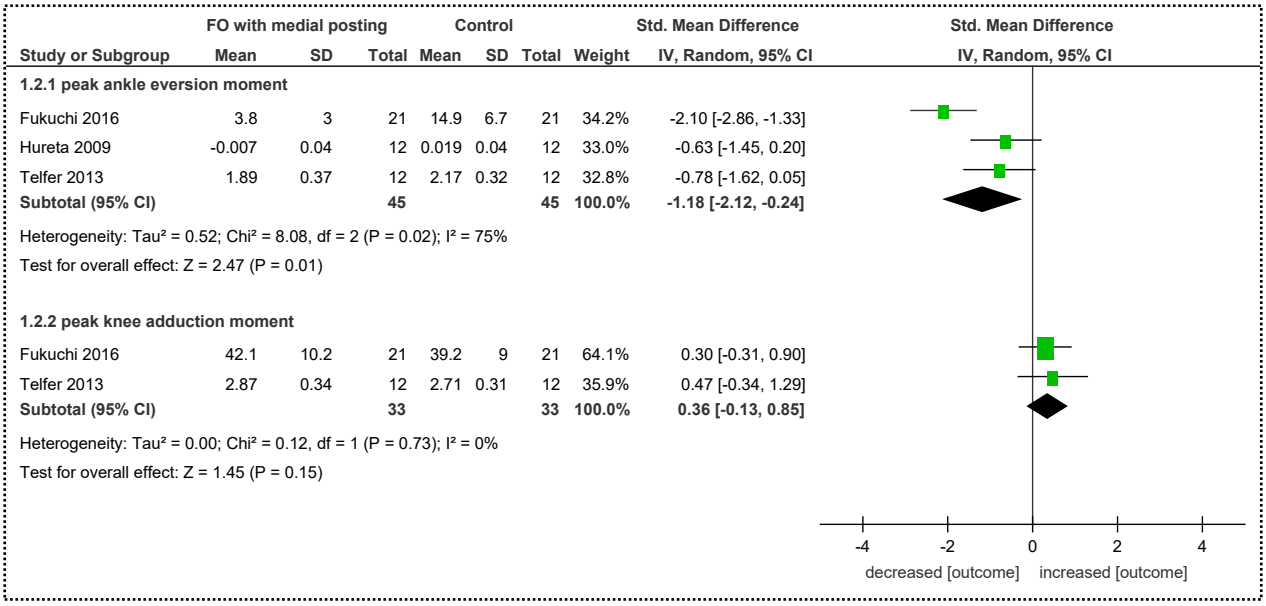

Figure 2.3 : Forest plot indicating the effect of foot orthosis with medial posting on lower extremity joint moments.

2.3.5. Lateral posting

For kinematics, the results of our meta-analysis showed a mean of 2.0° significant increase in peak ankle dorsiflexion during walking with- compared to without- orthosis (moderate ES 0.69; 95% CI 0.15 to 1.22, $p = 0.01$, minimal heterogeneity $I^2 = 0\%$) [210, 233]. In addition, 0.3° higher peak ankle eversion (small ES 0.34; 95% CI -0.51 to 1.19, $p = 0.43$, high heterogeneity $I^2 = 88$ %), 1.8° higher peak ankle plantarflexion (small ES 0.43; 95% CI -0.09 to 0.96, $p = 0.11$, minimal heterogeneity $I^2 = 0$ %), 1.7° lower peak ankle abduction (small ES -0.37; 95% CI -0.91 to 0.17, $p = 0.18$, minimal heterogeneity $I^2 = 0$ %), was achieved for differences in foot kinematics as an effect of walking with orthosis (Figure 2.4). However, these differences were not statistically significant due to insignificant results in individual studies and controversial effects between studies. In terms of knee kinematics, four studies reported peak knee flexion [229, 231, 233, 252], four studies peak knee adduction [229, 231, 233, 252], and two studies peak internal tibia rotation [173, 228]. However, our meta-analysis revealed no significant differences between control and orthosis conditions especially due to the fact that individual studies reported no significant effect (Figure 2.4). In addition, single studies compared peak external shank rotation relative to foot (inversion) [210], as well as peak hip flexion, extension and adduction [233] without reaching any significant differences between walking with- and without- orthosis (Table 2.4).

In terms of kinetics, walking with laterally posted led to significant increase in peak ankle abduction moment (large ES 1.70; 95% CI 0.83 to 2.57, $p = 0.0001$, high heterogeneity $I^2 = 78$ %), as reported in four studies [210, 213, 222, 230]. Meta-analysis on 14 studies [173, 213, 221-223, 229-232, 252-254, 256, 260] showed a decrease in peak knee adduction moment (moderate ES -0.55; 95% CI -0.85 to -0.24, $p = 0.0005$, moderate heterogeneity $I^2 = 69$ %), and on four studies [213, 216, 232, 252] indicated an increase in mediolateral GRF (small ES 0.44; 95% CI 0.02 to 0.87, $p = 0.04$, low heterogeneity $I^2 = 40\%$; Figure 2.5). In addition, meta-analysis was performed on four studies [173, 221, 228, 229] looking at the peak ankle eversion moment, two studies [229, 230] at the peak knee flexion moment, and four studies [213, 216, 232, 252] at the peak vertical GRF (Figure 2.5). However, no significant effect of using FO with lateral posting was reported there. A single study [230] reported peak knee adduction moment, without finding any significant effect of walking with lateral posting.

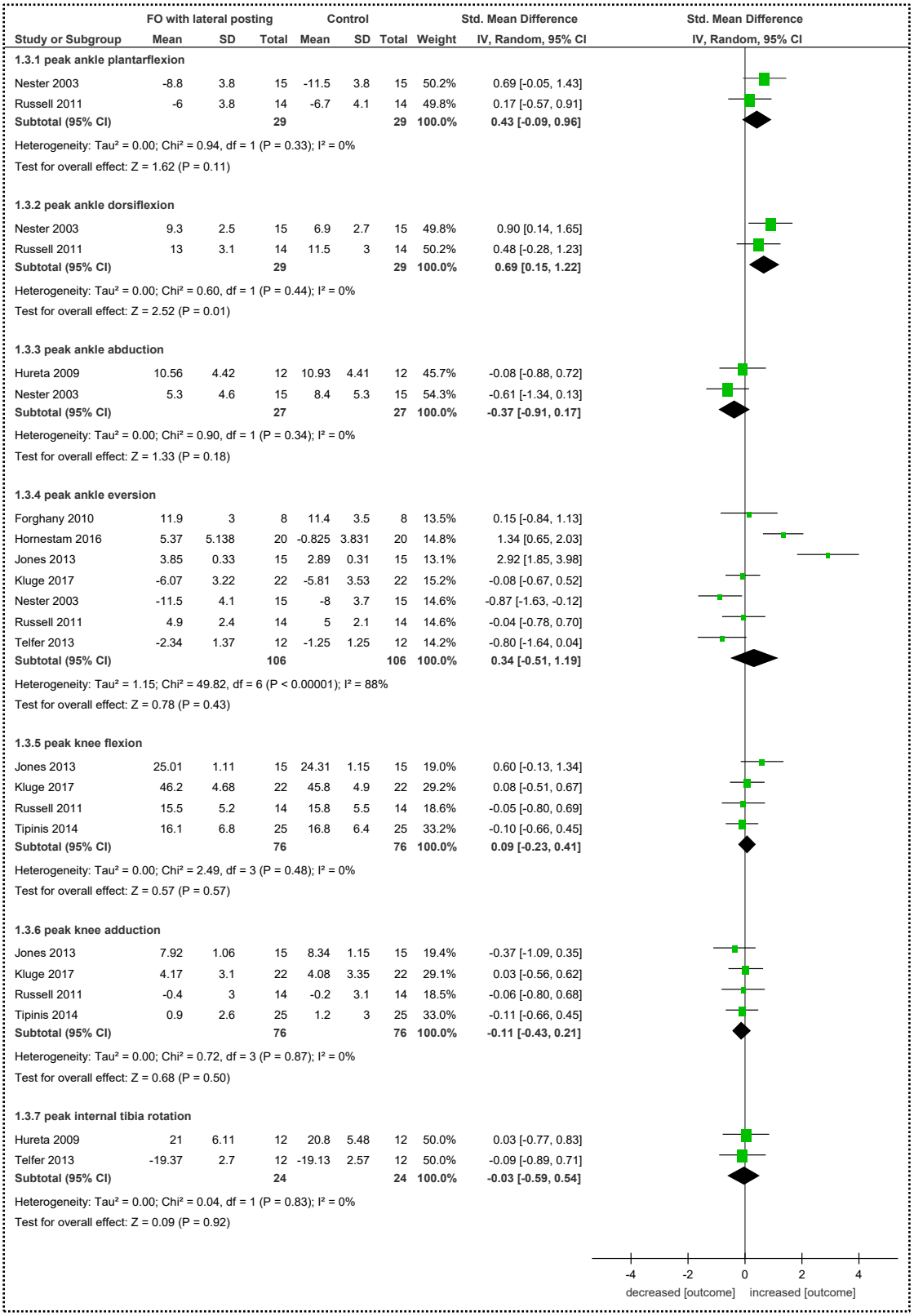

Figure 2.4 : Forest plot indicating the effect of foot orthosis with lateral posting on lower extremity kinematics.

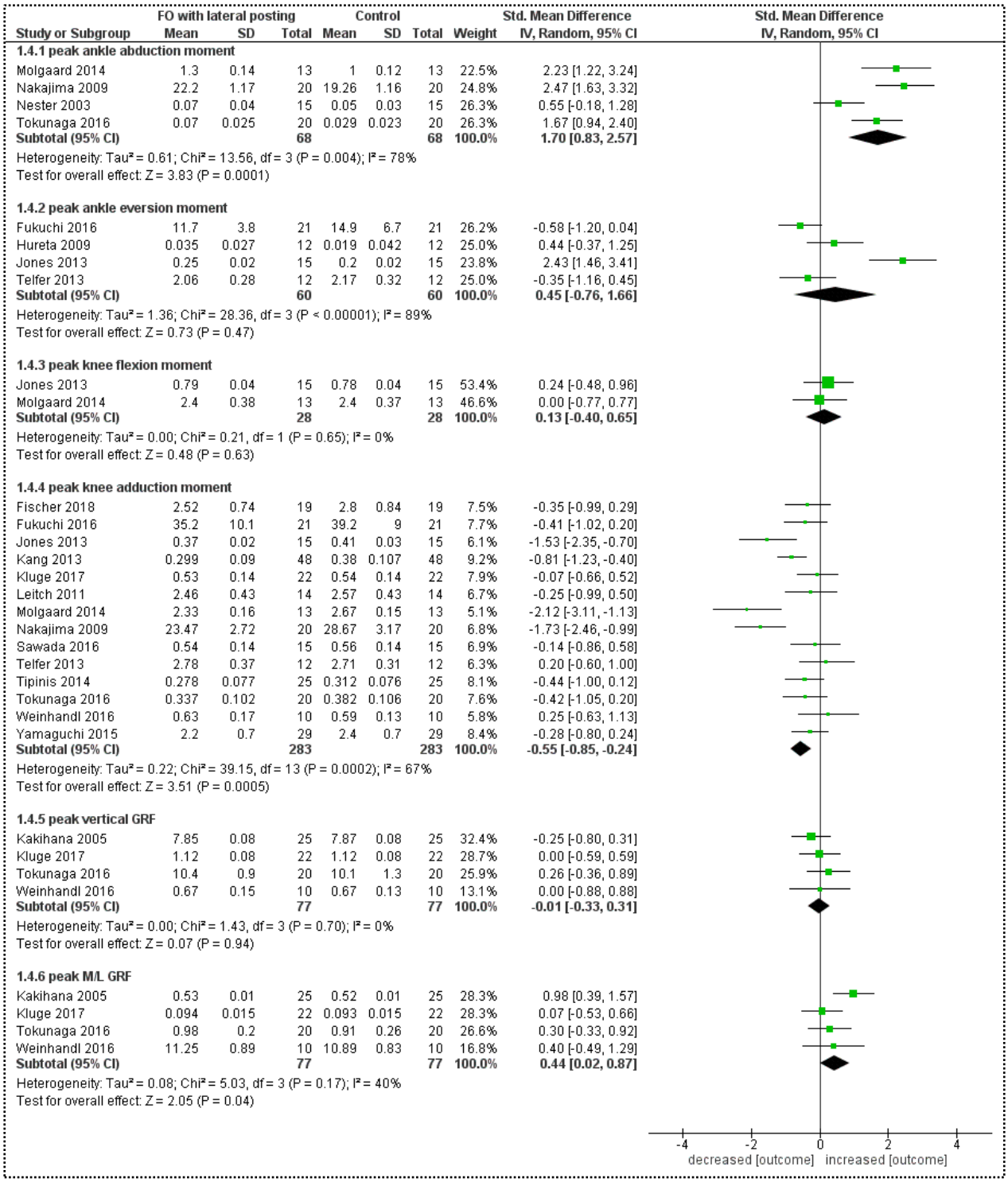

Figure 2.5 : Forest plot indicating the effect of foot orthosis with lateral posting on lower extremity joint moments and ground reaction force. The subtotal effect for each parameter and the total effect were calculated as standardized mean difference (95% CI). SD: standard deviation, std: standardized, CI: confidence interval, IV: inverse variance.

2.3.6. Arch support

One study [222] indicated a significant decrease of -1.36°in peak knee adduction (large ES -0.88; 95% CI -1.53 to -0.23, p = 0.008) when walking with arch-supported FO (Table 2.4). Regarding joint moments, one single study [222] showed that FO with arch support did not make any significant difference in either peak ankle abduction moment or peak knee adduction moment. Meta-analysis was only possible on peak vertical GRF reported by two studies [222, 226], where no significant effect of walking with arch-supported orthosis was found (trivial ES -0.08; 95% CI -0.59 to 0.43, p=0.42, minimal heterogeneity I^2 = 0%; Figure 2.6).

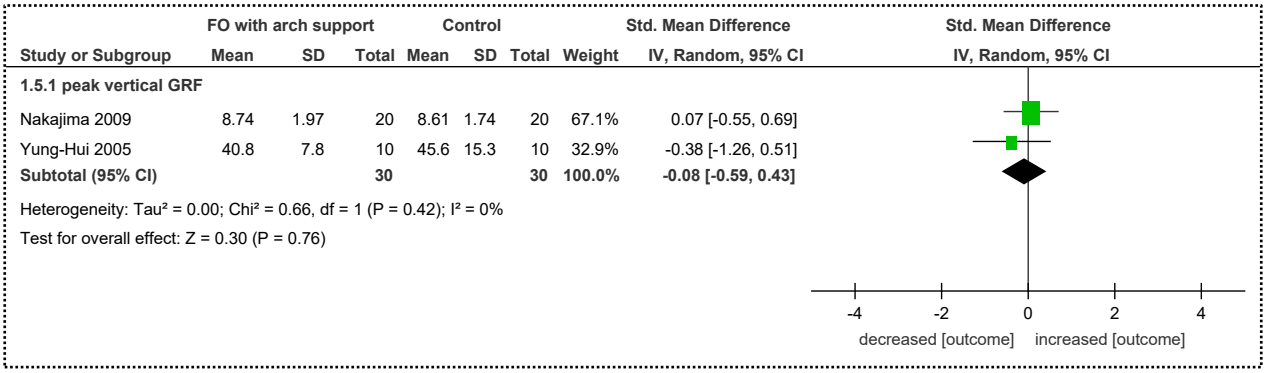

Figure 2.6 : Forest plot indicating the effect of foot orthosis with arch support on ground reaction force. The effect was calculated as standardized mean difference (95% CI). SD: standard deviation, std: standardized, CI: confidence interval, IV: inverse variance.

2.3.7. Arch & Heel support

No significant difference was observed in peak ankle eversion and peak internal tibia rotation during walking with- and without- arch & heel supported FO as reported by Wahmkow, et al. [217]. No single study reported either kinematic or kinetic parameters for this design of FO. Meta-analysis evaluation for peak vertical GRF showed no significant effect of walking with heel supported FO (trivial ES -0.20; 95% CI -0.58 to 0.19, p = 0.54, minimal heterogeneity I^2 = 0%; Figure 2.7) [224-226].

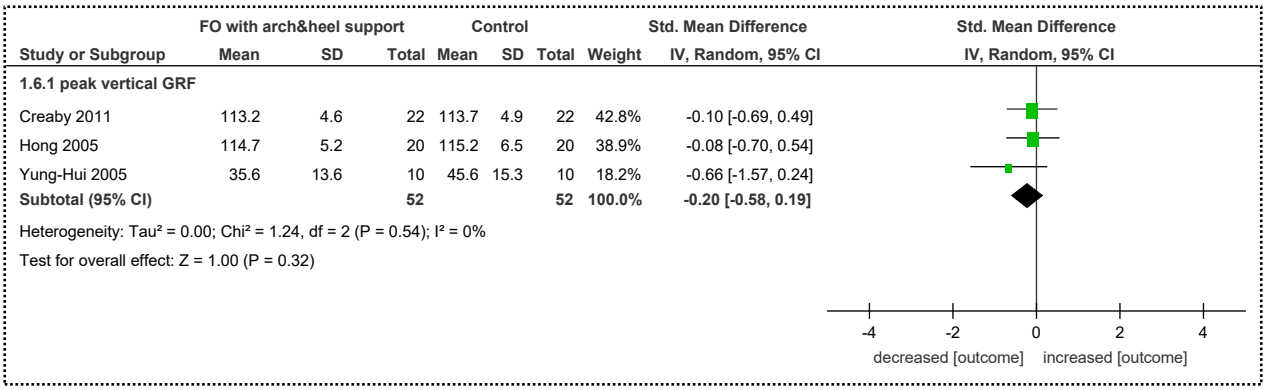

Figure 2.7 : Forest plot indicating the effect of foot orthosis with arch & heel support on ground reaction force. The effect was calculated as standardized mean difference (95% CI). SD: standard deviation, std: standardized, CI: confidence interval, IV: inverse variance

2.4. Discussion

Until now it was unclear how segment movement or inter-segment coordination are affected by various FO designs. Four categories of FO designs, namely FO with medial posting, lateral posting, arch support and arch & heel support, were selected as the available and common geometrical modifications to control lower extremity movements and absorb shock. Although the final optimal FO might be a combination of these designs, we basically aimed to detect their separate effects. Based on this systematic review and meta-analysis, postings either medially or laterally appear to function effectively to control the foot posture, lower extremity kinematics and moment arms. Arch supports could modify foot positioning partially as well as how the foot interacts with GRF. Heel supports have been reported to attenuate the impact of ground force and rate of loading. It can also be added that the control of GRF by arch supported FO goes toward the propulsion and stability of walking, while heel supported FO conducts the shock absorption rule.

2.4.1. Medial posting

FO with medial posting exhibited decrease in ankle eversion moment and slight increase in knee adduction moment. These effects have been referred to less everted position of foot, and the medial shift of center of pressure (CoP) imposed by this FO design [221]. Foot pronation is necessary during contact phase to provide foot flexibility and absorb the GRF impact [173, 211]. However, the foot needs to supinate and provide enough arch height for efficient propulsion. Otherwise,

excessive pronation, observed in flatfoot, over-pronated foot or plantar fasciitis, would impose higher load on musculoskeletal system, since the foot in unstable and the rigid lever required at toe off cannot be provided [264]. Our results showed that medial posting can be effective for reducing the pronation components, ankle eversion and ankle eversion moment, in this group of people. There, these individuals could have more support during midstance and propulsion. This FO design could actually behave as a supportive structure to decrease stress on tissues and avoid muscle fatigue [228, 265]. However, some studies reached a weak relationship between controlling the motion of pronated foot and reducing the rate of injury [266]. Medial posting has also been effective for lateral knee osteoarthritis and patellofemoral pain syndrome by reducing the lateral knee loading and pain [267, 268], which could be confirmed by our meta-analysis findings.

2.4.2. Lateral posting

Compared to medial posting, lateral posting showed a reverse effect for ankle eversion and knee adduction moment, as expected due to its mediolateral reverse inclination [216, 252]. There were more studies using FO with lateral posting compared to other categories during walking for healthy subjects. Therefore, more gait measures were available in this category for meta-analysis. Further observations were increase in peak ankle dorsiflexion, peak ankle abduction moment and peak mediolateral GRF during walking with- orthosis compared to without-orthosis. To our observation, the main application of this FO design for improving gait pattern in patients with medial knee osteoarthritis [222], has made it a quite popular target in research. Its efficiency to reduce knee adduction moment, medial knee contact force and loading has been stated in several studies [216, 222, 229], and confirmed by our meta-analysis. For patients with peroneal tendon problems, lateral ankle sprain, and supination injuries, the lateral posting can be a mechanical support to control the excessive motion of subtalar joint [216]. In fact, FO with lateral posting could assist heel bone to a pronated position by higher ankle eversion and higher ankle dorsiflexion, verified by our review findings [216, 269]. In addition, high arch in cavus foot is associated with a stiff and rigid foot, which transfer higher energy to tibia and femur, and increase their vulnerability to stress fracture [264]. Our meta-analysis showed that decreasing the arch height by lateral posting could decrease the loading on the frontal plane of knee. FO with lateral posting has also been thought to improve balance and gait and correct foot varus deformity for patients with stroke [251]. Irrespective of mechanical efficiency provided by lateral posting, some studies reported that they might neither

reduce pain [230] nor improve comfort [231]. Meta-analysis was not possible for the effect of lateral posting on hip loading, and the only available study did not report any changes. This effect needs to be considered in future studies.

2.4.3. Arch support

Meta-analysis about FO with arch support was just possible on vertical GRF without finding any significant effect. Medial arch support has been prescribed for low arch feet to avoid excessive pronation, anterior knee pain and arthritis symptoms. Through using this FO design, the medial arch is supported against depression during weight-bearing and the ground reaction impact force is reduced [217]. It was also shown to decrease the tension in plantar aponeurosis [209, 226]. FO with arch support has been reported to improve fit, balance and mechanical transfer of ground force to foot, and reduce pain [252, 270-274]. However, careful attention should be paid on their positioning to avoid bias in knee alignment [252]. Previous research did not show consistent results for the mechanical performance of arch supports. Franz, et al. [271] stated that arch-supported FO could increase the toe-out angle, decrease the moment arm of knee, and relieve knee pain. Mulford, et al. [273] also confirmed the effectiveness of arch- supported FO in improving balance and pain in elderly subjects. However, Nakajima, et al. [222] showed similar knee adduction moment and subtalar joint adduction moment for FO with arch support and flat insoles. To our observation, arch supported FO has been evaluated for balance and stability rather than modifying kinematics and kinetics. Therefore, further studies are required to response for the efficiency of FOs with arch support to alter foot kinematics.

2.4.4. Arch & Heel support

Heel cups are usually suggested to attenuate the force at the initial foot contact. At this moment, high impact force is induced on the foot, which is further transmitted to knee and hip. The long term effect of high impact forces and the rate of loading could be cartilage damage, overuse injuries, and knee osteoarthritis [225, 272]. Adding heel cup to arch supported FO can provide foot support in both rearfoot and medial arch which play an important role in balance and propulsion. Most of FOs with heel cup have been examined during running, where they have been reported to efficiently reduce the impact force [275, 276]. During walking, lower extremity kinematics and kinetics were assessed by three studies focusing on FO with arch and heel support. Yung-Hui and

Wei-Hsien [226] reported efficient attenuation of impact force and higher comfort with arch & heel supported FOs. However, Creaby, et al. [225] found flat material insole more efficient in reducing the peak impact forces between ground, foot, and knee compared to FO with arch & heel support. They inferred that while FO with heel cup could be quite effective for subjects with low intrinsic shock-absorbing capacity [277, 278], flat material insoles work better for young individuals during walking. In addition, Hong, et al. [224] did not find any significant effect of this FO on ground reaction force. Therefore, due to limited studies as well as controversial effects of heel cup in shock absorption during walking, more studies are required in this field.

2.4.5. Clinical considerations

It is quite important to see whether our findings on the association between FO designs and their corresponding biomechanical effects are meaningful with clinical perspective. Based on previous literature findings even small orientation changes, *i.e.* 1° to 2°, in the interaction between foot and ground could be effective to either reduce or overcome lower extremity pathologies [279-281]. It has also been mentioned that small changes in knee adduction angle could alter knee joint contact forces and stress distribution within the cartilage [282, 283]. Referring to these evidences, 2.15° decrease in peak ankle eversion with medial posting, 2.04° increase in peak ankle dorsiflexion with lateral posting, and 1.36° in peak knee adduction with arch supported FO, found in the present meta-analysis, could be clinically meaningful. Small non-significant difference was found for peak ankle eversion during walking with laterally posted FO which was due to inconsistent findings of included studies. Different methodological approach for kinematic analysis, differences in the FO design and material, and different populations can be stated as the source of inconsistencies. Using multi-segment foot models as well as standardizing and customizing FO design are suggested to be implemented in future studies to reach more reliable results.

A further clinically important point is to perceive the negative aspects of each FO design, and look for the possible solutions. Regardless of whether medial and lateral postings are used for modifying foot abnormality [173] or knee problems [216], they are susceptible to alter the kinematics and kinetics of ankle and knee simultaneously [173, 216, 229]. Rodrigues, et al. [268] reported that medial wedging for the treatment of valgus knee osteoarthritis might impose changes in talus and talocalcaneal kinematics at the same time. Therefore, modifying one abnormality might happen in cost of inducing another pathology if this important point is ignored in treatments with FO. Some

solutions have been suggested to overcome this problem: using appropriate dose of posting or controlling unfavorable movements with adding extra supports. A few studies evaluated the dose-effect of posting in terms of biomechanical changes and comfort [173, 221, 231]. Tipnis, et al. [231] showed a systematic decrease in knee adduction moment with increasing the dose of lateral posting, but comfort level worsened for higher doses of wedging (> 6°). Telfer, et al. [173] reported a linear relationship between dose of posting and mechanics of rearfoot and knee. Fukuchi, et al. [221] found higher positive correlation between CoP and ankle joint moment compared to knee joint moment. This might indicate that although lower dose of posting can be effective for ankle instabilities, it might not be capable to improve knee mechanics, and consequently overcome knee problems. In terms of extra supports, some studies suggested to add ankle support to control the movement of talus when posting was aimed to treat knee osteoarthritis [268, 284]. In addition, Nakajima, et al. [222] revealed that adding arch support to lateral posting for patients with osteoarthritis increase comfort and clinical efficiency. It was thought that an arch support could modulate the subtalar joint over-abduction imposed by lateral wedge. Based on these findings, we believe that optimal FO could be reached if specific pathological and individual needs in terms of dose of posting and support as well as combining different categories of FO designs are taken into account.

2.4.6. Methodological considerations

Although we did not focus on the material of FO, it has been reported that FOs made of materials of different rigidities impose changes on foot support and control effects [209]. Therefore, it is suggested that further research assess FOs with different materials as well as how the deformation of FO changes during walking as a function of FO rigidity. In addition, the medial and lateral posting categories included orthoses with rearfoot postings or full-length wedges. The rearfoot postings could just control foot contact to midstance not to late stance [269]. Higher and longer pronation, *i.e.* rearfoot eversion, forefoot abduction and forefoot plantarflexion, is just partially controlled by rearfoot posting. Therefore, it is important to suggest full-length posting when abnormalities are observed in forefoot motion or late stance phase. Otherwise, over-pronation might stress hip joint to response for inter-joint coordination, and provide a potential for hip pathology [218]. We believe that our findings in healthy subjects could provide a quite helpful database to suggest different FO designs based on the biomechanical needs to treat different

pathologies. However, this should not be ignored that the compensatory mechanisms employed by patients might interact with FO biomechanical effect. As a result, the effect of similar FO design might be different in healthy individuals *versus* patients. For example, as an effect of medial posting, Telfer, et al. [173] reported a decrease in forefoot adduction for healthy individuals in contrast to an increase for flatfoot individuals. To come up with this issue, it is important to verify the effect of FO design on any specific pathology before its clinical use.

Several inconsistencies for experimental measurement were observed between the included studies. While some studies asked subjects to walk barefoot, others used either standardized shoes or subject comfortable shoes. Discussing on which method could be more effective regarding FO measurements is beyond the goals of this review. However, synthesizing the results of all these conditions in this review might have imposed bias and heterogeneity in our results. The interaction between foot, FO, shoes and ground would be different among these conditions which effect on kinematics and kinetics [252, 285]. In addition, the kinematic analysis was based on the position of reflective markers in all included studies. However, they were not similar in terms of attaching the markers on skin or shoes, regarding foot as multiple segment, and attaching redundant markers on each segment. These variables would effect on the accuracy of foot kinematics due to more or less compensation for soft tissue artefacts [245, 286]. Walking on treadmill or along walkway as well as the walking speed should be added as other non-identical factors. For example, Hornestam, et al. [211] reported that healthy subjects exhibited a decrease in pronation during higher speed of walking with lateral wedges.

Some heterogeneous as well as unexpected results existed in the context of this meta-analysis which could be addressed to various methodological and biomechanical approaches. Fukuchi, et al. [221] showed a decrease in peak ankle eversion moment as an effect of walking with both medial and lateral posting. The high decrease of this gait parameter for FO with medial posting in this study led to high heterogeneity index in meta-analysis results. This high difference might be inferred to its low biomechanical quality in terms of selected foot model. Indeed, this study considered foot as single segment, and placed just three reflective markers on shoes to record foot kinematics. In addition, lateral posting, due to the effect of its geometry on foot positioning, was expected to increase ankle eversion moment. However, three out of four studies did not fulfill such an expectation: *(i)* Telfer, et al. [173] reported decrease in peak ankle eversion and peak ankle

eversion moment. This can be related to the contoured shape of their customized orthosis, which prevents the deformation of medial longitudinal arch; *(ii)* Fukuchi, et al. [221] mentioned that the increase in ankle eversion moment was only possible with higher degrees of wedges, and we may hypothesize that it might be partly related to its low biomechanical quality; *(iii)* Huerta, et al. [228] explained that peak ankle eversion moment occurs at initial contact, where the point of lateral heel contact cannot be deteriorated by lateral wedge. In this study, Helen Hayes marker set [262] was used for recording kinematics, the subjects walked barefoot, and the speed of walking was not monitored. All of these parameters could also have led to such unexpected finding. No systematic effect was found for changes in internal tibia rotation for any of medial/lateral posting or arch support. Previous studies referred this observation to high inter-individual variability in this gait measure depending on foot type [173, 217, 287]. Decrease in peak knee adduction moment during walking with lateral posting was confirmed by all studies, with different effect sizes, except by Telfer, et al. [173] and Weinhandl, et al. [232]. This controversial result was probably related to the contoured geometry of FO by Telfer, et al. [173], and to not controlling gait speed as well as no change in the range of motion for ankle due to putting markers on the shoes by Weinhandl, et al. [232]. In the category of FO with arch & heel support, high variability in the response of individuals to insoles prohibited us to find any effect in our meta-analysis. Creaby, et al. [225] stated that heel cup insoles might just be effective for some individuals and suggested to separate individuals with-effect and without-effect for future studies.

As it can be seen through this review, different methodological approach has given rise to controversial and heterogeneous outcomes, where it makes it hard to provide a comprehensive database for clinical use. We believe that further studies could be more qualified in terms of designing more thoughtful and standardized protocols as well as measurement approach.

2.5. Conclusion

Our meta-analysis found evidence for decrease in peak ankle eversion moment with medial posting. Increase in peak ankle dorsiflexion, peak ankle eversion, peak ankle abduction moment, and peak mediolateral GRF, as well as decrease in peak knee adduction moment were the effects of walking with lateral posting. No significant evidence was found for FO with arch support or arch & heel support through our meta-analysis. The heterogeneity between the findings of included studies and the limited number of available studies were the deterrent effects for finding more evidence in

different categories. Although the mechanical and clinical approach to reach the optimal FO design remains to be more elucidated, this meta-analysis is the first comprehensive study to examine the interplay between FO design and gait kinematics and kinetics in healthy individuals. We think that heterogeneity between studies could be reduced by introducing standard multi-segment foot models for kinematic analysis and making use of additive manufacturing technology to design customized foot orthosis based on individual needs.

2.6. Supplementary materials

Groups of keywords

Group #1: related to “foot orthosis”

[MeSH terms: "Foot Orthoses"

OR

Keywords (title, abstract, and keywords): insole OR "shoe insert" OR "foot orthosis" OR "foot orthotics" OR "foot orthoses"**]**

AND

Group #2: related to “design and geometrical modifications”

[MeSH terms: "Computer-Aided Design" OR "Evidence-Based Facility Design"

OR

Keywords (title, abstract, and keywords): Wedge* OR post OR posting OR posted OR heel* lift* OR flange* OR heel* spur* cut* OR metatars* cut* OR plantar* fascial* groov* OR navicul* shell* OR heel* cup* OR flat* OR arch* support* OR offload* OR heel* skive* OR cushion* OR slip* resist* OR Design* OR structure* OR model* OR geometr* **]**

AND

Group #3: related to “biomechanical and locomotion metrics”

[MeSH terms: "Locomotion" OR "Biomechanical Phenomena" OR "Mechanics" OR "Mechanical Phenomena" OR "Electromyography"

OR

Keywords (title, abstract, and keywords): Motion OR movement OR locomot* OR kinematic* OR kinetic* OR pressur* OR dynamic* OR load* OR biomech* mechanic* OR shock* absorb* OR shock* attenuat* OR friction* OR moment* OR angle* OR rotation* OR force* OR angular* impuls* OR EMG OR electromyograph* OR muscle* activity* OR torque* OR energy***]**

Table S 2.I: Methodological quality assessment, modified Downs and Black checklist

Category	#Question in downs & black checklist	Question	Hints for assigning scores
Reporting	1	Is the hypothesis/aim/objective of the study clearly described?	"1" if yes, "0" if no
	2	Are the main outcomes to be measured clearly described in the Introduction or Methods section?	"1" for papers describing outcomes before result section. Otherwise "no"
	3	Are the characteristics of the patients included in the study clearly described?	"1" for describing age, sex, and health of lower extremity, otherwise "no"
	4	Are the interventions of interest clearly described? Treatments and placebo (where relevant) that are to be compared should be clearly described [footwear design]	"1" if foot orthosis design (treatment) and the awareness/blinding of wearing orthosis (placebo) have been described, otherwise "no"
	5	Are the distributions of principal confounders in each group of subjects to be compared clearly described?	Principal confounders: walking speed, foot orthosis material and design, the proof of healthy foot, shoe model. "2" if all of the principal confounders are clarified, "1" if some of the are clarified, otherwise "0"
	6	Are the main findings of the study clearly described?	"1" if outcome data have been reported for major findings and analyses, otherwise "no"
	7	Does the study provide estimates of the random variability in the data for the main outcomes?	"1" if reporting standard deviation, standard error or confidence interval for results, otherwise "0"
	10	Have actual probability values been reported (*e.g.* 0.035 rather than <0.05) for the main outcomes except where the probability value is less than 0.001?	"1" if yes, otherwise "0"

Table S 2.I (continued)

Category	#Question in downs & black checklist	Question	Hints for assigning scores
External Validity	11	Were the subjects asked to participate in the study representative of the entire population from which they were recruited? where a list of all members of the relevant population	"1" if the study described the source population, and the approach of selecting participants, otherwise "0"
	12	Were those subjects who were prepared to participate representative of the entire population from which they were recruited?	"1" if the proportion of participants asked to attend, and agreed should be stated, otherwise "0"
Internal Validity (Bias)	15	Was an attempt made to blind those measuring the main outcomes of the intervention?	"1" if there was blinding for data processing, otherwise "0"
	16	If any of the results of the study were based on "data dredging", was this made clear?	"1" if there is not any report of unplanned analysis and results, otherwise "0"
	18	Were the statistical tests used to assess the main outcomes appropriate?	"1" if proper statistical tests had been used, otherwise "0"
	20	Were the main outcome measures used accurate (valid and reliable)?	"1" if any clue has been given for the validity and reliability of outcome measures, otherwise "0"
Internal Validity-confounding (selection bias)	21	Were the patients in different intervention groups (trials and cohort studies) or were the cases and controls (case control studies) recruited from the same population?	"1" If the groups were matched for age, sex, and level of daily activities, otherwise "0"
	22	Were study subjects in different intervention groups (trials and cohort studies) or were the cases and controls (case-control studies) recruited over the same period of time?	"1" If all the participants were recruited over a mentioned and limited period of time, otherwise "0"

Table S 2.I (continued)

Category	#Question in downs & black checklist	Question	Hints for assigning scores
Internal Validity-confounding (selection bias)	25	Was there adequate adjustment for confounding in the analyses from which the main findings were drawn?	"1" if walking speed and shoe model was not significantly different between participants, otherwise "0"
Power	27	Did the study have sufficient power to detect a clinically important effect where the probability value for a difference being due to chance is less than 5%?	"1" if the number of participants were selected based on any power or sample size calculation, otherwise "0"

Chapter 3 - Predicting Foot Orthosis Deformation Based on its Contour Kinematics During Walking

This chapter is presented as an article, published in *PLoS One* journal. This article was co-authored by Maryam Hajizadeh, Benjamin Michaud, Gauthier Desmyttere, Jean-Philippe Carmona, and Mickael Begon. Maryam hajizadeh had a major contribution and was the corresponding author for this article. The conceptualization and design of this study were developed by Maryam Hajizadeh, Mickael Begon, and Benjamin Michaud. The data were collected by Maryam Hajizadeh and Gauthier Desmyttere. Data analysis was performed by Maryam Hajizadeh and Benjamin Michaud. Other co-authors contributed to the validation of results. Maryam Hajizadeh wrote the paper and all co-authors reviewed and validated the writing.

Published as: Hajizadeh M, Michaud B, Desmyttere G, Carmona JP, Begon M (2020) Predicting foot orthosis deformation based on its contour kinematics during walking. *PLoS ONE;* 15(5): e0232677. https://doi.org/10.1371/journal.pone.0232677

Abstract

Background: Customized foot orthoses (FOs) are designed based on foot posture and function, while the interaction between these metrics and FO deformation remains unknown due to technical problems. Our aim was to predict FO deformation under dynamic loading using an artificial intelligence (AI) approach, and to report the deformation of two FOs of different stiffness during walking.

Methods: Each FO was fixed on a plate, and six triad reflective markers were fitted on its contour, and 55 markers on its plantar surface. Manual loadings with known magnitude and application point were applied to deform "sport" and "regular" (stiffer) FOs in all regions (training session). Then, 13 healthy male subjects walked with the same FOs inside shoes, where the triad markers were visible by means of shoe holes (walking session). The marker trajectories were recorded using optoelectronic system. A neural network was trained to find the dependency between the orientation of triads on FO contour and the position of markers on its plantar surface. After tuning hyperparameters and evaluating the performance of the model, marker positions on FOs surfaces were predicted during walking for each subject. Statistical parametric mapping was used to compare the pattern of deformation between two FOs.

Results: Overall, the model showed an average error of < 0.6 mm for predicting the marker positions on both FOs. The training setup was appropriate to simulate the range of displacement of triads and the peak loading on FOs during walking. Sport FO showed different pattern and significantly higher range of deformation during walking compared to regular FO.

Conclusion: Our technique enables an indirect and accurate estimation of FO surface deformation during walking. The AI model was capable to make a distinction between two FOs with different stiffness and between subjects. This innovative approach can help to optimally customize the FO design.

3.1. Introduction

The human foot plays an important role in propulsion, stability and efficiency [40, 288, 289]. If the foot architecture cannot support the biomechanical demands of different activities, various foot pathologies might occur [1, 290-292]. Foot orthoses (FOs) are getting more popular in clinics to treat several types of symptomatic feet [217]. FO comes into direct contact with the foot and is, therefore, subject to deformation during dynamic loading, such as walking. FO design and foot structure work in parallel to conduct the range and pattern of deformation. Therefore, the motion and function of symptomatic foot could be enhanced by managing FO deformation *via* FO design.

Previous literature suggests the dependency between FO design and different alterations in foot posture and pressure [173, 293]. FO with medial posting brings about lower ankle eversion during walking, while lateral posting exhibits a reverse effect [22, 173]. In addition, arch-conforming shape of FO as well as insole stiffness have been reported to exhibit important impact on reducing peak plantar pressure [109]. Heel lifts with higher thickness and material hardness lead to higher plantar pressure in forefoot and heel regions compared to medium and soft materials. Both inadequate support induced from softer heel lifts and decreased compliance from harder heel lifts could subsequently compromise dynamic stability and comfort [294]. Therefore, both shape and stiffness of FO could modify the altered foot motion pattern and plantar pressure related to pathologies.

While the interaction between FO design and foot motion and function has been already reported [26, 173, 264, 295], the behaviour of FO, *i.e.* its deformation, during dynamic loading remains unknown. The main issue is that it is not possible to directly capture FO deformation *via* optoelectronic system and reflective markers, since FO plantar surface is hidden by foot contact. Artificial intelligence (AI) and finite element analysis have the potential of estimating FO deformation as alternative techniques. AI has been increasingly implemented to accurately predict time series and sequences with complex patterns [296-298]. Since AI is a data-driven self-adaptive method, it needs much fewer humanly decided assumptions and simplifications than finite element analysis [297]. Through a training dataset, the AI responds to the information flowing into the network. A test session is then used to generate the output features as a response to previously unseen inputs, in order to assess the performance of generated model [296, 299]. Thereafter, the validated model would be used to predict the FO deformation during walking, where the FO plantar

surface is hidden by foot contact. The predicted FO deformation with AI could finally be used to estimate objective function for a finite element model to optimize the design of FO and improve foot posture and plantar pressure of symptomatic foot.

The objective of this study was to suggest a novel method to predict the deformation on plantar surface of FO based on the orientation of FO contour during dynamic loading. To this end, a setup was designed to provide a comprehensive dataset for training an AI model. The dataset obtained from this setup could simulate the walking condition by controlling the orientation and magnitude of applied loads. The validation of the AI model was examined *via* the test dataset. Finally, this model was used to predict the FO deformation during walking with two FOs of different stiffness. It was hypothesized that the AI model enabled us to differentiate between FOs in terms of different ranges or patterns of deformation.

3.2. Materials and Methods

A total of 13 healthy male subjects with normal feet (age = 25.9 ± 4.2 years old, height =176.2 ± 4.3 cm, weight= 74.6 ± 7.8 kg, shoe size 9-10) were recruited *via* call for volunteers at the School of Kinesiology. The inclusion criteria for participants was to be free from any limb injuries at the time of testing and having no known history of foot structural abnormalities or pathologies. The subjects were asked whether they have ever used foot orthosis or therapeutic insoles for any reason of pain or foot injuries especially flatfoot deformity. In addition, two observers, GD and MH, had to examine and include the subjects with normal medial arch during weight bearing/non weight bearing position and normal rearfoot orientation relative to tibia long axis. Ethical approval was obtained from University of Montreal (17-145-CERES-D approval), and all participants gave their written informed consent.

3.2.1. Setup design and data acquisition

A three-dimensional scan of a positive cast mold generated from the average foot shape of 2000 European males (foot size 10) was used to design a customized three-quarter length FO. The FO plantar surface followed the contour of foot (medial and lateral arch, heel cup) with 1.5 mm thickness superimposed to honeycombs. The height of the honeycomb cells was then changed to reach two different stiffness (termed as “sport” *versus* “regular” FO). The regular FO was stiffer, *i.e.* less deformable, as an effect of higher honeycombs compared to sport FO. The design also

included six double-cross slots on the FO contour allowing for fitting six triads, each consisting of three reflective markers mounted on branches of 20 mm in length. Both FOs and triads were 3D printed in nylon 12 (Figure 3.1-a). Data collection was performed in two measurement sessions: training and walking.

In the training session, each FO was placed and fixed at the heel region on a wooden plate covered with a soft material corresponding to a shoe midsole property. Fifty-five 3-mm hemispherical retroreflective markers were taped to the plantar surface of FO, and triads were fitted on its contour (Figure 3.1-a, b). After capturing an unloaded static position for each FO, a 20-cm long stick with a narrow circular shape at the tip (6-mm diameter) and equipped with a load cell (Model XLU68F-250, Full Scale Range 250 Lbs, Delta Metrics Inc., Worthington, Ohio) was used in order to deform FO. The load cell was primarily calibrated with compressive loads before training session (Supplementary materials: Figure S 3.1). Different loadings were applied to all FO regions using the stick. The application point and magnitude of applied load was controlled *via* four retroreflective markers placed on the stick and the load cell, respectively (Figure 3.1-a).

During the walking session, each FO was placed inside standard sports shoes (New Balance 860 v8), and Medilogic WLAN insole was placed on plantar surface of FO to record foot plantar pressure. Six circular holes (25-mm diameter) were made on the upper shoe allowing a direct access to the FO contour in order to fit the triads. Each participant was asked to walk on a treadmill for 5 minutes for habituation, where his comfortable speed was acquired for the following measurements (Supplementary materials: Table S 3.I). Then, the participant walked for 3 minutes at this acquired speed for each sport and regular FO condition (Figure 3.1-c). A rest period of 5 minutes was given between conditions to avoid fatigue effects. Data acquisition included the recording of walking on a treadmill for 3 minutes at self-selected comfortable speed for each subject with each FO (Figure 3.1-c). The last 30-s of walking were used for further processing.

In both sessions, the markers' trajectories were recorded using an 18-camera VICON^{TM} optoelectronic motion analysis system (Oxford Metrics Ltd, Oxford, UK) at a sampling rate of 100 Hz. In addition, the load cell data and foot plantar pressure were recorded at sampling rate of 1000 Hz and 400 Hz, respectively.

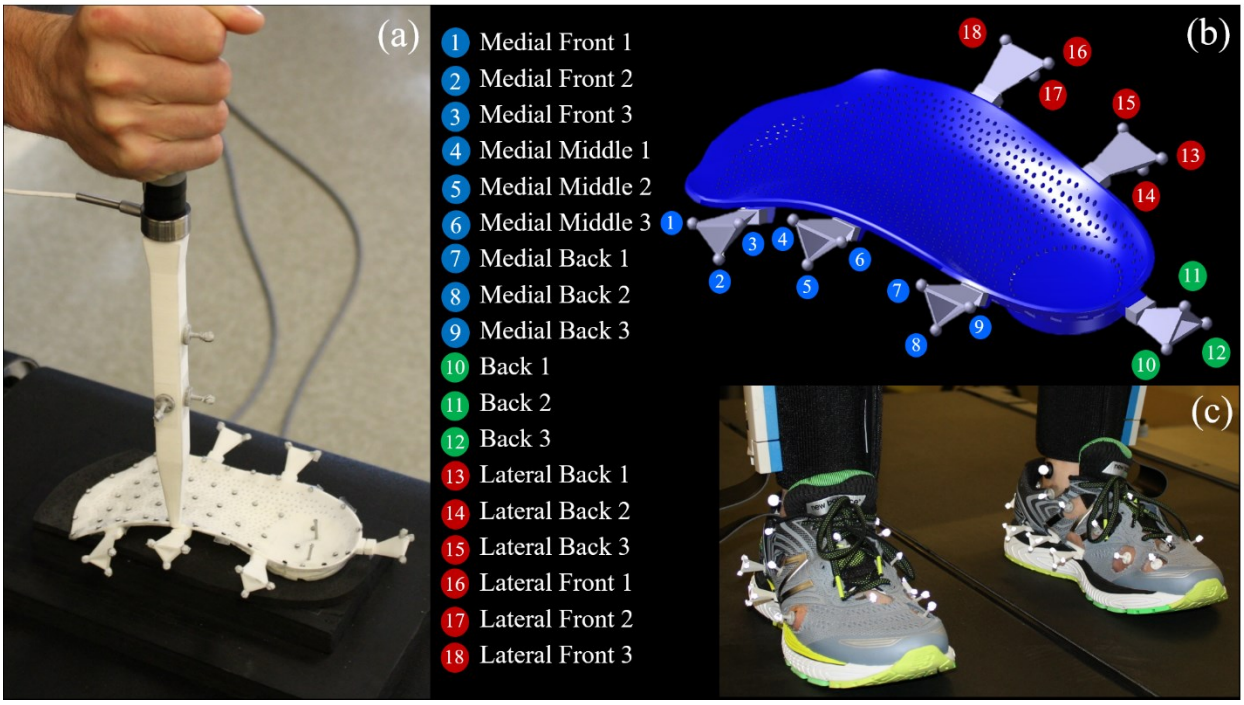

Figure 3.1: Set-up and markerset for two sessions. (a) *Training* session with attaching markers on plantar surface and triads on the contour of foot orthosis (FO), fixing FO on heel part, and load application. (b) The position and tag of triad markers fitted on foot orthosis contour. (c) *Walking* session with placing FO inside the shoe and inserting triads.

3.2.2. Deep learning for predicting FO deformation

The standardization of data was performed by expressing the data in a local coordinate system at each time frame. This local coordinate frame was defined from the position of three markers on triads (markers 4, 11, and 18 in Figure 3.1-b). The input data were the three-dimensional orientation of each triad relative to back triad, being computed by YXZ Cardan sequences. They were expressed as a vector of size OT = 15 (3 [relative orientation angle per triad] ×5 [triads]), trained over the number of time frames. The output feature was the position of markers on plantar surface of FO with the size of MPS=165 (3 [x, y, z] × 55 Markers on Plantar Surface) over the number of time frames.

A large amount of data was acquired for each FO in order to let load application in several FO regions. The frames without loading (< 0.1 N) was omitted from the acquired data, and the remained frames were then stratified based on 10 different regions of load application and got shuffled. These regions were defined as medial front, medial middle, medial back, back medial,

back, back lateral, lateral back, lateral middle, lateral front, and middle FO regions (Supplementary materials: Figure S 3.2). This method enabled us to control the proportion of different loadings over time and distribute them in the whole dataset.

The stratified shuffled data were split into learning set (85%) and test set (15%) for each FO. Data of *learning* set was used to tune the hyperparameters of the model, and *test* set was kept aside as unseen data to evaluate the performance of final selected model. Grid search algorithm with K-fold cross validation (K = 5) was used to tune the model. This algorithm performs exhaustive search to find the optimal parameters, where the 5-fold cross-validation splits the learning set into five different groups of train and validation sets to avoid overfitting. The tested hyperparameters were the number of layers at a range from 1 to 5, three optimizers namely "Adam", "Adadelta", and "Adagrad", learning rates of 0.01 and 0.005, batch size in the range of 16, 32, 64, and 128, and epoch in the range of 20, 50, and 100. The architecture of neural network was finally selected as densely connected neural network, with four layers (two hidden layers), optimizer "Adam" with learning rate of 0.005, loss function "mean square error", 100 epochs and batch size of 16, designed by TensorFlow [300]. These parameters provided the best accuracy (lowest loss) for learning the dependency between input (triads) and output (plantar surface markers).

3.2.3. Validation

A primary step for validation was to check whether the deformation and loading during the training session replicates what happens during walking. Regarding deformation, the ranges of displacement for 18 markers mounted on triads expressed in the local frame during *walking session* for all included subjects was compared to the corresponding ranges during *training* session for each sport and regular FO separately. This comparison was done for upward/downward displacement of triads, since it is the dominant component of displacement which can be considered for biomechanical behaviour of FO. For loading, the range of peak plantar pressure for all included subjects during walking was compared to the range of manual loading from stick during training session for each region of FO. The more overlap exists between the ranges of displacement and loading during *training* and *walking* sessions, the more accurate predictions would be expected [301, 302].

In addition, the generalization performance of the neural network was evaluated with the *test* set for each FO. The root mean square error (RMSE) was calculated as the difference between the "measured" and "predicted" marker positions on the FO plantar surface; normalized RMSE (NRMSE) were also estimated by normalizing the RMSE to the maximal deformation for each marker, calculated as the Euclidian distance between the position of MPSs on test set and reference position, *i.e.* unloaded static position.

3.2.4. Walking

The position of markers on plantar surface of both sport and regular FO were predicted using relative orientation of triads during the walking session for each subject. Similar to the training session, the coordinates of all available markers were expressed in the coordinate system generated by the three selected markers on triads for both sessions. This projection could reflect both rigid transformation (rotation and translation) and deformation of FO in the shoes during walking. Therefore, polar decomposition was used to calculate the optimal roto-translation between each time frame and the static condition to only extract the deformation [303, 304]. Finally, the 3D positions of optimally transformed markers were normalized to stance phase of walking, and the depression/reformation of each marker was calculated by subtracting its upward/downward position from its corresponding position at unloaded static position. For each subject, the pattern of FO deformation was displayed, and the magnitude of maximum depression and reformation was extracted for each stance phase of walking. Finally, in order to determine significant differences between the deformation of sport and regular FO, statistical parametric mapping (SPM1D) was used to conduct non-parametric paired *t*-test on 2D deformation matrices. These matrices were generated from the deformation of points on FO plantar surface at each time frame for each subject.

3.3. Results

The suggested technique to predict FO deformation was not only appropriate for simulating the loads and deformation during walking, but also accurate in terms of prediction error. As it was hypothesized, the AI model could also discriminate sport FO from regular FO.

3.3.1. Validation

3.3.1.1. Range of displacement

The ranges of upward/downward displacement of each triad marker during walking session were a subset of its displacement during training session for all included subjects (Figure 3.2). For sport FO, the subjects generated an average range of [6.0 ± 1.8; 6.1 ± 1.8; 7.0 ± 2.1 mm] on the medial front triad, [6.0 ± 1.8; 6.3 ± 1.9; 6.9 ± 2.0 mm] on the medial middle, and [4.3 ± 1.2; 4.8 ± 1.6; 6.1 ± 2.5 mm] on the medial back during walking compared to maximum amounts of [12.7; 14.6; 17.5 mm] on the medial front triad, [12.7; 13.7; 14.7 mm] on the medial middle, and [24.3; 23.6; 21.1 mm] on the medial back during training session. The back triad exhibited 12.1 ± 3.7 mm during walking for its three markers *versus* 25 mm during training. The markers of lateral back triad displaced within a range of [7.2 ± 2.1; 6.4 ± 1.8; 5.6 ± 1.7 mm] during walking, while they exhibited the maximum displacement of [18.8; 20.9; 23.9 mm] during training. In addition, the subjects generated an average range of [6.0 ± 1.8; 4.4 ± 1.3; 4.1 ± 1.1 mm] displacement on three markers of lateral front triad during walking, while we imposed a maximum displacement of [12.6, 10.1, and 7.7 mm] on this triad during training session.

For regular FO, the ranges of displacement were lower for all triads during walking and training sessions compared to sport FO. On the medial side of FO, the subjects displaced the triad markers with the ranges of [5.3 ± 1.7; 5.3 ± 1.8; 6.2 ± 2.3 mm] on the front, [5.3 ± 1.7; 5.5 ± 1.7; 6.2 ± 1.8 mm] on the middle, and [2.7 ± 0.7; 3.1 ± 1.3; 4.0 ± 1.5 mm] on the back during walking. During training these triad markers were displaced with maximum ranges of [10.0; 11.6; 13.5 mm], [10.0; 11.1; 12.1 mm], and [11.7; 11.0; 8.6 mm], respectively. The back triad moved [10.7 ± 3.5 mm] during walking compared to [19.9 mm] during training. The subjects showed an average of [4.0 ± 1.1; 4.0 ± 1.3; 4.2 ± 1.1 mm] for the lateral back triad and [5.3 ± 1.7; 4.3 ± 1.3; 4.1 ± 1.2 mm] for the lateral front triad during walking, while a maximum displacement of [12.0; 12.5; 14.4 mm] and [10.0; 7.8; 5.4 mm] was generated during training, respectively (Figure 3.2).

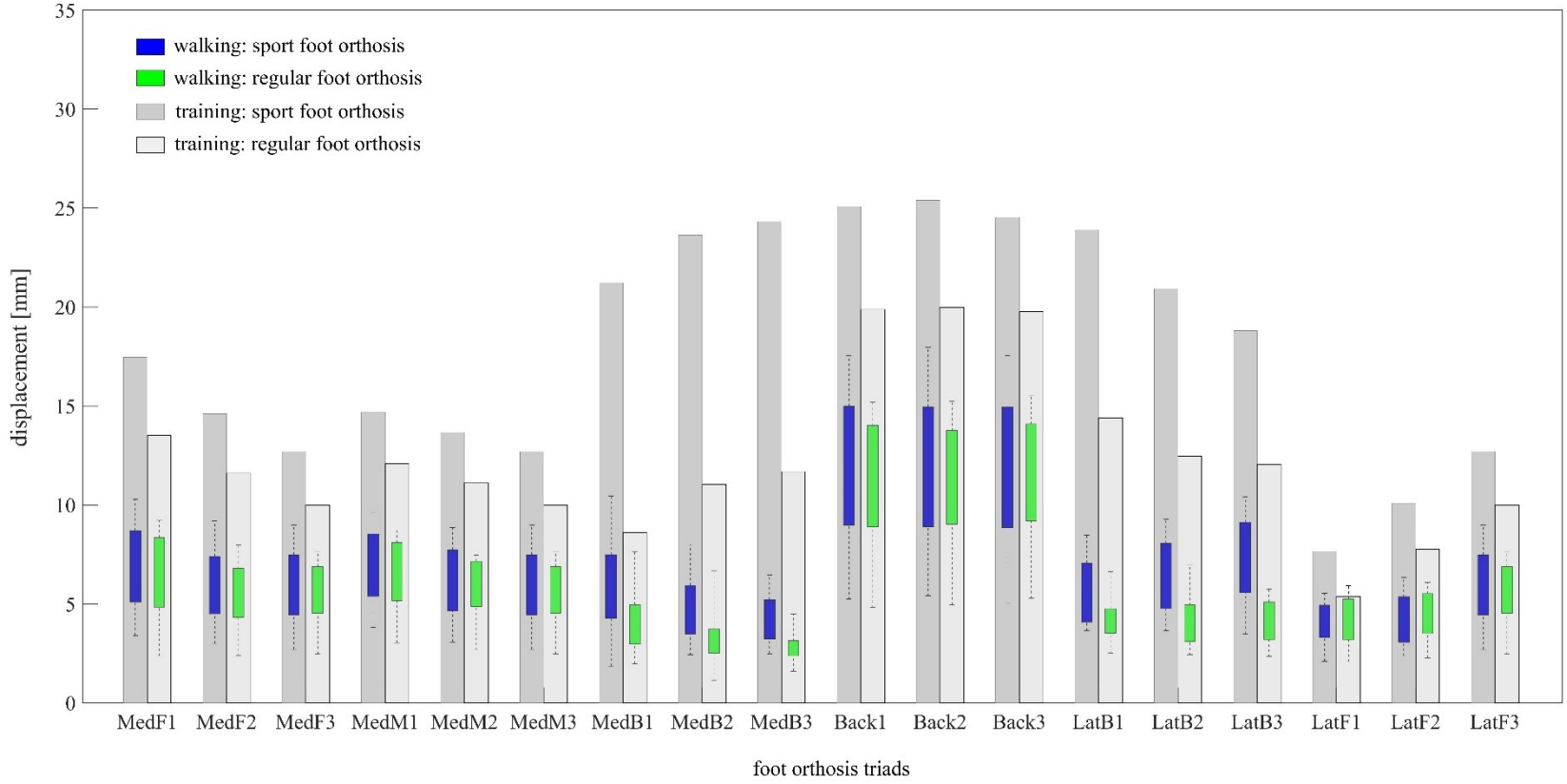

Figure 3.2: Comparing the range of displacement for triad markers during training session and walking session for both sport and regular foot orthosis. The displacement for walking session is the range generated by all included subjects. The horizontal axis shows each of 3 markers on each triad namely MedF: Medial Front, MedM: Medial Middle, MedB: Medial Back, Back, LatB: Lateral Back, LatF: Lateral Front. The position on each triad marker can be observed in Figure 3.1.

3.3.1.2. Range of loading

The results showed that the range of loading that was applied manually from stick to the FO during training session could cover the range of pressure that all subjects applied to each 10 regions of FO during walking for both FOs (Figure 3.3).

For sport FO, the subjects applied a range of 14.9 ± 5.9 N for peak force (peak pressure multiplied by sensor area) on the medial front region, 23.7 ± 5.6 N on the medial middle region and 25.7 ± 6.8 N on the medial back region. During training, maximum loads of 53.7 N, 70.1 N, and 65.8 N were applied to the medial front, middle, and back regions, respectively. On the back region, the subjects applied a range of 21.7 ± 12.2 N on medial back, 26.3 ± 11.4 N on central back, and 19.9 ± 10.7 N on the lateral back during walking compared to the exerted loads of 57.5 N, 53.5 N, and 62.0 N on these regions during training. On the lateral region, the range of peak force was 20.6±7.4 N, 25.3 ± 6.2 N, 24.7±6.3 N during walking on the front, middle, and back regions compared to 63.3 N, 53.9 N and 64.1 N during training. For the middle region, maximum force of 26.1 ± 7.9 N was applied during walking *versus* 73.2 N during training (Figure 3.3).

For regular FO, the average maximum forces for medial front, middle and back regions were 15.43 ± 4.4 N, 28.2 ± 6.5 N and 28.2 ± 11.3 N during walking *versus* 85.5 N, 104.4 N, and 102.2 N during training, respectively. On the back region, the subjects walked with applying maximum forces of 20.3 ± 12.1 N on medial back, 21.9 ± 9.2 N on central back, and 23.4 ± 13.5 N on lateral back, while the maximum stick load was 116.9 N, 52.0 N and 61.7 N on the corresponding regions. The FO experienced maximum forces of 21.6 ± 7.1 N, 34.2 ± 10.4 N, and 32.7 ± 13.0 N during walking at lateral front, lateral middle, and lateral back *versus* 53.5 N, 119.9 N, and 76.3 N during training. The walking session showed maximum force of 32.3 ± 9.6 N on the middle region of FO, while a maximum force of 98.6 N was applied to this region during training (Figure 3.3).

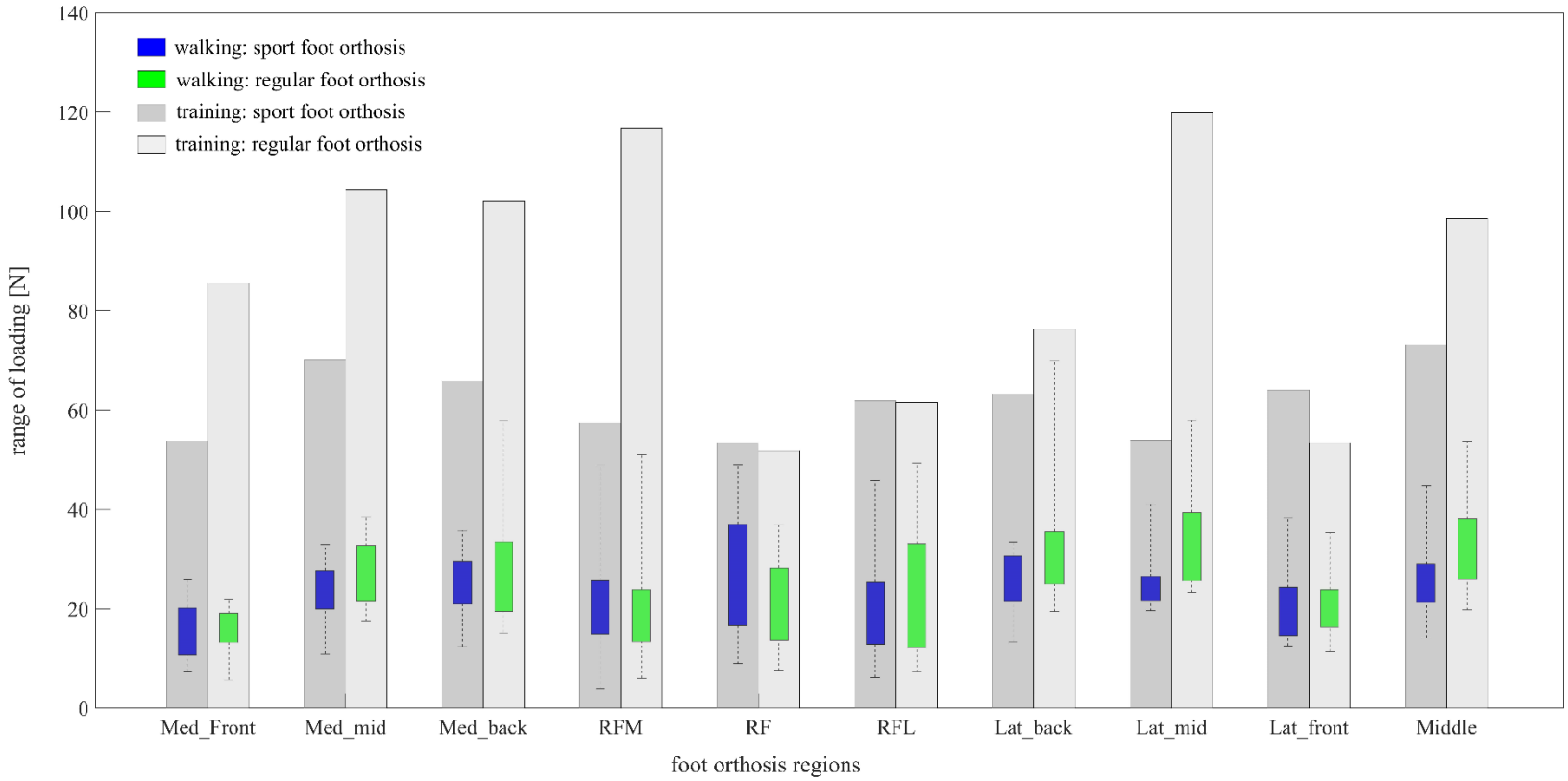

Figure 3.3: Comparing the range of loading on different regions of foot orthosis during training session and walking session for both sport and regular foot orthosis. The loading for walking session was calculated from the range of peak pressure generated by all included subjects.

3.3.1.3. Prediction error

The maximum deformation of the markers on plantar surface of FO ranged between 2.2 mm and 10.5 mm for sport FO and between 0.9 mm and 8.7 mm for regular FO with the largest deformation under the medial arch, lateral arch, and middle regions (Figure 3.4-c). The mean and standard deviation RMSE for the 55 markers on FO plantar surface was 0.3 ± 0.1 mm (95% confidence interval for RMSE= [0.31, 0.36] mm) for sport FO, and 0.6± 0.1 mm (95% confidence interval for RMSE= [0.53, 0.61] mm) for regular FO. The reconstruction error was higher for regular FO compared to sport FO (Figure 3.4-a). In addition, the normalized error was 8.2 ± 3.0 % for sport FO and 20.6 ± 12.6 % for regular FO (Figure 3.4-b). The highest NRMSE was observed on the back and medial/ lateral back regions of both FOs.

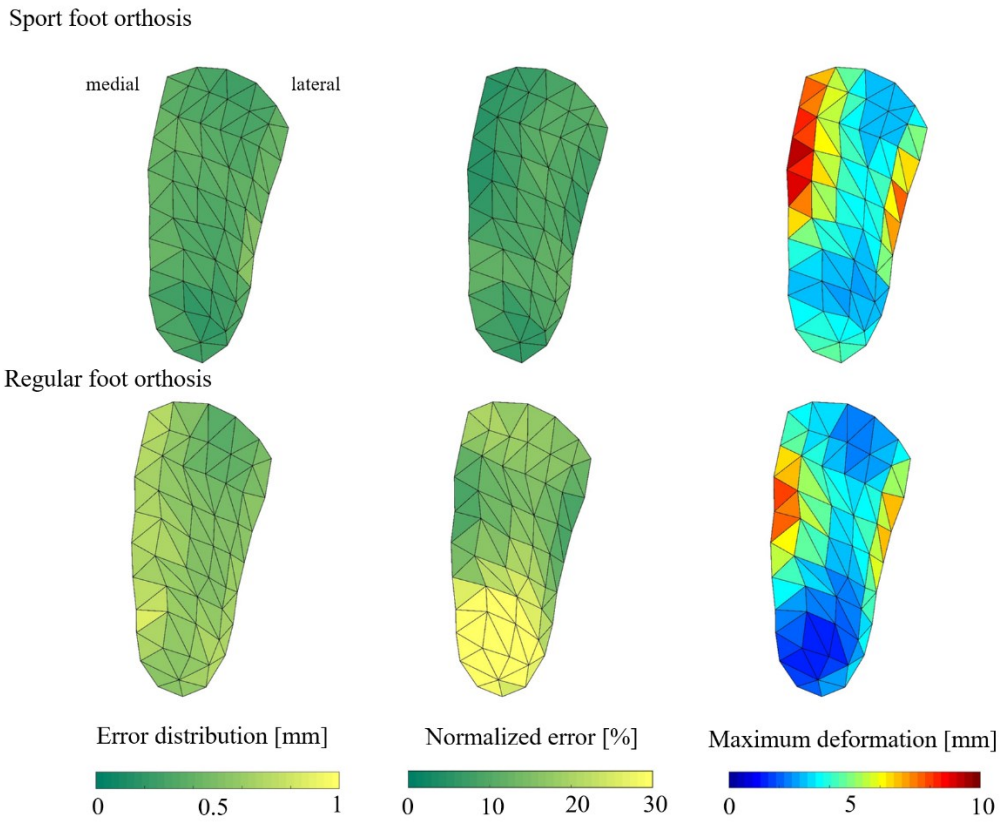

Figure 3.4: Distribution of reconstruction error for sport and regular foot orthosis (a) Colormap of prediction error on plantar surface of foot orthosis [mm]; (b) Colormap of prediction error normalized to maximum deformation [%]; (c) Maximum deformation on plantar surface of foot orthosis for test set [mm]. To show the error distribution on foot orthosis surface, the prediction error for each grid was calculated as the average error of its vertices.

3.3.2. Walking

Figure 3.5, Figure 3.6, and Figure 3.7 showed that subjects generated different magnitude and patterns of deformation across the plantar surface of sport compared to regular FO during walking. Small range of variability was observed between subjects in each group of FO, mostly for the magnitude of deformation.

In general, the collapse of the foot medial arch imposed depression on the medial region of sport FO from heel strike to midstance (50% stance phase), where it started to reform until toe off. The lateral region of FO showed a reverse deformation compared to medial region. A reformation of FO under lateral arch from heel strike to either flatfoot or midstance was followed by depression until toe off (Figure 3.5). The middle region of FO exhibited depression from heel strike to toe off with shifting its maximal depression from medial to lateral side during stance phase. The median of maximum depression varied from -5.6 to -10.6 mm, and the maximum reformation from 0.2 to 3.7 mm between subjects for sport FO (Figure 3.6-a).

For the regular FO, the depression of medial region from heel strike to either flatfoot or midstance was followed by a reformation until toe off with smaller range compared to sport FO (Figure 3.7). The lateral region of regular FO showed depression during either the whole stance phase or from heel strike to heel off. The depression on the lateral region was mostly focused on the frontal region rather than distributing in the whole lateral region in contrary to sport FO. The depression in the middle region of FO was mostly occurring from heel strike to heel off, which was accompanied with a shift from medial middle to lateral middle by advancing in stance phase. The median range of maximum depression changed from -4.0 to -6.8 mm between subjects, where they varied from 1.1 to 4.5 mm for maximum reformation (Figure 3.6-b).

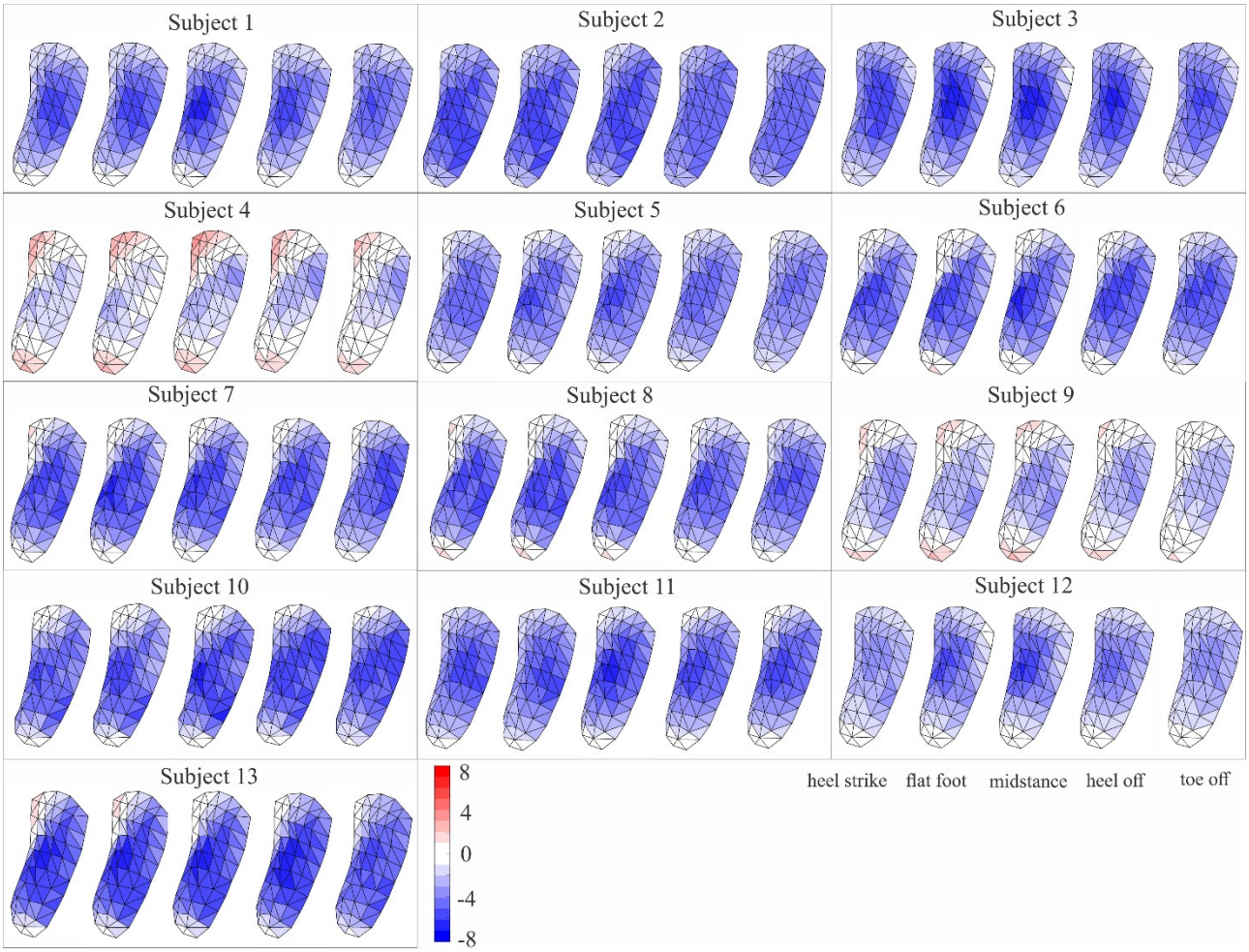

Figure 3.5: Colormap of depression/reformation of sport foot orthosis (FO) during different key events of stance phase of walking for each subject. The negative values show depression and positive values show reformation of FO. To show the deformation on FO surface, the deformation for each grid was estimated as the average deformation of its corresponding vertices.

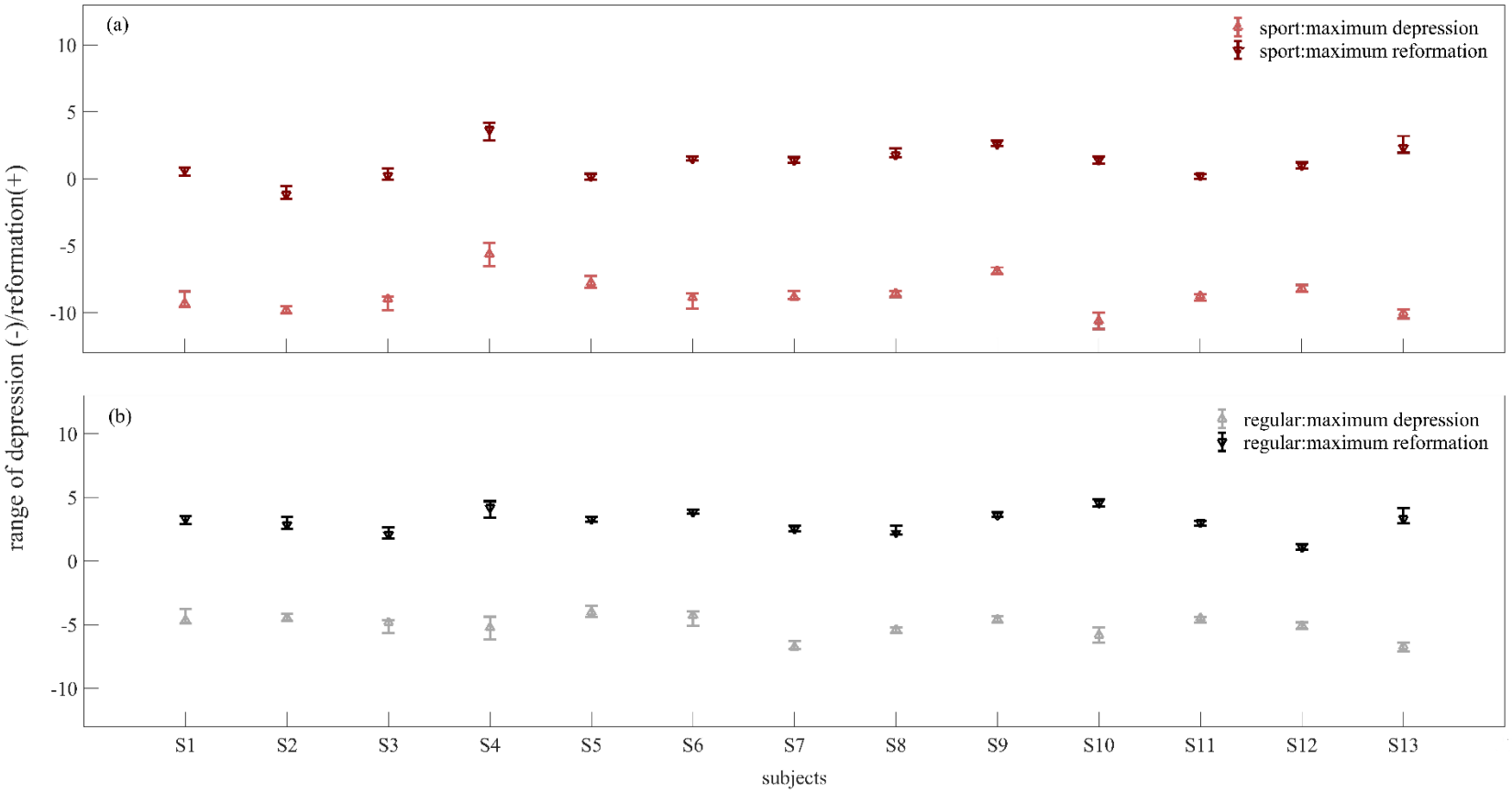

Figure 3.6: The range of maximum depression and maximum reformation for each subject during stance phase of walking with (a) Sport foot orthosis, (b) Regular foot orthosis.

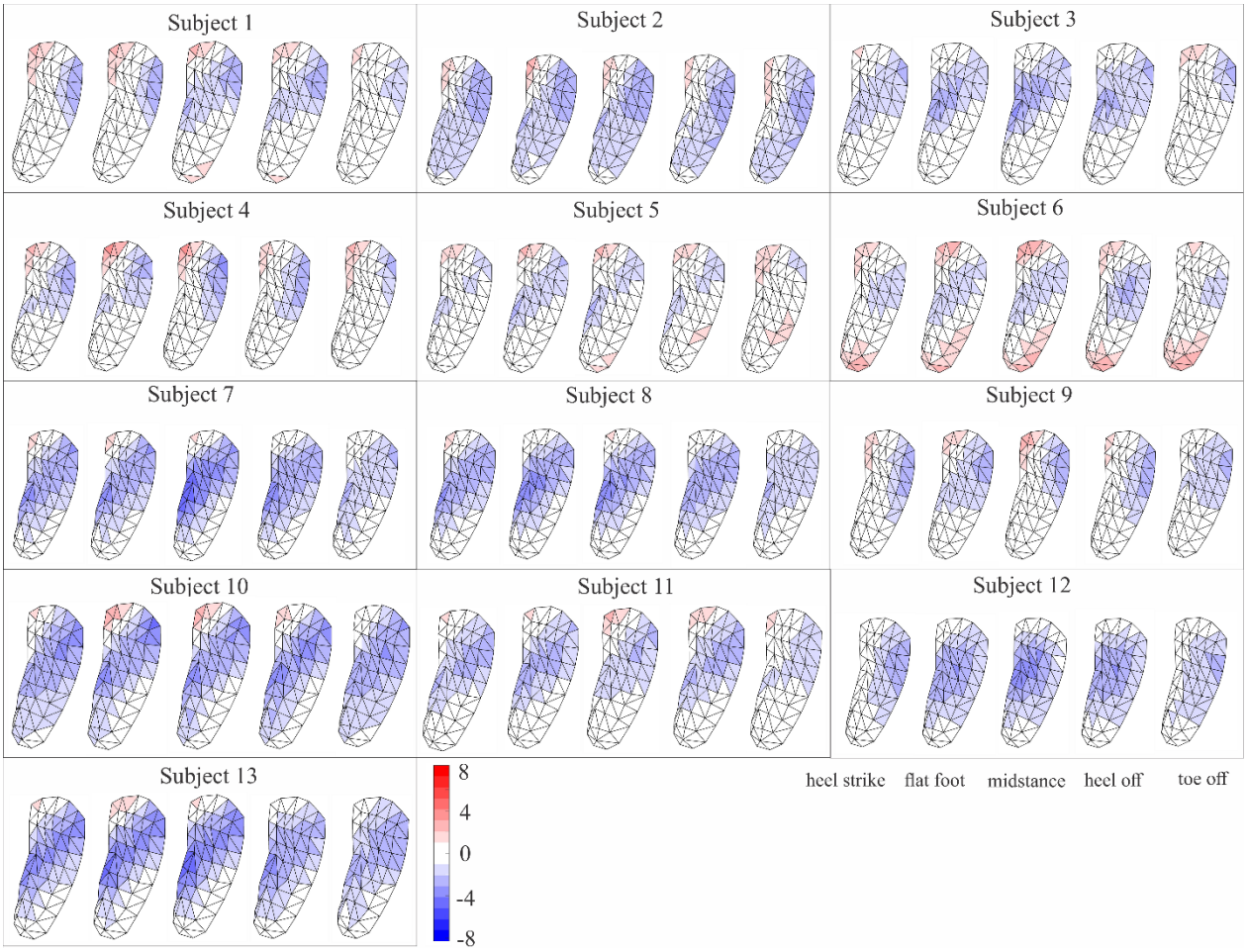

Figure 3.7: Colormap of depression/reformation of regular foot orthosis (FO) during different key events of stance phase of walking for each subject. The negative values show depression and positive values show reformation of FO. To show the deformation on FO surface, the deformation for each grid was estimated as the average deformation of its corresponding vertices.

The average range of depression/reformation was [-7.7 to 0.5] mm for sport FO *versus* [-3.9 to 2.5] mm for regular FO (Figure 3.8). Statistical analysis showed significant differences in deformation between sport and regular FO: the sport FO was more depressed on the middle region of FO, as well as the regions under medial and lateral arch compared to regular FO, from heel strike to toe off. In addition, the frontal extremity of lateral region and the back region showed more deformation in regular compared to sport FO.

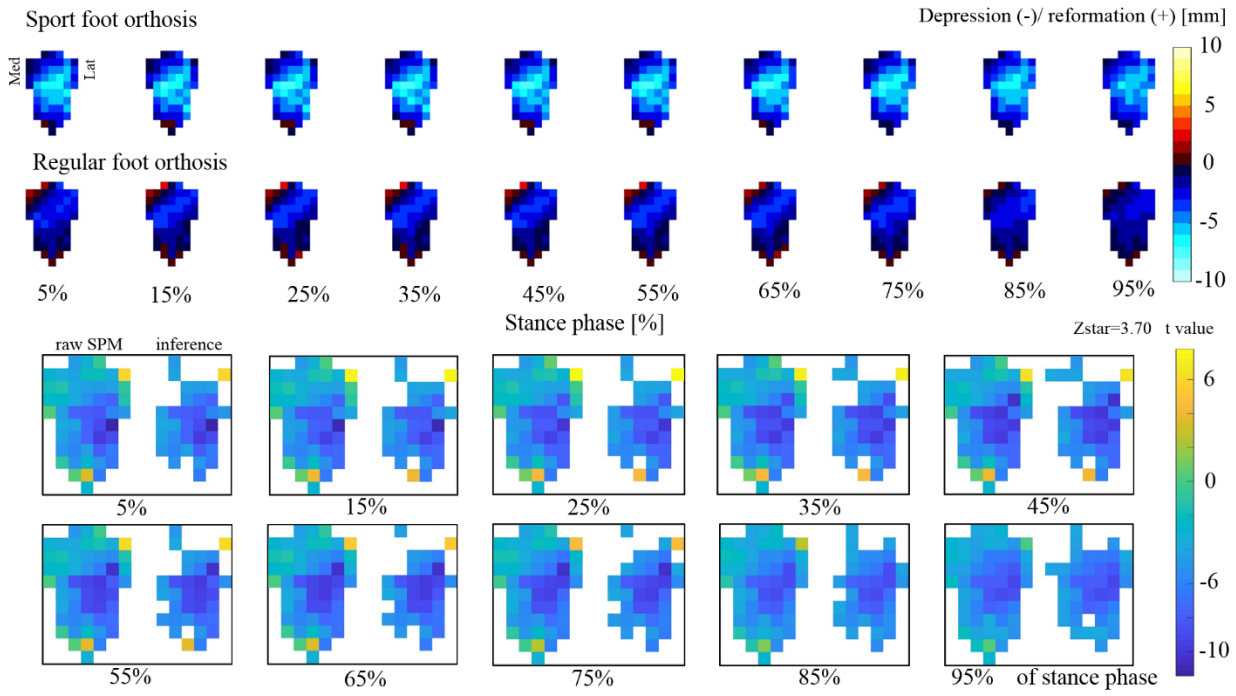

Figure 3.8: For each 10 percent of walking (a) The average range and pattern of deformation for sport and regular foot orthoses during walking for all participants, (b) Non-parametric paired t-test results using SPM1D to compare the deformation of sport *versus* regular foot orthosis. Each subplot shows raw SPM (at left side) and inference (on right side).

3.4. Discussion

Our study showed that FO deformation could be predicted from markers on removable triads fitted on the contour of the FO using an artificial neural network. The training session ensured a wide coverage of displacement of triads and applied loads on FOs that happens during walking, thanks to the designed setup. The average absolute prediction error on the plantar surface of FO was less than 0.6 mm for both FOs with different stiffness. In addition, the AI model was capable to distinguish the differences in the range and pattern of deformation between the sport and regular FO during walking for all included subjects. The model could also differentiate between subjects, as it could predict the small variability in the range of deformation as well as the gait moment of shifting depression onto reformation or *vice versa*.

The prediction error of markers on FO plantar surface during walking could not be calculated in similar way to the test set, since it was impossible to get makers' trajectories inside the shoes.

Therefore, the output results of this study were significantly dependent on the input data. Indeed, the prerequisite of reaching accurate predictions is the existence of good overlap between the input data in training and test sessions [302, 305, 306]. This aspect was considered by developing a setup through which FO deformation was controlled based on the known forces. In fact, the stick as the tool of manual loading was equipped to a load cell for capturing the applied forces as well as retroreflective markers to retrieve the location of loading on FO. Moreover, the FO was placed on wooden plate covered with a layer of midsole property in order to simulate the support of FO inside the shoes. The heel part of FO was fixed on the plate to avoid sliding of FO due to load application. Heel cup is the supportive region of the FO to absorb the ground reaction force at foot strike and represents the most difficult region to be deformed under body weight loading [307-309]. Consequently, fixing heel cup could minimally affect the FO deformation. The results showed that the setup was robust in terms of producing the ranges of displacements for triad markers as well as the applied forces on several FO regions during training. In fact, the training data from this setup could cover all existing displacements and forces for both sport and regular FO during walking. Therefore, it can be assumed that the accuracy of FO deformation during walking would remain in the range of accuracy that was predicted for the test set data.

The absolute prediction error showed an average of 0.3 mm for sport and 0.6 mm for regular FO, which was distributed almost evenly on the whole surface of both FOs. This might indicate that our AI model has been capable to provide similar accuracy for predicting the position of markers on different regions of FO. The normalized error was maximum on the back and medial/lateral back regions of regular FO. It could be due to the fact that the sport FO, and the regions under medial/lateral arch of regular FO were easier to deform due to the compliance and arch shape in contrast to medial/lateral back and back regions of regular FO during the training session. A previous research has reported 2.2 mm difference between arch deformation predicted from finite element model (9.9 mm) and experimental deformation (7.5 mm) in balanced standing position only [310]. Hence, in spite of maximum absolute error happening in the medial/lateral back regions of FO in this study, it was still lower than 1 mm during dynamic loading on FO, promising good prediction accuracy.

The deformation in several regions of FO during walking was extracted based on the predicted position of 55 markers spread out over the plantar surface of FO. The sport FO showed higher

magnitude of deformation under medial arch region and middle FO region compared to regular FO, suggesting the capability of regular FO for providing higher level of support at medial arch. Furthermore, the reformation of sport FO under lateral region from heel strike to midstance was followed by a depression phase. In contrast, the regular FO exhibited depression under lateral arch and frontal arch regions during the whole stance phase or until heel off. Statistical results showed that regular FO exhibited significantly lower deformation during the whole stance phase, which can be inferred as providing more support by regular FO at medial/lateral arch and middle region of foot. For healthy normal feet, the lengthening of medial longitudinal arch lets the elastic structures of the arch to absorb and store energy at early stance. This energy would then be released during the late stance when the medial longitudinal arch recoils, and may provide enough power for propulsion [311]. In fact, the structure of FO works in series with the triangular architecture of medial longitudinal arch to ameliorate its stiffness and facilitate the arch reforming [311, 312]. The extra support provided by regular FO might benefit flatfoot subjects by preventing their excessive collapse of medial arch during weight bearing phase [313]. Depression under medial arch was accompanied by depression on middle region as well as reformation under lateral arch region for sport FO. However, it was accompanied by depression of both middle and lateral regions for regular FO. Hence, the regular FO might have distributed the body weight on lateral regions more than sport FO. From midstance to toe off, both FOs were unloaded and reformed their shape under medial arch, while the FO deformation was transferred to the lateral middle and lateral arch regions. This could suggest that the stiffness of medial and lateral arches could control either foot posture such that the center of pressure is shifted medially/laterally, or foot function such that foot pressure distribution alters. It would subsequently change the forces and moment arm of the ground reaction force and consequently the ankle and knee joint moments. Excessive stiffness of FO can lead to further injuries in ankle, knee and hip such as osteoarthritis [314-316]. In order to optimize the functionality of FOs, it is necessary to customize the stiffness of FO based on foot motion, foot function and body weight. Reaching this goal primarily entails understanding which metrics for foot motion or foot function account for the most variability of FO deformation in different regions. The prediction of FO deformation will make it feasible for future studies to focus on this problem. The principal source of inter-subject variability might be due to using general prefabricated FOs for all included subjects, regardless of their weight and foot structure. It might also be due to

different compensatory strategies that healthy subjects execute to deal with FO as the intervening tool between foot and shoes [317].

A limitation of this study was that point forces were applied during training session to see the markers displacements, and not a distributed force to simulate pressure as in walking. New setups could be developed to apply forces at different regions of FO plantar surface at the same time. Finite element analysis might be used as an alternative technique to generate the training session. However, each simulation with a single point load will take some hours, while it could not provide enough accuracy due to modeling simplifications. Another limitation was that relative orientation of triads were used rather than the position of triad markers in order to predict the position of markers on plantar surface of FO. It was found out that the triads were not fitted in the same depth of slots inside the FO contour during training session and walking session. Using the position of the markers as the input for AI model could subsequently propagate this error in the position of predicted markers. This experimental error was hardly possible to avoid due to the difficulty of measuring the depth of triads' insertions especially during walking session. However, this experimental error could be exempted by using the orientation of triads instead of the position of their markers. The relative orientation of each triad was calculated relative to back triad, because it had the minimal displacement. Finally, as foot orthosis is in direct contact with both foot and shoe sole, the deformation of FO is affected by the loading from foot and the boundary conditions imposed from shoe sole. It means that depending on the shape and mechanical properties of the shoe sole, we would change the degree of freedom for the range of deformation on the plantar surface of FO. In order to modulate the effect of shoe sole on the variability of FO deformation between subjects, standard shoes (New Balance 860 v8) were used for all subjects during walking. However, it is necessary to address the difference in the effect of shoe sole during training *versus* walking session as a limitation of this study. In the training session, the FO was fitted on a wooden plate covered with a soft material corresponding to a shoe midsole property. The movement of the shoe sole was therefore constrained in the training session. In contrast, the shoe sole during walking was capable to move and deform. This would lead to differences in the boundary condition applied from shoe sole on the deformation of FO. This limitation might be figured out in future studies by improving the setup design.

It is suggested that future studies look at the deformation of customized FOs on subjects with symptomatic feet. More between subject variations in the predicted deformation might be observed in such studies due to the different behaviours of customized FOs and their interaction with symptomatic feet. In addition, modifications in the design of slots and mechanical fit between triads and FO contour might be considered in future studies to reduce the experimental error in the position of triad markers. Finally, our findings were limited to FO deformation, while the correlation between FO deformation and plantar pressure as well as the correlation between FO deformation, foot kinematics, and arch flexibility is still unknown. Such results could bring advantages to mechanical and clinical aspects of customized FOs.

3.5. Conclusions

Predicting FO deformation during dynamic activities is a novel and promising approach which reflects the direct interaction between the foot and FO design. The results showed an absolute error of less than one millimeter for predicting the deformation on the plantar surface of both FOs. Our artificial intelligence model could discriminate between two FOs with different stiffness, *i.e.* "sport" *versus* "regular", by estimating different ranges and patterns of deformation during walking. Our model could also differentiate between different key events of the stance phase. The trend of FO depression which shifted from the medial arch to the middle region and lateral arch by advancing in the stance phase seems realistic with a biomechanical perspective. Inter-subject variability in FO deformation can be referred to as the differences in weight and foot shape. However, this variability was small due to the fact that our population had normal foot type and wore the same prefabricated contoured FOs. Further studies are needed to investigate how such information can be helpful to improve FO design for better functionality in terms of relieving pain and pathological symptoms.

3.6. Supplementary materials

The raw data related to this study is available online in the section of supporting information at https://journals.plos.org/plosone/article?id=10.1371/journal.pone.0232677. These files present the following data:

S1 File. The pattern of foot orthosis depression/reformation for healthy subjects during walking with sport *versus* regular foot orthosis.

S2 File. Raw data for the training session of sport foot orthosis. This Excel file consists three sheets in which the position of triad markers, the orientation of triad markers and the position of markers on plantar surface of foot orthosis are provided respectively.

S3 File. Raw data for walking with sport foot orthosis. This Excel file consists two sheets in which the position of triad markers and the orientation of triad markers are provided respectively for subject 1.

S4 File. The results of each participant during walking with sport foot orthosis. This .mat file includes "DispEachPoint" and "DispEachPointMean" which shows the displacement of each predicted marker on foot orthosis plantar surface during stance phase of walking relative to its corresponding position in static non weight-bearing for each trial and the average of trials respectively. In addition, "loc_stance" and "loc_meanstance" show the location of each predicted marker during stance phase of walking. "peaks" and "peaksMean" represent the minimum (depression) and maximum (reformation) value of displacement during walking

S5 File. The results of each participant during walking with regular foot orthosis. This .mat file includes "DispEachPoint" and "DispEachPointMean" which shows the displacement of each predicted marker on foot orthosis plantar surface during stance phase of walking relative to its corresponding position in static non weight-bearing for each trial and the average of trials respectively. In addition, "loc_stance" and "loc_meanstance" show the location of each predicted marker during stance phase of walking. "peaks" and "peaksMean" represent the minimum (depression) and maximum (reformation) value of displacement during walking

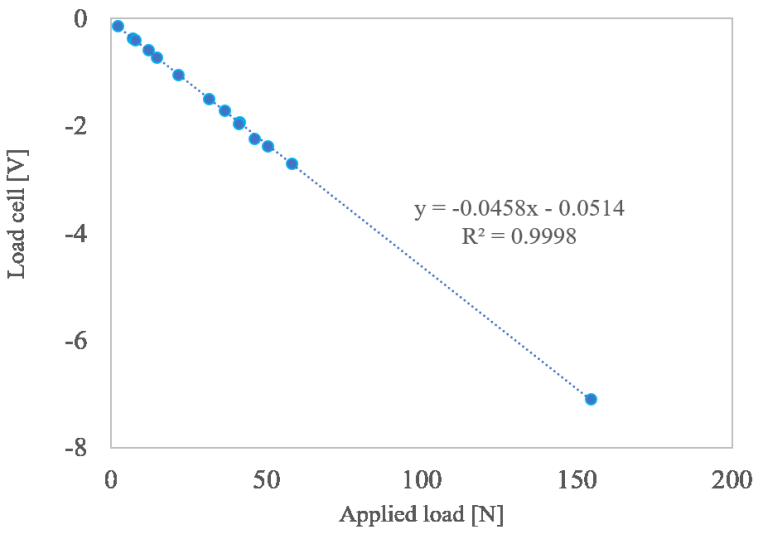

Figure S 3.1: The calibration session for extracting forces from load cell.

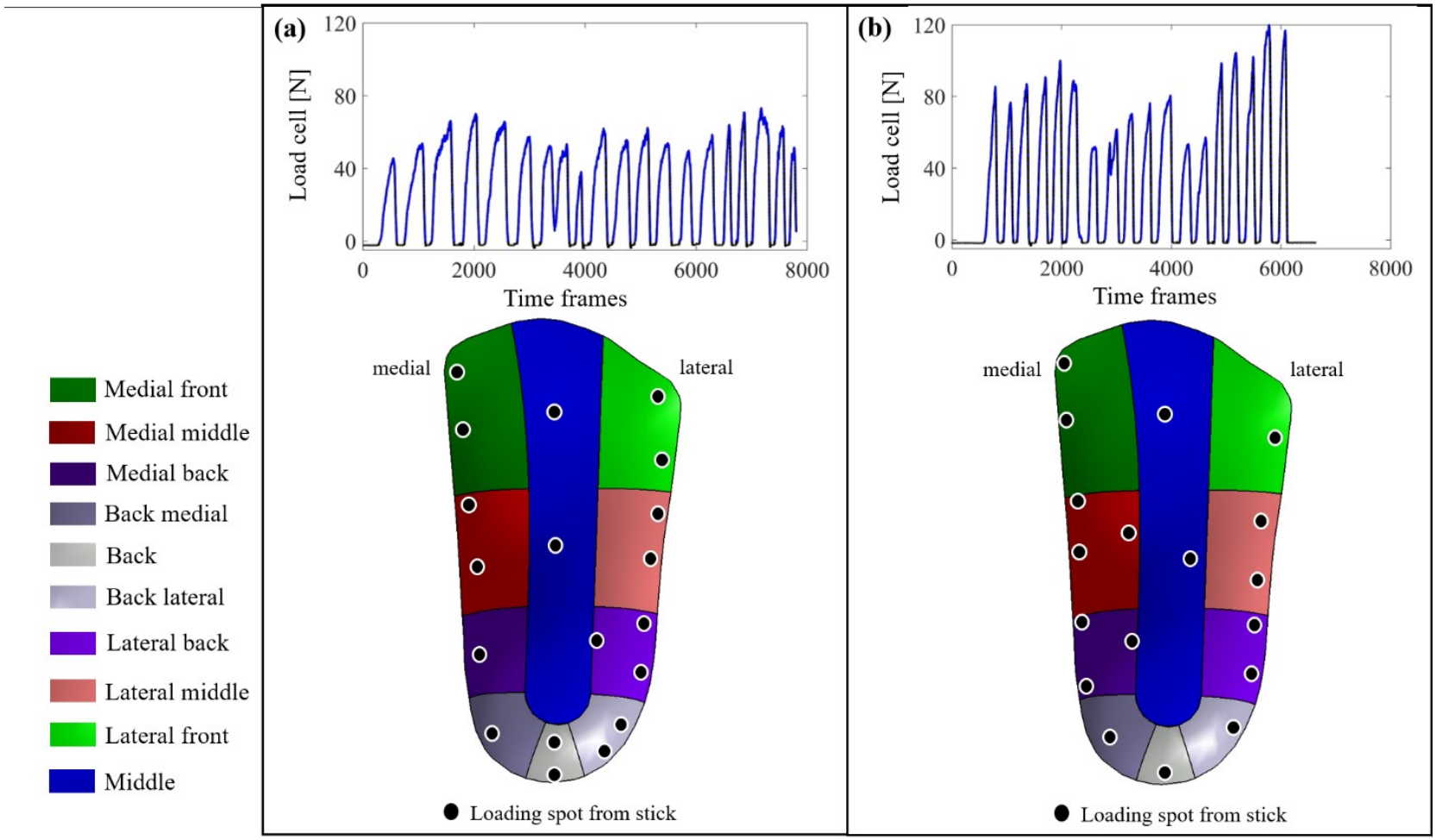

Figure S 3.2: The magnitude and location of loading applied from stick to deform foot orthosis in 10 regions: (a) Sport foot orthosis, (b) Regular foot orthosis.

Table S 3.I: The comfortable speed and step length of included participants

Subject #No.	Speed [m/s]	Step length [m]	
		Sport	Regular
1	0.8	0.53	0.52
2	1.1	0.39	0.46
3	0.7	0.48	0.46
4	1.0	0.56	0.55
5	1.0	0.48	0.47
6	0.9	0.52	0.52
7	1.1	0.59	0.59
8	1.0	0.56	0.53
9	1.0	0.60	0.64
10	1.0	0.57	0.56
11	1.0	0.51	0.51
12	0.8	0.49	0.50
13	1.2	0.62	0.60
mean ± SD	1.0 ± 0.1	0.53 ± 0.06	0.53 ± 0.05

Chapter 4 - Understanding the Role of Foot Biomechanics on Regional Foot Orthosis Deformation during Walking in Flatfoot Individuals

This chapter is presented as an article, submitted to *Journal of Biomechanics*. This article was co-authored by Maryam Hajizadeh, Gauthier Desmyttere, Anne-Laure Ménard, Jacinte Bleau, and Mickael Begon. Maryam Hajizadeh had a major contribution and was the corresponding author for this article. The conceptualization and design of this study were developed by Maryam Hajizadeh and Mickael Begon. The data were collected by Maryam Hajizadeh, Gauthier Desmyttere, and Anne-Laure Ménard. Data analysis was performed by Maryam Hajizadeh and Gauthier Desmyterre. Maryam Hajizadeh developed the statistical analysis approach, where it was validated and confirmed by Anne-Laure Ménard. Maryam Hajizadeh wrote the paper and all co-authors reviewed and validated the writing.

Submitted as: Hajizadeh M, Desmyttere G, Ménard AL, Bleau J, Begon M (2020) Understanding the role of foot biomechanics on regional foot orthosis deformation during walking in flatfoot individuals. *Journal of Biomechanics*

Abstract

Our objective was to determine the response of flatfoot individuals to foot orthosis (FO) deformation during walking as a function of their foot kinematics and plantar pressure distribution.

The kinematics of multi-segment foot and FO contour were recorded together with plantar pressure in 17 flatfoot individuals while walking with two rigidities of customized FOs. The deformation of the FO surface was predicted from its contour kinematics using an artificial neural network. Plantar pressure map and deformation were divided into five anatomically based regions defined by the corresponding foot segments. Forward stepwise linear mixed models were built for each of the four gait phases to determine the foot-FO interaction.

Foot kinematics and pressure showed small to moderate correlations with regional FO deformation. From heel-strike to foot-flat, the longitudinal arch angle was associated with FO deformation in the forefoot. From foot-flat to midstance, rearfoot eversion accounted for variations in the deformation of medial FO regions, and forefoot abduction for the lateral regions. From midstance to heel-off, rearfoot eversion, longitudinal arch angle, and plantar pressure played a significant role in FO deformation. Finally, from heel-off to toe-off, forefoot adduction influenced the deformation of forefoot and midfoot.

This study provides guidelines for designing customized FOs. Flatfoot individuals with excessive rearfoot eversion or very flexible medial arches require more support on medial FO regions, while the ones with excessive forefoot abduction need the support on lateral regions. The level of support, however, should be modulated with the level of increase in plantar pressure to avoid stress on foot structures.

Keywords: Foot orthosis deformation, Flatfoot, Kinematics, Foot plantar pressure, Linear mixed model

4.1. Introduction

Foot orthoses (FOs) can be used to alter abnormal foot motion and loading to prevent pain and overuse injuries [14]. In case of flexible flatfoot deformity, FOs are designed with the intent to reduce excessive rearfoot eversion and forefoot abduction [55], support medial longitudinal arch against collapsing [318], attenuate the impact force at heel-strike and distribute the pressure at midstance to facilitate proper push off [84]. These factors could expose flatfoot individuals to pain, fatigue, or further injuries [168, 319]. Previous studies have made efforts to identify the biomechanical factors that can estimate the response of flatfoot individuals to different designs of FOs, but controversial and limited evidence was achieved [25, 26, 28, 31]. This lack of evidence has left the customized FOs far behind their possible optimal design.

No standard approach for FO design has yet been introduced that can benefit all the flexible flatfoot individuals. For instance, medially posted FOs are commonly suggested to shift the subtalar joint towards its neutral position in order to reduce abnormal motion around this joint and decrease pressure in metatarsal and heel regions [2, 320]. While this mechanism works well for some flatfoot individuals [25, 26], neutralizing the static posture of the subtalar joint might not be a strong predictor of foot pronation response to FO during walking. Indeed some studies found no significant change in rearfoot eversion using medially posted FOs [2, 28, 31]. As an addition or alternative to medial posting, medial longitudinal arch supports have been used, but inconsistent effects on foot motion were reported. While some studies verified the efficiency of arch-supported FOs in reducing the level of pronation [158], preventing the deformation of the arch [26], and correcting the excessive deviation of the center of pressure [158], others rejected its efficiency to control rearfoot motion [321, 322]. Customized FOs provide more freedom for design and allow for adjusting the level of posting and arch support for each individual, which can be associated with more comfort [200]. The level of customization plays an important role in reaching an optimal FO design [13]. To explore this issue, dose-response effect of customized FOs was assessed by evaluating incremental levels of medially rearfoot postings that led to a linear decrease in rearfoot eversion [26]. However, a more robust basis for formulating the level of customization should be formed by recognizing multiple parameters of foot motion and loading that are likely to predict the dynamic characteristics of FOs in different regions.

Although foot motion and function of flatfoot individuals have been previously reported, limited knowledge exists on characterizing FOs. Time-dependent changes in FO deformation have the potential to characterize FO during dynamic activities. However, direct tracking of FO deformation by optoelectronic cameras is not possible since the FO surface is hidden by foot and shoe contacts. In a similar problem for estimating shoe deformation, Nishiwaki [106] inserted reflective markers on the contour of the shoe sole during running. However, the contour deformation cannot entirely represent the deformation of the whole FO surface. To overcome this limitation, alternative techniques were suggested. Finite element methods were used for either characterizing [115] or optimizing the design of FOs and shoes especially for diabetic feet [98] and athletes [103]. However, finite element simulation requires a large amount of information, which implies simplifications for generating the model and applying boundary conditions. Using mechanical testing, FOs with different materials and designs were characterized in four regions by defining their displacement and stiffness [102]. However, the characterization was based on applying sequential compressive loadings rather than the real dynamic loading during walking. Artificial intelligence represents a further alternative approach and has been validated for predicting FO deformation during walking in normal-arched feet [323]. This approach could yield the time-dependent deformation of FO plantar surface, could differentiate between FO designs, and did not need any simplifications for boundary conditions.

The inconsistent responses of flatfoot individuals to FOs might originate from subject-specific foot motion and loading. Therefore, our main objective was to determine the potential presence of dependencies between the region-dependent foot biomechanics and FO deformation during walking. Specifically, certain variables of foot motion and plantar pressure attributed to flatfoot deformity according to Desmyttere, et al. [22] were examined to clarify their relationship to the FO deformation. Furthermore, the foot-FO interaction was evaluated in different phases of the gait cycle to account for shifting of load between foot regions and consequently time-dependent changes in foot biomechanics and FO deformation.

4.2. Methods

4.2.1. Participants and customized foot orthosis

Seventeen participants (11 females, 6 males) with flexible flatfoot (age: 37.4±14.0 years, mass: 68.6±12.1 kg, height: 167.2±10.0 cm) were recruited from two podiatry clinics. All gave their written informed consent. The flexible flatfoot deformity was assessed by podiatrists in line with an arch height flexibility ≥ 16 mm/kN [69]. Other inclusion criteria were no history of wearing FO, no lower limb surgery, or injury during the last three months, and foot posture index (FPI > 6) [60]. Ethical approval was obtained from the University of Montreal (17-145-CERES-D).

Three-quarter length customized contoured FOs were designed based on the 3D surface scan of each participant's foot in its neutral subtalar joint position using SpecifX (Shapeshift3D, Canada). Each participant received two customized FOs (named "sport" *versus* "regular"), the regular FO being stiffer than the sport FO. Six double-cross slots were designed on FO contours for inserting marker triads. All FOs were 3D printed in Nylon12 (see Supplementary File 1: Details of customized foot orthosis design).

4.2.2. Data acquisition and processing

The data were collected in two sessions: FO calibration and walking. An 18-camera motion capture system (VICON, Oxford, UK) was used to record the kinematics at 100 Hz, and Medilogic WLAN plantar pressure system (T&T Medilogic Medizintechnik GmbH, Berlin, Germany) for recording plantar pressure at 400 Hz.

In FO calibration session, each FO was placed and fixed on a plate at the heel region, where repetitive compressive loads were applied on its plantar surface. The time-dependent FO deformations were recorded *via* the displacement of 55 reflective markers placed on the FO surface, simultaneously with the kinematics of FO contour *via* the marker triads. Briefly, to calculate the deformation, a densely connected neural network designed in Tensorflow [300] was trained to learn the dependency between the orientation of marker triads on FO contour and the position of markers on FO surface. The model was then used to predict the position of markers on FO surface during walking. The deformation was achieved by subtracting the position of predicted markers during walking from their corresponding position in unloaded static conditions. The

upward/downward deformation was used for further analysis. Details on the present set-up and analysis are provided in Hajizadeh, et al. [323].

In the walking session, one model of neutral running shoes (860 v8, New Balance, Boston, MA) was used for all participants. Circular holes (⌀2.5 cm) on shoes allowed for direct attachment of markers on the foot according to the Rizzoli foot model markerset [149] and the insertion of marker triads on FO contour into the double-cross slots. After a 5-min walk on the treadmill for acclimation and acquiring comfortable speed for each participant, a static trial was captured to personalize the multi-segment kinematics model. Then, walking trials were recorded for each FO in randomized blinded order. In addition to longitudinal arch angle (LAA) [65], the motion of rearfoot relative to the shank, midfoot relative to rearfoot, and forefoot relative to midfoot were calculated in sagittal (flexion/extension), frontal (eversion/inversion) and transverse (abduction/adduction) planes according to the generalized joint coordinates estimated using an extended Kalman filter [324] in Biorbd [325].

Data from foot kinematics and plantar pressure were synchronized offline by detecting the first foot contact with the ground, which was determined by foot velocity algorithm for kinematics data [326] and force detection algorithm with a 10% force threshold for pressure data [327].

4.2.3. Data reduction and analysis

The foot kinematics, plantar pressure, and FO deformation time histories were resampled over 100 points representing the percentages of the stance phase. Then, anatomically-based foot regions of interest (ROIs) were defined for these variables according to the position of reflective markers in the multi-segment foot model as described in Giacomozzi, et al. [178]. For each trial, FO surface markers and foot markers were projected onto the same plane as the pressure map at the midstance phase, when the foot is in full contact with its interacted surface (FO and plantar pressure insole). Then, an iterative closest point algorithm was used to find the rigid transformation between the borders of the plantar pressure map and the surface markers creating FO contour. The roto-translation matrix calculated from this algorithm was used to transform all foot markers and FO surface markers to match the plantar pressure map reference system. Then, the plantar pressure and FO surface markers were divided into five ROIs: medial and lateral rearfoot, medial and lateral midfoot, and forefoot (Figure 4.1). In this study, as ¾-length FOs were used, the forefoot region

was considered as the combination of forefoot and toes. Furthermore, the rearfoot region was divided into medial and lateral regions following the approach described in Stebbins, et al. [193].

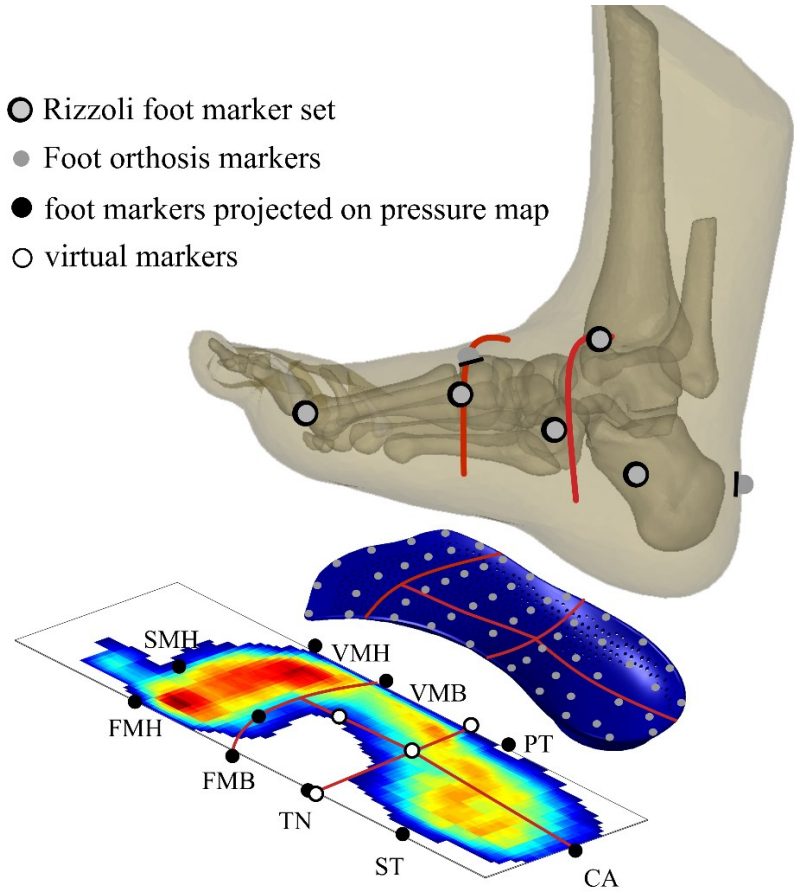

Figure 4.1: Anatomical masking to create integrated regions of interest for foot kinematics, foot plantar pressure, and foot orthosis deformation. The foot markers were attached based on the Rizzoli foot model [149], in which CA: the upper central ridge of the calcaneus posterior surface, ST: most medial apex of sustentaculum tali, TN: most medial apex of the navicular tuberosity, FMB: first metatarsal base, FMH: first metatarsal head, SMB: second metatarsal base, SMH: second metatarsal head, VMB: fifth metatarsal base, VMH: fifth metatarsal head, PT: lateral apex of peroneal tubercle.

For each participant, the first five cycles of walking were used for further analysis, leading to 170 cycles across all participants (17 participants× 2 FOs× 5 cycles). Four gait phases (GPs) were selected to extract the range of motion (RoM) of all variables termed as GP-1 (from heel-strike *i.e.* the primary contact of heel with the ground to foot-flat where the entire foot comes into contact with ground), GP-2 (from foot-flat to midstance where the entire foot is in contact with ground and the contralateral foot lifts off the ground), GP-3 (from midstance to heel-off where the heel elevates

off the ground), GP-4 (from heel-off to toe-off where the toe elevates off the ground). The foot RoM (3 joints× 3 rotations), LAA (1 rotation), and mean pressure normalized to the peak pressure (5 ROIs) were extracted for each gait phase (GP-1 to 4) to be considered as independent variables. Additionally, the RoM of FO deformation (5 ROIs) at each GP was used as a dependent variable. All analyses were performed using MATLAB (R2019a, The Mathworks, USA), except for FO deformation being predicted using Python 3.7.

4.2.4. Statistical analysis

Multicollinearity was examined between independent variables (foot kinematics and foot pressure components) using the variance inflation factor (VIF) with a threshold of 5. At each GP, repeated measure correlations (*rmcorr*) between all 15 independent variables and deformation at each ROI were conducted using the "*rmcorr*" R package [328]. The results of *rmcorr* yielded correlation coefficient r_{rm} and significance level p_{rm}, which helped to arrange the independent variables from the most to the least correlated variables. Twenty separate linear mixed models using restricted maximum likelihood estimation were built in SPSS v26.0 (IBM, Armonk, N.Y., USA) to detect the potential predictors of FO deformation at each ROI and each GP. Linear mixed effect models could consider within-subject correlations for cycles as well as FO type, and avoid biasing results. For all models, participants (n = 17) were regarded as a random effect, FO type (*sport* or *regular*) and cycles (n = 5) as correlated residuals within the random effect, deformation as the dependent variable, and all independent variables exhibiting $p_{rm} \leq 0.1$ from *rmcorr* as potential fixed effects prior to selecting the final model. A sequential introduction of potential fixed effects to the model was used, where the model formulation started with the most correlated variable, and the terms were added in the model if their contribution showed a significant effect ($p \leq 0.05$) or removed if $p > 0.05$ in stepwise procedure. Fixed effects selected through this procedure were used to create the final linear mixed model of FO deformations, as follows:

$$Deformation\ (ROI_{GP}) = intercept + \sum_{k=1}^{n_k} \beta_k . RoM_k + \sum_{p=1}^{n_p} \beta_p .\ RoM_p \qquad (1)$$

where β_k and β_p are the coefficients of k^{th} regressor among foot kinematic metrics and p^{th} regressor among foot plantar pressure metrics, respectively.

4.3. Results

The RoM of multi-segment foot kinematics varied across GPs especially for LAA and all rotations of rearfoot and forefoot (Figure S 4.1). The mean plantar pressure in the forefoot increased during the whole stance phase. In midfoot, the increase of pressure from heel-strike to heel-off was followed by a decrease until toe-off. In rearfoot, an increase from heel-strike to midstance was followed by a decrease until toe-off (Figure S 4.2). Regarding FO deformation, an increase in the range of deformation was observed from GP-1 to GP-3, following by a decrease in GP-4, and the dominant changes belonged to the midfoot region (Figure S 4.3).

No collinearity was observed between independent variables (all GPs, VIF $\leq$ 5). Preliminary analysis with *rmcorr* showed small to moderate correlations between foot kinematics and pressure parameters and FO deformation at each GP, from which the variables with significance level $p_{rm} \leq 0.1$ were selected as potential predictors.

Following forward stepwise iterations, linear mixed models were built for each FO region at each phase (Figure 4.2, Figure 4.3, Figure 4.4, Figure 4.5). For all models of FO deformation at GP-1 to GP-3, introducing intercepts to the model significantly enhanced the model fit ($p < 0.05$), indicating that significant offsets existed between participants (Figure 4.2, Figure 4.3, Figure 4.4). At **GP-1**, the forefoot and midfoot kinematics contributed dominantly to deform all FO regions. In this phase, flexion and eversion of the forefoot were negatively associated with the deformation of all regions. Regarding midfoot kinematics, LAA negatively affected the forefoot deformation, while midfoot abduction was positively correlated to the deformation of all FO regions (Figure 4.2). At **GP-2,** midfoot and rearfoot kinematics had significant positive associations with deformation of the forefoot, medial midfoot, and medial rearfoot regions, while the forefoot kinematics and pressure of forefoot accounted for the variations in lateral midfoot and lateral rearfoot deformations with positive correlations (Figure 4.3). At **GP-3**, LAA, rearfoot kinematics, and pressure of medial midfoot contributed to FO deformation at all regions. In this phase, LAA was positively associated with medial and lateral midfoot deformations, the increase in rearfoot eversion was associated with an increase in medial midfoot and rearfoot deformations, and the pressure of medial midfoot was negatively associated with the deformation of all regions except medial rearfoot (Figure 4.4). At **GP-4**, forefoot kinematics and pressure of forefoot played the most important role in FO deformation. Forefoot abduction exhibited a positive correlation with forefoot and midfoot

deformation, and forefoot eversion had a significant positive contribution to rearfoot deformation. In addition, the pressure of the forefoot was positively associated with forefoot, lateral midfoot, and medial rearfoot deformations (Figure 4.5).

ROI	Linear mixed models for deformation of each region Predictors	Estimate (SE)	*p* value	*rmcorrs* between each predictor (x axis) and deformation of each region (y axis)
Forefoot	Intercept LAA MF abduction	0.97 (0.13) -0.13 (0.04) 0.23 (0.08)	<0.001 <0.001 0.004	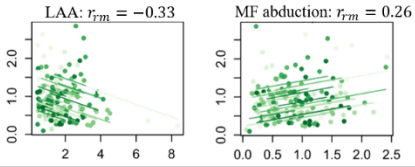
Medial midfoot	Intercept FF eversion MF abduction Pressure lateral MF	1.26 (0.37) -0.43 (0.15) 0.59 (0.19) 0.23 (0.05)	0.001 0.004 0.002 <0.001	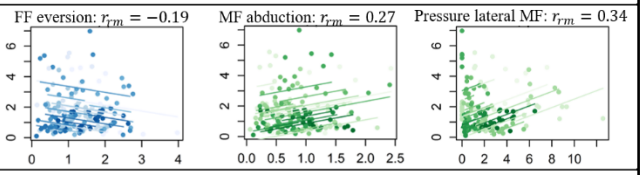
Lateral midfoot	Intercept FF flexion FF eversion MF abduction	1.06 (0.18) -0.09 (0.04) -0.15 (0.07) 0.39 (0.10)	<0.001 0.044 0.042 <0.001	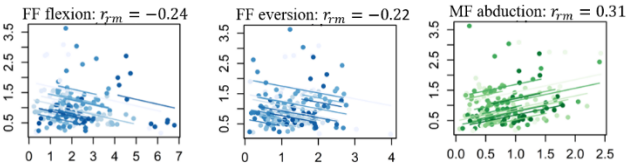
Medial rearfoot	Intercept FF eversion MF abduction Pressure lateral MF	0.57 (0.12) -0.15 (0.05) 0.21 (0.06) 0.07 (0.02)	<0.001 0.002 0.001 <0.001	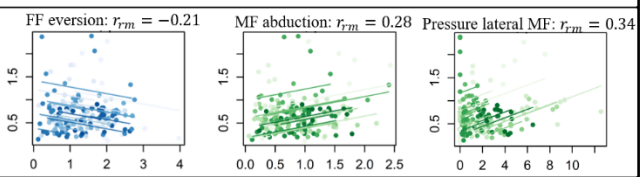
Lateral rearfoot	Intercept FF eversion MF abduction RF eversion	0.57 (0.08) -0.08 (0.03) 0.15 (0.04) -0.04 (0.02)	<0.001 0.019 <0.001 0.026	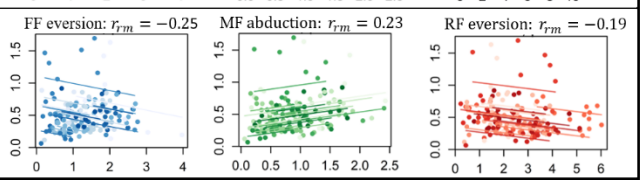

Figure 4.2: The linear mixed models for predicting foot orthosis deformation at five regions of interest, namely as forefoot, medial midfoot, lateral midfoot, medial rearfoot, lateral rearfoot, and the corresponding correlation coefficients between predictors of each region and deformation at Gait Phase 1, i.e. heel-strike to foot-flat (GP-1). For easier differentiation between regions, all variables of foot kinematics, plantar pressure, and orthosis deformation related to forefoot are shown in BLUE, midfoot in GREEN, and rearfoot in RED.

ROI	Linear mixed models for deformation of each region Predictors	Estimate (SE)	*p* value	*rmcorrs* between each predictor (x axis) and deformation of each region (y axis)
Forefoot	Intercept MF flexion RF abduction	0.59 (0.16) 0.10 (0.03) 0.07 (0.03)	<0.001 0.003 0.032	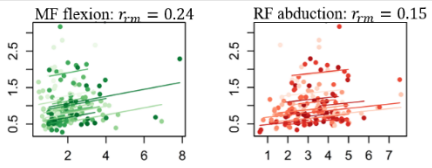
Medial midfoot	Intercept MF abduction RF eversion	1.72 (0.26) -0.50 (0.17) 0.16 (0.05)	<0.001 0.003 0.002	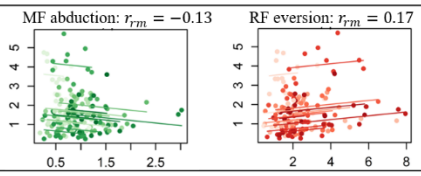
Lateral midfoot	Intercept FF abduction MF flexion Pressure FF	0.53 (0.20) 0.23 (0.11) 0.09 (0.04) 0.04 (0.01)	0.008 0.038 0.027 0.002	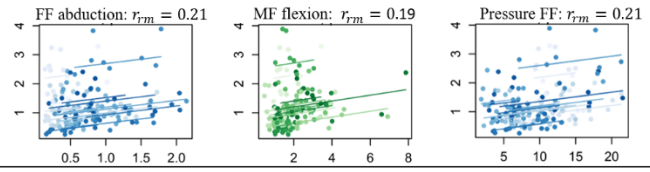
Medial rearfoot	Intercept MF eversion RF eversion Pressure lateral MF	0.65 (0.11) 0.09 (0.04) 0.05 (0.02) -0.01 (0.00)	<0.001 0.028 0.010 0.021	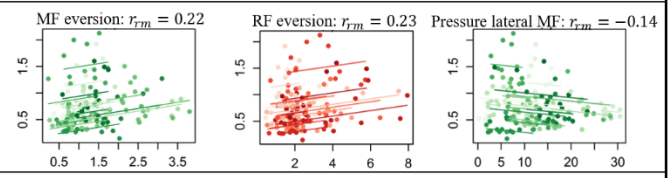
Lateral rearfoot	Intercept FF eversion FF abduction Pressure FF	0.26 (0.08) 0.16 (0.04) 0.10 (0.05) 0.01 (0.00)	0.001 <0.001 0.040 0.002	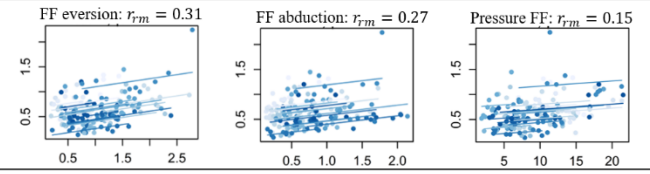

Figure 4.3: The linear mixed models for predicting foot orthosis deformation at five regions of interest, and the corresponding correlation coefficients between predictors of each region and deformation at Gait Phase 2, *i.e.* foot-flat to midstance (GP-2).

ROI	Linear mixed models for deformation of each region Predictors	Estimate (SE)	*p* value	*rmcorrs* between each predictor (x axis) and deformation of each region (y axis)
Forefoot	Intercept Pressure medial MF	1.27 (0.11) -0.02 (0.01)	<0.001 0.003	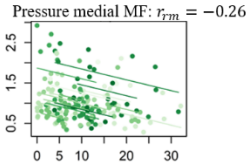
Medial midfoot	Intercept LAA RF eversion Pressure medial MF	0.71 (0.34) 0.10 (0.03) 0.21 (0.06) -0.03 (0.01)	0.006 0.002 0.001 0.016	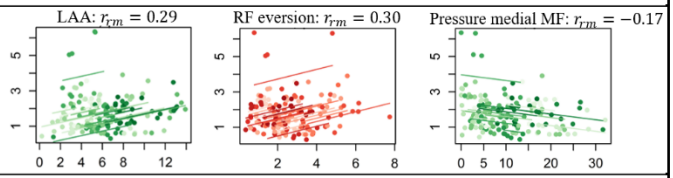
Lateral midfoot	Intercept LAA Pressure medial MF	1.11 (0.22) 0.08 (0.02) -0.03 (0.01)	<0.001 0.001 0.002	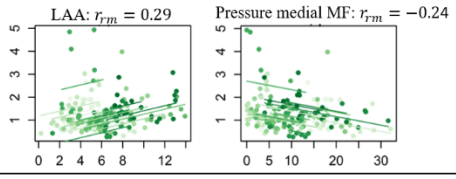
Medial rearfoot	Intercept RF eversion	0.68 (0.11) 0.07 (0.02)	<0.001 0.008	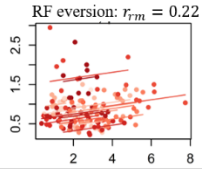
Lateral rearfoot	Intercept Pressure medial MF	0.80 (0.07) -0.01 (0.00)	<0.001 0.002	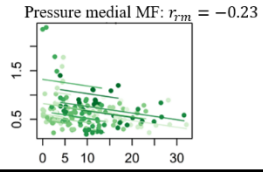

Figure 4.4: The linear mixed models for predicting foot orthosis deformation at five regions of interest, and the corresponding correlation coefficients between predictors of each region and deformation at Gait Phase 3, *i.e.* midstance to heel-off (GP-3).

ROI	Linear mixed models for deformation of each region Predictors	Estimate (SE)	*p* value	*rmcorrs* between each predictor (x axis) and deformation of each region (y axis)
Forefoot	Intercept FF abduction RF abduction Pressure FF	-0.06 (0.22) 0.12 (0.05) 0.07 (0.03) 0.02 (0.01)	0.797 0.006 0.016 0.026	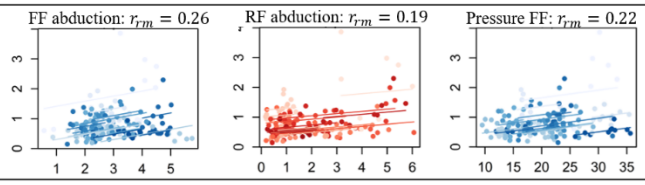
Medial midfoot	Intercept FF abduction Pressure lateral MF	0.06 (0.33) 0.27 (0.09) 0.32 (0.08)	0.857 0.003 <0.001	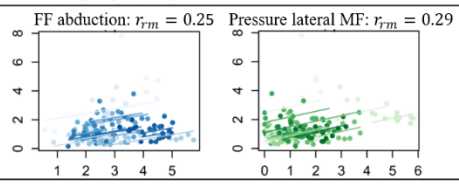
Lateral midfoot	Intercept FF abduction RF abduction Pressure FF	-0.46 (0.33) 0.22 (0.07) 0.09 (0.04) 0.04 (0.01)	0.156 0.001 0.030 0.002	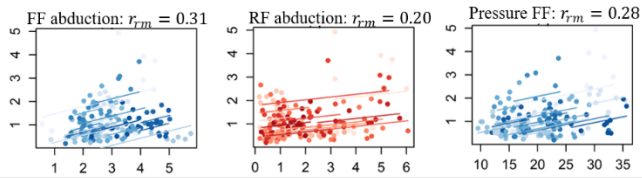
Medial rearfoot	Intercept FF eversion MF abduction Pressure FF	0.21 (0.13) 0.12 (0.04) -0.13 (0.04) 0.02 (0.01)	0.116 0.004 <0.001 <0.001	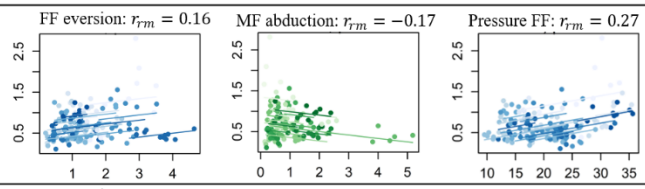
Lateral rearfoot	Intercept FF eversion	0.44 (0.06) 0.09 (0.03)	<0.001 0.002	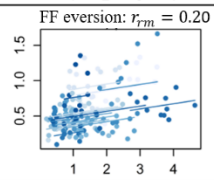

Figure 4.5: The linear mixed models for predicting foot orthosis deformation at five regions of interest, and the corresponding correlation coefficients between predictors of each region and deformation at Gait Phase 4, *i.e.* heel-off to toe-off (GP-4).

4.4. Discussion

This study examined the effect of foot biomechanics on region-dependent deformation of customized FOs in individuals with flexible flatfoot. Our findings confirm that the biomechanical alterations attributed to flatfoot deformity –foot pronation [318], LAA [55], and foot plantar pressure distribution [84]– play important roles in the response of flatfoot individuals to FOs' deformation. In addition, the dependency between foot biomechanics and FO deformation changed over the phases of the gait cycle. Specifically, *i)* rearfoot eversion contributed to the deformation of medial FO regions from foot-flat to heel-off; *ii*) a positive relationship between forefoot abduction and the deformation at lateral regions of FO was observed from foot-flat to midstance

iii) a positive association existed between the collapse of LAA and the deformation of both medial and lateral midfoot regions from midstance to heel-off , and *iv)* foot plantar pressure at medial midfoot was associated to the deformation of forefoot, midfoot and lateral rearfoot regions from midstance to heel-off.

Rearfoot eversion and forefoot abduction have been addressed as the key components of early and excessive pronation in flatfoot individuals [26]. Our linear mixed models showed that rearfoot eversion contributed significantly to the deformation of FO in medial midfoot and medial rearfoot regions from foot-flat to heel-off. In these phases, the maximum rearfoot eversion occurred and persisted before reaching heel-off (Figure 4.6-a). The relationship between rearfoot eversion and customized contoured FOs was also confirmed by Telfer, et al. [26], who showed that the increments in the level of medial posting had a linear relationship with changes in rearfoot eversion. Furthermore, Han, et al. [158] observed that modifying the FO design at medial midfoot, by adding arch support, would lead to lower peak rearfoot eversion in flexible flatfoot individuals. However, the responses of flatfoot individuals to customized FOs for reducing the rearfoot eversion have been inconsistent between studies [22]. This inconsistency might originate from either intrasubject variability in foot behaviour or differences in FO designs. Regarding this issue, Arnold, et al. [169] looked for the source of such inconsistency by comparing two groups with flatfoot deformity, including the ones that customized FOs either could (responders) or could not (non-responders) reduce their calcaneal eversion. They observed that responders exhibited significantly higher dynamic foot pronation compared to non-responders. These findings, in line with our results, suggest that for flatfoot individuals exhibiting excessive rearfoot eversion, it is important to design medially posted FOs or provide more rigidity and support in medial regions of FO, while the level of posting or rigidity should be modulated based on the level of individual excessive pronation. A further component of foot pronation was the maximum forefoot abduction, occurring from foot-flat to midstance, and significantly affected the FO deformation in lateral midfoot and lateral rearfoot (Figure 4.6-b). We suggest modifying the FO lateral region for flatfoot individuals who abduct their forefoot excessively.

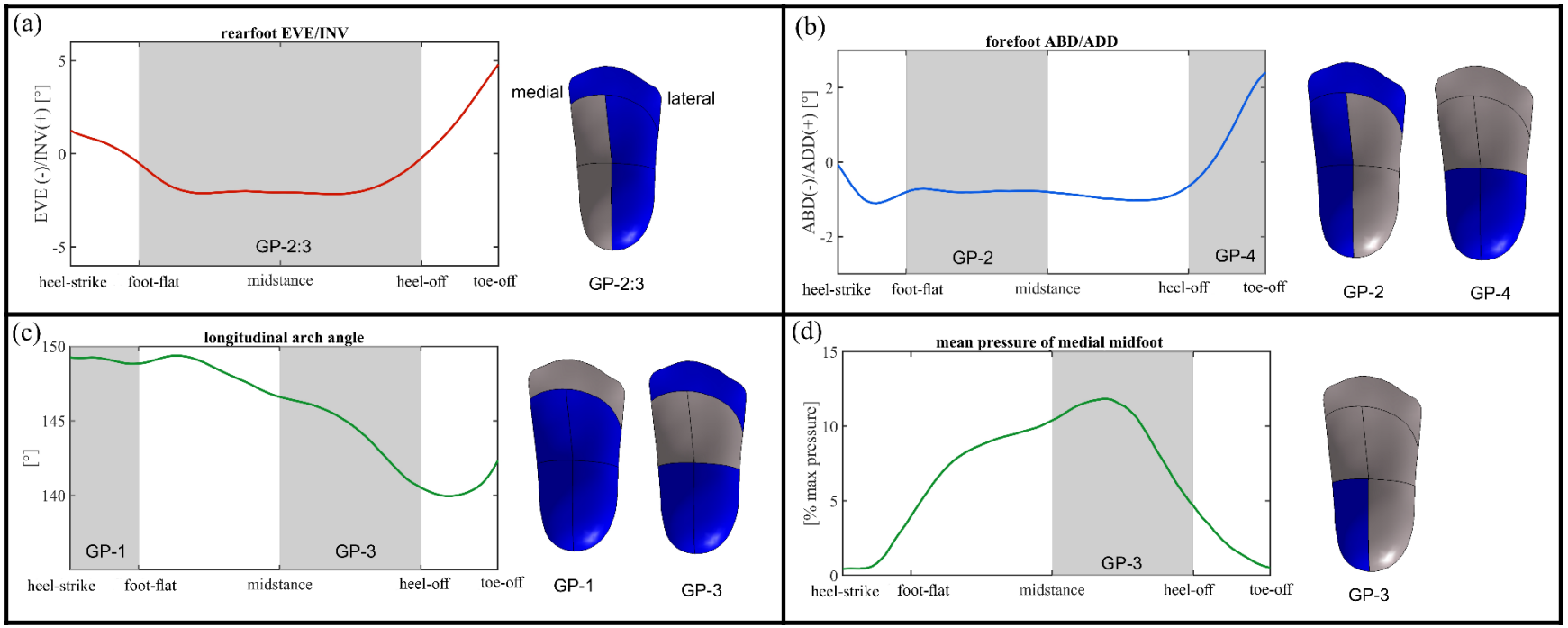

Figure 4.6: Summary of important findings from the linear mixed models. Gray shadows in kinematic and plantar pressure plots show the phases when they had significant association with foot orthosis deformation. The regions of foot orthosis shown with gray colors identify the regions affected by the corresponding kinematic or pressure parameters in each subplot.

In addition to excessive foot pronation, the medial longitudinal arch cannot recoil properly to provide rigid lever and sufficient stiffness in flatfoot individuals, leading to inefficient propulsion [55]. Our study showed a positive association between the collapse of LAA occurring from midstance to heel-off and the deformation of both medial and lateral midfoot regions (Figure 4.6-c). The design of FO on the medial region has been previously shown to mitigate the collapse of the medial arch, but the effect of FO design on the lateral region has not been reported. Balsdon, et al. [32] indicated that hard and soft customized FOs with Ethylene-Vinyl Acetate (EVA) posting were efficient to reduce the motion of medial longitudinal arch compared to prefabricated FOs. The relationship between LAA and the deformation of the lateral midfoot region might be referred to as the existing intra-correlation between the elevation/collapse of medial, lateral, and transverse arches [38]. Our outcomes suggest that for flexible flatfoot individuals with higher arch height flexibility, the design of FO at the midfoot region is vital, not only at the medial arch but also at the lateral arch.

Finally, foot plantar pressure usually increases under the medial arch region as a consequence of flatfoot deformity [99]. The linear mixed models showed that foot plantar pressure at medial midfoot was negatively associated with the deformation of forefoot, midfoot and lateral rearfoot regions, from midstance, where the maximum foot contact area occurs until heel-off (Figure 4.6-d). Increasing the plantar pressure might bring about higher stress in foot joints and ligaments [33]. The higher rigidity of FO has been associated with higher plantar pressure [329]. Therefore, the design of customized FOs should be a modulation between the level of correction in foot motion, the degree of supporting the medial arch, and the level of foot pressure increase. Our results emphasize the importance of utilizing the time-dependent as well as region-dependent foot motion and loading during dynamic activities as determinant factors to design customized FOs.

Some limitations are inherent in this study. The correlation coefficients extracted for the association between predictors and FO deformation were small to moderate ($0.14 \leq |r_{rm}| \leq 0.35$). A small sample size in our study also required a *priori* choice of potential predictors. Since linear mixed models are robust approaches and can account for more participants, a larger population must be sought in future studies to find stronger evidence for these relationships. In addition, foot kinematics and plantar pressure data were synchronized during postprocessing. Using a hardware trigger during data collection might yield more accurate synchronization. This study only

considered foot kinematics and plantar pressure to predict FO deformation, while joint moments, knee and hip motion, and static foot structure could be added as potential predictors. Finally, the predictions were performed based on ¾-length FOs, while flatfoot individuals might respond differently to full-length FOs. The alignment of the forefoot could be controlled by adding the forefoot posting under the first ray of full-length FOs, which would subsequently reduce abnormal rearfoot motion due to the coupling motion of three-foot segments.

In conclusion, this study provides preliminary hints for translating the biomechanical needs of individuals with flatfoot deformity into the design of customized FOs through a systematic, objective yet complex approach. The findings of this study might benefit clinicians for suggesting FOs based on foot motion and loading as well as engineers to ponder about adapting the design of FOs based on region-dependent mechanical properties rather than a homogenous structure over the whole surface of FO.

4.5. Supplementary materials

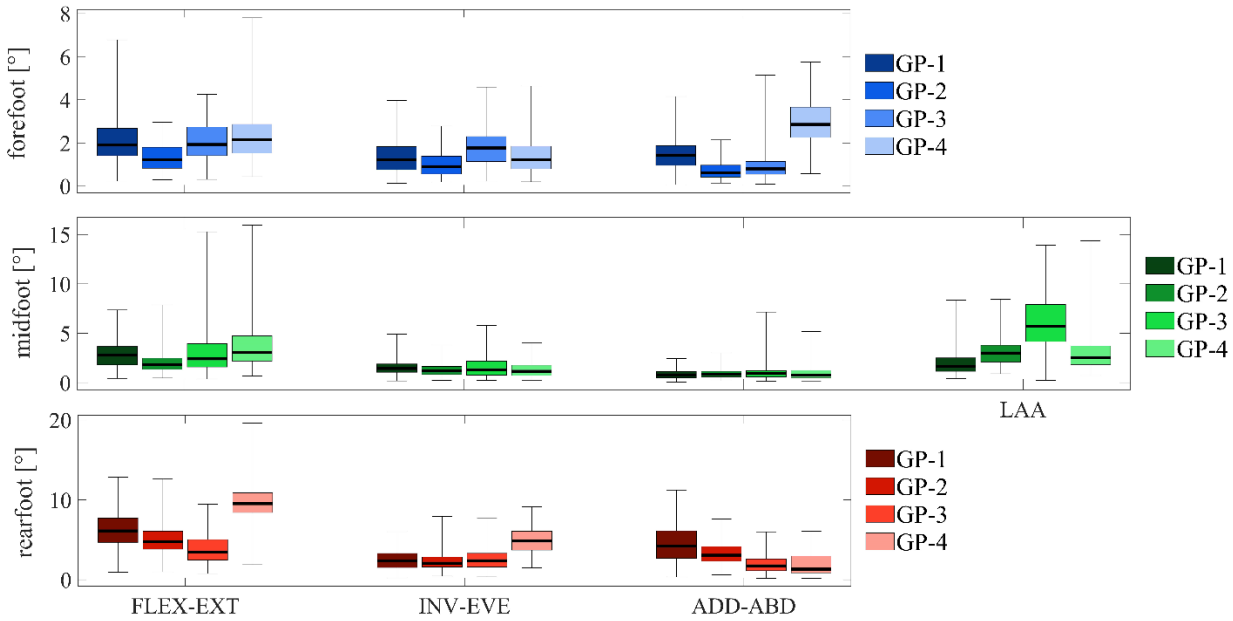

Figure S 4.1: The ranges of motion for multi-segment foot kinematics in forefoot, midfoot and rearfoot over the four phases of gait cycle.

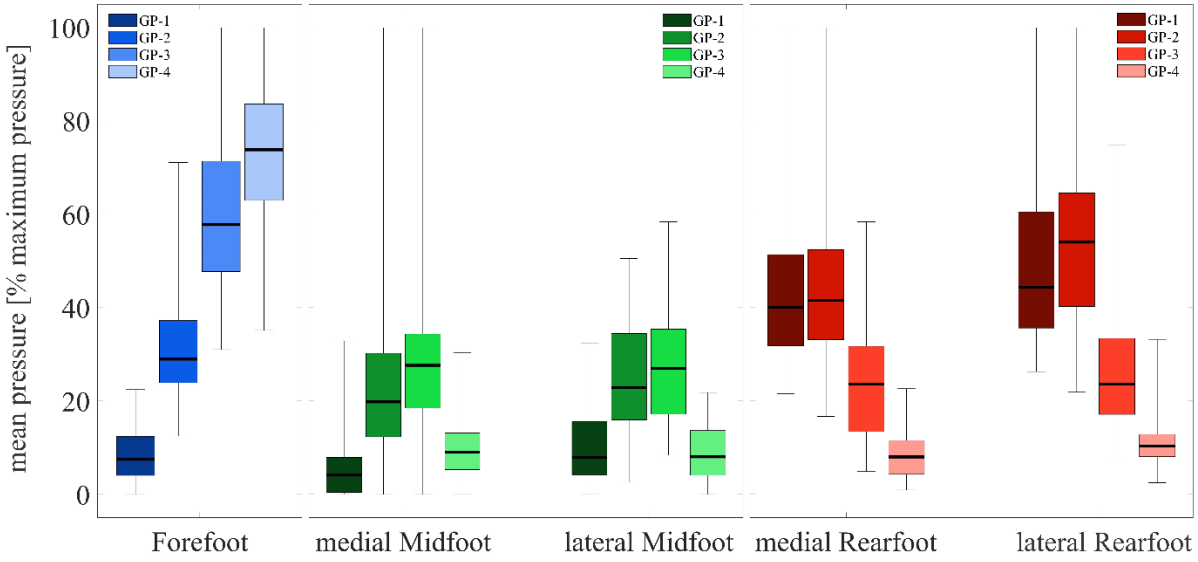

Figure S 4.2: The mean foot plantar pressure normalized to the maximum pressure in five regions of interest, namely forefoot, medial and lateral midfoot, medial and lateral rearfoot over the four phases of the gait cycle.

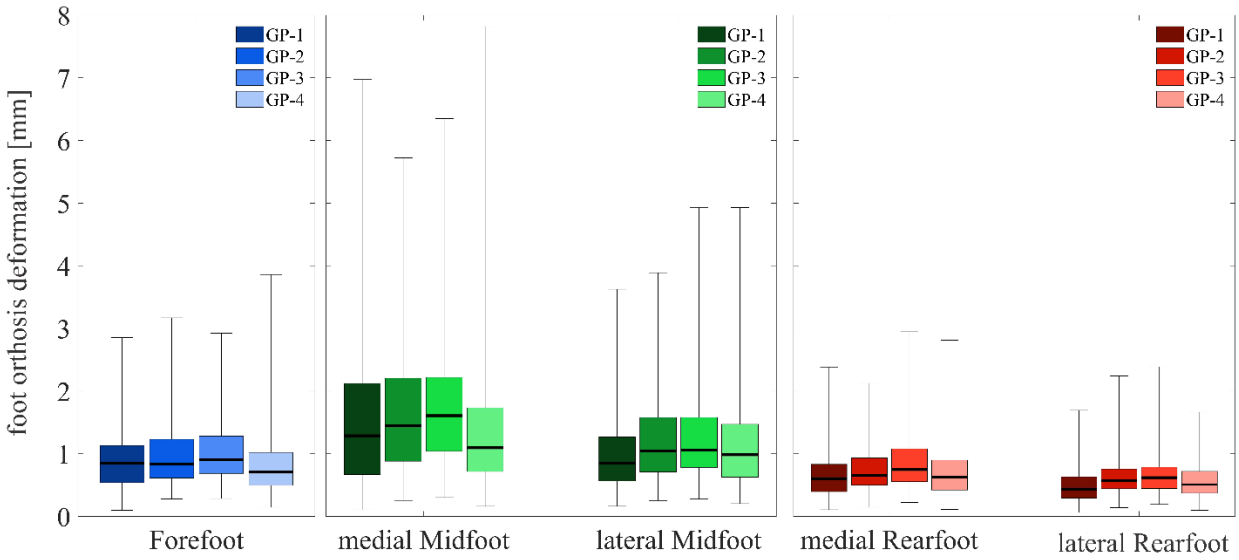

Figure S 4.3: Ranges of foot orthosis deformation in five regions of interest, namely forefoot, medial and lateral midfoot, medial, and lateral rearfoot over the four phases of the gait cycle.

Supplementary File 1: Details of customized foot orthosis design

The FO design consisted of a base layer superimposed on a layer with a honeycomb structure. Two parameters, namely arch height flexibility and body weight, were used to identify the height of honeycomb cells, which determined the FO stiffness. Two customized FOs (named "sport" *versus* "regular") were designed for each participant (Figure S 4.4). The height of honeycomb unit cells at the medial arch region had a range of 1.75 to 3.0 mm for sport FOs compared to a range of 2.25 to 5.25 mm for regular FOs, as the stiffer FO, between participants. The design of each FO also consisted of five double-cross slots, which enabled the insertion of marker triads on the contour of foot orthosis (Figure S 4.5). The kinematics of foot orthosis contour was acquired *via* the movement of these marker triads during both calibration and walking sessions.

The participants received their customized FOs four weeks prior to experiments and were asked to wear each FO during their regular daily activities for two weeks in a random order to get used to them. The participants were then invited to the lab for data acquisition.

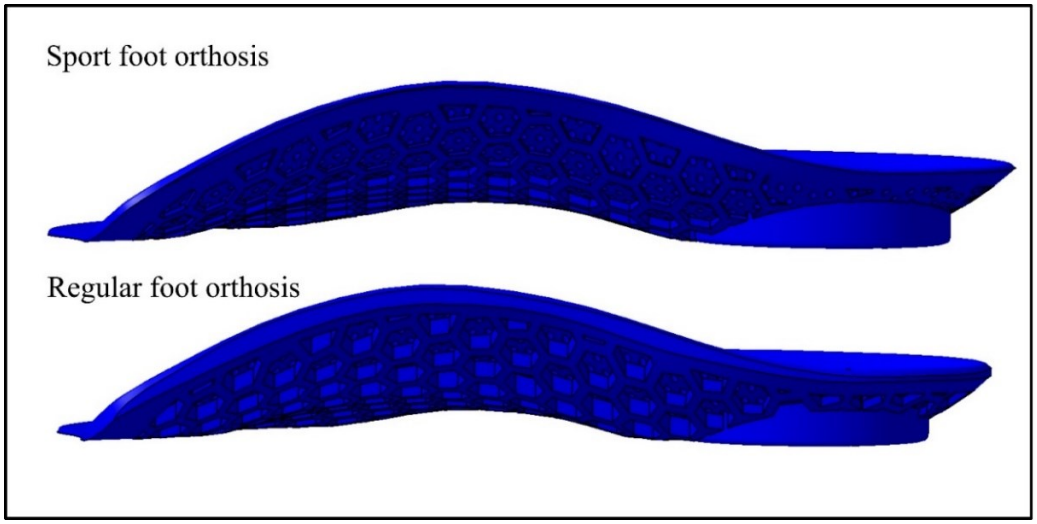

Figure S 4.4: An example of sport (lower height of honeycomb cells) *versus* regular (higher height of honeycomb cells) foot orthosis design for a flatfoot participant.

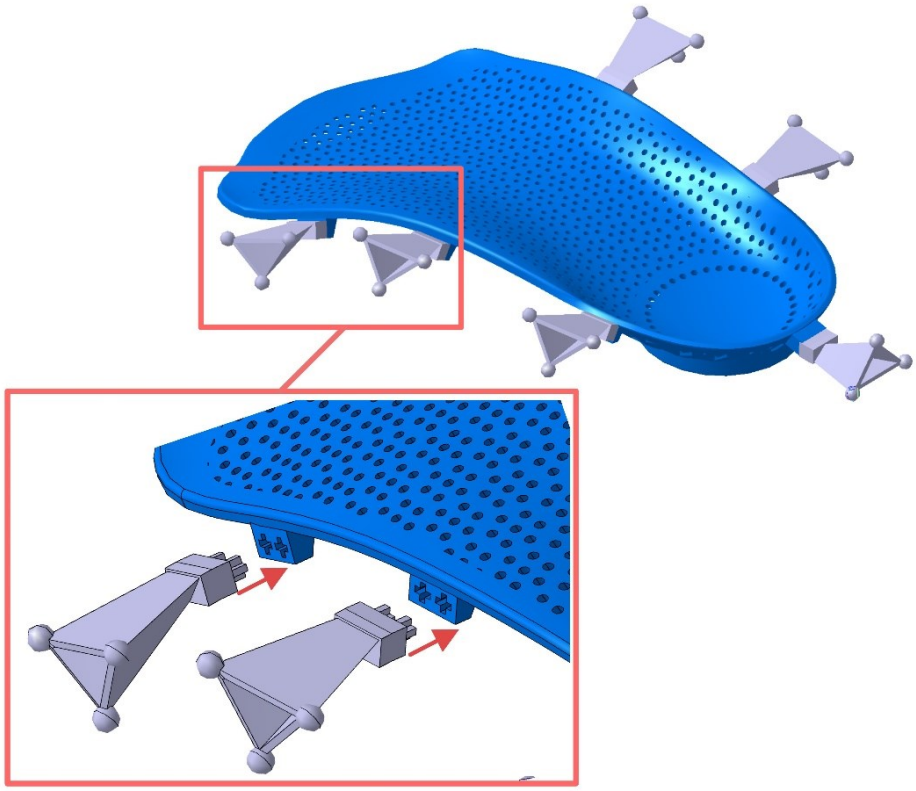

Figure S 4.5: The design of double-cross slots on foot orthosis contour for inserting marker triads during calibration and walking sessions.

Chapter 5 - General Discussion

The general objective of this thesis was to assess the function of foot orthoses (FOs) in association with foot biomechanics. To reach this aim, three specific objectives were defined as extracting the available knowledge and the level of evidence from available literature, quantifying the FO behaviour under dynamic loading, and finding the interaction between foot biomechanics and FO in a predictable manner.

The first objective was to conduct a comprehensive analysis of available literature to understand the biomechanical outcomes of common designs of FOs within individuals with normal-arched feet (Chapter 2). The level of evidence of the relationship between FO design and foot biomechanics was sought by extracting the relevant numeric data of kinematics and kinetics of the lower body from 25 included studies. Most studies focused on the biomechanical effects of lateral posting which is popular for patients with knee osteoarthritis for reducing their knee adduction moment. However, an insufficient number of studies existed in subgroups of medial posting, arch support, and heel support which are more commonly prescribed for individuals with flatfoot deformity. The assessment of data from included studies showed a large variation, which was likely caused by the variation in methodological approaches. Based on the statistical analysis of the reported data, normal arched feet responded to medially posted FOs by lowering the ankle eversion moment. However, no significant effect was observed for the decrease in impact force during walking with heel supported or arch supported FOs. The insight obtained from this systematic review enabled the proposition towards standardizations of methodological approach and revealed the necessity for further studies to clarify the relationship between FO design and foot motion.

The second objective of this thesis was to develop and validate an approach to quantify the behaviour of FO during dynamic activities. It was hypothesized that an artificial neural network could predict the deformation of FO on its plantar surface by using the kinematics of FO contour as the input. The findings of this article, presented in Chapter 3, confirmed this hypothesis. The developed model was capable to discriminate between different phases of the gait cycle as well as between individuals. Furthermore, the differences in the pattern and ranges of deformation during gait while wearing FOs with different rigidities could be detected by our model. Implementing this

approach to calculate the deformation of customized FOs in flatfoot individuals could provide improved insights on subject-specific response to FO design.

The third objective of this thesis was to determine whether any association exists between FO deformation and the determinants of foot biomechanics, *i.e.* kinematics and plantar pressure, in flatfoot individuals. It was hypothesized that the interaction between the foot and FO changes over different regions of the foot and the key phases of the gait cycle. The results of this article, presented in Chapter 4, confirmed our hypotheses. We found that the rearfoot eversion was dominantly controlled by medial regions of FOs, while the control of forefoot abduction was associated with lateral regions of FOs. In addition, the collapse of the medial arch was associated with the deformation of middle FO regions. Preliminary guidelines could be provided based on the findings of this chapter to be practiced in clinics and industry for enhancing the function of customized ¾-length contoured FOs.

In this chapter, each of these objectives and the link between them will be discussed to highlight the overall scope of the results and their importance in advancing the existing knowledge. Then, sections to summarize the general limitations of this thesis (section 5.5) and the perspectives for future research (section 5.6) will follow.

5.1. The function of foot orthoses during walking

The prescription of FOs is a complex approach, which is done following some visual inspections and anthropometrical measurements in clinical practice. In the case of flatfoot deformity, depending on the training and experience of clinical practitioners as well as the assessment of observations, highly variable designs of FOs might be prescribed [12]. Such variation in the design of FOs shows the lack of sufficient knowledge and the necessity of pursuing further research in this field. This thesis was part of a bigger project called *Functional Optimized Orthotic Trabecular Insole (FOOT¡)* which had industrial and clinical collaborators to specifically focus on the development and optimization of customized FO designs for flatfoot individuals. The main goals of this project were developing user-friendly software for automatic design of customized FOs from 3D foot scan images (SpecifX), optimizing the region-dependent mechanical properties of FOs by integrating different lattice structures within the design to enable proper shock absorption and propulsion for flatfoot individuals, and parametric design of customized FOs from clinical measures. To follow these goals, it was primarily required to gather the available knowledge on

common designs of FO and their applications for different foot types. Two parallel systematic reviews were conducted by our group (one as first author and one as the second author) to reach this objective by assessing the biomechanical function of different FO designs in two groups: individuals with normal-arched feet (Chapter 2) and individuals with flatfeet [22]. The key findings from both reviews about the effect of posting and arch support are discussed together in sections 5.1.1 and 5.1.2, respectively. These two adds-on of FOs can be regarded as the most common modifications for flatfoot deformity which aim to decrease the level of foot pronation as well as prevent medial arch depression during weight bearing. The results from normal-arched feet will provide useful information on the impact of FO design on foot biomechanics without having the foot deformity as an intervening parameter. On the other hand, a similar FO might exhibit different effects on the biomechanics of normal-arched feet *versus* flatfeet [22]. Therefore, a similar systematic review of flatfoot individuals could verify the impact of different FO designs before their clinical use.

5.1.1. The effect of posting on foot kinematics

The FOs are usually medially posted on rearfoot, forefoot, or a combination of rearfoot and forefoot for individuals with flatfoot to avoid excessive rearfoot eversion or forefoot abduction. Not only the placements of medial postings are different between studies, but also the level of posting (the inclination) and the material properties are not consistent. Our meta-analysis did not find any evidence for the effect of medial posting on the foot pronation of individuals with normal arched feet. Among the three included studies, two of them used rearfoot posting [173, 228] *versus* the other one using a full-length posting [210]. The levels of postings were also different between the three studies (6°, 7°, 10°). These differences in FO designs might be the source of high heterogeneity between studies. To reduce the effect of this heterogeneity in the systematic review conducted on flatfoot individuals, the medial posting was divided into four separate groups. These subgroups were medial rearfoot posting, medial forefoot posting, a combination of medial rearfoot and forefoot posting, and neutral posting. The results showed that medial forefoot posting and the combination of the medial forefoot and rearfoot postings could significantly reduce the excessive rearfoot eversion in flexible flatfoot individuals, but no evidence was found for the efficiency of rearfoot posting and neutral rearfoot posting. The efficiency of medial forefoot posting was referred to modifying the forefoot varus motion, which subsequently decreases the need for subtalar joint

pronation during the stance phase of flatfoot individuals [22]. The lack of evidence for rearfoot posting was referred to the contradictory results between studies. While three studies addressed a decrease in rearfoot eversion [24-26], two studies reported an increase [27, 28]. These inconsistent results are likely to be a cause of different criteria for recruiting participants, such as rearfoot eversion, arch height index, FPI-6, or other clinical observations. Differences in the foot structures of included participants in these studies could alter the foot motion and subsequently the response to similar designs of FOs. These findings emphasize the importance of FO design and individual foot characteristics on the response to FOs, which is in agreement with previous literature [21]. Even different placement and levels of postings would impose different alterations on foot biomechanics.

5.1.2. The effect of arch support on foot kinematics

Medial arch supports are supposed to keep the arch elevated during weight-bearing and help individuals with flatfoot to develop efficient propulsion [38, 217]. They are usually administered as the first choice to individuals with excessive rearfoot eversion in clinical practice [217]. However, our systematic reviews did not find any evidence for their efficiency in neither healthy nor flatfoot individuals. The lack of evidence for both populations could not be referred to heterogeneity between studies, because even single studies did not address any significant differences in foot motion or loading during walking with arch-supported FOs. The lack of evidence in single studies that calculated rearfoot kinematics from skin markers [217] as well as bone pin markers [330] has been referred to high inter-subject variation. It might also be due to considerable differences in the height and material properties (from flexible to rigid) of arch supports. Similar to the results for FOs with postings, these results also justify that different individuals react differently to similar designs of FOs. This factor should be considered in future research for reaching consistent results.

Comprehensive analysis of available literature did not find strong evidence for the application of different designs of FOs in healthy and flatfoot individuals. To our view, some steps should be taken in order to reach a consensus for prescribing and designing customized FOs and better consistency between studies: (1) There is a need to standardize the methodological approach. Similar criteria and tools should be used by clinical practitioners to quantify the foot type. In addition, multi-segment foot models to estimate foot kinematics and their calculation approach are

needed to be explicitly defined and standardized. (2) Standard approaches should be devised to design customized FOs based on the biomechanical needs of each individual. The variation in the response of individuals to customized FOs has been referred to the differences in their foot biomechanics [169]. However, we did not find any study that investigated the interaction between foot biomechanics and FO dynamics.

5.2. Quantifying foot orthosis deformation

Since FOs are placed between feet and shoes, they can work in parallel with feet to assist in favorable motions or prevent unwanted motions [97]. As foot and FO are in direct contact, their behaviour under dynamic loading should be coordinated. In order to assess the interaction between foot and FO, it is required to introduce some parameters to quantify both foot biomechanics and FOs. Multi-segment foot kinematics and foot plantar pressure were selected to represent foot biomechanics. In addition, the quantification of FO was defined as its deformation during the stance phase of walking. The characteristics of FOs depend on their geometrical features and material choice and play an important role in their biomechanical function [33]. The limited knowledge of FO behaviour under dynamic loading might be caused by the difficulty to estimate it directly. Indirect approaches such as finite element modeling [15, 98] and mechanical testing [102] have been implemented in a few studies to estimate the FO behaviour. In this thesis, an artificial neural network was validated for indirect estimation of FO deformation during walking.

The approach used in this study for quantifying FOs has some strong points compared to other approaches. In comparison to finite element analysis, our approach did not need any simplifications in the geometrical model and boundary conditions, and it was computationally less expensive. Using finite element models, it is difficult to assign the material properties and loading specific to each subject as well as developing alternative numerical solutions to find similar mechanical properties due to the expense and invasiveness of collecting such data [331]. In contrast, our model was capable to predict the deformation for the stance of walking without any need to measure material properties. Furthermore, contact properties are defined based on some assumptions and simplifications in finite element models concerning the shoe-orthosis interaction and the shoe-ground contact, but our model was predicted for real contact properties. Our approach was also more robust than mechanical testing in terms of identifying the deformation during walking as mechanical testing implies one-directional or multi-directional loading application in an

environment that would best mimic the experimental conditions. In fact, we used the data of the calibration session, which was similar to the mechanical testing procedure used by Cuppens, et al. [102], to provide the input data for building the neural network model. Then, the generated model was capable to predict the deformation of the FO surface during walking by looking for similar kinematics of FO contour in the calibration session. This added step was, therefore, the main strength of our approach compared to mechanical testing. Having access to such information enabled us to investigate the existence of any association between foot and FO during gait rather than under simulated loadings. After evaluating our technique with the data of healthy individuals, we generated subject specific models for each flatfoot participant to anticipate their pattern of deformation during walking. To our knowledge, no previous study had been developed to quantify the customized FOs on a patient-specific basis. Having access to the deformation of FO during walking in flatfoot individuals was a key parameter to understand the interaction between foot biomechanics and FO dynamic behaviour. The interaction between foot and FO could finally help us to provide preliminary guidelines to clinicians to decide about FO design and to engineers to integrate more details within the design of customized FOs. This could finally result in delivering more optimal designs of FOs to the flatfoot patients by correcting the foot posture more efficiently and avoiding the consequent clinical symptoms.

5.3. Interaction between foot and foot orthosis

The traditional theories to design FOs have been established based on static foot posture and loading. However, the static condition might not sufficiently represent the reality of dynamic loading and its requirements. Evaluating the foot-FO interaction during walking can provide primary information for designing FOs as a function of foot dynamics. To find the relationship between multiple variables for explaining complex physical and biological phenomena, multiple regression analysis, and linear mixed models have been introduced as useful statistical tools [176, 332, 333]. Using multiple regression analysis in SPSS v26.0 (IBM, Armonk, N.Y., USA), it is possible to find out how much variance in the dependent variable is accounted by independent variables (R^2). On the other hand, linear mixed models are useful tools to build the models based on the significant associations between potential predictors and dependent variables, but they do not yield the amount of variation accounted by predictors (R^2). The strength of the linear mixed model over multiple regression analysis is that it can account for the within-subject correlations

[334]. Since we used two customized FOs for each individual as well as different phases of the gait cycle, we needed to use linear mixed models to avoid biasing the results. In this thesis, we avoided to use non-linear regression models, because they might cause overfitting due to the complexity of the model. The overfitting would result in fitting the random noises in specific samples rather than reflecting the overall population. In addition, the non-linear regression models are more difficult to interpret compared to linear models. The key finding from these models was that FO behaviour changes over different phases of the gait cycle as well as different regions of FO. This aspect should be incorporated into the design of FOs to reach their optimal function.

Two customized FOs were designed and tested for each individual in this project, named as "sport" *versus* "regular". The sport FO was less stiff than regular FO due to the lower height of honeycomb cells. Based on the findings of this thesis, there is still ambiguity in whether any of the two rigidities of our customized FOs, 3D printed for the flatfoot people, were the optimal design. The interpretation of results from two different rigidities of FOs in Chapter 3 showed that sport FO exhibited the downward deformation under the medial arch region accompanied by upward deformation under the lateral arch region. On the other hand, the regular FO indicated the simultaneous downward deformation under the medial and lateral arch regions [323]. The opposite motion of medial and lateral regions in sport FO is not harmonized with the similar motion of medial and lateral arch of the foot indicated by Gwani, et al. [38]. In addition, according to our further article [335] in Chapter 4, it was found that the collapse of medial longitudinal arch is associated with the deformation of both medial and lateral FO regions, which also confirms the intra-correlation between the motion of foot arches in coordination with corresponding FO regions. These observations show that sport FO might prevent the coordinated elevation/depression of medial and lateral arches. On the other hand, rigid FO might apply excessive stress to foot structures due to higher pressure compared to sport FO [329]. Therefore, further research is needed to assess whether the level of higher pressure would result in higher stress in soft tissues *via* finite element analysis and further injuries *via* long-term experimental assessments. To conclude, the level of rigidity in several regions needs to be adjusted carefully not only for correcting foot motion but also for permitting the coordinated motion of foot joints and other functional mechanisms, while avoiding to impose immediate or long-term extra stress on soft tissues and bony structures.

5.4. Implications for clinical and industrial practice

The findings of this thesis could provide preliminary guidelines on the prescription and the design of customized FOs for flatfoot individuals. Our modeling technique to estimate the FO deformation was validated, affordable, non-invasive, and provided relevant and subject-specific information, which have been counted as primary criteria for a modeling approach to be applicable in clinical settings [331]. Based on our linear mixed models, if the goal of treatment is to reduce the subtalar joint eversion in order to prevent excessive and early pronation, clinicians could consider prescribing FOs which provide higher support on medial regions. This suggestion is in agreement with a previous study assessing the interaction between medial posting and foot biomechanics in a predictable dose-response manner and found out a linear relationship between the level of increase in medial posting and the amount of decrease in rearfoot eversion [173]. Furthermore, for individuals with very flexible arches, we suggested supporting their medial longitudinal arch by modifying the FO design under the medial arch and lateral arch regions. This finding is in agreement with a previous study that justified the efficiency of contoured customized FOs on supporting the medial longitudinal arch during the gait of flatfoot individuals using biplane x-ray fluoroscopy [32]. Although the reduction of rearfoot eversion and the support of longitudinal arch by increasing the level of medial posting or adding arch supports have been justified in some literature [26, 158], a threshold for a clinically meaningful effect simultaneous with maintaining the comfort level has not been established. This issue needs to be explored in future research. A further observation of our findings was that the response of flatfoot individuals to customized FOs is related to their foot biomechanics during dynamic activities, which has been also addressed in previous research [87, 179]. Therefore, the clinicians are suggested to complement the assessments of the foot in the static posture with other dynamic observations and measurements before prescribing FOs. Finally, we found that the relationship between FO and foot biomechanics varies over different regions of FO. This observation has been already come into practice by integrating different adds-on within the FO design such as postings, heel supports, and arch supports. The future direction of *FOOTi* Project is to implement this finding by integrating different lattice structures within FO design through an optimization approach, in order to adjust the region-dependent mechanical properties of FOs based on individual demands.

5.5. Limitations

This thesis generally aimed to provide insights on FO performance under dynamic loading. To this aim, two different methodological approaches were taken: (1) systematic review and meta-analysis of available literature, (2) indirect estimation of FO deformation, and evaluating the interaction between foot and FO. Some limitations are inherent within each of these methods.

The systematic review included in this thesis suffers from a limited number of studies considering the foot as a multi-segment foot model. Single-segment foot models cannot reflect the reality of foot motion and function during walking. The kinematics of forefoot and rearfoot, as well as medial arch angle, are among the parameters that alter as a consequence of flatfoot deformity and could be only estimated by applying multi-segment foot models. Furthermore, the included studies using multi-segment foot models did not use the same markerset and analysis techniques. A further limitation was that the designs of FOs in the same design category were not consistent. In fact, FOs were different in terms of their materials and the levels of posting, which could subsequently lead to heterogeneous outcomes. Care was taken to aggregate the data using similar foot models and FO designs, which consequently resulted in the exclusion of some available data from statistical analysis. This systematic review highlighted the limited number of available studies and the heterogeneity in their methodological approach. This information can strengthen future research by standardizing such inconsistent approaches.

Following the systematic review study, an artificial neural network was implemented to predict the deformation of FO. A calibration session was required to be captured before the walking session to provide the input data for generating the model. Therefore, a setup was designed for the calibration session, in which the kinematics of FO contour was recorded by attaching six marker triads on the FO contour and the surface deformation by attaching 55 markers on FO plantar surface. The model was then able to recognize the dependency between the orientation of marker triads and the position of markers on the FO surface in the calibration session in order to predict the position of surface markers during walking. The deformation of FO was finally calculated by subtracting the predicted position of markers during walking from their corresponding position in unloaded static conditions (Chapter 3). This prediction approach had some limitations as following which may impact the findings of Chapter 4:

I. Some limitations existed in the calibration session used to generate the neural network model. A primary limitation was that the loads to deform FOs were applied manually. Although the application point and the magnitude of loading were recorded in our set-up, the amount of loading and deformation varied over the surface of FO depending on the rigidity and design of each region. Applying the manual loads also influenced the orientation of forces. As a result, this data suffered from a standard and automatic approach of load application, which might have led to inconsistent calibration sessions. Since the quality of data in the calibration session could significantly affect the predictions, a more standard approach was likely to improve the accuracy and repeatability of results. Cuppens, et al. [102] used a texture analyzer to quantify several regions of FOs including the medial arch, heel, metatarsal heads, and forefoot. The advantage of this tool over our manual loading method was the possibility of applying consistent forces all over the FO surface, the repeatability of load application between FOs, accurate control over the orientation of applied forces, and reduced labor work. On the other hand, both manual loading methods applied point forces, while the load is distributed on a larger region of FO during walking depending on the foot contact area. In our calibration session, it would have been difficult to apply the distributed load, because the tool to generate this load could have hidden several markers on the FO surface. This difference in the type of loading between calibration and walking sessions might raise some levels of uncertainty in the predictions of the walking session, which needs further validation. To overcome this uncertainty, an indirect approach such as finite element modeling can be used to find the corresponding point forces that impose similar magnitude and pattern of deformation to the ones from distributed forces of foot contact during walking. Thereafter, using precise tools of load application, the equal point forces that represent the forces during walking can be applied in the calibration session.

II. Slight differences existed in the position of marker triads between the calibration and walking sessions. A deeper overlooking of data showed that the depth of insertion was not the same between sessions (< 1 mm on average) probably because of using different marker triads. Although the designs of all marker triads were the same, they might have been abraded due to their repeated insertion into the double-cross slots on FO contour. In order to remove this source of inaccuracy, the relative orientations of marker triads were just used to train the neural network instead of their position. This corresponded to the loss of information in input data,

since six degrees of freedom, including three orientation and three translation components, could be calculated from three markers of each triad. Future studies intending to use the contour of FOs to estimate the deformation are suggested to design more stable joints for attaching markers.

III. Some differences were spotted in the boundary conditions between the FO calibration session and the walking session. In the calibration session, the FO was fixed to the shoe sole so that the sole could not move or deform independently. In addition, the FO was not constrained by the shoe upper in the calibration session, meaning that no limitation was imposed on the side motion of FO. During walking, a proportion of FO deformation might be constrained by the side walls of shoes. To our view, this limitation is less likely to negatively influence our predictions, as a higher range of motion could be generated in the calibration session with fewer constraints from the shoe upper. Whether such differences in the boundary conditions between the two sessions would impact the predicted deformation during walking remains to be assessed in future research.

IV. The deformation of each FO during walking was predicted from a single recorded calibration session. Some steps were taken for validating the accuracy of our predictions. Primarily, different trials were recorded, in which we applied different loadings to deform one customized FO. The first trial was recorded by applying bending and torsional loads on all FO regions to simulate the motion in sagittal and frontal planes. This trial was used to generate the neural network model. Other trials were then recorded with the purpose of manually deforming the FO on different specific orientations, namely bending to simulate plantarflexion/dorsiflexion, bending the medial arch region to simulate eversion and arch collapse, and bending the region under the lateral arch to simulate inversion. These trials were used to assess and validate the generated model. The results showed that as long as the loadings and the resulted ranges of motion for marker triads in the test set remained as a subset of the corresponding variables in the training set, a good prediction accuracy (RMSE < 1 mm) would be achieved. Based on these findings, it was important that the loading and the range of motion of marker triads during the walking session were a subset of corresponding variables during the calibration session. Therefore, two steps were taken to ensure the accuracy of predictions during walking, which were presented in Chapter 3. In the first step, 15% of the data from the calibration session was kept as unseen data to test the model accuracy. In the second step, the peak pressure in 10

discrete regions of FO during the stance phase of walking was assessed to be subsets of the loads in corresponding regions during the calibration session. Furthermore, the ranges of deformation of marker triads during walking were assessed to ensure their coverage by the corresponding ranges of motion during the calibration session. However, we did not investigate whether similar deformations would be achieved by using different calibration sessions for the same FO. It is suggested to do repeatability tests for some customized FOs to confirm the reliability of prediction results. Adding this validation step could enhance the reliability of our predictions.

A further step for validating our model can be to take advantage of imaging techniques. Assessing the predictive performance of the artificial neural network model by independent and unseen validation set does not provide information on how well the model is able to accurately respond to the loading and the range of deformation during walking. Imaging techniques such as EOS (in statics) or videofluoroscopy (in dynamics) have the potential to capture the range and pattern of deformation of FO surface. According to our preliminary study, metal beads can be attached to the plantar surface of 3D printed FOs, while reconstructing the position of these metal beads from X-ray images during weight-bearing or walking could determine the FO deformation. The challenging point with this validation technique is the arrangement of beads' locations on the FO plantar surface so that they can be easily distinguished and registered after acquiring the images. Attaching fewer number of beads compared to the 55 surface markers as well as different sizes of beads on the plantar surface of FO might help to facilitate the image registration process. The FO deformation obtained from registered images could then be used to validate our neural network model.

V. The response of flatfoot individuals to customized FOs was assessed four weeks after receiving their orthoses, while they just wore each of the sport and regular FOs for two weeks in a randomized order. Therefore, the long-term effect of FOs during walking remains unknown. Previous research has shown that long-term use of rigid FOs in children with flatfoot was efficient to correct the rearfoot posture [336]. A systematic review reported that FOs did not exhibit any significant effect immediately after their application in pediatric flexible flatfoot individuals, but they could significantly improve some radiographical parameters and foot posture over time [337]. In addition, the long-term efficiency of laterally wedged insoles in improving the pain and physical function of patients with knee osteoarthritis [338], as well as

the textured insoles on postural stability of healthy elderly individuals [334], have been confirmed. The long-term efficiency of FOs on the level of comfort and pain, as well as correcting the motion and loading of lower body joints in flexible flatfoot individuals during gait should be assessed in future studies. The results from the long-term effect of FOs can finally be incorporated into the FO design and be applied for re-formulating the cost function to optimize the function of FOs.

5.6. Perspectives

The ongoing *FOOTi* project in the Laboratory of Simulation and Movement Modelling (S2M lab) aims to deliver the optimized design of customized FOs for flatfoot individuals. In this way, it is required to improve our understanding of the association between foot biomechanics and symptoms of flatfoot deformity. This can be achieved by complementing the results of foot kinematics and foot plantar pressure with joint moments and muscle activation. In addition, the relationship between the movement of the subtalar joint and medial arch motion as a functional mechanism of the foot and the impact of FO on this relationship should be estimated. Such relationships could enhance our understanding of coordinated foot function. They can also provide some alternative options for indirect correction of foot motion and function when a difficulty exists in the direct correction of that variable. This difficulty might appear in the form of imposing extra stress on bony structures and soft tissues or causing certain levels of discomfort for patients. Finally, these datasets can be used to extend the results for the interaction between foot and FOs, presented in this thesis, to determine the gold point that flatfoot individuals are favorable to reach by wearing FOs. This gold point is necessary to define a cost function to be applied in finite element analysis for optimizing the designs of FOs. A schematic of what has been done and the future direction of the project is illustrated in Figure 5.1.

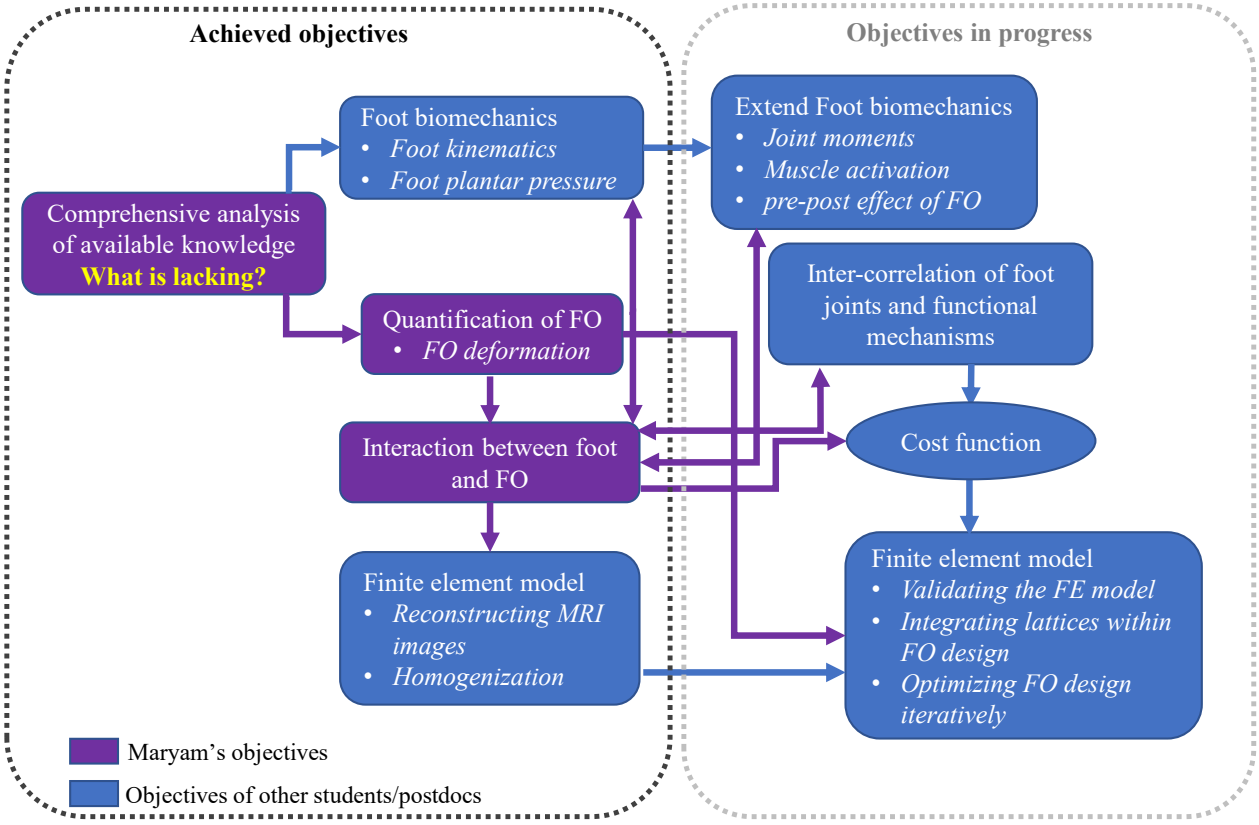

Figure 5.1: Flowchart to summarize the objectives of FOOT¡ project including the proportion of this thesis, what has been done, the future direction. Abbreviations: FO: foot orthosis, FE: finite element, MRI: magnetic resonance imaging.

Here, some relevant research perspectives are overviewed:

Validating the finite element model by FO deformation: It was previously mentioned that finite element models involve some simplifications and assumptions in generating the model, assigning the mechanical properties, and applying the constraints and boundary conditions. Therefore, these models need to be validated by experimental results. The geometry of a normal-arched foot and a flatfoot have been already reconstructed from MRI images and the model of foot-FO has been generated. A convergence study is primarily required to confirm meshing and sensitivity analysis to justify the boundary conditions, in order to ensure the reliability of results. Then, the point forces during the calibration session can be applied in the finite element model, so that the deformation of the FO plantar surface can be validated with the experimental results. A further step can be done by simulating the foot plantar pressure during walking in the model, which enables us to use the results of FO deformation, calculated in Chapter 3, to confirm and check the results of the finite

element approach. For a final validation of both modeling techniques, it is proposed to use the direct data from imaging techniques such as EOS during weight bearing or videofluoroscopy during walking.

Extending the relationships obtained from linear mixed models: In this thesis, the foot biomechanics of 17 individuals with flatfoot deformity and the dynamic behaviour of their customized FO were used to determine the foot-FO interaction using linear mixed models. The developed models helped us to suggest different designs of FOs for different symptoms of flatfoot deformity, which presented valuable preliminary guidelines for clinicians and industrial FO designers. However, to make these guidelines reliable and practical, it will be relevant to design different FOs, namely higher support in the medial region, higher support in the lateral region, and higher support on medial and lateral arches, and collect similar data on a larger sample size. Using these data, the efficiency of new FO designs on correcting foot motion and loading can be evaluated. In addition, following a discriminant function analysis, similar to Arnold, et al. [169], it would be possible to recognize the responders to each FO design. This will be a robust experimental approach to either confirm or reject the findings from our linear mixed models and present standard approaches for designing customized FOs with higher levels of certainty.

Optimizing the function of foot orthoses using finite element modeling: The designs of customized FOs in this study were formulated according to the experience of podiatrists and through discussions and consensus between our clinical and industrial partners. Although our FOs were designed in reliance on clinical and mechanical concepts, their performance was not evaluated before fabrication. Lochner, et al. [16] recommended integrating two simulation steps within the modern process of fabrication FO, explained in section 1.3.2. The first simulation step was recommended for postural adjustment of the foot to be replaced by the adjustment identified based on the visual and anthropometrical assessments by podiatrists. Some advantages such as automating the fabrication process, higher repeatability, and preventing the deformation of soft tissues can be gained by adding this simulation step. The second simulation step was supposed to be conducted after the CAD/CAM design of customized FOs to assess their function and iteratively optimize the design for reaching the favorable alterations in foot motion and loading. In order to optimize the FOs using finite element analysis in our project, it is required to devise a cost function based on our biomechanical interpretations. The results of this thesis could predict the deformation

of normal-ached feet *versus* flatfeet during walking. In addition, we identified the biomechanical parameters that had a higher impact on the deformation of each FO region. A primary cost function could be developed based on (a) detecting the alterations in the biomechanics of flatfoot individual, (b) finding the FO region that its deformation is significantly associated with the identified biomechanical alteration from our linear mixed models, (c) changing the structure of identified FO region with the objective of neutralizing the biomechanical alteration. The final design of FO can be achieved through an iterative optimization approach using finite element analysis.

Comparing the function of full-length FOs *versus* ¾-length FOs: The customized FOs could be designed as full-length which supports the whole length of foot or ¾- length where the area under the toes is not supported. Full-length FOs are commonly used when modification of FO in the forefoot region is required, such as forefoot postings. On the other hand, ¾-length FOs are easier to fit inside different shoes. The biomechanical performance of these two types of FOs was also shown to be different [339]. In this study, ¾-length FOs were 3D printed and evaluated. Previous studies showed that full-length FOs with forefoot posting could control the forefoot abduction and excessive rearfoot eversion in individuals with flatfoot deformity [25, 52], in addition to decreasing pressure in lateral and heel regions [52]. On the other hand, a further study observed that ¾-length FOs were less likely to impose a negative effect on pressure distribution compared to full-length FOs for individuals with hallux valgus deformity. The findings of this thesis suggested that excessive forefoot abduction could be controlled by adding rigidity or support to the lateral regions of ¾-length FOs. Additional rigidity, however, can result in higher plantar pressure and consequently pain and discomfort [33, 329]. Based on the existing evidence, it is difficult to conclude which FO design, full-length or 3/4 -length, is more efficient for flatfoot individuals, especially for the ones with excessive forefoot abduction. Due to the differences between the two FO types, the relationships between foot biomechanics and FO obtained in this study cannot be generalized to full-length FOs. Therefore, future research is required to compare the effect of these two FO types with similar designs on the same population.

Chapter 6 - Conclusion

This thesis aimed to deepen our understanding of foot orthosis function during walking. The three main studies presented in this thesis made it possible to find the level of evidence that exists in the available literature for the effect of orthosis design on the kinematics and kinetics of foot; to quantify the foot orthosis deformation during walking by developing a validated protocol; and to formulate the deformation of foot orthosis as a function of foot kinematics and plantar pressure.

Firstly, the systematic review conducted on the association between foot orthosis design and foot biomechanics made it possible to understand the available knowledge and what is lacking in the literature. The key observations of this review were that medially posted foot orthoses could control the foot posture and moment arms; arch supports could partially modify the foot positioning and maintain stability; and heel supports might attenuate the impact of ground force and provide shock absorption. However, low levels of evidence were found for these observations which could be due to the limited number of available studies and the heterogeneity between existing data caused by differences in their methodological approach. Therefore, standardizing the methodological approach for foot orthosis prescription, data collection, and data analysis are required. Then, more studies following such standard approaches are suggested to be developed to enhance our understanding of the biomechanical impact of foot orthoses.

The next step of this thesis was to quantify the foot orthosis deformation during walking by developing and validating an artificial neural network. A comprehensive set of data, covering a broader range of deformation and loading that happen during walking, was used to generate a robust model. The predictive performance of the model was additionally tested by a set of unseen data. The developed model was capable to recognize the pattern and range of deformation of customized orthoses during walking and to differentiate between the two foot orthoses with different rigidities. The deformation of orthoses, predicted in this step, could be used to represent their behaviour under dynamic loading. It could also be applied to validate the finite element models.

Finally, the response of individuals to customized foot orthoses was evaluated which is still a challenge in clinical practice. To explore this issue, linear mixed models were built to find direct interaction between foot and foot orthosis. For each orthosis region, we could rank the level of

dependency between foot biomechanics and foot orthosis deformation in order from largest to smallest. We showed that region-dependent deformations of customized foot orthoses were associated with foot kinematics and plantar pressure, while this dependency changed over the phases of the gait cycle. The results of this step provided useful guidelines to direct the clinical practitioners towards the key parameters for prescribing foot orthoses and the engineers towards applying functional gradient structural properties to the foot orthosis design for reaching their optimal function.

Bibliography

[1] M. S. Lee *et al.*, "Diagnosis and treatment of adult flatfoot," vol. 44, no. 2, pp. 78-113, 2005.

[2] H. A. Banwell, S. Mackintosh, D. J. J. o. f. Thewlis, and a. research, "Foot orthoses for adults with flexible pes planus: a systematic review," vol. 7, no. 1, p. 23, 2014.

[3] A.-V. Behling, S. Manz, V. von Tscharner, B. M. J. J. o. s. Nigg, and m. i. sport, "Pronation or foot movement—What is important," vol. 23, no. 4, pp. 366-371, 2020.

[4] F. Halabchi, R. Mazaheri, M. Mirshahi, and L. J. I. j. o. p. Abbasian, "Pediatric flexible flatfoot; clinical aspects and algorithmic approach," vol. 23, no. 3, p. 247, 2013.

[5] N. Rodriguez, R. G. J. C. i. p. m. Volpe, and surgery, "Clinical diagnosis and assessment of the pediatric pes planovalgus deformity," vol. 27, no. 1, pp. 43-58, 2010.

[6] T. Prachgosin, W. Leelasamran, P. Smithmaitrie, S. J. P. Chatpun, and o. international, "Effect of total-contact orthosis on medial longitudinal arch and lower extremities in flexible flatfoot subjects during walking," vol. 41, no. 6, pp. 579-586, 2017.

[7] L. Welte, L. A. Kelly, G. A. Lichtwark, and M. J. J. J. o. t. R. S. I. Rainbow, "Influence of the windlass mechanism on arch-spring mechanics during dynamic foot arch deformation," vol. 15, no. 145, p. 20180270, 2018.

[8] D. V. Flores, C. Mejía Gómez, M. Fernández Hernando, M. A. Davis, and M. N. J. R. Pathria, "Adult Acquired Flatfoot Deformity: Anatomy, Biomechanics, Staging, and Imaging Findings," vol. 39, no. 5, pp. 1437-1460, 2019.

[9] A. K. Buldt, P. Levinger, G. S. Murley, H. B. Menz, C. J. Nester, and K. B. Landorf, "Foot posture is associated with kinematics of the foot during gait: A comparison of normal, planus and cavus feet," *Gait & Posture,* vol. 42, no. 1, pp. 42-48, 2015/06/01/ 2015.

[10] R. T. Cheung, R. C. Chung, and G. Y. J. B. j. o. s. m. Ng, "Efficacies of different external controls for excessive foot pronation: a meta-analysis," vol. 45, no. 9, pp. 743-751, 2011.

[11] K.-W. Lin *et al.*, "Biomechanical Evaluation and Strength Test of 3D-Printed Foot Orthoses," vol. 2019, 2019.

[12] H. B. Menz, J. J. Allan, D. R. Bonanno, K. B. Landorf, and G. S. Murley, "Custom-made foot orthoses: an analysis of prescription characteristics from an Australian commercial orthotic laboratory," (in eng), *J Foot Ankle Res,* vol. 10, p. 23, 2017.

[13] H. B. J. J. o. f. Menz and a. research, "Foot orthoses: how much customisation is necessary?," vol. 2, no. 1, p. 23, 2009.

[14] O. Ciobanu, Y. Soydan, and S. Hizal, "Customized foot orthosis manufactured with 3D printers," in *Proceedings of IMS*, 2012, pp. 91-98.

[15] L. Tang *et al.*, "Functional gradient structural design of customized diabetic insoles," *Journal of the Mechanical Behavior of Biomedical Materials,* vol. 94, pp. 279-287, 2019/06/01/ 2019.

[16] S. J. Lochner, J. P. Huissoon, S. S. J. C.-A. D. Bedi, and Applications, "Simulation methods in the foot orthosis development process," vol. 11, no. 6, pp. 608-616, 2014.

[17] M. K. Nilsson, R. Friis, M. S. Michaelsen, P. A. Jakobsen, R. O. J. J. o. f. Nielsen, and a. research, "Classification of the height and flexibility of the medial longitudinal arch of the foot," vol. 5, no. 1, p. 3, 2012.

[18] R. A. Zifchock, C. Theriot, H. J. Hillstrom, J. Song, and M. Neary, "The Relationship Between Arch Height and Arch Flexibility: A Proposed Arch Flexibility Classification System for the Description of Multidimensional Foot Structure," *Journal of the American Podiatric Medical Association,* vol. 107, no. 2, pp. 119-123, 2017.

[19] D. S. Williams and I. S. J. P. t. McClay, "Measurements used to characterize the foot and the medial longitudinal arch: reliability and validity," vol. 80, no. 9, pp. 864-871, 2000.

[20] S. J. Lochner, "Computer aided engineering in the foot orthosis development process," 2013.

[21] A. E. Williams, A. Martinez-Santos, J. McAdam, C. J. J. J. o. F. Nester, and A. Research, "'Trial and error…','… happy patients' and '… an old toy in the cupboard': a qualitative investigation of factors that influence practitioners in their prescription of foot orthoses," vol. 9, no. 1, pp. 1-8, 2016.

[22] G. Desmyttere, M. Hajizadeh, J. Bleau, and M. J. C. B. Begon, "Effect of foot orthosis design on lower limb joint kinematics and kinetics during walking in flexible pes planovalgus: A systematic review and meta-analysis," vol. 59, pp. 117-129, 2018.

[23] M. Hajizadeh, G. Desmyttere, J.-P. Carmona, J. Bleau, and M. J. T. F. Begon, "Can foot orthoses impose different gait features based on geometrical design in healthy subjects? A systematic review and meta-analysis," vol. 42, p. 101646, 2020.

[24] P. Dedieu, C. Drigeard, L. Gjini, F. Dal Maso, and P.-G. Zanone, "Effects of foot orthoses on the temporal pattern of muscular activity during walking," *Clinical Biomechanics,* vol. 28, no. 7, pp. 820-824, 2013.

[25] M. A. Johanson, R. Donatelli, M. J. Wooden, P. D. Andrew, and G. S. J. P. T. Cummings, "Effects of three different posting methods on controlling abnormal subtalar pronation," vol. 74, no. 2, pp. 149-158, 1994.

[26] S. Telfer, M. Abbott, M. P. Steultjens, and J. J. J. o. b. Woodburn, "Dose–response effects of customised foot orthoses on lower limb kinematics and kinetics in pronated foot type," vol. 46, no. 9, pp. 1489-1495, 2013.

[27] A. Stacoff *et al.*, "Biomechanical effects of foot orthoses during walking," vol. 17, no. 3, pp. 143-153, 2007.

[28] R. A. Zifchock and I. J. C. b. Davis, "A comparison of semi-custom and custom foot orthotic devices in high-and low-arched individuals during walking," vol. 23, no. 10, pp. 1287-1293, 2008.

[29] C. Bishop, J. B. Arnold, and T. May, "Effects of Taping and Orthoses on Foot Biomechanics in Adults with Flat-Arched Feet," *Medicine and science in sports and exercise,* vol. 48, no. 4, pp. 689-696, 01 Apr 2016.

[30] G. P. Brown, R. Donatelli, P. A. Catlin, and M. J. Wooden, "The effect of two types of foot orthoses on rearfoot mechanics," *Journal of Orthopaedic and Sports Physical Therapy,* vol. 21, no. 5, pp. 258-267, 1995.

[31] W. J. Hurd, S. J. Kavros, and K. R. J. C. J. o. S. M. Kaufman, "Comparative biomechanical effectiveness of over-the-counter devices for individuals with a flexible flatfoot secondary to forefoot varus," vol. 20, no. 6, pp. 428-435, 2010.

[32] M. Balsdon, C. Dombroski, K. Bushey, T. R. J. P. Jenkyn, and o. international, "Hard, soft and off-the-shelf foot orthoses and their effect on the angle of the medial longitudinal arch: A biplane fluoroscopy study," vol. 43, no. 3, pp. 331-338, 2019.

[33] S. Su, Z. Mo, J. Guo, and Y. Fan, "The Effect of Arch Height and Material Hardness of Personalized Insole on Correction and Tissues of Flatfoot," (in eng), *J Healthc Eng,* vol. 2017, p. 8614341, 2017.

[34] D. R. Bonanno *et al.*, "The effect of different depths of medial heel skive on plantar pressures," vol. 5, no. 1, pp. 1-10, 2012.

[35] R. S. Goonetilleke, *The science of footwear*. CRC Press, 2012.

[36] F. Harrold, R. J. J. C. T. i. F. Abboud, and A. Surgery, "Biomechanics of the Foot and Ankle," ed: Cambridge: Cambridge University Press, 2018, pp. 22-43.

[37] H. J. C. O. Elftman and R. Research®, "The transverse tarsal joint and its control," vol. 16, pp. 41-46, 1960.

[38] A. S. Gwani, M. A. Asari, and Z. M. J. F. m. Ismail, "How the three arches of the foot intercorrelate," vol. 76, no. 4, pp. 682-688, 2017.

[39] T. Bito *et al.*, "Forefoot transverse arch height asymmetry is associated with foot injuries in athletes participating in college track events," vol. 30, no. 8, pp. 978-983, 2018.

[40] L. A. Kelly, G. Lichtwark, and A. G. J. J. o. T. R. S. I. Cresswell, "Active regulation of longitudinal arch compression and recoil during walking and running," vol. 12, no. 102, p. 20141076, 2015.

[41] J. Reeves, "The effect of foot orthoses on muscle activity and morphology, foot biomechanics and skin sensitivity," University of Salford, 2019.

[42] C.-B. Phan, G. Shin, K. M. Lee, and S. J. J. o. b. Koo, "Skeletal kinematics of the midtarsal joint during walking: Midtarsal joint locking revisited," vol. 95, p. 109287, 2019.

[43] J. J. J. o. a. Hicks, "The mechanics of the foot: II. The plantar aponeurosis and the arch," vol. 88, no. Pt 1, p. 25, 1954.

[44] D. A. Bruening, M. B. Pohl, K. Z. Takahashi, and J. A. Barrios, "Midtarsal locking, the windlass mechanism, and running strike pattern: A kinematic and kinetic assessment," *Journal of biomechanics,* vol. 73, pp. 185-191, 2018.

[45] J. Hicks, "The mechanics of the foot: II. The plantar aponeurosis and the arch," *Journal of anatomy,* vol. 88, no. Pt 1, p. 25, 1954.

[46] C. B. Blackwood, T. J. Yuen, B. J. Sangeorzan, and W. R. Ledoux, "The midtarsal joint locking mechanism," *Foot & ankle international,* vol. 26, no. 12, pp. 1074-1080, 2005.

[47] J. L. Tweed, J. Campbell, R. Thompson, and M. J. T. F. Curran, "The function of the midtarsal joint: a review of the literature," vol. 18, no. 2, pp. 106-112, 2008.

[48] N. Okita, S. A. Meyers, J. H. Challis, N. A. J. F. Sharkey, and A. International, "Midtarsal Kinematics While Walking," vol. 30, no. 8, p. 805, 2009.

[49] M. Razeghi, M. E. J. G. Batt, and posture, "Foot type classification: a critical review of current methods," vol. 15, no. 3, pp. 282-291, 2002.

[50] H. J. Hillstrom *et al.*, "Foot type biomechanics part 1: structure and function of the asymptomatic foot," vol. 37, no. 3, pp. 445-451, 2013.

[51] S. Pita-Fernandez *et al.*, "Flat foot in a random population and its impact on quality of life and functionality," vol. 11, no. 4, p. LC22, 2017.

[52] S. F.-T. Tang, C.-H. Chen, C.-K. Wu, W.-H. Hong, K.-J. Chen, and C.-K. Chen, "The effects of total contact insole with forefoot medial posting on rearfoot movement and foot pressure distributions in patients with flexible flatfoot," *Clinical Neurology and Neurosurgery,* vol. 129, pp. S8-S11, 2015/02/01/ 2015.

[53] M. Pfeiffer, R. Kotz, T. Ledl, G. Hauser, and M. J. P. Sluga, "Prevalence of flat foot in preschool-aged children," vol. 118, no. 2, pp. 634-639, 2006.

[54] S. N. K. Arachchige, H. Chander, and A. J. T. F. Knight, "Flatfeet: Biomechanical implications, assessment and management," vol. 38, pp. 81-85, 2019.

[55] D. B. Van, B. J. J. F. Sangeorzan, and a. clinics, "Biomechanics and pathophysiology of flat foot," vol. 8, no. 3, pp. 419-430, 2003.

[56] K. T. Haendlmayer, N. J. J. O. Harris, and Trauma, "(ii) Flatfoot deformity: an overview," vol. 23, no. 6, pp. 395-403, 2009.

[57] A. C. Redmond, J. Crosbie, and R. A. J. C. b. Ouvrier, "Development and validation of a novel rating system for scoring standing foot posture: the Foot Posture Index," vol. 21, no. 1, pp. 89-98, 2006.

[58] S. P. Shultz *et al.*, "An investigation of structure, flexibility, and function variables that discriminate asymptomatic foot types," vol. 33, no. 3, pp. 203-210, 2017.

[59] L. K. Dahle, M. Mueller, A. Delitto, J. E. J. J. o. O. Diamond, and S. P. Therapy, "Visual assessment of foot type and relationship of foot type to lower extremity injury," vol. 14, no. 2, pp. 70-74, 1991.

[60] S. C. Morrison, J. J. J. o. f. Ferrari, and a. research, "Inter-rater reliability of the Foot Posture Index (FPI-6) in the assessment of the paediatric foot," vol. 2, no. 1, p. 26, 2009.

[61] M. E. Bennett, J. Camilla Tulloch, K. W. Vlg, and C. L. J. J. o. p. h. d. Phillips, "Measuring orthodontic treatment satisfaction: questionnaire development and preliminary validation," vol. 61, no. 3, pp. 155-160, 2001.

[62] J. S. Lee, K. B. Kim, J. O. Jeong, N. Y. Kwon, and S. M. J. A. o. r. m. Jeong, "Correlation of foot posture index with plantar pressure and radiographic measurements in pediatric flatfoot," vol. 39, no. 1, p. 10, 2015.

[63] P. K. Levangie and C. C. J. P. F. D. C. Norkin, "Joint Structure and function: a comprehensive analysis. 3rd," 2000.

[64] L. S. R. Jonson, M. T. J. J. o. O. Gross, and S. P. Therapy, "Intraexaminer reliability, interexaminer reliability, and mean values for nine lower extremity skeletal measures in healthy naval midshipmen," vol. 25, no. 4, pp. 253-263, 1997.

[65] T. G. McPoil and M. W. J. J. o. t. A. P. M. A. Cornwall, "Use of the longitudinal arch angle to predict dynamic foot posture in walking," vol. 95, no. 2, pp. 114-120, 2005.

[66] T. W. Kernozek and M. D. J. A. P. M. R. Ricard, "Foot placement angle and arch type: effect on rearfoot motion," vol. 71, no. 12, pp. 988-991, 1990.

[67] D. J. T. o. c. o. n. A. Brody, "Techniques in the evaluation and treatment of the injured runner," vol. 13, no. 3, p. 541, 1982.

[68] A. M. Picciano, M. S. Rowlands, T. J. J. o. O. Worrell, and S. P. Therapy, "Reliability of open and closed kinetic chain subtalar joint neutral positions and navicular drop test," vol. 18, no. 4, pp. 553-558, 1993.

[69] R. A. Zifchock, C. Theriot, H. J. Hillstrom, J. Song, and M. J. J. o. t. A. P. M. A. Neary, "The Relationship between arch height and arch flexibility: a proposed arch flexibility classification system for the description of multidimensional foot structure," vol. 107, no. 2, pp. 119-123, 2017.

[70] J. Song *et al.*, "Comprehensive biomechanical characterization of feet in USMA cadets: Comparison across race, gender, arch flexibility, and foot types," vol. 60, pp. 175-180, 2018.

[71] R. J. Butler, H. Hillstrom, J. Song, C. J. Richards, and I. S. J. J. o. t. A. P. M. A. Davis, "Arch height index measurement system: establishment of reliability and normative values," vol. 98, no. 2, pp. 102-106, 2008.

[72] P. R. Cavanagh and M. M. J. J. o. b. Rodgers, "The arch index: a useful measure from footprints," vol. 20, no. 5, pp. 547-551, 1987.

[73] J. Hamill, B. Bates, K. Knutzen, and G. J. C. B. Kirkpatrick, "Relationship between selected static an dynamic lower extremity measures," vol. 4, no. 4, pp. 217-225, 1989.

[74] L. W. J. R. Q. A. P. E. A. Irwin, "A study of the tendency of school children to develop flat-footedness," vol. 8, no. 1, pp. 46-53, 1937.

[75] A. Simkin, I. Leichter, M. Giladi, M. Stein, C. J. F. Milgrom, and ankle, "Combined effect of foot arch structure and an orthotic device on stress fractures," vol. 10, no. 1, pp. 25-29, 1989.

[76] L. Smith, T. Clarke, C. Hamill, and F. J. J. o. t. A. P. M. A. Santopietro, "The effects of soft and semi-rigid orthoses upon rearfoot movement in running," vol. 76, no. 4, pp. 227-233, 1986.

[77] R. List, H. Gerber, M. Foresti, P. Rippstein, J. J. F. Goldhahn, and A. Surgery, "A functional outcome study comparing total ankle arthroplasty (TAA) subjects with pain to subjects with absent level of pain by means of videofluoroscopy," vol. 18, no. 4, pp. 270-276, 2012.

[78] S. C. Wearing, S. Urry, P. Perlman, J. Smeathers, P. J. F. Dubois, and a. international, "Sagittal plane motion of the human arch during gait: a videofluoroscopic analysis," vol. 19, no. 11, pp. 738-742, 1998.

[79] C. L. Saltzman, D. A. Nawoczenski, and K. D. Talbot, "Measurement of the medial longitudinal arch," *Archives of Physical Medicine and Rehabilitation,* vol. 76, no. 1, pp. 45-49, 1995/01/01/ 1995.

[80] A. Felfernig, G. Friedrich, and D. J. A. I. i. E. Jannach, "Conceptual modeling for configuration of mass-customizable products," vol. 15, no. 2, pp. 165-176, 2001.

[81] R. Majumdar *et al.*, "Development and evaluation of prefabricated antipronation foot orthosis," (in eng), *J Rehabil Res Dev,* vol. 50, no. 10, pp. 1331-42, 2013.

[82] B. Khodaei, H. Saeedi, M. Farzadi, and E. Norouzi, "Comparison of plantar pressure distribution in CAD–CAM and prefabricated foot orthoses in patients with flexible flatfeet," *The Foot,* vol. 33, pp. 76-80, 2017.

[83] S. Ki, A. Leung, and A. Li, "Comparison of plantar pressure distribution patterns between foot orthoses provided by the CAD-CAM and foam impression methods," *Prosthetics and orthotics international,* vol. 32, no. 3, pp. 356-362, 2008.

[84] B. Khodaei, H. Saeedi, M. Farzadi, and E. J. T. F. Norouzi, "Comparison of plantar pressure distribution in CAD–CAM and prefabricated foot orthoses in patients with flexible flatfeet," vol. 33, pp. 76-80, 2017.

[85] M. L. Root, "Normal and abnormal function of the foot," *Clinical biomechanics,* vol. 2, 1977.

[86] M. L. Root, W. P. Orien, J. H. Weed, and R. Hughes, "Biomechanical examination of the foot, Vol. 1," *Clinical Biomechanics Corp, Los Angeles,* pp. 42-123, 1971.

[87] H. L. Jarvis, C. J. Nester, P. D. Bowden, and R. K. Jones, "Challenging the foundations of the clinical model of foot function: further evidence that the root model assessments fail to appropriately classify foot function," *Journal of foot and ankle research,* vol. 10, no. 1, p. 7, 2017.

[88] P. Harradine and L. Bevan, "A review of the theoretical unified approach to podiatric biomechanics in relation to foot orthoses therapy," *Journal of the American Podiatric Medical Association,* vol. 99, no. 4, pp. 317-325, 2009.

[89] M. M. Lusardi, M. Jorge, and C. C. Nielsen, *Orthotics and Prosthetics in Rehabilitation-E-Book*. Elsevier Health Sciences, 2013.

[90] R. Phillips, R. Christeck, and R. Phillips, "Clinical measurement of the axis of the subtalar joint," *Journal of the American Podiatric Medical Association,* vol. 75, no. 3, p. 119, 1985.

[91] H. J. Dananberg, "Functional hallux limitus and its relationship to gait efficiency," *Journal of the American Podiatric Medical Association,* vol. 76, no. 11, pp. 648-652, 1986.

[92] H. Dananberg, "Lower extremity mechanics and their effect on lumbosacral function," *SPINE-PHILADELPHIA-HANLEY AND BELFUS-,* vol. 9, pp. 389-389, 1995.

[93] H. Dananberg, "Lower Back Pain: A Repetitive Motion Injury," *Movement, Stability and Low Back Pain: The Role of the Sacroiliac Joint,* 1997.

[94] H. J. Dananberg and M. Guiliano, "Chronic low-back pain and its response to custom-made foot orthoses," *Journal of the American Podiatric Medical Association,* vol. 89, no. 3, pp. 109-117, 1999.

[95] H. Dananberg, "Question and answer session," *The Podiatric Biomechanics Group Focus,* vol. 7, p. 7, 1999.

[96] K. A. Kirby, "Subtalar joint axis location and rotational equilibrium theory of foot function," *Journal of the American Podiatric Medical Association,* vol. 91, no. 9, pp. 465-487, 2001.

[97] J. Pallari *et al.*, "Design and additive fabrication of foot and ankle-foot orthoses," in *Proceedings of the 21st Annual International Solid Freeform Fabrication Symposium–An Additive Manufacturing Conference*, 2010, pp. 9-11.

[98] P. E. Chatzistergos, R. Naemi, N. J. M. e. Chockalingam, and physics, "A method for subject-specific modelling and optimisation of the cushioning properties of insole materials used in diabetic footwear," vol. 37, no. 6, pp. 531-538, 2015.

[99] A. K. Buldt, J. J. Allan, K. B. Landorf, H. B. J. G. Menz, and posture, "The relationship between foot posture and plantar pressure during walking in adults: a systematic review," vol. 62, pp. 56-67, 2018.

[100] C. Nicolopoulos, J. Black, and E. J. T. f. Anderson, "Foot orthoses materials," vol. 10, no. 1, pp. 1-3, 2000.

[101] D. Shurr, T. J. P. Cook, and O. U. S. R. P. Hall, "Methods, materials, and mechanics," pp. 17-29, 1990.

[102] K. Cuppens *et al.*, "Using a texture analyser to objectively quantify foot orthoses," in *2019 41st Annual International Conference of the IEEE Engineering in Medicine and Biology Society (EMBC)*, 2019, pp. 5348-5351: IEEE.

[103] D. Drougkas *et al.*, "Gait-Specific Optimization of Composite Footwear Midsole Systems, Facilitated through Dynamic Finite Element Modelling," (in eng), *Appl Bionics Biomech,* vol. 2018, p. 6520314, 2018.

[104] J. T.-M. Cheung, J. Yu, and M. J. K. J. o. S. B. Zhang, "Review of computational models for footwear design and evaluation," vol. 19, no. 1, pp. 13-25, 2009.

[105] A. Forestiero, A. Raumer, E. L. Carniel, A. N. J. P. o. t. I. o. M. E. Natali, Part P: Journal of Sports Engineering, and Technology, "Investigation of the interaction phenomena between foot and insole by means of a numerical approach," vol. 229, no. 1, pp. 3-9, 2015.

[106] T. J. S. T. Nishiwaki, "Running shoe sole stiffness evaluation method based on eigen vibration analysis," vol. 1, no. 1, pp. 76-82, 2008.

[107] Y.-C. Hsu *et al.*, "Using an optimization approach to design an insole for lowering plantar fascia stress—a finite element study," vol. 36, no. 8, p. 1345, 2008.

[108] J. T.-M. Cheung, J. Yu, D. W.-C. Wong, and M. J. F. s. Zhang, "Current methods in computer-aided engineering for footwear design," vol. 1, no. 1, pp. 31-46, 2009.

[109] J. T.-M. Cheung, M. J. M. e. Zhang, and physics, "Parametric design of pressure-relieving foot orthosis using statistics-based finite element method," vol. 30, no. 3, pp. 269-277, 2008.

[110] R. Verdejo and N. J. J. o. b. Mills, "Heel–shoe interactions and the durability of EVA foam running-shoe midsoles," vol. 37, no. 9, pp. 1379-1386, 2004.

[111] K. G. Gerritsen, A. J. van den Bogert, and B. M. J. J. o. b. Nigg, "Direct dynamics simulation of the impact phase in heel-toe running," vol. 28, no. 6, pp. 661-668, 1995.

[112] C. F. Munro, D. I. Miller, and A. J. J. J. o. b. Fuglevand, "Ground reaction forces in running: a reexamination," vol. 20, no. 2, pp. 147-155, 1987.

[113] P. J. M. Villaggio, "WJ Stronge, Impact Mechanics," vol. 35, no. 5, pp. 470-471, 2000.

[114] T. Nishiwaki and S. J. F. S. Nakaya, "Footwear sole stiffness evaluation method corresponding to gait patterns based on eigenvibration analysis," vol. 1, no. 2, pp. 95-101, 2009.

[115] M. Rupérez, C. Monserrat, M. J. I. J. o. I. D. Alcañiz, and Manufacturing, "Simulation of the deformation of materials in shoe uppers in gait. Force distribution using finite elements," vol. 2, no. 2, pp. 59-68, 2008.

[116] G. J. B.-m. m. Lewis and engineering, "Finite element analysis of a model of a therapeutic shoe: effect of material selection for the outsole," vol. 13, no. 1, pp. 75-81, 2003.

[117] P. Franciosa, S. Gerbino, A. Lanzotti, L. J. M. e. Silvestri, and physics, "Improving comfort of shoe sole through experiments based on CAD-FEM modeling," vol. 35, no. 1, pp. 36-46, 2013.

[118] G. Luo, V. L. Houston, M. A. Garbarini, A. C. Beattie, and C. J. J. o. b. Thongpop, "Finite element analysis of heel pad with insoles," vol. 44, no. 8, pp. 1559-1565, 2011.

[119] D. McKenzie, D. Clement, and J. J. S. m. Taunton, "Running shoes, orthotics, and injuries," vol. 2, no. 5, pp. 334-347, 1985.

[120] B. M. Nigg, J. Baltich, S. Hoerzer, and H. J. B. J. o. S. M. Enders, "Running shoes and running injuries: mythbusting and a proposal for two new paradigms:‘preferred movement path’and ‘comfort filter’," vol. 49, no. 20, pp. 1290-1294, 2015.

[121] S. Alemany, I. García, E. Alcántara, J. González, and L. Castillo, "Integration of plantar pressure measurements in a finite element model for the optimization of shankpiece design for high-heeled shoes," in *6th Symposium of Footwear Biomechanics*, 2003.

[122] S. Koike and S. J. P. E. Okina, "A modeling method of sport shoes for dynamic analysis of shoe-body coupled system," vol. 34, pp. 272-277, 2012.

[123] T. G. Havenhill, B. C. Toolan, and L. F. Draganich, "Effects of a UCBL orthosis and a calcaneal osteotomy on tibiotalar contact characteristics in a cadaver flatfoot model," (in eng), *Foot Ankle Int,* vol. 26, no. 8, pp. 607-13, Aug 2005.

[124] G. Kogler, S. Solomonidis, and J. J. C. B. Paul, "In vitro method for quantifying the effectiveness of the longitudinal arch support mechanism of a foot orthosis," vol. 10, no. 5, pp. 245-252, 1995.

[125] G. Kogler, S. Solomonidis, and J. J. C. B. Paul, "Biomechanics of longitudinal arch support mechanisms in foot orthoses and their effect on plantar aponeurosis strain," vol. 11, no. 5, pp. 243-252, 1996.

[126] Y. Saito, T. S. Chikenji, Y. Takata, T. Kamiya, and E. Uchiyama, "Can an insole for obese individuals maintain the arch of the foot against repeated hyper loading?," (in eng), *BMC Musculoskelet Disord,* vol. 20, no. 1, p. 442, Oct 11 2019.

[127] F. Horst *et al.*, "On the Understanding and Interpretation of Machine Learning Predictions in Clinical Gait Analysis Using Explainable Artificial Intelligence," 2019.

[128] J. Lawrence, *Introduction to neural networks*. California Scientific Software, 1993.

[129] T. Chau, "A review of analytical techniques for gait data. Part 2: neural network and wavelet methods," *Gait & Posture,* vol. 13, no. 2, pp. 102-120, 2001/04/01/ 2001.

[130] W. J. C. B. Schöllhorn, "Applications of artificial neural nets in clinical biomechanics," vol. 19, no. 9, pp. 876-898, 2004.

[131] J. Brownlee, "Crash Course On Multi-Layer Perceptron Neural Networks," 2016.

[132] J. TORRES. (2018). *Learning process of a neural network*. Available: https://towardsdatascience.com/how-do-artificial-neural-networks-learn-773e46399fc7

[133] A. Sayadi, M. Monjezi, N. Talebi, and M. Khandelwal, "A comparative study on the application of various artificial neural networks to simultaneous prediction of rock fragmentation and backbreak," *Journal of Rock Mechanics and Geotechnical Engineering,* vol. 5, no. 4, pp. 318-324, 2013/08/01/ 2013.

[134] J. Brownlee. (2019). *How to use Data Scaling Improve Deep Learning Model Stability and Performance*. Available: https://machinelearningmastery.com/how-to-improve-neural-network-stability-and-modeling-performance-with-data-scaling/

[135] R. Kirk, M. Carre, S. Haake, and G. Manson, "Using neural networks to understand relationships in the traction of studded footwear on sports surfaces," 2006.

[136] C.-C. Wang, C.-H. Yang, C.-S. Wang, D. Xu, and B.-S. Huang, "Artificial neural networks in the selection of shoe lasts for people with mild diabetes," *Medical Engineering & Physics,* vol. 64, pp. 37-45, 2019/02/01/ 2019.

[137] M. José Rupérez, J. D. Martín-Guerrero, C. Monserrat, S. Alemany, and M. Alcañíz, "MODELLING THE CONTACT OF FOOT SURFACE AND SHOE UPPER USING ARTIFICIAL NEURAL NETWORKS," *Journal of Biomechanics,* vol. 41, p. S479, 2008/07/01/ 2008.

[138] M. J. Rupérez, J. D. Martín-Guerrero, C. Monserrat, and M. Alcañiz, "Artificial neural networks for predicting dorsal pressures on the foot surface while walking," *Expert Systems with Applications,* vol. 39, no. 5, pp. 5349-5357, 2012/04/01/ 2012.

[139] J. Wang, T. J. A. o. b. Zielińska, and biomechanics, "Gait features analysis using artificial neural networks: testing the footwear effect," vol. 19, no. 1, pp. 17--32, 2017.

[140] J. Barton, A. J. M. Lees, B. Engineering, and Computing, "Comparison of shoe insole materials by neural network analysis," vol. 34, no. 6, pp. 453-459, 1996.

[141] P. Lundgren *et al.*, "Invasive in vivo measurement of rear-, mid-and forefoot motion during walking," vol. 28, no. 1, pp. 93-100, 2008.

[142] P. Wolf *et al.*, "Functional units of the human foot," vol. 28, no. 3, pp. 434-441, 2008.

[143] C. Bishop, G. Paul, and D. J. J. o. b. Thewlis, "Recommendations for the reporting of foot and ankle models," vol. 45, no. 13, pp. 2185-2194, 2012.

[144] L. Rankine, J. T. Long, K. Canseco, and G. F. J. C. R. i. B. E. Harris, "Multisegmental foot modeling: a review," vol. 36, no. 2-3, 2008.

[145] S. M. Kidder, F. S. Abuzzahab, G. F. Harris, and J. E. J. I. t. o. r. e. Johnson, "A system for the analysis of foot and ankle kinematics during gait," vol. 4, no. 1, pp. 25-32, 1996.

[146] M. Carson, M. Harrington, N. Thompson, J. O'connor, and T. J. J. o. b. Theologis, "Kinematic analysis of a multi-segment foot model for research and clinical applications: a repeatability analysis," vol. 34, no. 10, pp. 1299-1307, 2001.

[147] J. Simon *et al.*, "The Heidelberg foot measurement method: development, description and assessment," vol. 23, no. 4, pp. 411-424, 2006.

[148] S. Rao, C. Saltzman, and H. J. J. C. B. Yack, "Segmental foot mobility in individuals with and without diabetes and neuropathy," vol. 22, no. 4, pp. 464-471, 2007.

[149] A. Leardini *et al.*, "Rear-foot, mid-foot and fore-foot motion during the stance phase of gait," vol. 25, no. 3, pp. 453-462, 2007.

[150] E. S. Grood and W. J. Suntay, "A joint coordinate system for the clinical description of three-dimensional motions: application to the knee," 1983.

[151] A. Leardini and P. Caravaggi, "Kinematic Foot Models for Instrumented Gait Analysis," in *Handbook of Human Motion*, B. Müller *et al.*, Eds. Cham: Springer International Publishing, 2017, pp. 1-24.

[152] P. Caravaggi, M. G. Benedetti, L. Berti, and A. Leardini, "Repeatability of a multi-segment foot protocol in adult subjects," *Gait & Posture,* vol. 33, no. 1, pp. 133-135, 2011/01/01/ 2011.

[153] K. Deschamps *et al.*, "Body of evidence supporting the clinical use of 3D multisegment foot models: a systematic review," vol. 33, no. 3, pp. 338-349, 2011.

[154] S. van Hoeve, M. J. T. J. o. F. Poeze, and A. Surgery, "Multisegment Foot Models and Clinical Application After Foot and Ankle Trauma: A Review," vol. 58, no. 4, pp. 748-754, 2019.

[155] R. Mahaffey, S. C. Morrison, W. I. Drechsler, M. C. J. J. o. f. Cramp, and a. research, "Evaluation of multi-segmental kinematic modelling in the paediatric foot using three concurrent foot models," vol. 6, no. 1, p. 43, 2013.

[156] W. Pirker and R. J. W. K. W. Katzenschlager, "Gait disorders in adults and the elderly," vol. 129, no. 3-4, pp. 81-95, 2017.

[157] N. Shibuya, D. C. Jupiter, L. J. Ciliberti, V. VanBuren, J. J. T. J. o. f. La Fontaine, and a. surgery, "Characteristics of adult flatfoot in the United States," vol. 49, no. 4, pp. 363-368, 2010.

[158] K. Han, K. Bae, N. Levine, J. Yang, J.-S. J. M. s. m. i. m. j. o. e. Lee, and c. research, "Biomechanical Effect of Foot Orthoses on Rearfoot Motions and Joint Moment Parameters in Patients with Flexible Flatfoot," vol. 25, p. 5920, 2019.

[159] P. Levinger *et al.*, "A comparison of foot kinematics in people with normal-and flat-arched feet using the Oxford Foot Model," vol. 32, no. 4, pp. 519-523, 2010.

[160] S. A. Dugan, K. P. J. P. M. Bhat, and R. Clinics, "Biomechanics and analysis of running gait," vol. 16, no. 3, pp. 603-621, 2005.

[161] J. N. Zhai, J. Wang, and Y. S. J. J. o. P. T. S. Qiu, "Plantar pressure differences among adults with mild flexible flatfoot, severe flexible flatfoot and normal foot when walking on level surface, walking upstairs and downstairs," vol. 29, no. 4, pp. 641-646, 2017.

[162] I. Van den Herrewegen *et al.*, "Dynamic 3D scanning as a markerless method to calculate multi-segment foot kinematics during stance phase: Methodology and first application," *Journal of Biomechanics,* vol. 47, no. 11, pp. 2531-2539, 2014/08/22/ 2014.

[163] S. M. Mosier, G. Pomeroy, A. J. C. o. Manoli 2nd, and r. research, "Pathoanatomy and etiology of posterior tibial tendon dysfunction," no. 365, pp. 12-22, 1999.

[164] A. E. Hunt and R. M. J. C. b. Smith, "Mechanics and control of the flat versus normal foot during the stance phase of walking," vol. 19, no. 4, pp. 391-397, 2004.

[165] M. Hösl, H. Böhm, C. Multerer, L. J. G. Döderlein, and posture, "Does excessive flatfoot deformity affect function? A comparison between symptomatic and asymptomatic flatfeet using the Oxford Foot Model," vol. 39, no. 1, pp. 23-28, 2014.

[166] C. B. Hirose, J. E. J. F. Johnson, and a. international, "Plantarflexion opening wedge medial cuneiform osteotomy for correction of fixed forefoot varus associated with flatfoot deformity," vol. 25, no. 8, pp. 568-574, 2004.

[167] R. S. Silva, A. L. G. Ferreira, L. M. Veronese, and F. V. J. J. o. t. A. P. M. A. Serrão, "Forefoot varus predicts subtalar hyperpronation in young people," vol. 104, no. 6, pp. 594-600, 2014.

[168] H. A. Banwell, D. Thewlis, and S. J. T. F. Mackintosh, "Adults with flexible pes planus and the approach to the prescription of customised foot orthoses in clinical practice: a clinical records audit," vol. 25, no. 2, pp. 101-109, 2015.

[169] J. B. Arnold, T. May, and C. J. C. J. o. S. M. Bishop, "Predictors of the Biomechanical Effects of Customized Foot Orthoses in Adults With Flat-Arched Feet," vol. 28, no. 4, pp. 398-400, 2018.

[170] R. Donatelli, C. Hurlbert, D. Conaway, R. J. J. o. O. St. Pierre, and S. P. Therapy, "Biomechanical foot orthotics: a retrospective study," vol. 10, no. 6, pp. 205-212, 1988.

[171] M. L. J. C. b. Root, "Normal and abnormal function of the foot," vol. 2, 1977.

[172] M. H. J. P. M. Yamashita and R. Clinics, "Evaluation and selection of shoe wear and orthoses for the runner," vol. 16, no. 3, pp. 801-829, 2005.

[173] S. Telfer, M. Abbott, M. P. M. Steultjens, and J. Woodburn, "Dose-response effects of customised foot orthoses on lower limb kinematics and kinetics in pronated foot type," *Journal of Biomechanics,* vol. 46, no. 9, pp. 1489-1495, 31 May 2013.

[174] M. N. Orlin and T. G. J. P. t. McPoil, "Plantar pressure assessment," vol. 80, no. 4, pp. 399-409, 2000.

[175] S. S. Zulkifli and W. P. Loh, "A state-of-the-art review of foot pressure," *Foot and Ankle Surgery,* vol. 26, no. 1, pp. 25-32, 2020/01/01/ 2020.

[176] P. Caravaggi, A. Leardini, and C. J. J. o. b. Giacomozzi, "Multiple linear regression approach for the analysis of the relationships between joints mobility and regional pressure-based parameters in the normal-arched foot," vol. 49, no. 14, pp. 3485-3491, 2016.

[177] P. Dixon, M. Bowtell, J. J. G. Stebbins, and posture, "The use of regression and normalisation for the comparison of spatio-temporal gait data in children," vol. 40, no. 4, pp. 521-525, 2014.

[178] C. Giacomozzi, A. Leardini, and P. J. J. o. b. Caravaggi, "Correlates between kinematics and baropodometric measurements for an integrated in-vivo assessment of the segmental foot function in gait," vol. 47, no. 11, pp. 2654-2659, 2014.

[179] R. T. Lewinson *et al.*, "Foot structure and knee joint kinetics during walking with and without wedged footwear insoles," *Journal of Biomechanics,* vol. 73, pp. 192-200, 2018/05/17/ 2018.

[180] Q. Mei *et al.*, "Foot shape and plantar pressure relationships in shod and barefoot populations," pp. 1-14, 2019.

[181] S. Xiong, R. S. Goonetilleke, W. A. S. Rodrigo, and J. J. A. e. Zhao, "A model for the perception of surface pressure on human foot," vol. 44, no. 1, pp. 1-10, 2013.

[182] A. H. Abdul Razak, A. Zayegh, R. K. Begg, and Y. J. S. Wahab, "Foot plantar pressure measurement system: A review," vol. 12, no. 7, pp. 9884-9912, 2012.

[183] W. R. Ledoux *et al.*, "Diabetic foot ulcer incidence in relation to plantar pressure magnitude and measurement location," vol. 27, no. 6, pp. 621-626, 2013.

[184] C. Price, D. Parker, C. J. G. Nester, and posture, "Validity and repeatability of three in-shoe pressure measurement systems," vol. 46, pp. 69-74, 2016.

[185] M. Koch, L.-K. Lunde, M. Ernst, S. Knardahl, and K. B. Veiersted, "Validity and reliability of pressure-measurement insoles for vertical ground reaction force assessment in field situations," *Applied Ergonomics,* vol. 53, pp. 44-51, 2016/03/01/ 2016.

[186] *Medilogic WLAN insole*. Available: https://medilogic.com/en/medilogic-wlan-insole/

[187] J. DeBerardinis, J. S. Dufek, M. B. Trabia, D. E. J. J. o. r. Lidstone, and a. t. engineering, "Assessing the validity of pressure-measuring insoles in quantifying gait variables," vol. 5, p. 2055668317752088, 2018.

[188] S. J. Ellis, H. Stoecklein, C. Y. Joseph, G. Syrkin, H. Hillstrom, and J. T. J. H. j. Deland, "The accuracy of an automasking algorithm in plantar pressure measurements," vol. 7, no. 1, pp. 57-63, 2011.

[189] C. Giacomozzi, P. Caravaggi, J. A. Stebbins, and A. Leardini, "Integration of Foot Pressure and Foot Kinematics Measurements for Medical Applications," in *Handbook of Human Motion*, B. Müller *et al.*, Eds. Cham: Springer International Publishing, 2016, pp. 1-22.

[190] A. M. Galica *et al.*, "Hallux valgus and plantar pressure loading: the Framingham foot study," vol. 6, no. 1, p. 42, 2013.

[191] C. Xu *et al.*, "Normal foot loading parameters and repeatability of the Footscan® platform system," vol. 10, no. 1, p. 30, 2017.

[192] J. Pauk, K. Daunoraviciene, M. Ihnatouski, J. Griskevicius, and J. V. J. A. B. B. Raso, "Analysis of the plantar pressure distribution in children with foot deformities," vol. 12, no. 1, pp. 29-34, 2010.

[193] J. Stebbins *et al.*, "Assessment of sub-division of plantar pressure measurement in children," vol. 22, no. 4, pp. 372-376, 2005.

[194] J. Stebbins, M. Harrington, C. Giacomozzi, N. Thompson, and T. Theologis, "Measurement of Foot Kinematics and Plantar Pressure in Children Using the Oxford Foot Model," ed: Bethesday, MD: Proceedings of Pediactric and Adult Foot and Ankle: New …, 2003.

[195] Z. Sawacha *et al.*, "Integrated kinematics–kinetics–plantar pressure data analysis: A useful tool for characterizing diabetic foot biomechanics," vol. 36, no. 1, pp. 20-26, 2012.

[196] C. Giacomozzi, M. G. Benedetti, A. Leardini, V. Macellari, and S. J. J. o. t. A. P. M. A. Giannini, "Gait analysis with an integrated system for functional assessment of talocalcaneal coalition," vol. 96, no. 2, pp. 107-115, 2006.

[197] J. Stebbins, C. Giacomozzi, T. J. J. o. F. Theologis, and A. Research, "Correlation between plantar pressure and Oxford Foot Model kinematics," vol. 1, no. 1, pp. 1-2, 2008.

[198] J. K. Gurney, U. G. Kersting, D. J. G. Rosenbaum, and posture, "Between-day reliability of repeated plantar pressure distribution measurements in a normal population," vol. 27, no. 4, pp. 706-709, 2008.

[199] B. Chuckpaiwong, J. A. Nunley, N. A. Mall, R. M. J. G. Queen, and posture, "The effect of foot type on in-shoe plantar pressure during walking and running," vol. 28, no. 3, pp. 405-411, 2008.

[200] R. Xu *et al.*, "Comparative Study of the Effects of Customized 3D printed insole and Prefabricated Insole on Plantar Pressure and Comfort in Patients with Symptomatic Flatfoot," (in eng), *Med Sci Monit,* vol. 25, pp. 3510-3519, May 12 2019.

[201] A. C. Redmond, K. B. Landorf, A.-M. J. J. o. F. Keenan, and A. Research, "Contoured, prefabricated foot orthoses demonstrate comparable mechanical properties to contoured, customised foot orthoses: a plantar pressure study," vol. 2, no. 1, p. 20, 2009.

[202] H. L. Jarvis, C. J. Nester, P. D. Bowden, R. K. J. J. o. f. Jones, and a. research, "Challenging the foundations of the clinical model of foot function: further evidence that the root model assessments fail to appropriately classify foot function," vol. 10, no. 1, p. 7, 2017.

[203] M. J. J. o. t. A. P. A. Root, "Biomechanical examination of the foot," vol. 63, no. 1, p. 28, 1973.

[204] A. K. Buldt, S. Forghany, K. B. Landorf, P. Levinger, G. S. Murley, and H. B. Menz, "Foot posture is associated with plantar pressure during gait: A comparison of normal, planus and cavus feet," (in eng), *Gait Posture,* vol. 62, pp. 235-240, May 2018.

[205] C. J. Nester, H. L. Jarvis, R. K. Jones, P. D. Bowden, A. J. J. o. f. Liu, and a. research, "Movement of the human foot in 100 pain free individuals aged 18–45: implications for understanding normal foot function," vol. 7, no. 1, p. 51, 2014.

[206] A. Mündermann, B. M. Nigg, R. N. Humble, D. J. J. M. Stefanyshyn, S. i. Sports, and Exercise, "Orthotic comfort is related to kinematics, kinetics, and EMG in recreational runners," vol. 35, no. 10, pp. 1710-1719, 2003.

[207] S. Telfer, M. Abbott, M. Steultjens, D. Rafferty, J. J. G. Woodburn, and posture, "Dose–response effects of customised foot orthoses on lower limb muscle activity and plantar pressures in pronated foot type," vol. 38, no. 3, pp. 443-449, 2013.

[208] S. Su, Z. Mo, J. Guo, and Y. J. J. o. h. e. Fan, "The Effect of Arch Height and Material Hardness of Personalized Insole on Correction and Tissues of Flatfoot," vol. 2017, 2017.

[209] G. F. Kogler, S. E. Solomonidis, and J. P. Paul, "Biomechanics of longitudinal arch support mechanisms in foot orthoses and their effect on plantar aponeurosis strain," *Clinical Biomechanics,* vol. 11, no. 5, pp. 243-252, 1996.

[210] C. J. Nester, M. L. Van Der Linden, and P. Bowker, "Effect of foot orthoses on the kinematics and kinetics of normal walking gait," *Gait and Posture,* vol. 17, no. 2, pp. 180-187, April 2003.

[211] J. F. Hornestam, T. R. Souza, P. Arantes, J. Ocarino, and P. L. Silva, "The effect of walking speed on foot kinematics is modified when increased pronation is induced," *Journal of the American Podiatric Medical Association,* Article vol. 106, no. 6, pp. 419-426, 2016.

[212] H. Akuzawa, A. Imai, S. Iizuka, N. Matsunaga, and K. Kaneoka, "Calf muscle activity alteration with foot orthoses insertion during walking measured by fine-wire electromyography," *Journal of Physical Therapy Science,* Article vol. 28, no. 12, pp. 3458-3462, 2016.

[213] K. Tokunaga *et al.*, "Effect of foot progression angle and lateral wedge insole on a reduction in knee adduction moment," *Journal of Applied Biomechanics,* vol. 32, no. 5, pp. 454-461, October 2016.

[214] C. Riegger-Krugh and J. J. Keysor, "Skeletal malalignments of the lower quarter: correlated and compensatory motions and postures," *Journal of Orthopaedic & Sports Physical Therapy,* vol. 23, no. 2, pp. 164-170, 1996.

[215] T. R. Souza *et al.*, "Clinical measures of hip and foot–ankle mechanics as predictors of rearfoot motion and posture," *Manual therapy,* vol. 19, no. 5, pp. 379-385, 2014.

[216] W. Kakihana, S. Torii, M. Akai, K. Nakazawa, M. Fukano, and K. Naito, "Effect of a lateral wedge on joint moments during gait in subjects with recurrent ankle sprain," *American Journal of Physical Medicine and Rehabilitation,* vol. 84, no. 11, pp. 858-864, November 2005.

[217] G. Wahmkow, M. Cassel, F. Mayer, and H. Baur, "Effects of different medial arch support heights on rearfoot kinematics," *PLoS ONE,* vol. 12 (3) (no pagination), no. e0172334, 01 Mar 2017.

[218] W. H. Hsu, C. L. Lewis, G. M. Monaghan, E. Saltzman, J. Hamill, and K. G. Holt, "Orthoses posted in both the forefoot and rearfoot reduce moments and angular impulses on lower extremity joints during walking," *Journal of Biomechanics,* vol. 47, no. 11, pp. 2618-2625, 22 Aug 2014.

[219] K. D. Gross *et al.*, "Varus foot alignment and hip conditions in older adults," *Arthritis & Rheumatology,* vol. 56, no. 9, pp. 2993-2998, 2007.

[220] R. Chang, P. A. Rodrigues, R. E. Van Emmerik, and J. Hamill, "Multi-segment foot kinematics and ground reaction forces during gait of individuals with plantar fasciitis," *Journal of biomechanics,* vol. 47, no. 11, pp. 2571-2577, 2014.

[221] C. A. Fukuchi, R. T. Lewinson, J. T. Worobets, and D. J. Stefanyshyn, "Effects of lateral and medial wedged insoles on knee and ankle internal joint moments during walking in healthy men," *Journal of the American Podiatric Medical Association,* Article vol. 106, no. 6, pp. 411-418, 2016.

[222] K. Nakajima *et al.*, "Addition of an arch support improves the biomechanical effect of a laterally wedged insole," *Gait and Posture,* Article vol. 29, no. 2, pp. 208-213, 2009.

[223] A. G. Fischer, B. Ulrich, L. Hoffmann, B. M. Jolles, and J. Favre, "Effect of lateral wedge length on ambulatory knee kinetics Arielle," *Gait & Posture,* vol. 63, pp. 114-118, Jun 2018.

[224] W. H. Hong, Y. H. Lee, H. C. Chen, Y. C. Pei, and C. Y. Wu, "Influence of heel height and shoe insert on comfort perception and biomechanical performance of young female adults during walking," *Foot and Ankle International,* vol. 26, no. 12, pp. 1042-1048, December 2005.

[225] M. W. Creaby, K. May, and K. L. Bennell, "Insole effects on impact loading during walking," *Ergonomics,* vol. 54, no. 7, pp. 665-671, Jul 2011.

[226] L. Yung-Hui and H. Wei-Hsien, "Effects of shoe inserts and heel height on foot pressure, impact force, and perceived comfort during walking," *Applied Ergonomics,* vol. 36, no. 3, pp. 355-362, May 2005.

[227] K. Holt and J. Hamill, "Running injuries and treatment: a dynamic approach," *Rehabilitation of the Foot and Ankle,* vol. 1, p. 241, 1995.

[228] J. P. Huerta, J. M. R. Moreno, K. A. Kirby, F. J. G. Carmona, and A. M. O. Garcia, "Effect of 7-degree rearfoot varus and valgus wedging on rearfoot kinematics and kinetics during the stance phase of walking," *Journal of the American Podiatric Medical Association,* vol. 99, no. 5, pp. 415-421, September-October 2009.

[229] R. K. Jones, M. Zhang, P. Laxton, A. H. Findlow, and A. Liu, "The biomechanical effects of a new design of lateral wedge insole on the knee and ankle during walking," *Human Movement Science,* vol. 32, no. 4, pp. 596-604, August 2013.

[230] C. M. Molgaard, T. Graven-Nielsen, O. Simonsen, and U. G. Kersting, "Potential interaction of experimental knee pain and laterally wedged insoles for knee off-loading during walking," *Clinical Biomechanics,* vol. 29, no. 8, pp. 848-854, 2014.

[231] R. A. Tipnis, P. A. Anloague, L. L. Laubach, and J. A. Barrios, "The dose-response relationship between lateral foot wedging and the reduction of knee adduction moment," *Clinical Biomechanics,* vol. 29, no. 9, pp. 984-989, 01 Nov 2014.

[232] J. T. Weinhandl, S. E. Sudheimer, B. L. Van Lunen, K. Stewart, and M. C. Hoch, "Immediate and 1 week effects of laterally wedge insoles on gait biomechanics in healthy females," *Gait and Posture,* vol. 45, pp. 164-169, March 01 2016.

[233] E. M. Russell and J. Hamill, "Lateral wedges decrease biomechanical risk factors for knee osteoarthritis in obese women," *Journal of Biomechanics,* vol. 44, no. 12, pp. 2286-2291, 11 August 2011.

[234] H. A. Banwell, S. Mackintosh, and D. Thewlis, "Foot orthoses for adults with flexible pes planus: a systematic review," *Journal of foot and ankle research,* vol. 7, no. 1, p. 23, 2014.

[235] K. Mills, P. Blanch, A. R. Chapman, T. G. McPoil, and B. Vicenzino, "Foot orthoses and gait: a systematic review and meta-analysis of literature pertaining to potential mechanisms," *British journal of sports medicine,* p. bjsports66977, 2010.

[236] S. H. Downs and N. Black, "The feasibility of creating a checklist for the assessment of the methodological quality both of randomised and non-randomised studies of health care

interventions," *Journal of Epidemiology & Community Health,* vol. 52, no. 6, pp. 377-384, 1998.

[237] M. Fernando *et al.*, "Biomechanical characteristics of peripheral diabetic neuropathy: a systematic review and meta-analysis of findings from the gait cycle, muscle activity and dynamic barefoot plantar pressure," *Clinical biomechanics,* vol. 28, no. 8, pp. 831-845, 2013.

[238] M. Hajizadeh, A. H. Oskouei, F. Ghalichi, and G. Sole, "Knee kinematics and joint moments during stair negotiation in participants with anterior cruciate ligament deficiency and reconstruction: a systematic review and meta-analysis," *PM&R,* vol. 8, no. 6, pp. 563-579. e1, 2016.

[239] R. L. Brennan and D. J. Prediger, "Coefficient kappa: Some uses, misuses, and alternatives," *Educational and psychological measurement,* vol. 41, no. 3, pp. 687-699, 1981.

[240] J. R. Landis and G. G. Koch, "The measurement of observer agreement for categorical data," *biometrics,* pp. 159-174, 1977.

[241] D. J. Geerse, B. H. Coolen, and M. Roerdink, "Walking-adaptability assessments with the Interactive Walkway: Between-systems agreement and sensitivity to task and subject variations," *Gait & Posture,* vol. 54, no. Supplement C, pp. 194-201, 2017/05/01/ 2017.

[242] C. E. Milner and R. A. Brindle, "Reliability and minimal detectable difference in multisegment foot kinematics during shod walking and running," *Gait & Posture,* vol. 43, no. Supplement C, pp. 192-197, 2016/01/01/ 2016.

[243] M. Almarwani, S. Perera, J. M. VanSwearingen, P. J. Sparto, and J. S. Brach, "The test–retest reliability and minimal detectable change of spatial and temporal gait variability during usual over-ground walking for younger and older adults," *Gait & Posture,* vol. 44, no. Supplement C, pp. 94-99, 2016/02/01/ 2016.

[244] F. Riva, M. C. Bisi, and R. Stagni, "Gait variability and stability measures: Minimum number of strides and within-session reliability," *Computers in Biology and Medicine,* vol. 50, no. Supplement C, pp. 9-13, 2014/07/01/ 2014.

[245] T. Monnet, M. Begon, C. Vallée, and P. Lacouture, "Improvement of the input data in biomechanics: kinematic and body segment inertial parameters," *Biomech Princ Trends Appl,* 2010.

[246] D. Laroche *et al.*, "Test–retest reliability of 3D kinematic gait variables in hip osteoarthritis patients," *Osteoarthritis and cartilage,* vol. 19, no. 2, pp. 194-199, 2011.

[247] Y. Xu *et al.*, "Full Step Cycle Kinematic and Kinetic Comparison of Barefoot Walking and a Traditional Shoe Walking in Healthy Youth: Insights for Barefoot Technology," *Applied bionics and biomechanics,* vol. 2017, 2017.

[248] X. Zhang, M. R. Paquette, and S. Zhang, "A comparison of gait biomechanics of flip-flops, sandals, barefoot and shoes," *Journal of Foot and Ankle Research,* journal article vol. 6, no. 1, p. 45, November 06 2013.

[249] R. Shultz, T. B. Birmingham, and T. R. Jenkyn, "Differences in neutral foot positions when measured barefoot compared to in shoes with varying stiffnesses," *Medical Engineering & Physics,* vol. 33, no. 10, pp. 1309-1313, 2011/12/01/ 2011.

[250] C. Pothrat, G. Authier, E. Viehweger, E. Berton, and G. Rao, "One- and multi-segment foot models lead to opposite results on ankle joint kinematics during gait: Implications for clinical assessment," *Clinical Biomechanics,* vol. 30, no. 5, pp. 493-499, 2015/06/01/ 2015.

[251] S. Forghany, R. Jones, S. Preece, C. Nester, and S. Tyson, "Early observations of the effects of lateral wedge orthoses on lower limb muscle length and potential for exacerbating spasticity," *Prosthetics and Orthotics International,* vol. 34, no. 3, pp. 319-326, September 2010.

[252] F. Kluge, S. Krinner, M. Lochmann, and B. M. Eskofier, "Speed dependent effects of laterally wedged insoles on gait biomechanics in healthy subjects," *Gait and Posture,* vol. 55, pp. 145-149, 01 Jun 2017.

[253] T. Sawada *et al.*, "Foot alignments influence the effect of knee adduction moment with lateral wedge insoles during gait," *Gait and Posture,* vol. 49, pp. 451-456, 01 Sep 2016.

[254] S. Yamaguchi, M. Kitamura, T. Ushikubo, A. Murata, R. Akagi, and T. Sasho, "Effect of laterally wedged insoles on the external knee adduction moment across different reference frames," *PLoS ONE,* vol. 10 (9) (no pagination), no. e0138554, 23 Sep 2015.

[255] R. W. Bohannon and A. W. Andrews, "Normal walking speed: a descriptive meta-analysis," *Physiotherapy,* vol. 97, no. 3, pp. 182-189, 2011.

[256] K. M. Leitch, T. B. Birmingham, I. C. Jones, J. R. Giffin, and T. R. Jenkyn, "In-shoe plantar pressure measurements for patients with knee osteoarthritis: Reliability and effects of lateral heel wedges," *Gait and Posture,* vol. 34, no. 3, pp. 391-396, July 2011.

[257] J. Burston, J. Richards, and J. Selfe, "The effects of three quarter and full length foot orthoses on knee mechanics in healthy subjects and patellofemoral pain patients when walking and descending stairs," *Gait and Posture,* Article vol. 62, pp. 518-522, 2018.

[258] J. J. McGough and S. V. Faraone, "Estimating the size of treatment effects: moving beyond p values," *Psychiatry (Edgmont),* vol. 6, no. 10, p. 21, 2009.

[259] J. P. Higgins, S. G. Thompson, J. J. Deeks, and D. G. Altman, "Measuring inconsistency in meta-analyses," *BMJ: British Medical Journal,* vol. 327, no. 7414, p. 557, 2003.

[260] J. W. Kang, H. S. Park, C. K. Na, J. W. Park, J. Hong, and S. H. Lee, "Immediate coronal plane kinetic effects of novel lateral-offset sole shoes and lateral-wedge insole shoes in healthy individuals," *Orthopedics,* vol. 36, no. 2, pp. e165-e171, February 2013.

[261] M. Carson, M. Harrington, N. Thompson, J. O'connor, and T. Theologis, "Kinematic analysis of a multi-segment foot model for research and clinical applications: a repeatability analysis," *Journal of biomechanics,* vol. 34, no. 10, pp. 1299-1307, 2001.

[262] M. P. Kadaba, H. Ramakrishnan, and M. Wootten, "Measurement of lower extremity kinematics during level walking," *Journal of orthopaedic research,* vol. 8, no. 3, pp. 383-392, 1990.

[263] C. J. Nester, S. Hutchins, and P. Bowker, "Effect of foot orthoses on rearfoot complex kinematics during walking gait," *Foot and Ankle International,* Article vol. 22, no. 2, pp. 133-139, 2001.

[264] M. Razeghi and M. E. Batt, "Biomechanical analysis of the effect of orthotic shoe inserts," *Sports Medicine,* vol. 29, no. 6, pp. 425-438, 2000.

[265] J. Nilsson and A. Thorstensson, "Ground reaction forces at different speeds of human walking and running," *Acta Physiologica,* vol. 136, no. 2, pp. 217-227, 1989.

[266] M. B. Ryan, G. A. Valiant, K. McDonald, and J. E. Taunton, "The effect of three different levels of footwear stability on pain outcomes in women runners: a randomised control trial," *British journal of sports medicine,* p. bjsports69849, 2010.

[267] J. J. Eng and M. R. Pierrynowski, "The effect of soft foot orthotics on three-dimensional lower-limb kinematics during walking and running," *Physical Therapy,* vol. 74, no. 9, pp. 836-844, 1994.

[268] P. T. Rodrigues, A. F. Ferreira, R. M. Pereira, E. Bonfa, E. F. Borba, and R. Fuller, "Effectiveness of medial-wedge insole treatment for valgus knee osteoarthritis," *Arthritis Care & Research,* vol. 59, no. 5, pp. 603-608, 2008.

[269] C. L. MacLean, R. van Emmerik, and J. Hamill, "Influence of custom foot orthotic intervention on lower extremity intralimb coupling during a 30-minute run," *Journal of Applied Biomechanics,* Clinical Trial

Research Support, Non-U.S. Gov't vol. 26, no. 4, pp. 390-9, 2010.

[270] H. Bateni, "Changes of postural steadiness following use of prefabricated orthotic insoles," *Journal of Applied Biomechanics,* Article vol. 29, no. 2, pp. 174-179, 2013.

[271] J. R. Franz, J. Dicharry, P. O. Riley, K. Jackson, R. P. Wilder, and D. C. Kerrigan, "The Influence of arch supports on knee torques relevant to knee osteoarthritis," *Medicine and Science in Sports and Exercise,* Article vol. 40, no. 5, pp. 913-917, 2008.

[272] O. N. Martins, A. Schinkel-Ivy, B. D. Cotter, and J. D. M. Drake, "Changes in spatio-temporal gait parameters following immediate and sustained use of insoles with a progressive system of increasing arch support," *Footwear Science,* Article vol. 8, no. 3, pp. 147-154, 2016.

[273] D. Mulford, H. M. Taggart, A. Nivens, and C. Payrie, "Arch support use for improving balance and reducing pain in older adults," *Applied Nursing Research,* vol. 21, no. 3, pp. 153-158, 2008.

[274] B. Najafi, D. Miller, B. D. Jarrett, and J. S. Wrobel, "Does footwear type impact the number of steps required to reach gait steady state?: An innovative look at the impact of foot orthoses on gait initiation," *Gait and Posture,* Article vol. 32, no. 1, pp. 29-33, 2010.

[275] S. J. Dixon, "Influence of a commercially available orthotic device on rearfoot eversion and vertical ground reaction force when running in military footwear," *Military medicine,* vol. 172, no. 4, p. 446, 2007.

[276] D. C. Low and S. J. Dixon, "The influence of shock-pad density and footwear cushioning on heel impact and forefoot loading during running and turning movements," *International Journal of Surface Science and Engineering,* Conference Paper vol. 10, no. 1, pp. 86-99, 2016.

[277] E. Alcántara, A. Forner, E. Ferrús, A.-C. García, and J. Ramiro, "Influence of age, gender, and obesity on the mechanical properties of the heel pad under walking impact conditions," *Journal of Applied Biomechanics,* vol. 18, no. 4, pp. 345-356, 2002.

[278] H. Kinoshita, P. R. Francis, T. Murase, S. Kawai, and T. Ogawa, "The mechanical properties of the heel pad in elderly adults," *European journal of applied physiology and occupational physiology,* vol. 73, no. 5, pp. 404-409, 1996.

[279] J. M. Genova and M. T. Gross, "Effect of foot orthotics on calcaneal eversion during standing and treadmill walking for subjects with abnormal pronation," *Journal of Orthopaedic & Sports Physical Therapy,* vol. 30, no. 11, pp. 664-675, 2000.

[280] K. Myers, J. Long, J. Klein, J. Wertsch, D. Janisse, and G. Harris, "Biomechanical implications of the negative heel rocker sole shoe: gait kinematics and kinetics," *Gait & posture,* vol. 24, no. 3, pp. 323-330, 2006.

[281] C. Neville and J. Houck, "Choosing among 3 ankle-foot orthoses for a patient with stage II posterior tibial tendon dysfunction," *journal of orthopaedic & sports physical therapy,* vol. 39, no. 11, pp. 816-824, 2009.

[282] M. Hall, C. A. Stevermer, and J. C. Gillette, "Gait analysis post anterior cruciate ligament reconstruction: knee osteoarthritis perspective," *Gait & posture,* vol. 36, no. 1, pp. 56-60, 2012.

[283] M. Kaur, D. C. Ribeiro, J.-C. Theis, K. E. Webster, and G. Sole, "Movement patterns of the knee during gait following ACL reconstruction: a systematic review and meta-analysis," *Sports Medicine,* vol. 46, no. 12, pp. 1869-1895, 2016.

[284] Y. Toda, N. Segal, A. Kato, S. Yamamoto, and M. Irie, "Effect of a novel insole on the subtalar joint of patients with medial compartment osteoarthritis of the knee," *The Journal of rheumatology,* vol. 28, no. 12, pp. 2705-2710, 2001.

[285] G. S. Keenan, J. R. Franz, J. Dicharry, U. Della Croce, and D. C. Kerrigan, "Lower limb joint kinetics in walking: the role of industry recommended footwear," *Gait & posture,* vol. 33, no. 3, pp. 350-355, 2011.

[286] A. Leardini, M. Benedetti, L. Berti, D. Bettinelli, R. Nativo, and S. Giannini, "Rear-foot, mid-foot and fore-foot motion during the stance phase of gait," *Gait & posture,* vol. 25, no. 3, pp. 453-462, 2007.

[287] A. Liu *et al.*, "Effect of an antipronation foot orthosis on ankle and subtalar kinematics," *Medicine and Science in Sports and Exercise,* Article vol. 44, no. 12, pp. 2384-2391, 2012.

[288] N. L. W. Keijsers, N. M. Stolwijk, J. W. K. Louwerens, and J. Duysens, "Classification of forefoot pain based on plantar pressure measurements," *Clinical Biomechanics,* vol. 28, no. 3, pp. 350-356, 2013/03/01/ 2013.

[289] Q. Wang, Y. Huang, J. Zhu, L. Wang, and D. Lv, "Effects of foot shape on energetic efficiency and dynamic stability of passive dynamic biped with upper body," *International Journal of Humanoid Robotics,* vol. 7, no. 02, pp. 295-313, 2010.

[290] N. Farahpour, A. Jafarnezhad, M. Damavandi, A. Bakhtiari, and P. J. J. o. b. Allard, "Gait ground reaction force characteristics of low back pain patients with pronated foot and able-bodied individuals with and without foot pronation," vol. 49, no. 9, pp. 1705-1710, 2016.

[291] S. T. J. D. s. T. c. s. f. Hansen and ankle, "Adult consequences of pediatric foot disorders," vol. 2, pp. 526-530, 2010.

[292] M. Vlutters, E. Van Asseldonk, and H. J. J. o. b. Van Der Kooij, "Reduced center of pressure modulation elicits foot placement adjustments, but no additional trunk motion during anteroposterior-perturbed walking," vol. 68, pp. 93-98, 2018.

[293] K. Mills, P. Blanch, A. R. Chapman, T. G. McPoil, and B. Vicenzino, "Foot orthoses and gait: a systematic review and meta-analysis of literature pertaining to potential mechanisms," *British journal of sports medicine,* vol. 44, no. 14, pp. 1035-1046, Nov 2010.

[294] X. Zhang and B. Li, "Influence of in-shoe heel lifts on plantar pressure and center of pressure in the medial-lateral direction during walking," *Gait and Posture,* vol. 39, no. 4, pp. 1012-1016, April 2014.

[295] C. A. Fukuchi, R. T. Lewinson, J. T. Worobets, and D. J. J. J. o. t. A. P. M. A. Stefanyshyn, "Effects of Lateral and Medial Wedged Insoles on Knee and Ankle Internal Joint Moments During Walking in Healthy Men," vol. 106, no. 6, pp. 411-418, 2016.

[296] M. Blazkiewicz and A. Wit, "Artificial neural network simulation of lower limb joint angles in normal and impaired human gait," (in eng), *Acta Bioeng Biomech,* vol. 20, no. 4, pp. 43-49, 2018.

[297] M. Khashei and M. J. E. S. w. a. Bijari, "An artificial neural network (p, d, q) model for timeseries forecasting," vol. 37, no. 1, pp. 479-489, 2010.

[298] P. Osateerakun, G. Barton, R. Foster, S. Bennett, and R. Lakshminarayan, "P 037 – Prediction of moments from movements without force platforms using artificial neural networks: A pilot test," *Gait & Posture,* vol. 65, pp. 299-300, 2018/09/01/ 2018.

[299] S.-B. Joo, S. E. Oh, and J. H. Mun, "Improving the ground reaction force prediction accuracy using one-axis plantar pressure: Expansion of input variable for neural network," *Journal of Biomechanics,* vol. 49, no. 14, pp. 3153-3161, 2016/10/03/ 2016.

[300] M. Abadi *et al.*, "Tensorflow: A system for large-scale machine learning," in *12th {USENIX} symposium on operating systems design and implementation ({OSDI} 16)*, 2016, pp. 265-283.

[301] R. G. Pearson, C. J. Raxworthy, M. Nakamura, and A. J. J. o. b. Townsend Peterson, "Predicting species distributions from small numbers of occurrence records: a test case using cryptic geckos in Madagascar," vol. 34, no. 1, pp. 102-117, 2007.

[302] D. R. Stockwell and A. T. J. E. m. Peterson, "Effects of sample size on accuracy of species distribution models," vol. 148, no. 1, pp. 1-13, 2002.

[303] T. Monnet, A. Thouzé, M. T. Pain, M. J. M. e. Begon, and physics, "Assessment of reproducibility of thigh marker ranking during walking and landing tasks," vol. 34, no. 8, pp. 1200-1208, 2012.

[304] M. Müller, B. Heidelberger, M. Teschner, and M. Gross, "Meshless deformations based on shape matching," in *ACM transactions on graphics (TOG)*, 2005, vol. 24, no. 3, pp. 471-478: ACM.

[305] K.-R. Mun, S. Chun, J. Hong, and J. J. H. f. Kim, "The Relationship Between Foot Feature Parameters and Postural Stability in Healthy Subjects," p. 0018720819828545, 2019.

[306] H. White, *Artificial neural networks: approximation and learning theory*. Blackwell Publishers, Inc., 1992.

[307] L. Li *et al.*, "3D printing individualized heel cup for improving the self-reported pain of plantar fasciitis," vol. 16, no. 1, p. 167, 2018.

[308] S. Perhamre, F. Lundin, M. Klässbo, R. J. S. j. o. m. Norlin, and s. i. sports, "A heel cup improves the function of the heel pad in sever's injury: effects on heel pad thickness, peak pressure and pain," vol. 22, no. 4, pp. 516-522, 2012.

[309] C.-L. Wang, C.-K. Cheng, Y.-H. Tsuang, Y.-S. Hang, and T.-K. J. C. B. Liu, "Cushioning effect of heel cups," vol. 9, no. 5, pp. 297-302, 1994.

[310] J. T.-M. Cheung, M. Zhang, and K.-N. J. C. B. An, "Effect of Achilles tendon loading on plantar fascia tension in the standing foot," vol. 21, no. 2, pp. 194-203, 2006.

[311] R. Ker, M. Bennett, S. Bibby, R. Kester, and R. M. J. N. Alexander, "The spring in the arch of the human foot," vol. 325, no. 6100, p. 147, 1987.

[312] L. A. Kelly, G. A. Lichtwark, D. J. Farris, and A. J. J. o. T. R. S. I. Cresswell, "Shoes alter the spring-like function of the human foot during running," vol. 13, no. 119, p. 20160174, 2016.

[313] S. Dars, H. Uden, H. A. Banwell, and S. J. P. o. Kumar, "The effectiveness of non-surgical intervention (Foot Orthoses) for paediatric flexible pes planus: A systematic review: Update," vol. 13, no. 2, p. e0193060, 2018.

[314] K. D. Gross *et al.*, "Association of flat feet with knee pain and cartilage damage in older adults," *Arthritis care & research,* vol. 63, no. 7, pp. 937-944, 2011.

[315] G. L. Hatfield *et al.*, "Knee and ankle biomechanics with lateral wedges with and without a custom arch support in those with medial knee osteoarthritis and flat feet," *Journal of Orthopaedic Research,* vol. 34, no. 9, pp. 1597-1605, 2016.

[316] K. Oh and S. J. J. o. b. Park, "The bending stiffness of shoes is beneficial to running energetics if it does not disturb the natural MTP joint flexion," vol. 53, pp. 127-135, 2017.

[317] A. Stacoff *et al.*, "Effects of foot orthoses on skeletal motion during running," vol. 15, no. 1, pp. 54-64, 2000.

[318] M. Kido *et al.*, "Effect of therapeutic insoles on the medial longitudinal arch in patients with flatfoot deformity: a three-dimensional loading computed tomography study," vol. 29, no. 10, pp. 1095-1098, 2014.

[319] N. Collins, L. Bisset, T. McPoil, B. J. F. Vicenzino, and a. international, "Foot orthoses in lower limb overuse conditions: a systematic review and meta-analysis," vol. 28, no. 3, pp. 396-412, 2007.

[320] K. A. Kirby, *Foot and lower extremity biomechanics: A ten year collection of precision intricast newsletters*. Precision Intricast, Incorporated, 1997.

[321] G. P. Brown, R. Donatelli, P. A. Catlin, M. J. J. J. o. O. Wooden, and S. P. Therapy, "The effect of two types of foot orthoses on rearfoot mechanics," vol. 21, no. 5, pp. 258-267, 1995.

[322] S. C. Cobb, L. L. Tis, J. T. Johnson, Y. T. Wang, and M. D. Geil, "Custom-Molded Foot-Orthosis Intervention and Multisegment Medial Foot Kinematics During Walking," *Journal of Athletic Training,* vol. 46, no. 4, pp. 358-365, 2011.

[323] M. Hajizadeh, B. Michaud, G. Desmyttere, J.-P. Carmona, and M. Begon, "Predicting foot orthosis deformation based on its contour kinematics during walking," *PLOS ONE,* vol. 15, no. 5, p. e0232677, 2020.

[324] V. Fohanno, M. Begon, P. Lacouture, and F. J. M. S. D. Colloud, "Estimating joint kinematics of a whole body chain model with closed-loop constraints," vol. 31, no. 4, pp. 433-449, 2014.

[325] B. Michaud and M. Begon, "BIORBD: Toolbox for biomechanical analyses," 2020.

[326] C. M. O'Connor, S. K. Thorpe, M. J. O'Malley, C. L. J. G. Vaughan, and posture, "Automatic detection of gait events using kinematic data," vol. 25, no. 3, pp. 469-474, 2007.

[327] P. Catalfamo, D. Moser, S. Ghoussayni, D. J. G. Ewins, and posture, "Detection of gait events using an F-Scan in-shoe pressure measurement system," vol. 28, no. 3, pp. 420-426, 2008.

[328] J. Z. Bakdash and L. R. J. F. i. p. Marusich, "Repeated measures correlation," vol. 8, p. 456, 2017.

[329] G. Desmyttere, S. Leteneur, M. Hajizadeh, J. Bleau, and M. Begon, "Effect of 3D printed foot orthoses stiffness and design on foot kinematics and plantar pressures in healthy people," *Gait & Posture,* 2020.

[330] A. Stacoff *et al.*, "Effects of foot orthoses on skeletal motion during running," *Clinical Biomechanics,* vol. 15, no. 1, pp. 54-64, 2000/01/01/ 2000.

[331] S. Behforootan, P. Chatzistergos, R. Naemi, N. J. M. e. Chockalingam, and physics, "Finite element modelling of the foot for clinical application: a systematic review," vol. 39, pp. 1-11, 2017.

[332] J. M. Smoliga, L. A. Wirfel, D. Paul, M. Doarnberger, and K. R. J. J. o. b. Ford, "Effects of unweighting and speed on in-shoe regional loading during running on a lower body positive pressure treadmill," vol. 48, no. 10, pp. 1950-1956, 2015.

[333] B. Stansfield, K. Hawkins, S. Adams, D. J. G. Church, and posture, "Spatiotemporal and kinematic characteristics of gait initiation across a wide speed range," vol. 61, pp. 331-338, 2018.

[334] R. H. Carlson Jr *et al.*, "Treadmill gait speeds correlate with physical activity counts measured by cell phone accelerometers," vol. 36, no. 2, pp. 241-248, 2012.

[335] M. Hajizadeh, G. Desmyttere, A.-L. Ménard, J. Bleau, and M. Begon, "Understanding the role of foot biomechanics on regional foot orthosis deformation during walking in flatfoot individuals."

[336] K.-J. Youn, S. Y. Ahn, B.-O. Kim, I. S. Park, and S.-K. J. A. o. r. m. Bok, "Long-Term Effect of Rigid Foot Orthosis in Children Older Than Six Years With Flexible Flat Foot," vol. 43, no. 2, p. 224, 2019.

[337] A. Jane MacKenzie, K. Rome, and A. M. Evans, "The Efficacy of Nonsurgical Interventions for Pediatric Flexible Flat Foot: A Critical Review," *Journal of Pediatric Orthopaedics,* vol. 32, no. 8, 2012.

[338] H.-C. Yeh *et al.*, "Immediate efficacy of laterally wedged insoles with arch support on walking in persons with bilateral medial knee osteoarthritis," vol. 95, no. 12, pp. 2420-2427, 2014.

[339] J. F. Doty, R. G. Alvarez, T. B. Ervin, A. Heard, J. Gilbreath, and N. S. Richardson, "Biomechanical Evaluation of Custom Foot Orthoses for Hallux Valgus Deformity," *The Journal of Foot and Ankle Surgery,* vol. 54, no. 5, pp. 852-855, 2015/09/01/ 2015.

[340] H. Lal, M. K. J. J. o. c. o. Patralekh, and trauma, "3D printing and its applications in orthopaedic trauma: a technological marvel," vol. 9, no. 3, pp. 260-268, 2018.

[341] C. Giacomozzi, V. Macellari, A. Leardini, M. J. M. Benedetti, B. Engineering, and Computing, "Integrated pressure-force-kinematics measuring system for the characterisation of plantar foot loading during locomotion," vol. 38, no. 2, pp. 156-163, 2000.

Appendices

Appendix 1. Foot Orthosis Deformations Following Dynamic Loading: A 3D Finite Element Study

Maryam Hajizadeh[1], Anne-Laure Ménard[2], Gauthier Desmyttere[2], Laure Lagarenne[2], Jean-Philippe Carmona[3], Mickaël Begon[1, 2]

[1]Institute of Biomedical Engineering, Université de Montréal, Montréal, QC, Canada [2] School of Kinesiology and Exercise Science, Université de Montréal, Montréal, QC, Canada, [3]Caboma, Montréal, QC, Canada

This study includes preliminary results on the estimation of foot orthosis deformation using finite element analysis, which was presented in ISB conference 2019- Calgary, Canada.

Summary

3D printing is increasingly used to design patient-specific medical products [340], such as orthoses. Indeed, 3D printed foot orthoses (FO) have an interesting potential as they can include optimized patterns to locally adjust the mechanical properties according to each patient's gait pattern. Modelling FO is key to optimize its design and properties. This study aimed at quantifying FO displacement following loading, using finite-element modelling (FEM). An experimental setup included VICON motion analysis system to capture FO deformation and a custom-designed stick equipped to a load cell to manually apply controlled dynamic loading. A FEM was developed and tested mimicking the experimental conditions. Results showed that FEM could yiled similar range of displacement values as the experimental setup. FEM is promising for future patient-specific applications.

Introduction

The designs of customized FO have been commonly based on foot type, foot function or patient's weight [16]. However, the interaction between these two parameters has not been considered yet. This study aimed at quantifying displacements of a FO following dynamic loading using FEM.

Methods

A size-10 3D printed FO was fixed to a plate using three nails on the heel. In total, 55 retroreflective markers were positioned on the plantar surface of FO, and 18 markers on six removable triads on the FO edges (Figure S- I). An 18-camera motion capture system (VICON, Oxford, UK) recorded positions of markers at a frequency of 100 Hz. A custom-designed stick equipped with a uni-directional load cell was calibrated and synchronized with the kinematics. Force was manually applied with the stick (Figure S- I) at different locations on the FO, where the orientation of loading was captured with four markers attached to the stick.

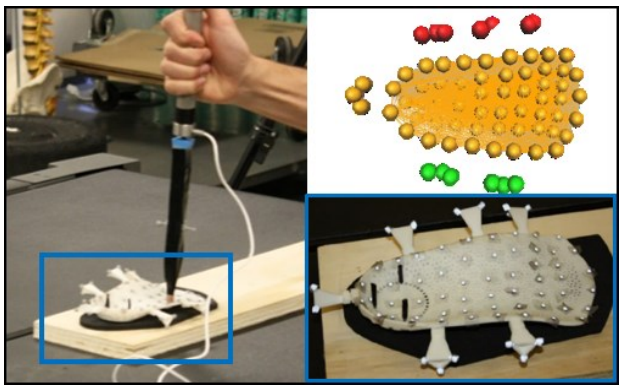

Figure S- I: Experimental setup and load application.

FO geometry was imported and meshed using Hypermesh (Altair HyperWorks 14.0, Altair Engineering inc., MI, USA). The orthosis mesh was assigned Nylon 12 linear elastic properties (E= 1700 MPa, ν = 0.30). The underneath plate was modelled as a shell with steel material properties. A contact surface with non-linear contact properties was defined between FO (slave) and plate (master). All translations were fixed at the heel using three groups of nodes representing nails. Loading direction was obtained from the four markers on the stick projected on the FO. Loading was spread across nodes equivalent to the stick area. Four loading locations were chosen on distant edges of the FO to validate displacements.

Results and Discussion

The FE model (Figure S- II- A) was able to predict similar displacements patterns as the experimental values (Figure S- II- B) following different loading application points on both medial and lateral sides of the FO. Loading on the FO medial arch generated high deformation on both

medial and lateral sides, similar to the loading on the lateral arch. The heel support experienced the least deformation for all loadings.

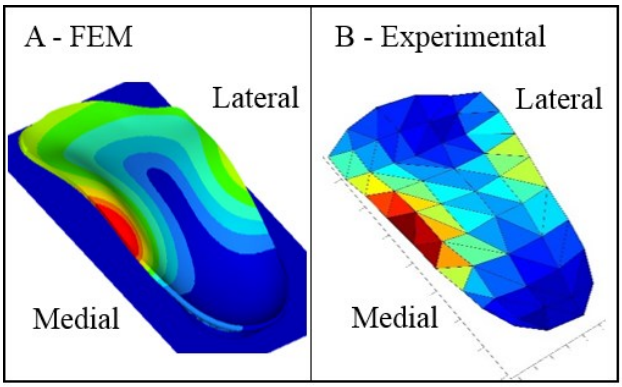

Figure S- II: FO deformations results: experimental and FEM.

Conclusions

FEM enabled the prediction of FO deformation following dynamic loading. This model should be further used to optimize FO design following patient-specific variations.

Appendix 2. Anatomically based integration of foot pressure and foot kinematics

The details for anatomical masking of foot regions is summarized in this section for Rizzoli foot model [149], which is the multi-segment foot model used in this thesis. The details for integrated anatomical masking using other foot kinematics models could be found elsewhere [189].

Following the temporal synchronization of foot kinematics and plantar pressure dataset, it is required to align the markers constituting multi-segment foot model, surface markers on foot orthosis obtained from artificial intelligence and plantar pressure images (Figure S- III). The midstance phase of walking would be used for the purpose of masking, where the vertical distance of markers from the pressure plate has its minimum sum, a minimum skin motion artefact occurs, and the foot plantar surface is the closest to flat surface [189]. The next step would be to identify different regions of interest (ROIs) based on the association between anatomical markers and functional structure of the foot in accordance with the foot model [178, 189, 341]. In addition to available foot markers in Rizzoli foot model (Figure S- III- a), four virtual markers was defined for identifying the regions: “M1” as the midpoint between ST and FMB, “M2” as the midpoint between PT and VMB, “M3” as the midpoint between M1 and M2, and “M4” as the midpoint between FMB and VMB. The borders of regions were then determined by passing some lines and arcs from the real and virtual markers as following:

- Line passing M1 and M2, to define rearfoot region posterior to the line
- Line passing M3 and M4, to separate the medial from the lateral region of midfoot
- Arc to resemble the contour of metatarsal base and define the border between midfoot and forefoot. This arc was made from the center located in ST and the radius equal to the vector ST-VMB in the literature. In this study, the arc was modified as the one passing the three markers of FMB, SMB and VMB located on metatarsal base. These anatomical markers were located on the bony landmarks of metatarsal, and to our observation could better resemble the contour of metatarsal.
- Arc to resemble the contour of metatarsal head and define the border between forefoot and toes. The arc center was at ST and the radius was equal to the vector ST- (the point at one-third of the line HLX-FMH).
- Line passing M4 and SMH to separate the hallux from other toes.

For the purpose of this thesis, the rearfoot was also separated to medial and lateral by a line passing M3 and CA. In addition, the combination of forefoot, hallux and other toes ROIs were regarded as one single ROI since the FOs used in this study were ¾-length FOs. Figure S- III-a shows the location of markers for Rizzoli foot model on foot skeleton, aligning the foot markers and plantar pressure images, and anatomical masking based on the location of anatomical landmarks. As it can be observed in Figure S- III-b, the foot plantar surface was divided to five ROIs for this study.

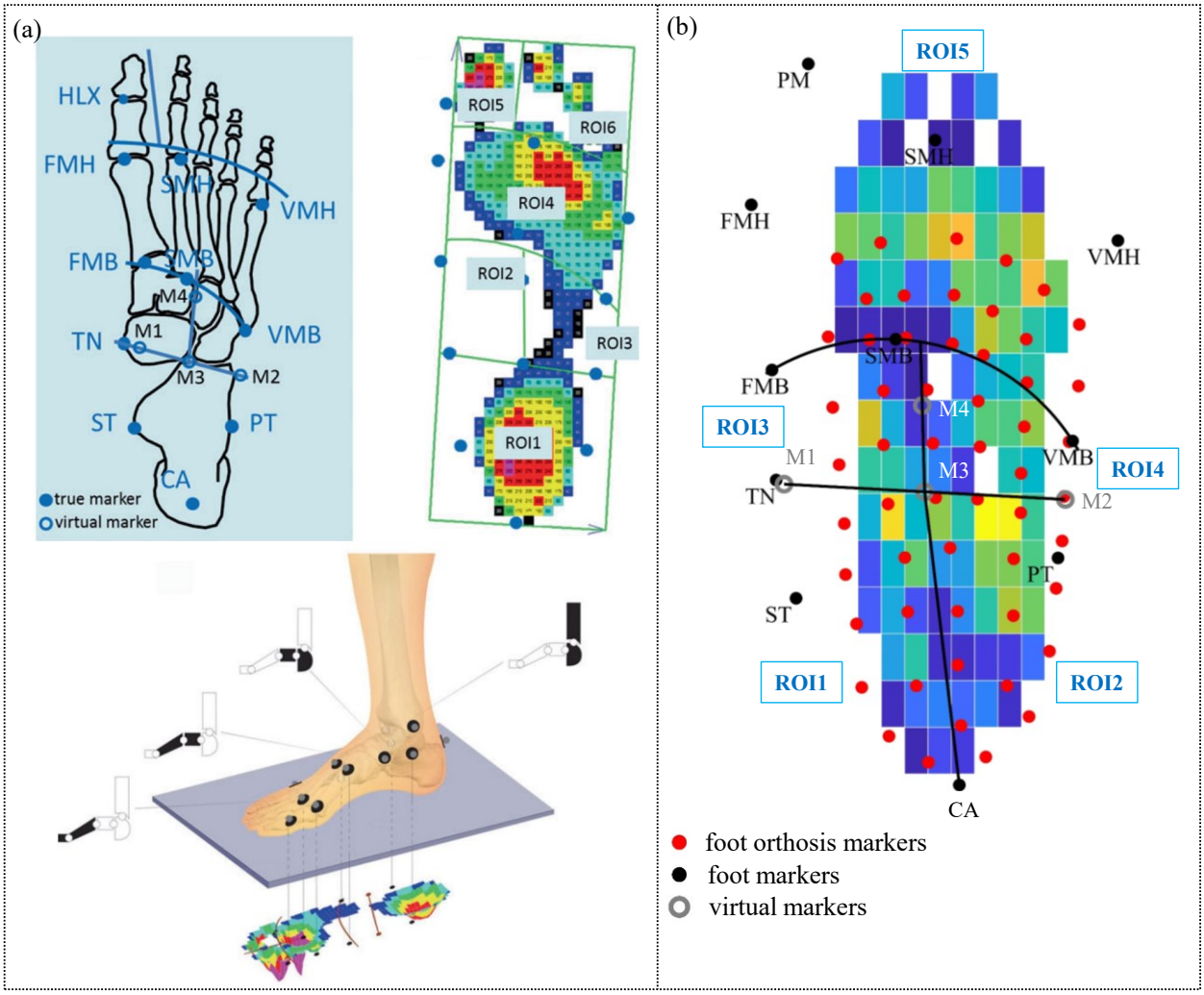

Figure S- III: Anatomical masking based on Rizzoli foot model [149]: (a) Integration of foot kinematics, and plantar pressure depicted by Giacomozzi, et al. [189]; Copyright (2020) with permission from Springer Nature (b) Integration of foot kinematics, plantar pressure, and foot orthosis surface markers implemented by S2M lab.